



THE UNIVERSITY OF QUEENSLAND
AUSTRALIA

Tensor Network States and Algorithms
in the presence of
Abelian and non-Abelian Symmetries

By

Sukhbinder Singh

B.E. Comp. Sci. (2003), Thapar University, India.

A thesis submitted for the degree of Doctor of Philosophy at
The University of Queensland in November 2024
School of Mathematics and Physics

© Sukhbinder Singh, 2024
(except as otherwise indicated).

Produced in L^AT_EX 2_ε.

Declaration by author

This thesis is composed of my original work, and contains no material previously published or written by another person except where due reference has been made in the text. I have clearly stated the contribution by others to jointly-authored works that I have included in my thesis.

I have clearly stated the contribution of others to my thesis as a whole, including statistical assistance, survey design, data analysis, significant technical procedures, professional editorial advice, and any other original research work used or reported in my thesis. The content of my thesis is the result of work I have carried out since the commencement of my research higher degree candidature and does not include a substantial part of work that has been submitted to qualify for the award of any other degree or diploma in any university or other tertiary institution. I have clearly stated which parts of my thesis, if any, have been submitted to qualify for another award.

I acknowledge that an electronic copy of my thesis must be lodged with the University Library and, subject to the General Award Rules of The University of Queensland, immediately made available for research and study in accordance with the *Copyright Act 1968*.

I acknowledge that copyright of all material contained in my thesis resides with the copyright holder(s) of that material.

Statement of Contributions to Jointly Authored Works Contained in this Thesis

This thesis is partly by publication. It contains the following publications, which I have co-authored as the first author, directly as Chapters 2,3 and 4.

(Singh et al., 2010a) - Incorporated as *Chapter 2*. The details of the SU(2) symmetric iTEBD algorithm were developed by myself and Prof. Guifre Vidal. The implementation of the algorithm in MATLAB and numerical simulations was performed by myself. Most of the manuscript was prepared by Prof. Guifre Vidal. Section 5, which describes the details

of the symmetric iTEBD algorithm, and Figs. 3 and 4 were prepared by myself. Prof. Huan-Zhou Qiang was responsible for clarifying several results from the representation theory of $SU(2)$ that were crucial to the development of the algorithm. He also pointed out the exact results that were used in Fig. 4 to draw a comparison with the numerical results.

(Singh et al., 2010b) - Incorporated as *Chapter 3*. The theoretical formalism presented in this paper was developed mostly by myself and Prof. Guifre Vidal. Robert N. C. Pfeifer joined the effort at an advanced stage of the project and contributed ideas that were important for the final presentation of the formalism. The manuscript was mostly written by Prof. Guifre Vidal, in close correspondence with myself and Robert N. C. Pfeifer. Implementation in MATLAB and numerical simulations were performed by me. However, these results were not included in the final draft of the manuscript.

(Singh et al., 2011) - Incorporated as *Chapter 4*. The theoretical ideas presented in this paper were developed mostly by myself and Prof. Guifre Vidal. The MATLAB implementation and numerical results reported in the manuscript were performed by myself. Robert N. C. Pfeifer also independently and simultaneously coded an implementation in MATLAB that was an important support for the validity of the ideas presented in the paper. Myself and Robert N. C. Pfeifer jointly proposed a precomputation scheme that was used in both the implementations. The main structure and content of the paper, including all the figures, was prepared by myself in close supervision of Prof. Guifre Vidal. The final draft was critically revised by Prof. Guifre Vidal. Robert. N.C. Pfeifer also contributed to the corrections of the figures and the manuscript at a pre-submission stage, and assisted in writing the Appendix.

Statement of Contributions by Others to the Thesis as a Whole

The overall motivation and research direction of this thesis was provided by Prof. Guifre Vidal.

Statement of Parts of the Thesis Submitted to Qualify for the Award of Another Degree

None.

Published Works by the Author Incorporated into the Thesis

(Singh et al., 2010a) - Incorporated as Chapter 2.

(Singh et al., 2010b) - Incorporated as Chapter 3.

(Singh et al., 2011) - Incorporated as Chapter 4.

Additional Published Works by the Author Relevant to the Thesis but not Forming Part of it

None.

Acknowledgments

The completion of this thesis would have been impossible without the tireless supervision and wise guidance of Guifre Vidal. From him I have learnt numerous practical aspects of both research and life. For that my gratitude remains well beyond words.

I thank all my fellow research group members: Philippe Corboz, Glen Evenbly, Andy Ferris, Jacob Jordan, Ian McCulloch, Roman Orus, Robert Pfeifer and Luca Tagliacozzo, for providing me with an intellectually rich and competitive research environment. I also acknowledge the support of Huan-Qiang Zhou, whose research group I visited twice during the completion of this work. I thank him for always putting palpable enthusiasm into physics and physics into words.

My personal perseverance was fueled by my parents who have made me what I am today, and by Meru, my dear friend, who has been like my shadow in the last few years, especially during the strenuous times of this project.

Finally, I would like to make a special mention of the blessings of my grandsire figure, Sant Baba Pritam Das Ji, who forever nourishes my spirit.

Abstract

Understanding and classifying phases of matter is a vast and important area of research in modern physics. Of special interest are phases at low temperatures where quantum effects are dominant. Theoretical progress is thwarted by a general lack of analytical solutions for quantum many-body systems. Moreover, perturbation theory is often inadequate in the strongly interacting regime. As a result, numerical approaches have become an indispensable tool to address such problems. In recent times, numerical approaches based on tensor networks have caught widespread attention. Tensor network algorithms draw on insights from Quantum Information theory to take advantage of special entanglement properties of low energy quantum many-body states of lattice models. Examples of popular tensor networks include Matrix Product States, Tree tensor Network, Multi-scale Entanglement Renormalization Ansatz and Projected Entangled Pair States. The main impediment of these methods comes from the fact that they can only represent states with a limited amount of entanglement. On the other hand, exploitation of symmetries, a powerful asset for numerical methods, has remained largely unexplored for a broad class of tensor networks algorithms.

In this thesis we extend the formalism of tensor network algorithms to incorporate global internal symmetries. We describe how to both numerically *protect* the symmetry and *exploit* it for computational gain in tensor network simulations. Our formalism is generic. It can readily be adapted to specific tensor network representations and to a wide spectrum of physical symmetries. The latter includes conservation of total particle number (U(1) symmetry) and of total angular momentum (SU(2) symmetry), and also more exotic symmetries (anyonic systems). The generality of the formalism is due to the fact that the symmetry constraints are imposed at the level of individual tensors, in a way that is

independent of the details of the tensor network. As a result, we are led to a framework of symmetric tensors. Such tensors are then used as building blocks for tensor network representations of quantum-many states in the presence of symmetry.

For a long time several physical problems of immense interest have remained elusive to numerical methods mostly owing to extremely high simulation costs. These include systems of frustrated magnets and interacting fermions that are relevant in the context of quantum magnetism and high temperature superconductivity. With symmetry now as a potent ally, tensor network algorithms may finally be used to draw positive insights about such systems.

Keywords: tensor networks, symmetry, $U(1)$, $SU(2)$, MERA, MPS, spin networks, anyons

Australian and New Zealand Standard Research Classifications (ANZSRC):

020401 Condensed Matter Characterisation Technique Development (50%)

020603 Quantum Information, Computation and Communication (50%).

Contents

List of Tables	xiii
List of Figures	xv
1 Introduction	1
1.1 Tensor network states and algorithms	2
1.2 Symmetries	4
1.3 Incorporating symmetries into tensor network algorithms	5
1.4 Plan of the thesis	8
2 Exploiting symmetries in MPS algorithms: An Example	11
3 Tensor networks and symmetries: Theoretical formalism	25
3.1 Errata	31
4 Implementation of Abelian symmetries	33
5 Implementation of non-Abelian symmetries I	57

5.1	Preparatory Review: Tensor network formalism	58
5.2	Representations of the group $SU(2)$	68
5.3	Tensor product of representations	79
5.4	Review: Fusion trees	89
5.5	Block structure of $SU(2)$ -invariant tensors	98
5.6	Manipulations of $SU(2)$ -invariant tensors	109
5.7	Supplement: Examples of evaluating a spin network	120
6	Implementation of non-Abelian symmetries II	125
6.1	Tensor networks with $SU(2)$ symmetry: A practical demonstration	142
7	Conclusions and Outlook	153
	References	157

List of Tables

1.1	Popular tensor networks in one and two spatial dimensions.	4
1.2	Examples of global internal physical symmetries.	5
6.1	Example of spin assignment in an SU(2) MERA for the anti-ferromagnetic spin chain with $L = 54$ sites (or 108 spins).	147

List of Figures

- 1.1 Computational gain obtained by exploiting the symmetry in an MPS algorithm. Computation time (in seconds) for one iteration of the infinite TEBD algorithm, as a function of the MPS bond dimension χ is shown. Here χ is a refinement parameter, a larger χ leads to a better accuracy of the method. For sufficiently large χ , exploiting symmetry leads to reductions in computation time. The horizontal line on this graph shows that this reduction in computation time equates to the ability to evaluate MPSs with a higher bond dimension χ : For the same cost per iteration incurred when optimizing a regular MPS in MATLAB with bond dimension $\chi = 220$, one may choose instead to optimize a U(1)-symmetric MPS with $\chi = 380$ or an SU(2)-symmetric MPS with $\chi = 1300$ 7
- 5.1 Graphical representation of tensors by means of a shape e.g. circle or a “blob” with emanating lines corresponding to indices of the tensor. Indices may be incoming or outgoing as indicated by arrows. (i) Graphical representations of tensors with rank 0, 1 and 2, corresponding to a complex number $c \in \mathbb{C}$, a vector $|v\rangle \in \mathbb{C}^{[i]}$ and a matrix $\hat{M} \in \mathbb{C}^{|a| \times |b|}$. (ii) Graphical representation of a tensor \hat{T} with components \hat{T}_{abcd} with directions $\vec{D} = \{\text{‘in’}, \text{‘out’}, \text{‘in’}, \text{‘out’}\}$. Notice that the indices emerge in a counter-clockwise order, perpendicular to the boundary of the blob; the first index is identified by the presence of by a dot within the blob close to the index. All arrows in a tensor diagram point downwards, that may be interpreted as choosing a metaphorical “time” that flows downwards. 59

5.2	Transformations of a tensor: (i) Reversing direction of an index, Eq. (5.3). (ii) Permutation of indices, Eq. (5.4). (ii) Fusion of indices a and b into $d = a \times b$, Eq. (5.5); splitting of index $d = a \times b$ into a and b , Eq. (5.6). . .	61
5.3	(i) Graphical representation of the matrix multiplication of two matrices \hat{R} and \hat{S} into a new matrix \hat{T} , Eq. (5.7). (ii) Graphical representation of an example of the multiplication of two tensors \hat{R} and \hat{S} into a new tensor \hat{T} , Eq. (5.8).	62
5.4	Graphical representations of the five elementary steps 1-5 into which one can decompose the multiplication of the tensors of Eq. (5.8).	63
5.5	(i) Factorization of a matrix \hat{T} according to a singular value decomposition, Eq. (5.14). (ii) Factorization of a rank-4 tensor \hat{T} according to one of several possible singular value decompositions.	65
5.6	(i) Example of a tensor network \mathcal{N} . (ii) Tensor \hat{T} of which the tensor network \mathcal{N} could be a representation. (iii) Tensor \hat{T} can be obtained from \mathcal{N} through a sequence of contractions of pairs of tensors. Shading indicates the two tensors to be multiplied together at each step. The product tensor is depicted by a blob that covers the two tensors that are multiplied. . . .	66
5.7	(i) The graphical representation of the Clebsch-Gordan tensors: C^{fuse} and C^{split} . (ii) Tensors C^{fuse} and C^{split} are isometries and thus yield the Identity when contracted pairwise either as (i) or (ii), Eq. (5.72).	82
5.8	The graphical representations of (i) the fusing tensor Υ^{fuse} and (ii) the splitting tensor. For fixed values of j_A, j_B and j_{AB} each of these tensors factorizes into a X and a C tensor.	85
5.9	Tensors Υ^{fuse} and Υ^{split} are unitary and thus yield the Identity when con- tracted pairwise either as (i) or (ii).	88

5.10	Examples of two fusion trees τ and τ' that describe two different ways of considering the tensor product of (i) three vector spaces $\mathbb{V}^{(A)}, \mathbb{V}^{(B)}$ and $\mathbb{V}^{(C)}$ and (ii) four vector spaces $\mathbb{V}^{(A)}, \mathbb{V}^{(B)}, \mathbb{V}^{(C)}$ and $\mathbb{V}^{(D)}$. Fusion proceeds from top to bottom.	90
5.11	(i) In the tensor product of three irreps, two coupled bases that are labeled by fusion trees τ (5.100) and τ' (5.101) are related to one another by means of the recoupling coefficients $\hat{F}_{j_A j_B j_C j_{ABC}}^{j_D j_E}$. (ii) A recoupling coefficient is given as the ‘scalar product’ of \hat{Q} and \hat{Q}'	92
5.12	(i) The change of basis from the product basis to two different coupled bases in the fusion of three reducible representations is given in terms of two fusing tensors. (ii) The two coupled basis are related by means of the matrix $\hat{\Gamma}$ [Eq. (5.114)] that is obtained by contracting a tensor network made of tensors Υ^{fuse} and tensors Υ^{split} . (iii) The components of $\hat{\Gamma}$ are given in terms of recoupling coefficients. This can be seen by performing the contraction piecewise. For fixed values of spins $j_A, j_B, j_C, j_{ABC}, j_D$ and j_E the tensor network decomposes into a tensor network made of X tensors and a spin network. The former is contracted to obtain a matrix \hat{D}' whereas the latter can be replaced by the Identity $\hat{I}_{2j_{ABC}+1}$ and a recoupling coefficient [Fig. 5.11(ii)].	95
5.13	The spin network that relates two coupled bases labeled by fusion trees τ and τ' . The spin network is proportional to the Identity, the proportionality factor is the coefficient $\hat{S}_{j_A j_B j_C j_D j}^{j_E j_F j_G j_H}$, which can be shown to be the product of two recoupling coefficients.	96
5.14	The transformation $\hat{\Gamma}$ that relates two different coupled bases, labeled by fusion trees τ and τ' , when fusing four reducible representations. Matrix $\hat{\Gamma}$ decomposes into a degeneracy matrix \hat{D}_j and the Identity.	97

5.15	Implication of the symmetry constraints fulfilled by a rank-1 $SU(2)$ -invariant tensor with (i) an outgoing index, and (ii) an incoming index. The only allowed spin on the one index is $j = 0$	100
5.16	Implication of the symmetry constraints fulfilled by rank-2 $SU(2)$ -invariant tensors as resulting in the decomposition of the tensors into degeneracy tensors \hat{P} and structural tensors.	102
5.17	Examples of the constraints fulfilled by rank-3 $SU(2)$ -invariant tensors and their implication as resulting in the decomposition of the tensors into degeneracy tensors \hat{P} and a Clebsch-Gordan tensors.	105
5.18	Two equivalent canonical decompositions of a rank-4 $SU(2)$ -invariant tensor corresponding to two different ways of fusing the three incoming indices into the outgoing index.	107
5.19	(i) Graphical representation of the cup tensor. For simplicity, we choose the same graphical representation for a cup tensor applied to an index that carries a single spin j as well as for one that is applied on an index i that carries several spins j (possibly with degeneracy d_j). ($c = 2j + 1$ is a normalization constant.) (ii) The analogous graphical representation of the cap tensor. (iii) Multiplying together a cup tensor and a cap tensor yields the Identity.	110

5.20	Reversing an index of an SU(2)-invariant tensor by means of a cup tensor.	
	(i) Reversing an index of an SU(2)-invariant tensor \hat{T} with two outgoing indices to obtain a matrix \hat{T}' . (ii) The reversal in (i) as performed on the canonical form of \hat{T} . The degeneracy index can be reversed without affecting the components of the degeneracy tensor \hat{P} . The reversal of the spin index equates to replacing the shaded region with a Clebsch-Gordan tensor and a numerical factor $\frac{1}{2^{j+1}}$, which is absorbed into \hat{P} to obtain \hat{P}' . (iii) Reversing an index of a rank-3 SU(2)-invariant tensor. (iv) The reversal in (iii) as performed on the canonical form of \hat{T} . The reversal of the spin index equates to replacing the shaded region with a Clebsch-Gordan tensor and a recoupling coefficient $\hat{F}_{0j_b j_a j_c}^{j_a j_b}$. The recoupling coefficient appears as a result of introducing a resolution of Identity [Fig. 5.7(iii)] on the spins j_b and j_a and then simplifying the resulting diagram by applying the equality in Fig. 5.11(ii).	111
5.21	Permutation of indices [Fig. 5.2(ii)] as performed on the canonical form of a rank-3 SU(2)-invariant tensor. The permutation decomposes into permutation of the degeneracy indices and permutation of the spin indices. The latter equates to replacing the Clebsch-Gordan tensor and a ‘cross’ with a Clebsch-Gordan tensor and a numerical factor $R_{j_a, j_b \rightarrow j_c}^{\text{swap}}$.	114
5.22	Illustration of the property that reversal of indices “commutes” with a permutation of them.	115
5.23	(i) Fusion of two outgoing indices of an SU(2)-invariant tensor by means of the fusing tensor Υ^{fuse} . (ii) Fusion in the canonical form of the tensor decomposes into the fusion of the degeneracy indices using tensor X^{fuse} , and the fusion of the spin indices using tensor C^{fuse} . The latter can be performed for free since the loop can directly be replaced with a straight line [Fig. 5.7(ii)]. (iii) Splitting of an outgoing index into two indices by means of the splitting tensor Υ^{split} . (iv) Splitting the index in the canonical form of the tensor.	117

5.24 (i) Fusion of two incoming indices into an incoming index, and (ii) splitting an incoming index into two incoming indices can be performed in one of two way. 118

5.25 Computation times (in seconds) required to permute indices of a rank-four tensor \hat{T} , as a function of the size of the indices. All four indices of \hat{T} have the same size $9d$, and therefore the tensor contains $|\hat{T}| = 9^4 d^4$ coefficients. The figures compare the time required to perform these operations using a regular tensor and an $SU(2)$ -invariant tensor, where in the second case each index contains three different values of spin $j = 0, 1, 2$, each with degeneracy d , and the canonical form of Eq. (5.161) is used. The upper figure shows the time required to permute two indices: For large d , exploiting the symmetry of an $SU(2)$ -invariant tensor by using the canonical form results in shorter computation times. The lower figure shows the time required to fuse two adjacent indices. In this case, maintaining the canonical form requires more computation time. Notice that in both figures the asymptotic cost scales as $O(d^4)$, or the size of \hat{T} , since this is the number of coefficients which need to be rearranged. We note that the fixed-cost overheads associated with symmetric manipulations could potentially vary substantially with choice of programming language, compiler, and machine architecture. The results given here show the performance of our MATLAB implementation of $SU(2)$ symmetry. 122

5.26 Computation times (in seconds) required to multiply two matrices (upper panel) and to perform a singular value decomposition (lower panel), as a function of the size of the indices. Matrices of size $9d \times 9d$ are considered. The figures compare the time required to perform these operations using regular matrices and SU(2)-invariant matrices, where for the SU(2) matrices each index contains three different values of the spin $j = 0, 1, 2$, each with degeneracy d , and the canonical form of Eq. (5.137) is used. That is, each matrix decomposes into three blocks of size $d \times d$. For large d , exploiting the block diagonal form of SU(2)-invariant matrices results in shorter computation time for both multiplication and singular value decomposition. The asymptotic cost scales with d as $O(d^3)$, while the size of the matrices grows as $O(d^2)$. (For matrix multiplication, a tighter bound of $O(d^{2.5})$ for the scaling of computational cost with d is seen in this example.) We note that the fixed-cost overheads associated with symmetric manipulations could potentially vary substantially with choice of programming language, compiler, and machine architecture. The results given here show the performance of our MATLAB implementation of SU(2) symmetry. . . . 123

5.27 Illustration of evaluating a spin network. 124

6.1 A tree decomposition $\mathcal{D}(\hat{T})$ of a rank-6 SU(2)-invariant tensor \hat{T} with indices $\{i_1, i_2, \dots, i_6\}$. (All internal indices are summed over.) The tree decomposition consists of an SU(2)-invariant vector \hat{v} , a set of splitting tensors and cup tensors that are attached to the incoming indices of \hat{T} . The tree decomposition is obtained by applying a resolution of Identity $\mathcal{I}(\boldsymbol{\tau})$ on the tensor. The fusing and splitting tensors that constitute $\mathcal{I}(\boldsymbol{\tau})$ are connected together according to the fusion tree $\boldsymbol{\tau}$ 127

- 6.2 (i) Two different, but equivalent, tree decompositions $\mathcal{D}^X(\hat{T})$ and $\mathcal{D}^Y(\hat{T})$ of a rank-4 SU(2)-invariant tensor \hat{T} . The two decompositions are characterized by different fusion trees τ^X and τ^Y . (ii) Tree decompositions $\mathcal{D}^X(\hat{T})$ and $\mathcal{D}^Y(\hat{T})$ are obtained by applying the resolutions of Identity $\mathcal{I}(\tau^X)$ and $\mathcal{I}(\tau^Y)$ on \hat{T} 128
- 6.3 Mapping a tree decomposition $\mathcal{D}^X(\hat{T})$ of an SU(2)-invariant tensor \hat{T} to another tree decomposition $\mathcal{D}^Y(\hat{T})$ by applying a resolution of Identity $\mathcal{I}(\tau^Y)$ to $\mathcal{D}^X(\hat{T})$. We obtain an intermediate matrix $\hat{\Gamma}(\tau^X, \tau^Y)$ by contracting together the splitting tensors in $\mathcal{D}^X(\hat{T})$ and the fusing tensors in $\mathcal{I}(\tau^Y)$ and then multiply it with vector \hat{v}^X to obtain vector \hat{v}^Y 130
- 6.4 Permuting indices of a rank-4 SU(2)-invariant tensor \hat{T} given in a tree decomposition. The “crossings” in the diagram can be absorbed into the tree by applying a resolution of Identity $\mathcal{I}(\tau')$ (for a given fusion tree τ'). An intermediate matrix $\hat{\Gamma}(\tau, \mathbf{p}, \tau')$ is obtained by contracting together the splitting tensors in $\mathcal{D}(\hat{T})$, the permutation \mathbf{p} and the fusing tensors in $\mathcal{I}(\tau')$. The matrix is multiplied with the vector \hat{v} to determine the updated vector \hat{v}' 132
- 6.5 (i) Fusion of two adjacent indices that belong to the same node of the tree decomposition proceeds by simply deleting the node to obtain the updated tree decomposition. (ii) Splitting an index corresponds to concatenating a new node to the tree decomposition. 137
- 6.6 The block-diagonal form of an SU(2)-invariant matrix is obtained from its tree decomposition by performing two multiplications. At each step the tensors within the shaded region are multiplied together. The same steps are also shown in the canonical form. 138

6.7	The five steps of tensor multiplication [Fig. 5.4] as adapted to the presence of the symmetry. For simplicity, the tree decompositions are not explicitly shown; the circle representing a tensor masks the tree decomposition of the tensor.	139
6.8	The number of spin networks to be evaluated when permuting or reshaping an $SU(2)$ -invariant tensor, as a function of the number of indices of the tensor and the number of different spins j assigned to each index of the tensor. The plot shows the increase in the number of spin networks that are evaluated when reshaping tensors with increasing number of indices. It also illustrates the corresponding increase that results from increasing the number of different values of spin j that are assigned to the indices of the tensor. (Note that the number of spin networks does not depend on the degeneracy dimension of a spin j .) Consequently, the cost of reshaping tensors with a large number of indices may potentially become significant.	140
6.9	A tensor network \mathcal{N} made of $SU(2)$ -invariant tensors represents an $SU(2)$ -invariant tensor \hat{T} . This is seen by means of two equalities. The first equality is obtained by inserting resolutions of the Identity $\hat{I} = \hat{W}_{\mathbf{r}}\hat{W}_{\mathbf{r}}^{\dagger}$ on each index connecting two tensors in \mathcal{N} . The second equality follows from the fact that each tensor in \mathcal{N} is $SU(2)$ -invariant.	142
6.10	MERA for a system of $L = 2 \times 3^2 = 18$ sites, made of two layers of disentanglers \hat{u} and isometries \hat{w} , and a top tensor \hat{t}	143
6.11	Error in ground state energy ΔE as a function of χ for the Heisenberg model with $2L = 108$ spins and periodic boundary conditions, in the singlet sector, $J = 0$. The error is calculated with respect to the exact solutions, and is seen to decay polynomially with χ for the particular choice of spins listed in Table 6.1.	146

- 6.12 Low energy spectrum of \hat{H} with $L = 54$ sites (=108 spins). Depicted states have spin J of zero (\times , blue loops), one ($+$, red loops), or two (\circ , green loop). The superscript 2 close to the boundary of a loop indicates that the loop encloses two-fold degenerate states e.g., the second, third and fourth spin-1 triplets are twofold degenerate. The inset shows a zoom in of the region enclosed within the box. It compares the energies of the two-fold degenerate spin-one states within the box with those obtained using the regular MERA (black asterix points). Since the symmetry is not protected, the states obtained with the regular MERA corresponding to different m_J do not have the same energies. 148
- 6.13 Memory cost (in number of components) for storing the MERA as a function of the bond dimension χ . The horizontal line on this graph shows that this reduction in memory cost equates to the ability to store MERAs with a higher bond dimension χ : For the same amount of memory required to store a MERA with bond dimension $\chi = 15$, one may choose instead to store a U(1)-symmetric MERA with $\chi = 26$ or an SU(2)-symmetric MERA with $\chi = 39$ 149
- 6.14 Computation time (in seconds) for one iteration of the MERA energy minimization algorithm, as a function of the bond dimension χ . For sufficiently large χ , exploiting the SU(2) symmetry leads to reductions in computation time. The horizontal line on this graph shows that this reduction in computation time equates to the ability to evaluate MERAs with a higher bond dimension χ : For the same cost per iteration incurred when optimizing a regular MERA in MATLAB with bond dimension $\chi = 18$, one may choose instead to optimize a U(1)-symmetric MERA with $\chi = 26$ or an SU(2)-symmetric MERA $\chi = 33$ 150

CHAPTER 1

Introduction

The study of quantum many-body phenomena is of pivotal interest in modern physics. Important areas of research, such as the characterization of exotic phases of quantum matter and of quantum phase transitions (Sachdev, 1999), or even the possible realization (Kitaev, 2003; Nayak et al., 2008) of a quantum computer, rely on our understanding of collective phenomena in quantum many-body systems. Theoretical progress in these research areas is hindered both by a general lack of analytical results as well as the inadequacy of perturbation theory in the strongly interacting regime where the interesting physics often lies. As a result, development of numerical approaches to probe such systems has become a flourishing research industry. However, numerical methods are limited by staggering computational costs.

The number of parameters required to describe a generic quantum many-body wavefunction on a lattice grows exponentially with the number of sites in the lattice. An immediate consequence is that exact diagonalization can only be applied to small systems. In particular, thermodynamic properties often remain inaccessible by this method. Conventional alternatives include Quantum Monte Carlo sampling techniques. These are well established numerical methods that have been used extensively in several areas of Mathematics and Physics. Of interest here is that these techniques have been applied (Evertz, 2003; Prokofev et al., 1998; Sandvik, 2005; Syljuasen and Sandvik, 2002) successfully to several quantum lattice models. On the other hand, Quantum Monte Carlo techniques suffer from the notorious sign problem (Henelius and Sandvik, 2000; Loh and Gubernatis, 1990)

that hinders their application to certain systems of immense interest. Notable examples include systems of frustrated magnets and of interacting fermions that are relevant in the context of quantum magnetism and high temperature superconductivity(Anderson, 1987).

In recent years, new approaches based on tensor networks have caught widespread attention. Such approaches can be regarded as generalizations of the density matrix renormalization group (DMRG) method(McCulloch, 2008; Schollwock, 2005a; White, 1992, 1993), which is highly successful for one-dimensional systems. The potential of tensor network algorithms relies on the fact that, as DMRG, they can address systems of frustrated spins and interacting fermions but, unlike DMRG, they can also be applied to two dimensional systems, both of large size and of infinite size. The main impediment of such methods comes from the fact that simulation costs increase rapidly with the amount of entanglement in the system. Consequently, tensor networks can only represent states with a limited amount of entanglement. On the other hand, exploitation of symmetries has remained largely unexplored for a broad class of tensor networks algorithms.

Symmetries, of fundamental importance in physics, require special treatment in numerical studies. Unless explicitly preserved at the algorithmic level, they are bound to be destroyed by the accumulation of small errors, in which case significant features of the system might be concealed. On the other hand, when properly handled, the presence of a symmetry can be exploited to reduce simulation costs.

The goal of this thesis is to extend the tensor network formalism to the presence of symmetries. We develop a generic framework that can be applied to adapt any given tensor network representation and algorithm to both numerically protect symmetries and exploit them for computational gain.

1.1 Tensor network states and algorithms

Tensor networks are an efficient parameterization of low energy quantum many-body states of lattice models. The degrees of freedom of the model are arranged on a lattice

\mathcal{L} made of L sites where each site is described by a Hilbert space of dimension d . As a result, the Hilbert space dimension of \mathcal{L} grows exponentially with the number of sites L . Thus, a generic quantum many-body state on the lattice is parameterized by exponentially many parameters. On the other hand, the dynamics of the system are typically governed by a *local* Hamiltonian \hat{H} , that is, \hat{H} decomposes as the sum of terms involving only a small number of sites, and whose strength decays with the distance between the sites. The locality of the dynamics often implies that only a relatively small amount of entanglement is present in the ground state. In such circumstances, tensor networks offer a good description of the ground state. Moreover, the description is efficient, in that the total number of parameters encoded into the tensor networks grows roughly linearly with L .

Examples of tensor network states for one dimensional systems include the matrix product state (Fannes et al., 1992; Ostlund and Rommer, 1995; Perez-Garcia et al., 2007) (MPS), which results naturally from both Wilson’s numerical renormalization group (Wilson, 1975) and White’s DMRG and is also used as a basis for simulation of time evolution, e.g. with the time evolving block decimation (TEBD) (Vidal, 2003, 2004, 2007a) algorithm and variations thereof, often collectively referred to as time-dependent DMRG (Daley et al., 2004; Schollwöck, 2005b; Vidal, 2003, 2004, 2007a; White and Feiguin, 2004); the tree tensor network (Shi et al., 2006) (TTN), which follows from coarse-graining schemes where the spins are blocked hierarchically; and the multi-scale entanglement renormalization ansatz (Evenbly and Vidal, 2009a; Giovannetti et al., 2008; Pfeifer et al., 2009; Vidal, 2007b, 2008, 2010) (MERA), which results from a renormalization group procedure known as entanglement renormalization (Vidal, 2007b, 2010). For two dimensional lattices there are generalizations of these three tensor network states, namely projected entangled pair states (Gu et al., 2008; Jiang et al., 2008; Jordan et al., 2008; Murg et al., 2007, 2009; Nishino and Okunishi, 1998; Nishio et al., 2004; Sierra and Martin-Delgado, 1998; Verstraete and Cirac, 2004; Xie et al., 2009) (PEPS), 2D TTN (Murg et al., 2010; Tagliacozzo et al., 2009) and 2D MERA (Aguado and Vidal, 2008; Cincio et al., 2008; Evenbly and Vidal, 2009b, 2010a,b; König et al., 2009) respectively. As variational ansätze, PEPS and 2D MERA are particularly interesting since they can be used to address large two-dimensional lattices, including systems of frustrated spins (Evenbly and Vidal, 2010a;

<i>One dimensional</i>	<i>Two dimensional</i>
MPS	PEPS
1D TTN	2D TTN
1D MERA	2D MERA

Table 1.1 – Popular tensor networks in one and two spatial dimensions.

Murg et al., 2009) and interacting fermions, (Barthel et al., 2009; Corboz and Vidal, 2009; Corboz et al., 2010a,b; Gu et al., 2010; Kraus et al., 2010; Pineda et al., 2010; Pizorn and Verstraete, 2010; Shi et al., 2009) where Monte Carlo techniques fail due to the sign problem.

Some popular tensor networks are summarized in table 1.1.

1.2 Symmetries

The presence of symmetries is a universal trait of physical theories. Symmetry has become one of the most powerful tools of theoretical physics, as it has become evident that practically all laws of nature originate in symmetries. The importance of symmetries in physical theories was firmly grounded by the famous *Noether's theorem*, a rigorous result that links the presence of a symmetry to the conservation of a physical quantity.

In this thesis we will be concerned with symmetries exhibited in quantum lattice models. The many-body Hamiltonian \hat{H} may be invariant under certain transformations, which form a group \mathcal{G} of symmetries (Cornwell, 1997). Under the action of the symmetry transformation, the Hilbert space of the theory is divided into symmetry sectors labeled by quantum numbers or conserved charges. The symmetry group \mathcal{G} may be *Abelian* or *non-Abelian*, depending on whether or not the total effect of applying two symmetry transformations depends on the order in which the transformations are applied. The symmetry sectors associated with an Abelian symmetry correspond to one-dimensional invariant subspaces. In contrast, the dimension of the symmetry sectors associated with a non-Abelian symmetry may be larger than one.

<i>Conserved physical quantity</i>	<i>Symmetry group</i>	<i>Abelian/non-Abelian</i>
Parity of particle number	Z_2	Abelian
Particle number, spin projection	$U(1)$	Abelian
Total angular momentum, total spin	$SU(2)$	non-Abelian
Particle number and spin	$U(1) \times SU(2)$	non-Abelian
Spin and isospin	$SU(2) \times SU(2)$	non-Abelian
Total anyonic charge	e.g. $SU(2)_k$	e.g., non-Abelian

Table 1.2 – Examples of global internal physical symmetries.

On the lattice, one can distinguish between *space* symmetries, which correspond to some permutation of the sites of the lattice, and *internal* symmetries, which act on the vector space of each site. An example of space symmetry is invariance under translations by some unit cell, which leads to conservation of quasi-momentum. An example of internal symmetry is $SU(2)$ invariance, e.g. spin isotropy in a quantum spin model. An internal symmetry can in turn be *global*, if it transforms the space of each of the lattice sites according to the same transformation (e.g. a spin independent rotation); or *local*, if each lattice site is transformed according to a different transformation (e.g. a spin-dependent rotation), as it is in the case of lattice gauge models. A global internal $SU(2)$ symmetry gives rise to conservation of total spin. Table 1.2 lists some examples of Abelian and non-Abelian physical symmetries.

By targeting a specific symmetry sector during a calculation, computational costs can often be significantly reduced while explicitly preserving the symmetry. It is therefore not surprising that symmetries play an important role in numerical approaches.

1.3 Incorporating symmetries into tensor network algorithms

Exploiting symmetries has been of great interest in numerical approaches, since it allows selection of a specific charge sector within the kinematic Hilbert space, and leads to

significant reduction of computational costs.

In the context of tensor network algorithms, benefits of exploiting the symmetry have been extensively demonstrated especially in the context of MPS. Both *space* and *internal* symmetries, Abelian and non-Abelian, have been thoroughly incorporated into DMRG code and have been exploited to obtain computational gains (Bergkvist et al., 2006; McCulloch, 2007; McCulloch and Gulacsi, 2002; Ostlund and Rommer, 1995; Perez-Garcia et al., 2008; Pittel and Sandulescu, 2006; Ramasesha et al., 1996; Sanz et al., 2009; Schollwock, 2005b; Sierra and Nishino, 1997; Tatsuaki, 2000; White, 1992).

Symmetries have also been used in more recent proposals to simulate time evolution with MPS (Cai et al., 2010; Daley et al., 2004, 2005; Danshita et al., 2007; Mishmash et al., 2009; Muth et al., 2010; Schollwock, 2005b; Singh et al., 2010a; Vidal, 2004, 2007a; White and Feiguin, 2004).

Figure 1.1 is demonstrative of the colossal computational gain that has been obtained by exploiting the symmetry in the context of the MPS. (In Fig. 6.14 we show an analogous comparison for exploiting symmetries in the context of the MERA.)

However, when considering symmetries, it is important to notice that an MPS is a trivalent tensor network. That is, in an MPS each tensor has at most three indices. The Clebsch-Gordan coefficients (Cornwell, 1997) (or coupling coefficients) of a symmetry group are also trivalent, and this makes incorporating the symmetry into an MPS by considering symmetric tensors particularly simple. In contrast, tensor network states with a more elaborate network of tensors, such as MERA or PEPS, consist of tensors having a larger number of indices. In this case a more general formalism is required in order to exploit the symmetry.

In this thesis we will describe how to incorporate a global internal symmetry, given by a compact and reducible group \mathcal{G} , into tensor network algorithms. We will develop a generic strategy that is independent of the details of the underlying tensor network. We will do this by imposing the symmetry constraints at the level of individual tensors that constitute the tensor network. We will then also describe how symmetric tensors are

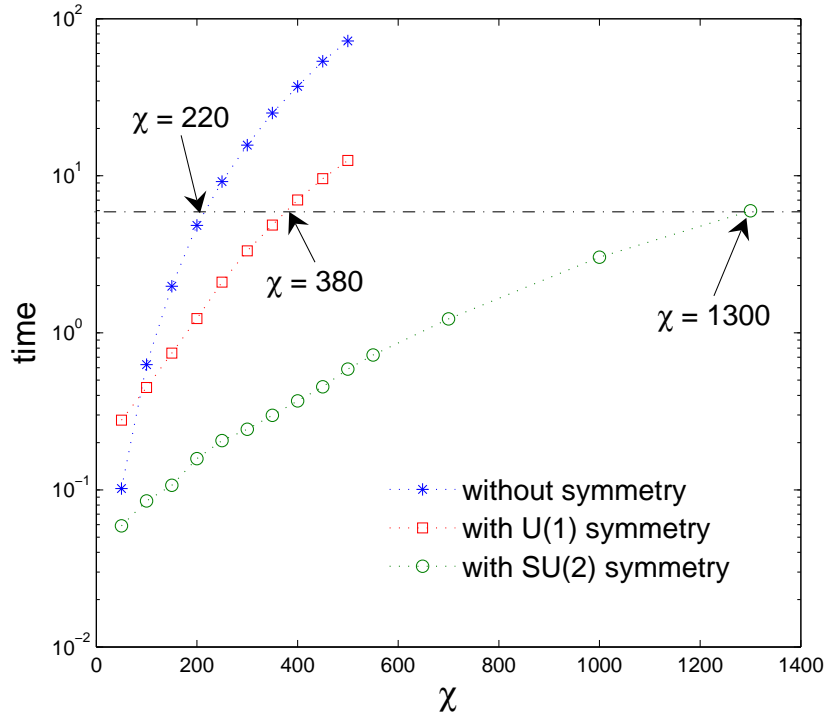


Figure 1.1 – Computational gain obtained by exploiting the symmetry in an MPS algorithm. Computation time (in seconds) for one iteration of the infinite TEBD algorithm, as a function of the MPS bond dimension χ is shown. Here χ is a refinement parameter, a larger χ leads to a better accuracy of the method. For sufficiently large χ , exploiting symmetry leads to reductions in computation time. The horizontal line on this graph shows that this reduction in computation time equates to the ability to evaluate MPSs with a higher bond dimension χ : For the same cost per iteration incurred when optimizing a regular MPS in MATLAB with bond dimension $\chi = 220$, one may choose instead to optimize a U(1)-symmetric MPS with $\chi = 380$ or an SU(2)-symmetric MPS with $\chi = 1300$.

manipulated such that the symmetry is both *preserved* and *exploited* for computational gain. Having built a framework of symmetric tensors, we will adapt an arbitrary tensor network to the presence of symmetry by using symmetric tensors as building blocks for the tensor network. The resulting tensor network represents a class of quantum many-body wavefunctions that are invariant (or more generally covariant) under the symmetry transformation. Algorithms based on such symmetric tensor networks will also be adapted to the presence of symmetry. This will be achieved by expressing each step of an algorithm

in terms of symmetric manipulations of the tensors.

As a concrete illustration, we will extensively describe the implementation of $U(1)$ and $SU(2)$ symmetries into the MPS and MERA. With these implementations at hand, we will demonstrate the colossal benefits of incorporating the symmetry into tensor network algorithms. These include addressing specific symmetry sectors of the Hilbert space, compactification of the tensor network representation and computational speedup in numerical simulations. For example, in a lattice spin model endowed with spin isotropy the ground state is constrained to the spin zero or singlet sector of the Hilbert space. Therefore, in a numerical probing for the state, it is sufficient to restrict attention to the singlet subspace. This can, in turn, potentially result in a substantial reduction of computational costs.

1.4 Plan of the thesis

This thesis is comprised of three published papers corresponding to chapters 2,3 and 4 and additional chapters 5 and 6. The material in chapters 5 and 6 was under preparation for publication at the time of submitting this thesis. The following is a brief summary of all the chapters.

In Chapter 2 we dive straight into the core of the problem. We describe the implementation of a non-Abelian symmetry for the case of the simplest tensor network: the MPS. This will serve to illustrate the key points that are required to be considered when implementing symmetries into tensor network algorithms. In addition, this chapter also demonstrates the benefits of exploiting symmetries in the case of MPS algorithms. We adapt the infinite time evolving block decimation (iTEBD) algorithm to the presence of a global $SU(2)$ symmetry. This is of interest in its own right since the iTEBD algorithm has been immensely successful in simulations of infinite 1D quantum many-body systems. This is also the first implementation of a non-Abelian symmetry into the iTEBD algorithm and has resulted in a significant enhancement of this algorithm.

In Chapter 3 we go beyond the class of MPS algorithms. We describe the general strategy to incorporate a wide spectrum of symmetries into more complex tensor network states and

algorithms. We consider tensor networks made of symmetric tensors, that is, tensors that are invariant under the action of the symmetry. We develop a formalism to characterize and manipulate symmetric tensors.

In Chapter 4 we implement the general formalism for the case of an Abelian symmetry. The implementation of an Abelian symmetry is simplified by the fact that symmetric tensors are easier to characterize. In a basis labeled by the charges of the symmetry, a symmetric tensor has a sparse block structure. We explain how this block structure can be exploited for computational gain in a practical implementation of the symmetry. The benefits of exploiting the symmetry are numerically demonstrated by exploiting $U(1)$ symmetry in the context of the MERA.

In Chapters 5 and 6 we describe the implementation of a non-Abelian symmetry. The details of implementing the symmetry are more involved, since the structural tensors are highly non-trivial. However, the computational gain that results from exploiting a non-Abelian symmetry is significantly larger than that obtained by exploiting an Abelian symmetry. Moreover, the practical scheme presented to implement a non-Abelian symmetry can be readily extended to incorporate more exotic symmetry constraints such as those corresponding to the presence of anyonic degrees of freedom. The benefits of exploiting a non-Abelian symmetry are numerically demonstrated by means of our implementation of $SU(2)$ symmetry in the context of the MERA.

Finally, in Chapter 7 we draw conclusions and discuss potential applications and future directions of this work.

Note on References: In addition to the references listed at the end of the thesis, chapter wise references appear at the end of chapters 2, 3 and 4 that correspond to published papers.

Exploiting symmetries in MPS algorithms: An Example

We kick start the main discussion of the thesis by describing how to incorporate an $SU(2)$ symmetry into a specific MPS algorithm: the iTEBD algorithm. The iTEBD algorithm has been immensely successful in simulations of infinite 1D quantum many-body systems.

We follow a straightforward implementation of the symmetry into the algorithm. We consider an MPS that is made of trivalent $SU(2)$ invariant tensors. A trivalent $SU(2)$ invariant tensor decomposes into two pieces. One piece contains the degrees of freedom whereas the other corresponds to the Clebsch-Gordan coefficients of $SU(2)$. We describe how the iTEBD algorithm can be enhanced by exploiting this decomposition of the MPS tensors. The resulting symmetric algorithm is obtained to be 300 times faster (See Fig. 1.1). We use the symmetric algorithm for a numerical study of a critical quantum spin chain.

This chapter serves to illustrate the main conceptual ingredients that are required to incorporate symmetries into tensor network algorithms. In the next chapter, we will generalize these ingredients by going beyond the specific details of the $SU(2)$ symmetry group and the MPS representation.

Simulation of one-dimensional quantum systems with a global SU(2) symmetry

Sukhwinder Singh^{1,3}, Huan-Qiang Zhou² and Guifre Vidal¹

¹ School of Physical Sciences, University of Queensland, Brisbane QLD 4072, Australia

² Department of Physics, Chongqing University, Chongqing 400044, People's Republic of China

E-mail: ssingh@physics.uq.edu.au

New Journal of Physics **12** (2010) 033029 (12pp)

Received 15 December 2009

Published 16 March 2010

Online at <http://www.njp.org/>

doi:10.1088/1367-2630/12/3/033029

Abstract. In this paper, we describe a refined matrix product representation for many-body states that are invariant under SU(2) transformations and use it to extend the time-evolving block decimation (TEBD) algorithm to the simulation of time evolution in the presence of an SU(2) symmetry. The resulting algorithm, when tested in a critical quantum spin chain, proved to be more efficient than the standard TEBD.

Contents

1. Introduction	2
2. Total spin basis	2
3. Bipartite decomposition	3
4. Matrix product decomposition	4
5. Simulation of time evolution	6
6. Example	8
7. Final remarks	10
Acknowledgments	11
References	11

³ Author to whom any correspondence should be addressed.

1. Introduction

Quantum many-body systems are characterized by a large Hilbert space, one whose dimension grows exponentially with the system's size. This makes the numerical study of generic quantum many-body phenomena computationally difficult. However, quantum systems are governed by Hamiltonians made of local interactions, that is, by highly non-generic operators. As a result, physically relevant states are atypical vectors in the Hilbert space and can sometimes be described efficiently. Systems in one spatial dimension are a prominent example. Here, the geometry of local interactions induces an anomalously small amount of bipartite correlations and an effective representation is often possible in terms of a trial wave function known as the *matrix product state* (MPS) [1, 2]. This, in turn, underlies the success of the density matrix renormalization group (DMRG) [3], which is an algorithm to compute ground states, and of several recent extensions of it [4, 5], including the time-evolving block decimation (TEBD) algorithm to simulate time evolution [4].

Symmetries, of fundamental importance in physics, require special treatment in numerical studies. Unless explicitly preserved at the algorithmic level, they are bound to be destroyed by the accumulation of small errors, in which case significant features of the system might be concealed. On the other hand, when properly handled, the presence of a symmetry can be exploited to reduce simulation costs. The latter has long been realized in the context of DMRG [3, 6]. More recently, the Abelian U(1) symmetry has been incorporated into the TEBD algorithm [7].

In this paper, we study how to enhance the TEBD algorithm in systems that are invariant under the action of a more general (possibly non-Abelian) symmetry, as given by a compact, completely reducible group G . (This includes finite groups as well as Lie groups such as $O(n)$, $SO(n)$, $U(n)$ and $SU(n)$.) We present an explicit theoretical construction of a refined MPS representation with built-in symmetry and put forward a significantly faster TEBD algorithm that both preserves and exploits the symmetry. For simplicity and concreteness, we analyze the smallest non-Abelian case, the $SU(2)$ group, which is relevant in the context of isotropic quantum spin systems. In contrast to the much simpler case of an Abelian U(1) symmetry [7], the analysis of the $SU(2)$ symmetry already contains the major ingredients of an arbitrary compact, completely reducible group G . In addition, it can be cast in the language of spin operators, which is often more familiar to physicists when compared with group representation theory. As a test, we have computed the ground state of the spin-1/2 antiferromagnetic Heisenberg chain, obtaining remarkably precise two-point correlators for both short and long distances.

In preparation for describing the $SU(2)$ MPS, we start by introducing a convenient vector basis and discuss the bipartite decomposition of states that are invariant under $SU(2)$.

2. Total spin basis

Let V be a vector space on which $SU(2)$ acts unitarily by means of transformations $e^{i\vec{v}\cdot\vec{S}}$, where matrices S_x , S_y and S_z close the Lie algebra $SU(2)$, namely $[S_\alpha, S_\beta] = i\epsilon_{\alpha\beta\gamma}S_\gamma$, and $\vec{v} \in \mathbb{R}^3$. A total spin basis (TSB) $|_{jtm}^{[V]}\rangle \in V$ satisfies the eigenvalue relations

$$\vec{S}^2 |_{jtm}^{[V]}\rangle = j(j+1) |_{jtm}^{[V]}\rangle, \quad S_z |_{jtm}^{[V]}\rangle = m |_{jtm}^{[V]}\rangle, \quad (1)$$

and is associated with the direct sum decomposition of V into irreducible representations (irreps) of $SU(2)$ [8],

$$V \cong \bigoplus_j (\tilde{V}^{(j)} \otimes V^{(j)}). \quad (2)$$

Here, $\tilde{V}^{(j)}$ is a d_j -dimensional space that accounts for the *degeneracy* of the spin- j irrep and has basis $|_{jt}^{[V]}\rangle \in \tilde{V}^{(j)}$, where $t = 1, \dots, d_j$, whereas $V^{(j)}$ is a $(2j + 1)$ -dimensional space that accommodates a spin- j irrep and has basis $|_{jm}^{[V]}\rangle \in V^{(j)}$, where m is the projection of the spin in the z -direction, $m = -j, \dots, j$. Each vector of the TSB factorizes into degeneracy and irrep parts as $|_{jtm}^{[V]}\rangle = |_{jt}^{[V]}\rangle |_{jm}^{[V]}\rangle$, where equation (1) determines only $|_{jm}^{[V]}\rangle$.

3. Bipartite decomposition

Consider an operator $\Theta : A \rightarrow B$ that acts from vector space A to B and that commutes with the action of $SU(2)$. Let $\vec{S}^{[A]}$ and $\vec{S}^{[B]}$ generate the action of the group on A and B . Then we have

$$\Theta S_\alpha^{[A]} = S_\alpha^{[B]} \Theta, \quad \alpha = x, y, z. \quad (3)$$

Describing A and B with a TSB and employing Schur's lemma [8], Θ splits into degeneracy and irrep parts as

$$\begin{aligned} \Theta &= \sum_{j_1 t_1 m_1} \sum_{j_2 t_2 m_2} \Theta_{j_2 t_2 m_2}^{j_1 t_1 m_1} |_{j_1 m_1 t_1}^{[A]}\rangle \langle_{j_2 t_2 m_2}^{[B]}| \\ &= \sum_j \left(\sum_{t_1 t_2} T_{t_1 t_2}^j |_{j t_1}^{[A]}\rangle \langle_{j t_2}^{[B]}| \right) \left(\sum_m |_{jm}^{[A]}\rangle \langle_{jm}^{[B]}| \right). \end{aligned} \quad (4)$$

The operator Θ is dual to a pure state $|\Psi\rangle$ of a bipartite system with vector space $A \otimes B$ by taking

$$\begin{aligned} \langle_{j_2}^{[B]}| &\rightarrow |_{j_2}^{[B]}\rangle, \\ \langle_{jm}^{[B]}| &\rightarrow \omega_m^j |_{j-m}^{[B]}\rangle, \end{aligned} \quad (5)$$

where ω is completely determined in terms of the Clebsch–Gordan coefficients $\langle j_1 j_2 m_1 m_2 | j_1 j_2; jm \rangle$ (see, for instance, [10]), namely

$$\omega_m^j \equiv (-1)^{2j+m+1} (2j+1)^{-1/2}, \quad (6)$$

$$\langle j_1 j_2 m_1 m_2 | j_1 j_2; 00 \rangle = \delta_{j_1, j_2} \delta_{m_1, -m_2} \omega_{m_1}^{j_1}. \quad (7)$$

and where $|\Psi\rangle$ is an $SU(2)$ *singlet*, that is, invariant under transformations acting simultaneously on A and B , or

$$(\vec{S}^{[A]} + \vec{S}^{[B]})^2 |\Psi\rangle = 0, \quad (S_z^{[A]} + S_z^{[B]}) |\Psi\rangle = 0. \quad (8)$$

Under the transformation in equation (5), equation (4) becomes

$$\begin{aligned} |\Psi\rangle &= \sum_{j_1 t_1 m_1} \sum_{j_2 t_2 m_2} N_{j_2 t_2 m_2}^{j_1 t_1 m_1} |_{j_1 m_1 t_1}^{[A]}\rangle |_{j_2 t_2 m_2}^{[B]}\rangle \\ &= \sum_j \left(\sum_{t_1 t_2} T_{t_1 t_2}^j |_{j t_1}^{[A]}\rangle |_{j t_2}^{[B]}\rangle \right) \left(\sum_m \omega_m^j |_{jm}^{[A]}\rangle |_{j-m}^{[B]}\rangle \right). \end{aligned} \quad (9)$$

The above decomposition is quite sensible: it shows that a coefficient $N_{j_2 t_2 m_2}^{j_1 t_1 m_1}$ may be nonzero only if

- (i) $j_1 = j_2$ (only the product of two spin j irreps can give rise to a spin 0 irrep, that is, the singlet $|\Psi\rangle$) and
- (ii) $m_1 = -m_2$, which guarantees that the z -component of the spin vanishes.

In addition, equation (9) embodies the essence of our strategy: to isolate the degrees of freedom that are not determined by the symmetry—in this case the degeneracy tensor $T_{t_1 t_2}^j$. We now consider the singular value decomposition (SVD)

$$T_{t_1 t_2}^j = \sum_t (R^j)_{t_1 t} (\eta^j)_t (S^j)_{t t_2} \quad (10)$$

of the tensor $T_{t_1 t_2}^j$ for a fixed j , and define

$$|\Psi_{j t}^{[A]}\rangle \equiv \sum_{t_1} R_{t_1 t}^j |\Psi_{j t_1}^{[A]}\rangle, \quad |\Psi_{j t}^{[B]}\rangle \equiv \sum_{t_2} S_{t t_2}^j |\Psi_{j t_2}^{[B]}\rangle. \quad (11)$$

By combining equations (9)–(11), we arrive at our canonical symmetric bipartite decomposition (CSBD)

$$|\Psi\rangle = \sum_j \left(\sum_t \eta_t^j |\Psi_{j t}^{[A]}\rangle |\Psi_{j t}^{[B]}\rangle \right) \left(\sum_m \omega_m^j |j m\rangle |j -m\rangle \right), \quad (12)$$

which is related to the Schmidt decomposition

$$|\Psi\rangle = \sum_{\alpha} \lambda_{\alpha} |\Phi_{\alpha}^{[A]}\rangle |\Phi_{\alpha}^{[B]}\rangle \quad (13)$$

by the identifications $\alpha \rightarrow (j t m)$, $\lambda_{\alpha} \rightarrow \eta_t^j \omega_m^j$ and

$$|\Phi_{\alpha}^{[A]}\rangle \rightarrow |\Psi_{j t}^{[A]}\rangle |j m\rangle, \quad |\Phi_{\alpha}^{[B]}\rangle \rightarrow |\Psi_{j t}^{[B]}\rangle |j -m\rangle, \quad (14)$$

where some of the Schmidt coefficients λ_{α} are negative. (If one prefers to work with non-negative Schmidt coefficients, negative signs can be absorbed into e.g. $|\Phi_{\alpha}^{[B]}\rangle$.)

More generally, a state $|j t m\rangle^{[CD]}$ of a bipartite system $C \otimes D$ can be expressed in terms of TSBs for C and D as [9]

$$|j t m\rangle^{[CD]} = \sum_{j_1 j_2} \left(\sum_{t_1 t_2} X_{j_1 t_1 j_2 t_2}^{j t} |j_1 t_1\rangle^{[C]} |j_2 t_2\rangle^{[D]} \right) \left(\sum_{m_1 m_2} C_{j_1 m_1 j_2 m_2}^{j m} |j_1 m_1\rangle^{[C]} |j_2 m_2\rangle^{[D]} \right), \quad (15)$$

where tensor X relates to degeneracy degrees of freedom and tensor C is given by the Clebsch–Gordan coefficients

$$C_{j_1 m_1 j_2 m_2}^{j m} = \langle j_1 j_2 m_1 m_2 | j_1 j_2; j m \rangle. \quad (16)$$

4. Matrix product decomposition

We now consider a chain of n quantum spins with spin s , represented by a one-dimensional (1D) lattice where each site, labeled r ($r = 1, \dots, n$), carries a $(2s + 1)$ -dimensional irrep of $SU(2)$.

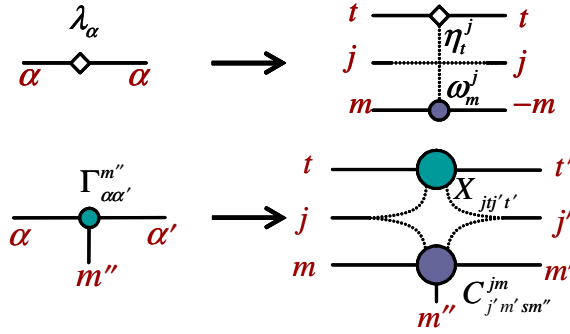


Figure 1. Diagrammatic representation of tensors λ and Γ of a MPS and tensors (η, ω) and (X, \tilde{C}) of a SU(2) MPS.

The coefficients $c_{m_1 m_2 \dots m_n}$ of a state $|\Psi\rangle$ of the lattice,

$$|\Psi\rangle = \sum_{m_1=1}^{2s+1} \cdots \sum_{m_n=1}^{2s+1} c_{m_1 m_2 \dots m_n} |_{m_1}^{[1]}\rangle |_{m_2}^{[2]}\rangle \cdots |_{m_n}^{[n]}\rangle, \quad (17)$$

where $\{|_{m}^{[r]}\rangle\}$ is a basis for site r with $S_z^{[r]} |_{m}^{[r]}\rangle = m |_{m}^{[r]}\rangle$, can be codified as a MPS [1, 2],

$$c_{m_1 \dots m_n} = \sum_{\alpha_1 \dots \alpha_{n-1}} \Gamma_{\alpha_1}^{[1]m_1} \lambda_{\alpha_1}^{[1]} \Gamma_{\alpha_1 \alpha_2}^{[2]m_2} \lambda_{\alpha_2}^{[2]} \cdots \Gamma_{\alpha_{n-1}}^{[n]m_n}. \quad (18)$$

Following the conventions of Vidal's paper [4], here $\lambda_\alpha^{[r]}$ are the Schmidt coefficients of $|\Psi\rangle$ according to the bipartition $[1 \cdots r] : [r+1 \cdots n]$ of the spin chain and the tensor $\Gamma_{\alpha\beta}^{[r]m}$ relates the Schmidt vectors for consecutive bipartitions,

$$|\Phi_\alpha^{[r \cdots n]}\rangle = \sum_{m=1}^{2s+1} \Gamma_{\alpha\beta}^{[r]m} \lambda_\beta^{[r]} |_{m}^{[r]}\rangle |\Phi_\beta^{[r+1 \cdots n]}\rangle. \quad (19)$$

When $|\Psi\rangle$ is a singlet, that is,

$$\left(\sum_r \vec{S}^{[r]} \right)^2 |\Psi\rangle = 0, \quad \sum_r S_z^{[r]} |\Psi\rangle = 0, \quad (20)$$

equations (12) and (15) supersede equations (13) and (19) and each tensor λ and Γ in equation (18) decomposes into degeneracy and irrep parts, see figure 1,

$$\lambda_\alpha = \lambda_{(jtm)} \rightarrow \eta_t^j \omega_m^j, \quad (21)$$

$$\Gamma_{\alpha\alpha'}^{m''} = \Gamma_{(jtm)(j't'm')}^{(sm'')} \rightarrow X_{jtj't'} \tilde{C}_{j'm'sm''}^{jm}, \quad (22)$$

where \tilde{C} is related to the Clebsch–Gordan coefficients C by

$$\tilde{C}_{j'm'j''m''}^{jm} \equiv (-1)^{2j'} (\omega_{m'}^{j'})^{-1} C_{j'm'j''m''}^{jm}. \quad (23)$$

Here, the term $(\omega_{m'}^{j'})^{-1}$ arises in conjunction with the transformation equation (5).

The SU(2) MPS is defined by equations (21) and (22). In this representation, the constraints imposed by the symmetry are used to our advantage. By splitting tensors λ and Γ , we achieve

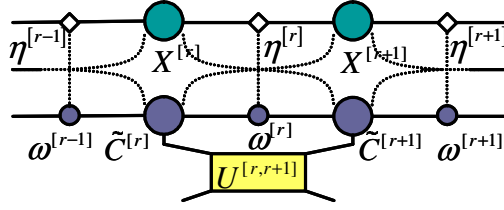


Figure 2. The TEBD algorithm is based on updating the MPS when a gate U acts on two neighboring sites. This diagram generalizes figure 3(i) of [11] after the replacements $\lambda \rightarrow (\eta, \omega)$ and $\Gamma \rightarrow (X, \tilde{C})$ of equations (21) and (22) for a $SU(2)$ MPS.

two goals simultaneously. On the one hand, the resulting MPS is guaranteed, by construction, to be invariant under $SU(2)$ transformations. That is, any algorithm based on this representation will preserve the symmetry exactly and permanently. On the other hand, all the degrees of freedom of $|\Psi\rangle$ are concentrated in smaller tensors η and X (tensors ω and \tilde{C} are specified by the symmetry), and thus the $SU(2)$ MPS is a more economical representation. If $|\cdot|$ denotes the number of coefficients of a tensor, then

$$|\lambda| \equiv \sum_j (2j+1)d_j \rightarrow |\eta| \equiv \sum_j d_j, \quad (24)$$

$$|\Gamma| = (2s+1)|\lambda||\lambda'| \rightarrow |X| \equiv \sum_{(j,j')} d_j d_{j'}, \quad (25)$$

where λ and λ' are the tensors to the left and to the right of Γ and where, following spin composition rules, the last sum is restricted to pairs (j, j') such that $|j - j'| \leq s$.

5. Simulation of time evolution

Our next step is to generalize the TEBD algorithm [4] to the simulation of $SU(2)$ -invariant time evolution. This reduces to explaining how to update the $SU(2)$ MPS when an $SU(2)$ -invariant gate U acts between contiguous sites, see figure 2. The update is achieved by following steps analogous to those of the regular TEBD algorithm, see figure 3 of [11], involving tensor multiplications and one SVD (figure 3). Following the procedure described in [11], we first absorb the gate into the tensors of the MPS by contracting the tensor network in figure 3. Here V_{Xi} and V_{Ci} enact a change of basis from the product basis $\{|j_1 m_1 t_1\rangle\} \otimes \{|j_p m_p t_p\rangle\}$ to the coupled basis $\{|j m t\rangle\}$. Specifically, V_{Ci} are the Clebsch–Gordan coefficients that describe the change of basis $|j_1 m_1\rangle \otimes |j_p m_p\rangle \rightarrow |j m\rangle$, and V_{Xi} denotes the change of basis $|j_1 t_1\rangle \otimes |j_p t_p\rangle \rightarrow |j t\rangle$. A straightforward choice for V_{Xi} is an invertible linear map that uniquely associates each pair j, t to a tuple j_1, t_1, j_p, t_p . Define $(V_{Xi})_{j_1 t_1 j_p t_p}^{j t} = 1$ for each such unique association and as 0 otherwise. The network contraction in figure 3 is a sum of the terms corresponding to various compatible values of j_1, j_2 and j_3 . For each such term, the top line of tensors comprising the η 's, X 's and V_X 's are multiplied together. By Schur's lemma, the product of the tensors ω 's, \tilde{C} 's, V_C 's and U on the lower leg is proportional to ω , with a proportionality constant α that depends on j, j_1, j_2, j_3 and j_p and that can be pre-computed because none of these tensors depend on $|\Psi\rangle$. α is then absorbed into the product of the degeneracy matrices, which are then

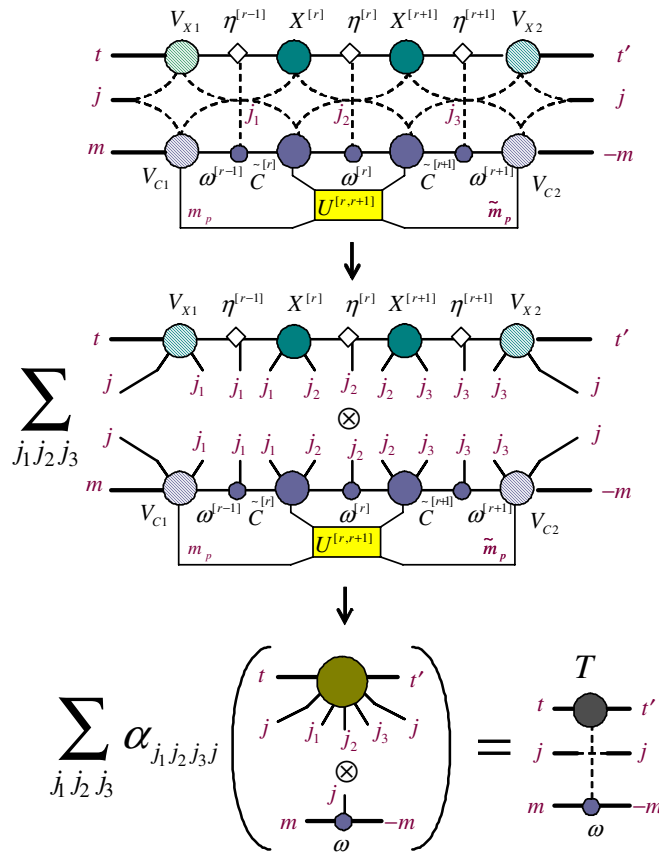


Figure 3. Key steps of the TEBD algorithm for a SU(2) MPS, analogous to figures 3(i)–(iii) of [11] for a regular MPS. Once U has been applied to two spins, additional tensors V_{X_i} and V_{C_i} implement a unitary transformation required to reabsorb these spins into blocks and obtain an updated representation for the bipartition $[1 \cdots r] : [r + 1 \cdots n]$. Then, for each fixed value of the j indices (discontinuous lines), the η 's, X 's and V_X 's are multiplied together and the result, with a weight $\alpha_{j_1 j_2 j_3 j}$ coming from the product of the ω 's, C 's, V_C 's and U (that can be pre-computed because none of these tensors depend on $|\Psi\rangle$), is added together to give rise to tensor T .

added together to give rise to tensor T . A SVD of the tensor $T_{j_t j_{t'}}$ ensues (equation (10)), giving rise to tensors R and S and the updated tensor $\eta^{[r]}$. The coupled basis $|jmt\rangle$ is reorganized back into product basis by contracting R and S with $(V_{X_i})^{-1}$ (shown in figure 4(B) for R only). Once again, the contraction is effected by multiplying $(V_{X_i})^{-1}$ with R (or S) for each value of j . Finally, contract \tilde{R} (and \tilde{S}) with $(\eta^{[r-1]})^{-1}$ (and $(\eta^{[r+1]})^{-1}$) to obtain the updated tensors $X^{[r]}$ and $X^{[r+1]}$.

Note that all matrix multiplications and SVDs now involve smaller tensors, and only tensors X and η of the SU(2) MPS need to be updated. This results in a substantial reduction in computational space and time and thus an increase in performance. For instance, the SVD of Θ in figure 3 of [11], where $|\Theta| \approx (2s + 1)^2 |\lambda|^2$ is now replaced with the SVD of $\Omega_{j_t j_{t'}}$

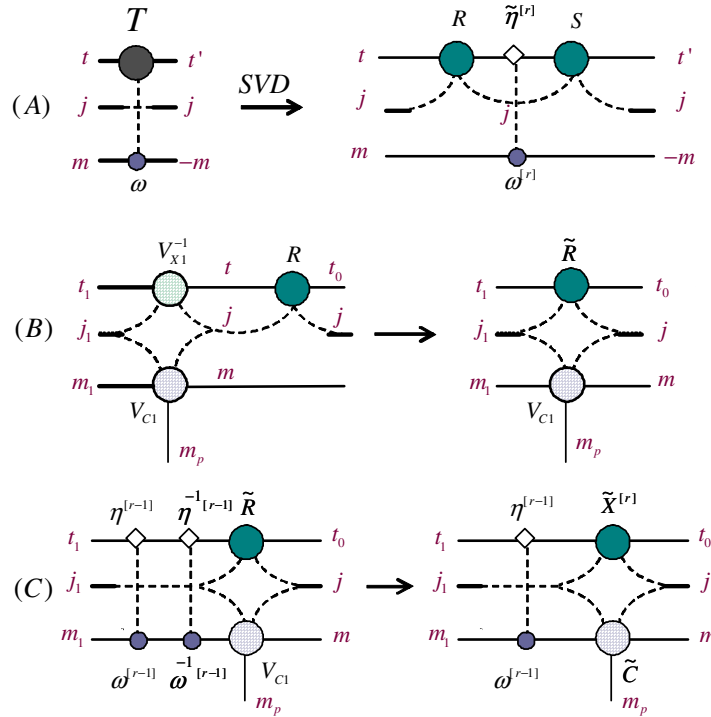


Figure 4. The remaining steps of the TEBD algorithm. (A) The tensor T is singular value decomposed into R and S and an updated $\eta^{[r]}$. In (B) and (C), the tensors R and S are reorganized into the updated tensors $X^{[r]}$ and $X^{[r+1]}$.

(see figure 3) for each value of j , where $|\Omega_{jtjt'}| = (\sum_{j' \geq j-2s}^{j+2s} d_{j'})^2$. The cost $c_{\text{svd}}(A)$ of computing the SVD of a matrix A grows roughly as $|A|^{3/2}$ and is the most expensive manipulation of the TEBD algorithm. We obtain the following comparative costs:

$$c_{\text{svd}}(\Theta) \sim \left((2s+1) \sum_j [(2j+1)d_j] \right)^3, \quad (26)$$

$$c_{\text{svd}}(\Omega) \sim \sum_j \left(\sum_{j' \geq j-2s}^{j+2s} d_{j'} \right)^3. \quad (27)$$

6. Example

For illustrative purposes, we consider a quantum spin chain with $s = 1/2$ and with the Hamiltonian

$$H = \sum_r (S_x^{[r]} S_x^{[r+1]} + S_y^{[r]} S_y^{[r+1]} + S_z^{[r]} S_z^{[r+1]}), \quad (28)$$

that is, the spin-1/2 antiferromagnetic Heisenberg model, which is $SU(2)$ invariant and quantum critical at zero temperature. Representing the ground state of this model with a MPS is

challenging, because both the critical character of the system and the presence of the SU(2) symmetry contribute to its entanglement. As a result, compared to a gapped system or a system with smaller symmetry, an accurate MPS approximation to the ground state of (28) requires a larger value of χ . We have computed a SU(2) MPS approximation to the ground state of H , in the limit $n \rightarrow \infty$ of an infinite chain, by simulating imaginary-time evolution [11] starting from a state made of nearest-neighbor singlets $(|_{1/2}^{[r]}|_{-1/2}^{[r+1]} - |_{-1/2}^{[r]}|_{1/2}^{[r+1]})/\sqrt{2}$. With the constraint $\sum_j d_j = 600$, we have obtained that the following irreps j , with degeneracies d_j , contribute to the odd and even bipartitions⁴ of the resulting state:

j	0	1	2	3	4	j	$\frac{1}{2}$	$\frac{3}{2}$	$\frac{5}{2}$	$\frac{7}{2}$	$\frac{9}{2}$
d_j	117	247	176	55	5	d_j	220	242	115	22	1

Equations (24)–(27) show substantial computational gains,

$$\frac{|\Gamma|}{|X|} \approx \frac{10^7}{2 \times 10^5} = 50, \quad \frac{c_{\text{svd}}(\Theta)}{c_{\text{svd}}(\Omega)} \approx \frac{9 \times 10^{10}}{3 \times 10^8} = 300; \quad (29)$$

that is, with a regular MPS, storing the same state would require about 50 times more computer memory, whereas performing each SVD would be about 300 times slower.

We have computed the two-point correlators⁵ $C_2^\Delta(r) \equiv \langle S_z^{[0]} S_z^{[r]} \rangle$, and $C_2^\nabla(r) \equiv \langle S_z^{[1]} S_z^{[r+1]} \rangle$, and the average $C_2(r) \equiv (C_2^\Delta(r) + C_2^\nabla(r))/2$. For small r , they read as follows:

r	$C_2^\Delta(r)$	$C_2^\nabla(r)$	$C_2(r)$
1	−0.148 002 247 48	−0.147 429 206 05	−0.147 715 726[7]
2	0.060 679 769 82	0.060 679 769 91	0.060 679 769[9]
3	−0.050 378 609 08	−0.050 118 645 81	−0.050 248 627[4]
4	0.034 652 776 14	0.034 652 776 45	0.034 652 776[3]
5	−0.030 978 529 6	−0.030 802 190 1	−0.030 890 36[0]
6	0.024 446 726	0.024 446 726	0.024 446 7[26]
7	−0.022 565 932	−0.022 430 482	−0.022 498 2[1]

where, for $C_2(r)$, the square brackets show the first digits that differ from the exact solution ([12] and reference therein), from which we recover e.g. nine significant digits for $r = 1$. An expression for the correlator $C_2(r)$ is also known for large r ⁶. There, for $r \approx 4000$, 10 000 and 13 000, our results approximate the asymptotic solution with errors of 1, 5 and 10%, respectively, see figure 5. In comparison, with a regular MPS and similar computational resources, we lose three digits of precision for $r = 1$, whereas a 10% error is already achieved for $r \approx 500$ instead of $r \approx 13 000$.

It is important to note that the appearance of two different correlators $C_2^\Delta(r)$ and $C_2^\nabla(r)$ is an artifact of the present algorithm and that the average $C_2(r) \equiv (C_2^\Delta(r) + C_2^\nabla(r))/2$ is a legitimate procedure to eliminate it, since it corresponds to taking as the ground state of the infinite chain an equally weighted superposition of the MPS and its translation by one site. It is also of interest to note the effect that a finite χ in the MPS has on symmetries. If the infinite Heisenberg chain is

⁴ For semi-integer spins, e.g. $s = \frac{1}{2}$, the CSBD of equation (12) for a partition $[1 \dots r] : [r+1 \dots n]$ of the chain has only integer (semi-integer) values of j when r is even (odd).

⁵ $C_2^w(1)$ ($w = \Delta, \nabla$) are computed by contracting a small tensor network involving the tensors (η, ω) and (X, \tilde{C}) for two contiguous sites. For $r > 1$, $C_2^w(r)$ is computed in the same way, but first we simulate $r - 1$ (SU(2) invariant) swap gates that bring the two relevant sites together.

⁶ We use $c = 1.05$ in equation (5.25) of Lukganov and Terras [13].

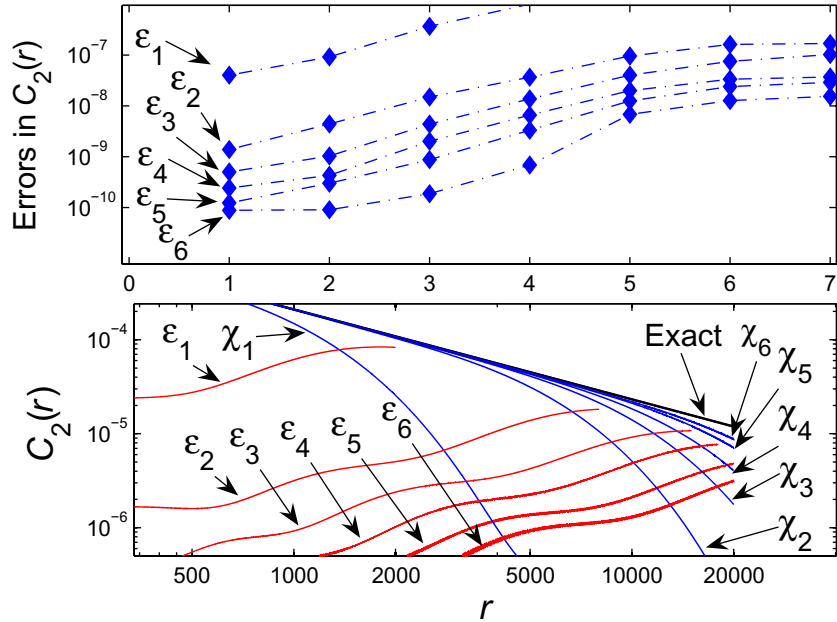


Figure 5. Top: errors in the two-point correlator $C_2(r)$ for $1 \leq r \leq 7$ when using SU(2) MPSs of different sizes $\chi_i \in \{350, 700, 1110, 1450, 1800, 2200\}$. Here, χ is roughly $|\lambda|$ in equation (24), that is, the rank of an equivalent (regular) MPS. The lowest line, $\chi_6 = 2200$, shows the errors in the data presented in the table. Bottom: numerical results for $C_2(r)$ for up to $r = 20\,000$ sites, for different sizes χ_i , together with corresponding errors ϵ_i .

addressed with a standard MPS, translation invariance is largely preserved but SU(2) invariance is clearly broken. If a SU(2) MPS is used instead, SU(2) invariance is exactly preserved but translation invariance is clearly broken. The extent to which either symmetry is broken decreases with increasing χ .

7. Final remarks

The above test with a critical spin-1/2 chain unambiguously demonstrates the superiority of the SU(2) MPS and TEBD with respect to their non-symmetric versions. Promisingly, these techniques can now be used to address systems that remain otherwise largely inaccessible to numerical analysis due to the large dimension of the local Hilbert space. These systems include a chain made of large spins, say $s = 4$, or a spin ladder with several legs. We regard the latter as a chain with several spins per site, where each site decomposes into SU(2) irreps as in equation (2) [9].

In addition, the SU(2) MPS is not restricted to the representation of SU(2) singlets. On the one hand, it can be used to represent *any* SU(2) invariant mixed state ρ of the chain, which decomposes as (see equation (2))

$$\rho = \bigoplus_j \rho_j \otimes I_{2j+1}. \quad (30)$$

This is achieved by attaching, to the end of the chain, an environment E that duplicates the subspace V of the chain on which ρ is supported and by considering a singlet purification $|\Psi_\rho^{VE}\rangle$, where $\rho = \text{tr}_E |\Psi_\rho^{VE}\rangle \langle \Psi_\rho^{VE}|$. We first build a SU(2) MPS for the purification and then trace out E . The resulting structure is a matrix product representation that retains the advantages of the SU(2) MPS. In particular, note that when ρ corresponds to a single irrep j ,

$$\rho = \frac{1}{2j+1} \sum_{m=-j}^m |_{jm}^{[V]} \rangle \langle_{jm}^{[V]}|, \quad (31)$$

the environment is a site with a spin j , and the chain together with the environment is just an extended spin chain, with the purification being of the form

$$|\Psi_\rho\rangle = \frac{1}{\sqrt{2j+1}} \sum_{m=-j}^j |_{jm}^{[V]} \rangle |_{jm}^{[E]} \rangle. \quad (32)$$

On the other hand, the SU(2) MPS can also be modified to represent any pure state $|_{jm}^{[V]} \rangle$ of the chain with well defined j and m . To achieve this, we first consider a mixed state ρ as in equation (31), that is, a symmetrization of $|_{jm}^{[V]} \rangle$, and then consider a purification $|\Psi_\rho\rangle$ for ρ as in equation (31), for which we can build a SU(2) MPS. Finally, we recall that $|_{jm}^{[V]} \rangle = \langle_{jm}^{[E]} | \Psi_\rho \rangle$, which leads to a simple, SU(2) MPS-like representation for $|_{jm}^{[V]} \rangle$ in terms of the SU(2) MPS for the purification $|\Psi_\rho\rangle$. The time-evolution simulation techniques described in this paper can be applied to the above generalized representations.

After nearly completing the original manuscript, we became aware of the related results obtained by I McCulloch, which were derived independently in the context of DMRG [14].

Acknowledgments

The authors thank S Lukyanov for helpful communications. GV acknowledges support from the Australian Research Council through a Federation Fellowship.

References

- [1] Fannes M, Nachtergaele B and Werner R F 1992 *Commun. Math. Phys.* **144** 3 443–590
Östlund S and Rommer S 1995 *Phys. Rev. Lett.* **75** 19 3537
- [2] Perez-Garcia D, Verstraete F, Wolf M M and Cirac J I 2007 *Quantum Inf. Comput.* **7** 401 (arXiv:quant-ph/0608197)
- [3] White S R 1992 *Phys. Rev. Lett.* **69** 2863
White S R 1993 *Phys. Rev. B* **48** 10345
Schollwoeck U 2005 *Rev. Mod. Phys.* **77** 259 (arXiv:cond-mat/0409292)
- [4] Vidal G 2003 *Phys. Rev. Lett.* **91** 147902 (arXiv:quant-ph/0301063)
Vidal G 2004 *Phys. Rev. Lett.* **93** 040502 (arXiv:quant-ph/0310089)
- [5] White S R and Feiguin A E 2004 *Phys. Rev. Lett.* **93** 076401
Verstraete F *et al* 2004 *Phys. Rev. Lett.* **93** 227205
- [6] Sierra G and Nishino T 1997 *Nucl. Phys.* **456** 505
Ramasesha S *et al* 1996 *Phys. Rev. B* **54** 7598
Tatsuaki W 2000 *Phys. Rev. E* **61** 3199
Rommer S and Ostlund S 1997 *Phys. Rev. B* **55** 2164

- McCulloch I P and Gulácsi M 2002 *Europhys. Lett.* **57** 852
Bergkvist S *et al* 2006 arXiv:cond-mat/0606265
Pittel S and Sandulescu N 2006 *Phys. Rev. C* **73** 014301
- [7] Daley A J *et al* 2004 *J. Stat. Mech.* P04005 (arXiv:cond-mat/0403313)
Daley A J *et al* 2005 *Phys. Rev. A* **72** 043618
Danshita I *et al* 2007 *Phys. Rev. A* **76** 043606
Zi Cai *et al* 2009 arXiv:0911.3457
Muth D *et al* 2009 arXiv:0910.1749
Mishmash R V and Carr L D 2009 *Math. Comput. Sim.* in press (arXiv:0810.2593)
- [8] Cornwell J F (ed) 1997 *Group Theory in Physics* (New York: Academic)
- [9] Singh S, Pfeifer R N C and Vidal G 2009 arXiv:0907.2994
- [10] http://en.wikipedia.org/wiki/Clebsch-Gordan_coefficients
- [11] Vidal G 2007 *Phys. Rev. Lett.* **98** 070201 (arXiv:cond-mat/0605597)
- [12] Sato J, Shiroishi M and Takahashi M 2005 *Nucl. Phys. B* **729** 441
- [13] Lukyanov S and Terras V 2003 *Nucl. Phys. B* **654** 323–56 (arXiv:hep-th/0206093)
- [14] McCulloch I 2007 *J. Stat. Mech.* P10014

Tensor networks and symmetries: Theoretical formalism

In this chapter we develop a generic theoretical formalism to incorporate a symmetry into tensor network algorithms. We consider a wide class of symmetries that are described by a compact and reducible group \mathcal{G} that is multiplicity free, that is, the tensor product of two charges of the group does not contain multiple copies of a charge. Our strategy revolves around tensors that are invariant under the action of the symmetry. As a result, we formulate a framework of symmetric tensors.

A symmetric tensor transforms covariantly (or remains invariant) under the action of the symmetry. In a basis labeled by the symmetry charges, the tensor decomposes into a set of *degeneracy tensors* and *structural tensors*. While the degeneracy tensors contain the degrees of freedom, the components of the structural tensors are generalizations of the coupling coefficients of the group, and are determined completely by the symmetry. Moreover, any symmetry preserving manipulation of the tensor can be performed in parts. For instance, a permutation of the indices of a symmetric tensor breaks into the permutation of the corresponding degeneracy indices and the permutation of the corresponding structural indices. Therefore, this *canonical decomposition* of a symmetric tensor allows for both a compact description of the tensor and a computational speedup in numerical manipulations of it.

We also point out a numerical connection to the formalism of *spin networks* (Major, 1999;

Penrose, 1971). A spin network is a mathematical object that appears, for example, in Loop Quantum Gravity (Rovelli, 1998), where it is used (Rovelli and Smolin, 1995) to facilitate a description of quantum spacetime. In our formalism, a tensor network made of symmetric tensors decomposes into a linear superposition of spin networks. Also, manipulating a symmetric tensor network requires *evaluating* a spin network. Thus, our work highlights the importance of spin networks in the context of tensor network algorithms, thus setting the stage for cross-fertilization between these two areas of research.

Tensor network decompositions in the presence of a global symmetry

Sukhwinder Singh, Robert N. C. Pfeifer, and Guifré Vidal

University of Queensland, Department of Physics, Brisbane, Queensland 4072, Australia

(Received 20 July 2009; revised manuscript received 11 October 2010; published 8 November 2010)

Tensor network decompositions offer an efficient description of certain many-body states of a lattice system and are the basis of a wealth of numerical simulation algorithms. We discuss how to incorporate a global symmetry, given by a compact, completely reducible group \mathcal{G} , in tensor network decompositions and algorithms. This is achieved by considering tensors that are invariant under the action of the group \mathcal{G} . Each symmetric tensor decomposes into two types of tensors: degeneracy tensors, containing all the degrees of freedom, and structural tensors, which only depend on the symmetry group. In numerical calculations, the use of symmetric tensors ensures the preservation of the symmetry, allows selection of a specific symmetry sector, and significantly reduces computational costs. On the other hand, the resulting tensor network can be interpreted as a superposition of exponentially many spin networks. Spin networks are used extensively in loop quantum gravity, where they represent states of quantum geometry. Our work highlights their importance in the context of tensor network algorithms as well, thus setting the stage for cross-fertilization between these two areas of research.

DOI: [10.1103/PhysRevA.82.050301](https://doi.org/10.1103/PhysRevA.82.050301)

PACS number(s): 03.67.Hk, 03.65.Ud, 05.50.+q, 89.75.Hc

Locality and symmetry are pivotal concepts in the formulation of physical theories. In a quantum many-body system, locality implies that the dynamics are governed by a Hamiltonian H that decomposes as the sum of terms involving only a small number of particles and whose strength decays with the distance between the particles. In turn, a symmetry of the Hamiltonian H allows us to organize the kinematic space of the theory according to the irreducible representations of the symmetry group.

Both symmetry and locality can be exploited to obtain a more compact description of many-body states and to reduce computational costs in numerical simulations. In the case of symmetries, this has long been understood. Space symmetries, such as invariance under translations or rotations, as well as internal symmetries, such as particle number conservation or spin isotropy, divide the Hilbert space of the theory into sectors labeled by quantum numbers or charges. The Hamiltonian H is by definition block-diagonal in these sectors. If, for instance, the ground state is known to have zero momentum, it can be obtained by just diagonalizing the (comparatively small) zero-momentum block of H .

In recent times, the far-reaching implications of locality for our ability to describe many-body systems have also started to unfold. The local character of the Hamiltonian H limits the amount of entanglement that low-energy states may have, and in a lattice system, restrictions on entanglement can be exploited to succinctly describe these states with a tensor network (TN) decomposition. Examples of TN decompositions include matrix product states (MPS's) [1], projected entangled-pair states [2], and the multiscale entanglement renormalization ansatz (MERA) [3]. It is important to note that in a lattice made of N sites, where the Hilbert space dimension grows exponentially with N , TN decompositions often offer an efficient description (with costs that scale roughly as N). This allows for scalable simulations of quantum lattice systems, even in cases that are beyond the reach of standard Monte Carlo sampling techniques. As an example, the MERA has been recently used to investigate ground states of frustrated antiferromagnets [4].

In this article we investigate how to incorporate a global symmetry into a TN, so as to be able to simultaneously exploit both the locality and the symmetries of physical Hamiltonians to describe many-body states. Specifically, in order to represent a symmetric state that has a limited amount of entanglement, we use a TN made of symmetric tensors. This leads to an *approximate*, efficient decomposition that preserves the symmetry *exactly*. Moreover, a more compressed description is obtained by breaking each symmetric tensor into several degeneracy tensors (containing all the degrees of freedom of the original tensor) and structural tensors (completely fixed by the symmetry). This decomposition leads to a substantial reduction in computational costs and reveals a connection between TN algorithms and the formalism of spin networks [5] used in loop quantum gravity [6].

In the case of an MPS, global symmetries have already been studied by many authors (see, e.g., [1,7]) in the context of both one-dimensional quantum systems and two-dimensional (2D) classical systems. An MPS is a trivalent TN (i.e., each tensor has at most three indices) and symmetries are comparatively easy to characterize. The present analysis applies to the more challenging case of a generic TN decomposition (where tensors typically have more than three indices).

We consider a lattice \mathcal{L} made of N sites, where each site is described by a complex vector space \mathbb{V} of finite dimension d . A pure state $|\Psi\rangle \in \mathbb{V}^{\otimes N}$ of the lattice can be expanded as

$$|\Psi\rangle = \sum_{i_1, i_2, \dots, i_N=1}^d (\Psi)_{i_1 i_2 \dots i_N} |i_1, i_2, \dots, i_N\rangle, \quad (1)$$

where $|i_s\rangle$ denotes a basis of \mathbb{V} for site $s \in \mathcal{L}$. For our purposes, a TN decomposition for $|\Psi\rangle$ consists of a set of tensors $T^{(v)}$ and a network pattern or graph characterized by a set of vertices and a set of directed edges. Each tensor $T^{(v)}$ sits at a vertex v of the graph, and is connected with neighboring tensors by bond indices according to the edges of the graph. The graph also contains N open edges, corresponding to the N physical indices i_1, i_2, \dots, i_N . The d^N coefficients $(\Psi)_{i_1 i_2 \dots i_N}$

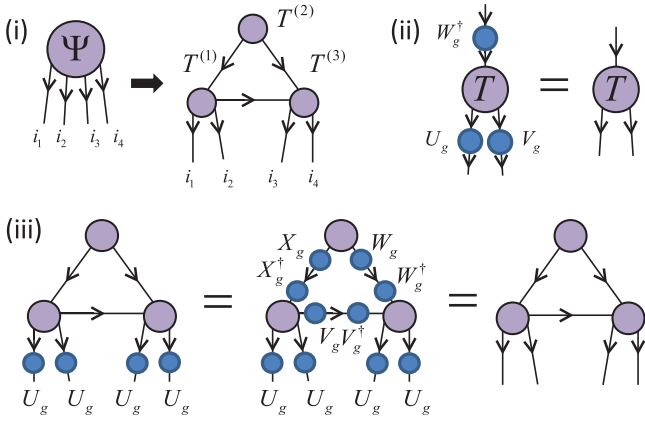


FIG. 1. (Color online) (i) Four-site state $|\Psi\rangle$ expressed in terms of a tensor network made of three tensors connected according to a directed graph. (ii) Invariance of tensor T in Eq. (7). (iii) Invariance of a tensor network of symmetric tensors, Eq. (3).

are expressed as [Fig. 1(i)]

$$(\Psi)_{i_1 i_2 \dots i_N} = \text{tTr} \left(\bigotimes_v T^{(v)} \right), \quad (2)$$

namely, as the tensor product of the tensors $T^{(v)}$ on all the vertices v , where the tensor trace tTr contracts all bond indices, so that only the physical indices i_1, i_2, \dots, i_N remain on the right-hand side of Eq. (2).

We also introduce a compact, completely reducible group \mathcal{G} . This includes finite groups as well as Lie groups such as $O(n)$, $SO(n)$, $U(n)$, and $SU(n)$. Let $U : \mathcal{G} \rightarrow L(\mathbb{V})$ be a unitary matrix representation of \mathcal{G} on the space \mathbb{V} of one site, so that for each $g \in \mathcal{G}$, $U_g : \mathbb{V} \rightarrow \mathbb{V}$ denotes a unitary matrix and $U_{g_1 g_2} = U_{g_1} U_{g_2}$. Here we are interested in states $|\Psi\rangle$ that are invariant under transformations of the form $U_g^{\otimes N}$ [8],

$$(U_g)^{\otimes N} |\Psi\rangle = |\Psi\rangle, \quad \forall g \in \mathcal{G}. \quad (3)$$

The space \mathbb{V} of one site decomposes as the direct sum of irreducible representations (irreps) of \mathcal{G} ,

$$\mathbb{V} \cong \bigoplus_a d_a \mathbb{V}^a \cong \bigoplus_a (\mathbb{D}^a \otimes \mathbb{V}^a), \quad (4)$$

where \mathbb{V}^a denotes the irrep labeled with charge a and d_a is the number of times \mathbb{V}^a appears in \mathbb{V} . We denote by $a = 0$ the charge corresponding to the trivial irrep, so that $\mathbb{V}^0 \cong \mathbb{C}$ and $U_g^a = 1$. In Eq. (4) we have also rewritten the same decomposition in terms of a d_a -dimensional degeneracy space \mathbb{D}^a . We choose a local basis $|i\rangle = |a, \alpha_a, m_a\rangle$ in \mathbb{V} , where α_a labels states within the degeneracy space \mathbb{D}^a (i.e., $\alpha_a = 1, \dots, d_a$) and m_a labels states within irrep \mathbb{V}^a . In this basis, U_g reads

$$U_g = \bigoplus_a (\mathbb{I}^a \otimes U_g^a). \quad (5)$$

Recall that an operator $M : \mathbb{V} \rightarrow \mathbb{V}$ that commutes with the group, $[M, U_g] = 0$ for all $g \in \mathcal{G}$, decomposes as [9]

$$M = \bigoplus_a (M^a \otimes \tilde{\mathbb{I}}^a) \quad (6)$$

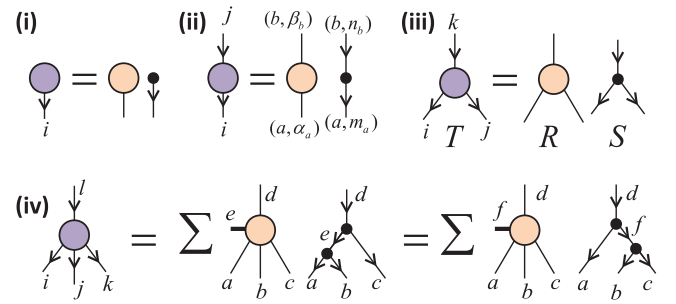


FIG. 2. (Color online) Decomposition of tensors with one to four indices. The sums in (iv) run over the intermediate indices (e, ϵ_e, q_e) and (f, ζ_f, r_f) in Eqs. (11) and (12).

(Schur's lemma). Our goal is to characterize a TN made of symmetric tensors, namely, tensors that are invariant under the simultaneous action of \mathcal{G} on all their indices. A symmetric tensor T with, for example, two outgoing indices i and j and one incoming index k , fulfills [Fig. 1(ii)]

$$\sum_{ijk} (U_g)_{ii'} (V_g)_{j'j} (T)_{ijk} (W_g^\dagger)_{kk'} = (T)_{i'j'k'}, \quad \forall g \in \mathcal{G}, \quad (7)$$

where U , V , and W denote unitary matrix representations of \mathcal{G} . Clearly, this choice guarantees that Eq. (3) is satisfied [Fig. 1(iii)]. Standard group representation theory results [9] imply that each symmetric tensor can be further decomposed in such a way that the degrees of freedom that are not fixed by the symmetry can be isolated (Fig. 2). Next we discuss the cases of tensors with a small number of indices. Recall that an index i of a tensor is associated with a vector space that decomposes as in Eq. (4); therefore, we can write $i = (a, \alpha_a, m_a)$, $j = (b, \beta_b, n_b)$, $k = (c, \gamma_c, o_c)$, and so on.

One leg. A tensor T with only one index i is invariant only if \mathcal{G} acts on it trivially, so the only relevant irrep is $a = 0$, and the index $i = \alpha_0$ labels states within the degeneracy space \mathbb{V}^0 .

Two legs. Schur's lemma [9] establishes that a symmetric tensor T with one outgoing index i and one incoming index j decomposes as [cf. Eq. (6)]

$$(T)_{ij} = (P^{ab})_{\alpha_a \beta_b} (Q^{ab})_{m_a n_b}, \quad Q^{ab} = \delta_{ab} \delta_{m_a n_b}. \quad (8)$$

Thus, for fixed values of the charges a and b , $(T)_{ij}$ breaks into a degeneracy tensor P^{ab} (where only $a = b$ is relevant) and another tensor Q^{ab} . P^{ab} contains all the degrees of freedom of T that are not fixed by the symmetry, whereas Q^{ab} is completely determined by \mathcal{G} . Another combination of outgoing and incoming indices, for example, two incoming indices, leads to a different form for tensor Q^{ab} .

Three legs. The tensor product of two irreps with charges a and b can be decomposed as the direct sum of irreps,

$$\mathbb{V}^a \otimes \mathbb{V}^b \cong \bigoplus_c N_{ab}^c \mathbb{V}^c, \quad (9)$$

where N_{ab}^c denotes the number of copies of \mathbb{V}^c that appear in the tensor product. For notational simplicity, from now on we assume that \mathcal{G} is multiplicity-free [10], that is, $N_{ab}^c \leq 1$, and denote by $(Q^{abc})_{m_a n_b o_c}$ the change of basis between the product basis $|a, m_a\rangle \otimes |b, n_b\rangle$ and the coupled basis $|c, o_c\rangle$. The Wigner-Eckart theorem states that a symmetric tensor T

with, for example, two outgoing indices i, j and one incoming index k , decomposes as

$$(T)_{ijk} = (P^{abc})_{\alpha_a \beta_b \gamma_c} (Q^{abc})_{m_a n_b o_c}. \quad (10)$$

As before, for fixed values of the charges a, b , and c , $(T)_{ijk}$ factorizes into degeneracy tensors P^{abc} with all the degrees of freedom and structural tensors Q^{abc} (the Clebsch-Gordan coefficients) completely determined by the group \mathcal{G} . An analogous decomposition with different Q^{abc} holds for other combinations of incoming and outgoing indices.

Four legs. The tensor product of three irreps $\mathbb{V}^a \otimes \mathbb{V}^b \otimes \mathbb{V}^c$ may contain several copies of an irrep \mathbb{V}^d . Let e be the charge that results from fusing a and b , $\mathbb{V}^a \otimes \mathbb{V}^b = \bigoplus_e N_{ab}^e \mathbb{V}^e$. We can use the values of e for which $N_{ab}^e N_{ec}^d \neq 0$ (i.e., such that a and b fuse to e and e and c fuse to d) to label the different copies of \mathbb{V}^d that appear in $\mathbb{V}^a \otimes \mathbb{V}^b \otimes \mathbb{V}^c$. Let $(Q_e^{abcd})_{m_a n_b o_c p_d q_e}$ denote the change of basis between the product basis $|am_a\rangle \otimes |bn_b\rangle \otimes |co_c\rangle$ and the coupled basis $|dp_d; e\rangle$ obtained by fusing to the intermediate basis $|eq_e\rangle \in \mathbb{V}^e$. Then a symmetric tensor T with three outgoing indices i, j , and k and one incoming index $l = (d, \delta_d, p_d)$ decomposes as

$$(T)_{ijkl} = \sum_{e, \epsilon_e, q_e} (P_e^{abcd})_{\alpha_a \beta_b \gamma_c \delta_d \epsilon_e} (Q_e^{abcd})_{m_a n_b o_c p_d q_e}, \quad (11)$$

where the sum is over all relevant values of the intermediate indices (e, ϵ_e, q_e) . Alternatively, T can be decomposed as

$$(T)_{ijkl} = \sum_{f, \zeta_f, r_f} (\tilde{P}_f^{abcd})_{\alpha_a \beta_b \gamma_c \delta_d \zeta_f} (\tilde{Q}_f^{abcd})_{m_a n_b o_c p_d r_f}, \quad (12)$$

where $(\tilde{Q}_f^{abcd})_{m_a n_b o_c p_d}$ denotes the change of basis to another coupled basis $|dp_d; f\rangle$ of \mathbb{V}^d obtained by fusing first b and c into f , and then a and f into d , involving a different set of intermediate indices (f, ζ_f, r_f) . The two coupled bases are related by a unitary transformation given by the 6-index tensor F [e.g., the 6- j symbols for $\mathcal{G} = \text{SU}(2)$] such that

$$\tilde{Q}_f^{abcd} = \sum_e (F_d^{abc})_f^e Q_e^{abcd}. \quad (13)$$

Since Eqs. (11) and (12) represent the same tensor T , the degeneracy tensors P and \tilde{P} are related by

$$\tilde{P}_f^{abcd} = \sum_e (F_d^{abc*})_f^e P_e^{abcd}. \quad (14)$$

More generally, a symmetric tensor T with t indices $i_s = (a_s, \alpha_a, m_a)$, where $s = 1, \dots, t$, decomposes as

$$(T)_{i_1 i_2 \dots i_t} = \sum (P_{e_1 \dots e_{t'}}^{a_1 \dots a_t})_{\alpha_{a_1} \dots \alpha_{a_t}, \alpha_{e_1} \dots \alpha_{e_{t'}}} \times (Q_{e_1 \dots e_{t'}}^{a_1 \dots a_t})_{m_{a_1} \dots m_{a_t}, m_{e_1} \dots m_{e_{t'}}}, \quad (15)$$

where the sum is over the intermediate indices $(e_k, \alpha_{e_k}, m_{e_k}), k = 1, \dots, t'$. The degeneracy tensors $P_{e_1 \dots e_{t'}}^{a_1 \dots a_t}$ contain all the degrees of freedom of T , whereas the structural tensors $Q_{e_1 \dots e_{t'}}^{a_1 \dots a_t}$ are completely determined by the symmetry. Here $e_1, e_2, \dots, e_{t'}$ are intermediate charges that decorate the inner branches of a trivalent tree used to label a basis in the space of intertwining operators between the tensor products of incoming and outgoing irreps. A different choice of tree will produce different sets of tensors \tilde{P} and \tilde{Q} , related to P and Q by F-moves [11].

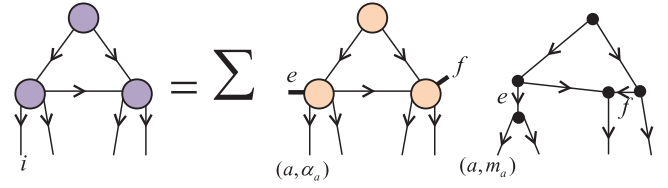


FIG. 3. (Color online) A TN for a symmetric state $|\Psi\rangle \in \mathbb{V}^{\otimes N}$ of lattice \mathcal{L} (Fig. 1) is expressed as a linear superposition of spin networks. The sum runs over the intermediate indices that carry charges e and f (shown explicitly) as well as all indices shared by two tensors.

We can now investigate how the TN decomposes if we write each of its tensors T in the (P, Q) form of Eq. (15) (see Fig. 3). For any fixed value of all the charges, the whole TN factorizes into two terms. The first one is a TN of degeneracy tensors. The second one is a directed graph with edges labeled by irreps of \mathcal{G} and vertices labeled by intertwining operators. This is nothing other than a spin network [5], a well-known object in mathematical physics and, especially, in loop quantum gravity [6], where it is used to describe states of quantum geometry. Accordingly, a symmetric TN for the state $|\Psi\rangle \in \mathbb{V}^{\otimes N}$ of a lattice \mathcal{L} of N sites can be regarded as a linear superposition of spin networks with N open edges. The number of spin networks in the linear superposition grows exponentially with the size of the TN. The expansion coefficients are given by the degeneracy tensors.

Computationally, the present characterization of a symmetric TN is of interest for several reasons. First of all, it allows us to describe a state $|\Psi\rangle^{\otimes N}$ with specific quantum numbers, which are preserved exactly during approximate numerical simulations. Let us consider as an example the group $U(1)$, with charge n corresponding to particle number ($n = 0, \pm 1, \pm 2, \dots$), and the group $SU(2)$, with charge j corresponding to the spin ($j = 0, 1/2, 1, 3/2, \dots$). The symmetric TN can be used to describe a state with, for example, zero particles ($n = 0$) and zero spin ($j = 0$), respectively or, more generally, covariant states with any value of n and j [8].

Second, the (P, Q) -decomposition (15) concentrates all the degrees of freedom of a symmetric tensor T in the degeneracy tensors P , producing a more compact description. For instance, for the $U(1)$ and $SU(2)$ groups, an approximation of the ground state of the antiferromagnetic Heisenberg spin- $\frac{1}{2}$ chain with a MERA of bond dimension $\chi = 21$ requires five and thirty-five times fewer parameters than with nonsymmetric tensors, respectively [12, 13].

In addition, the (P, Q) -decomposition (15) lowers the cost of simulations significantly. Consider the multiplication of two tensors (Fig. 4) that is central to most TN algorithms. Cost reductions come from two fronts:

(i) *Block-sparse matrices.* The most costly step in multiplying two tensors T' and T'' consists of multiplying two matrices M' and M'' obtained from T' and T'' . These matrices are of the form of Eq. (6), and therefore their multiplication can be done blockwise:

$$M = M' M'' = \bigoplus_a [(M'^a M''^a) \otimes \tilde{1}^a]. \quad (16)$$

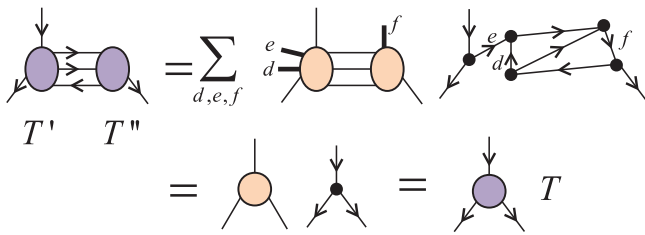


FIG. 4. (Color online) Product of two symmetric tensors. Only the intermediate charges d , e , and f are explicitly shown. Additional sums apply to all indices shared by two tensors. The computation involves evaluating spin networks.

(ii) *Precomputation.* Given a (P, Q) -decomposition of tensor T , another (\tilde{P}, \tilde{Q}) -decomposition (as required, e.g., to obtain matrices M' and M'') involves a linear map Γ :

$$\tilde{P} = \Gamma(P). \quad (17)$$

This map Γ , of which Eq. (14) is an example, is completely determined by the symmetry. In those TN algorithms that proceed by repeating a sequence of manipulations, map Γ

can be computed once and stored in memory for repeated usage.

A more detailed explanation of algorithmic details, as well as practical examples of the gains obtained using invariant tensors, is presented in Refs. [12] and [13] for the groups $U(1)$ and $SU(2)$, respectively. Reference [4] exploited the $U(1)$ symmetry in a 2D MERA calculation that involved tensors with up to twelve indices.

Finally, the connection between symmetric TNs and spin networks allows us to import into the context of TN algorithm techniques developed to evaluate spin networks in loop quantum gravity. Such techniques can be used, for example, to compute the linear map Γ of Eq. (17). Conversely, TN algorithms may also prove useful in loop quantum gravity, since they allow the efficient manipulation of superpositions of an exponentially large number of spin networks, for example.

We thank Ian McCulloch for continued discussions. Support from the Australian Research Council (APA, FF0668731, DP0878830) is acknowledged.

-
- [1] S. Ostlund and S. Rommer, *Phys. Rev. Lett.* **75**, 3537 (1995); M. Fannes, B. Nachtergaele, and R. Werner, *Commun. Math. Phys.* **144**, 443 (1992).
- [2] F. Verstraete and J. I. Cirac, e-print [arXiv:cond-mat/0407066v1](https://arxiv.org/abs/cond-mat/0407066v1); G. Sierra and M. A. Martin-Delgado, e-print [arXiv:cond-mat/9811170v3](https://arxiv.org/abs/cond-mat/9811170v3).
- [3] G. Vidal, *Phys. Rev. Lett.* **99**, 220405 (2007); **101**, 110501 (2008).
- [4] G. Evenbly and G. Vidal, *Phys. Rev. Lett.* **104**, 187203 (2010).
- [5] R. Penrose, *Angular Momentum: An Approach to Combinatorial Space-time*, 1971 [<http://math.ucr.edu/home/baez/penrose/>].
- [6] C. Rovelli and L. Smolin, *Phys. Rev. D* **52**, 5743 (1995); C. Rovelli, *Living Rev. Relativity* **11** (2008) [<http://www.livingreviews.org/lrr-2008-5>].
- [7] S. R. White, *Phys. Rev. Lett.* **69**, 2863 (1992); S. Ostlund and S. Rommer, *ibid.* **75**, 3537 (1995); G. Sierra and T. Nishino, *Nucl. Phys. B* **495**, 505 (1997); I. McCulloch and M. Gulacsı, *Europhys. Lett.* **57**, 852 (2002); I. McCulloch, *J. Stat. Mech.* (2007) P10014; S. Singh, H.-Q. Zhou, and G. Vidal, *New J. Phys.* **12**, 033029 (2010); D. Perez-Garcia *et al.*, *Phys. Rev. Lett.* **100**, 167202 (2008); M. Sanz *et al.*, *Phys. Rev. A* **79**, 042308 (2009).
- [8] A set of states $|\Psi_t\rangle$ that transform covariantly, $(U_g)^{\otimes N}|\Psi_t\rangle = \sum_{t'} (W_g)_{tt'}|\Psi_{t'}\rangle$, where W is a unitary representation of \mathcal{G} , can be represented by an invariant pure state $|\Phi\rangle \propto \sum_t |\Psi_t\rangle|t\rangle$ of lattice \mathcal{L} and one additional site on which the group acts with W_g^\dagger .
- [9] J. F. Cornwell, *Group Theory in Physics* (Academic, New York, 1997).
- [10] In non-multiplicity-free groups, such as $SU(3)$, where N_{ab}^c might be larger than 1, the coupled basis $|c, o_c, \mu\rangle$ and tensor S_{μ}^{abc} must include an extra index $\mu = 1, \dots, N_{ab}^c$. See, for example, R. N. C. Pfeifer *et al.*, *Phys. Rev. B* **82**, 115126 (2010).
- [11] When \mathcal{G} is an Abelian group, such as $U(1)$, the tensor product $\mathbb{V}^a \otimes \mathbb{V}^b$ of two irreps only gives rise to one irrep \mathbb{V}^c , so that no intermediate charges e_1, e_2, \dots, e_r need to be specified in Eq. (15), simplifying significantly the decomposition of symmetric tensors.
- [12] S. Singh, R. Pfeifer, and G. Vidal, e-print [arXiv:1008.4774v1](https://arxiv.org/abs/1008.4774v1).
- [13] S. Singh and G. Vidal (unpublished).

3.1 Errata

The following equations appear erroneously in the publication. They are to be corrected as follows.

The tensors P and Q that appear in Eqs.11 and 12 do not carry degeneracy indices and spin indices corresponding to the coupled charges e and f , since these indices are summed over in the description.

In Eq. 11 the components of P and Q read as $(P_e^{abcd})_{\alpha_a\beta_b\gamma_c\delta_d}$ and $(Q_e^{abcd})_{m_a n_b o_c p_d}$ respectively and the sum is only over different values of charge e . The corrected equation reads,

$$(T)_{ijkl} = \sum_e (P_e^{abcd})_{\alpha_a\beta_b\gamma_c\delta_d} (Q_e^{abcd})_{m_a n_b o_c p_d}, \quad (11)$$

In Eq. 12 the components of P and Q read as $(\tilde{P}_f^{abcd})_{\alpha_a\beta_b\gamma_c\delta_d}$ and $(\tilde{Q}_f^{abcd})_{m_a n_b o_c p_d}$ respectively and the sum is only over different values of charge f . The corrected equation reads,

$$(T)_{ijkl} = \sum_f (\tilde{P}_f^{abcd})_{\alpha_a\beta_b\gamma_c\delta_d} (\tilde{Q}_f^{abcd})_{m_a n_b o_c p_d}, \quad (12)$$

A similar correction holds for Eq. 15 which is a generalization of Eqs.11 and 12. The sum is only over different values of the intermediate charges $e_1 \dots e_{t'}$. The corrected equation reads,

$$(T)_{i_1 i_2 \dots i_t} = \sum_{e_1 \dots e_{t'}} (P_{e_1 \dots e_{t'}}^{a_1 \dots a_t})_{\alpha_{a_1} \dots \alpha_{a_{t'}}} (Q_{e_1 \dots e_{t'}}^{a_1 \dots a_t})_{m_{a_1} \dots m_{a_{t'}}}, \quad (15)$$

Implementation of Abelian symmetries

In this chapter we specialize the general formalism to the case of Abelian symmetries. Abelian symmetries appear frequently in the context of lattice models with particles (bosons or fermions) as well as those with spins. In the former, they include particle number conservation and parity conservation, whereas in the latter they appear as conservation of spin projection.

The analysis of exploiting an Abelian symmetry is made simple by the fact that the structural tensors in this case are trivial. On the other hand, an implementation of an Abelian symmetry serves to expose the practical difficulties that are encountered when incorporating symmetries into complicated tensor networks. We pay special attention to such implementation level concerns. Certain operations in the algorithm depend only on the symmetry and not on the components of the tensors involved. We exploit this fact to *precompute* the output of such operations and store their result in memory. This is particularly advantageous in an *iterative* algorithm where tensor components are updated or optimized by repeating a set of computations. The runtime cost of the iterative algorithm can be significantly reduced by reusing the precomputed results from memory. By making use of precomputation we obtained a substantial computational gain from exploiting the symmetry in our MATLAB implementation. However, this was achieved at the expense of storing potentially large amounts of precomputed data.

The discussion is conducted in the specific context of $U(1)$ symmetry associated, for

example, with conservation of particle number or of spin projection. We describe how to implement elementary tensor manipulations such as permutation and reshape of indices in a $U(1)$ symmetric way. We also present a concrete implementation of the $U(1)$ symmetry in the context of the MERA. We consider a MERA that is made of $U(1)$ symmetric tensors. Then using the $U(1)$ MERA we demonstrate the benefits of including symmetries into tensor networks.

Tensor network states and algorithms in the presence of a global U(1) symmetry

Sukhwinder Singh, Robert N. C. Pfeifer, and Guifre Vidal

Department of Physics, The University of Queensland, Brisbane QLD 4072, Australia

(Received 12 October 2010; published 15 March 2011)

Tensor network decompositions offer an efficient description of certain many-body states of a lattice system and are the basis of a wealth of numerical simulation algorithms. In a recent paper [*Phys. Rev. A* **82**, 050301 (2010)] we discussed how to incorporate a global internal symmetry, given by a compact, completely reducible group \mathcal{G} , into tensor network decompositions and algorithms. Here we specialize to the case of Abelian groups and, for concreteness, to a U(1) symmetry, associated, e.g., with particle number conservation. We consider tensor networks made of tensors that are invariant (or covariant) under the symmetry, and explain how to decompose and manipulate such tensors in order to exploit their symmetry. In numerical calculations, the use of U(1)-symmetric tensors allows selection of a specific number of particles, ensures the exact preservation of particle number, and significantly reduces computational costs. We illustrate all these points in the context of the multiscale entanglement renormalization *Ansatz*.

DOI: [10.1103/PhysRevB.83.115125](https://doi.org/10.1103/PhysRevB.83.115125)

PACS number(s): 03.65.Ud, 03.67.Hk

I. INTRODUCTION

Tensor networks are becoming increasingly popular as a tool to represent wave functions of quantum many-body systems. Their success is based on the ability to efficiently describe the ground state of a broad class of local Hamiltonians on the lattice. Tensor network states are used both as a variational *Ansatz* to numerically approximate ground states and as a theoretical framework to characterize and classify quantum phases of matter.

Examples of tensor network states for one-dimensional systems include the matrix product state^{1–3} (MPS), which results naturally from both Wilson’s numerical renormalization group⁴ and White’s density-matrix renormalization group^{5–8} (DMRG) and is also used as a basis for simulation of time evolution, e.g., with the time evolving block decimation (TEBD)^{9–11} algorithm and variations thereof, often collectively referred to as time-dependent DMRG;^{9–14} the tree tensor network¹⁵ (TTN), which follows from coarse-graining schemes where the spins are blocked hierarchically; and the multiscale entanglement renormalization *Ansatz*^{16–21} (MERA), which results from a renormalization-group procedure known as entanglement renormalization.^{16,21} For two-dimensional (2D) lattices there are generalizations of these three tensor network states, namely projected entangled pair states^{22–31} (PEPS), 2D TTN,^{32,33} and 2D MERA,^{34–40} respectively. As variational *Ansätze*, PEPS and 2D MERA are particularly interesting since they can be used to address large two-dimensional lattices, including systems of frustrated spins^{31,40} and interacting fermions,^{41–50} where Monte Carlo techniques fail due to the sign problem.

A many-body Hamiltonian \hat{H} may be invariant under certain transformations that form a group of symmetries.⁵¹ The symmetry group divides the Hilbert space of the theory into symmetry sectors labeled by quantum numbers or conserved charges. On a lattice one can distinguish between *space* symmetries, which correspond to some permutation of the sites of the lattice, and *internal* symmetries, which act on the vector space of each site. An example of space symmetry is invariance under translations by some unit cell, which leads to conservation of momentum. An example of internal symmetry

is SU(2) invariance, e.g., spin isotropy in a quantum spin model. An internal symmetry can in turn be *global*, if it transforms the space of each of the lattice sites according to the same transformation (e.g., a spin independent rotation); or *local*, if each lattice site is transformed according to a different transformation (e.g., a spin dependent rotation), as it is in the case of gauge symmetric models. A global internal SU(2) symmetry gives rise to conservation of total spin. By targeting a specific symmetry sector during a calculation, computational costs can often be significantly reduced while explicitly preserving the symmetry. It is therefore not surprising that symmetries play an important role in numerical approaches.

In Ref. 52 we described a formalism for incorporating global internal symmetries into a generic tensor network algorithm. Both Abelian and non-Abelian symmetries were considered. The purpose of this paper is to address, at a pedagogical level, the implementation of Abelian symmetries into tensor networks. We will also discuss several practical aspects of the exploitation of Abelian symmetries not covered in Ref. 52. For concreteness we will concentrate on the U(1) symmetry, but extending our results to any Abelian group is straightforward. A similar analysis of non-Abelian groups will be considered in Ref. 53.

In tensor network approaches, the exploitation of global internal symmetries has a long history, especially in the context of MPSs. Both Abelian and non-Abelian symmetries have been thoroughly incorporated into DMRG code and have been exploited to obtain computational gains.^{2,5,14,54–62} Symmetries have also been used in more recent proposals to simulate time evolution with MPSs.^{10–14,63–68}

When considering symmetries, it is important to notice that an MPS is a trivalent tensor network. That is, in an MPS each tensor has at most three indices. The Clebsch-Gordan coefficients⁵¹ (or coupling coefficients) of a symmetry group are also trivalent, and this makes incorporating the symmetry into an MPS by considering symmetric tensors particularly simple. In contrast, tensor network states with a more elaborate network of tensors, such as MERA or PEPS, consist of tensors having a larger number of indices. In this case a more general formalism is required in order to exploit the symmetry. As

explained in Ref. 52, a generic symmetric tensor can be decomposed into a *degeneracy* part, which contains all degrees of freedom not determined by symmetry, and a *structural* part, which is completely determined by symmetry and can be further decomposed as a trivalent network of Clebsch-Gordan coefficients.

The use of symmetric tensors in more complex tensor networks has also been discussed in Refs. 69,70. In particular, Ref. 69 has shown that under convenient conditions (injectivity), a PEPS that represents a symmetric state can be represented with symmetric tensors, generalizing similar results for MPSs obtained in Ref. 61. Notice that these studies are not concerned with how to decompose symmetric tensors so as to computationally protect or exploit the symmetry. On the other hand, exploitation of U(1) symmetry for computational gain in the context of PEPS was reported in Ref. 70, although no implementation details were provided. Finally, several aspects of *local* internal symmetries in tensor network algorithms have been addressed in Refs. 71–74.

The paper is organized in sections as follows. Section II contains a review of the tensor network formalism and introduces the nomenclature and diagrammatical representation of tensors used in the rest of the paper. It also describes a set \mathcal{P} of primitives for manipulating tensor networks, consisting of manipulations that involve a single tensor (permutation, fusion, and splitting of the indices of a tensor) and matrix operations (multiplication and factorization).

Section III reviews basic notions of representation theory of the Abelian group U(1). The action of the group is analyzed first on a single vector space, where U(1)-symmetric states and U(1)-invariant operators are decomposed in a compact, canonical manner. This canonical form allows us to identify the degrees of freedom which are not constrained by the symmetry. The action of the group is then also analyzed on the tensor product of two vector spaces and, finally, on the tensor product of a finite number of vector spaces.

Section IV explains how to incorporate the U(1) symmetry into a generic tensor network algorithm, by considering U(1)-invariant tensors in a canonical form, and by adapting the set \mathcal{P} of primitives for manipulating tensor networks. These include the multiplication of two U(1)-invariant matrices in their canonical form, which is at the core of the computational savings obtained by exploiting the symmetry in tensor network algorithms.

Section V illustrates the practical exploitation of the U(1) symmetry in a tensor network algorithm by presenting MERA calculations of the ground state and low-energy states of two quantum spin chain models. Section VI contains some conclusions.

The canonical form offers a more compact description of U(1)-invariant tensors, and leads to faster matrix multiplications and factorizations. However, there is also an additional cost associated with maintaining an invariant tensor in its canonical form while reshaping (fusing and/or splitting) its indices. In some situations, this cost may offset the benefits of using the canonical form. In the Appendix we discuss a scheme to lower this additional cost in tensor network algorithms that are based on iterating a repeated sequence of transformations. This is achieved by identifying, in the manipulation of a tensor, operations which only depend on the symmetry. Such

operations can be *precomputed* once at the beginning of a simulation. Their result, stored in memory, can be reused at each iteration of the simulation. The Appendix describes two such specific precomputation schemes.

II. REVIEW: TENSOR NETWORK FORMALISM

In this section we review background material concerning the formalism of tensor networks, without reference to symmetry. We introduce basic definitions and concepts, as well as the nomenclature and graphical representation for tensors, tensor networks, and their manipulations, that will be used throughout the paper.

A. Tensors

A tensor \hat{T} is a multidimensional array of complex numbers $\hat{T}_{i_1 i_2 \dots i_k} \in \mathbb{C}$. The *rank* of tensor \hat{T} is the number k of indices. For instance, a rank-0 tensor ($k = 0$) is a complex number. Similarly, rank-1 ($k = 1$) and rank-2 ($k = 2$) tensors represent vectors and matrices, respectively. The *size* of an index i , denoted $|i|$, is the number of values that the index takes, $i \in \{1, 2, \dots, |i|\}$. The size of a tensor \hat{T} , denoted $|\hat{T}|$, is the number of complex numbers it contains, namely $|\hat{T}| = |i_1| \times |i_2| \times \dots \times |i_k|$. In this paper we will use the hat, $\hat{}$, to indicate that an object is a tensor. We include vectors in this convention, writing their components as, e.g., $\hat{\Psi}_i$, although for simplicity we will omit the hat when a vector is written in bra or ket form, e.g., $|\Psi\rangle$.

It is convenient to use a graphical representation of tensors, as introduced in Fig. 1, where a tensor \hat{T} is depicted as a circle (more generally some shape, e.g., a square) and each of its indices is represented by a line emerging from it. In order to specify which index corresponds to which emerging line, we follow the prescription that the lines corresponding to indices $\{i_1, i_2, \dots, i_k\}$ emerge in counterclockwise order. Unless stated otherwise, the first index will correspond to the line emerging at nine o'clock (or the first line encountered while proceeding counterclockwise from nine o'clock).

Two elementary ways in which a tensor \hat{T} can be transformed are by *permuting* and *reshaping* its indices. A *permutation* of indices corresponds to creating a new tensor \hat{T}' from \hat{T} by simply changing the order in which the indices appear, e.g.,

$$(\hat{T}')_{acb} = \hat{T}_{abc}. \quad (1)$$

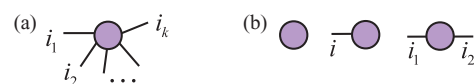


FIG. 1. (Color online) (a) Graphical representation of a tensor \hat{T} of rank k and components $\hat{T}_{i_1 i_2 \dots i_k}$. The tensor is represented by a shape (circle) with k emerging lines corresponding to the k indices i_1, i_2, \dots, i_k . Notice that the indices emerge in counterclockwise order. (b) Graphical representation of tensors with rank $k = 0, 1$, and 2 , corresponding to a complex number $c \in \mathbb{C}$, a vector $|v\rangle \in \mathbb{C}^{|i|}$, and a matrix $\hat{M} \in \mathbb{C}^{|i_1| \times |i_2|}$, respectively.

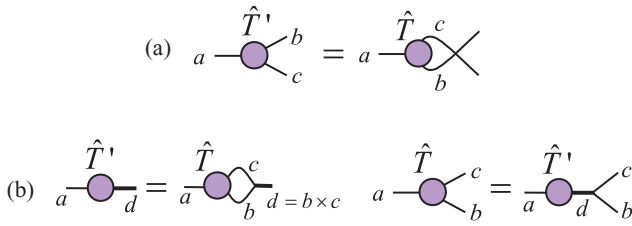


FIG. 2. (Color online) Transformations of a tensor: (a) Permutation of indices b and c . (b) Fusion of indices b and c into $d = b \times c$; splitting of index $d = b \times c$ into b and c .

On the other hand, a tensor \hat{T} can be *reshaped* into a new tensor \hat{T}' by “fusing” and/or “splitting” some of its indices. For instance, in

$$(\hat{T}')_{ad} = \hat{T}_{abc}, \quad d = b \times c, \quad (2)$$

tensor \hat{T}' is obtained from tensor \hat{T} by fusing indices $b \in \{1, \dots, |b|\}$ and $c \in \{1, \dots, |c|\}$ together into a single index d of size $|d| = |b| \cdot |c|$ that runs over all pairs of values of b and c , i.e., $d \in \{(1,1), (1,2), \dots, (|b|, |c| - 1), (|b|, |c|)\}$, whereas in

$$\hat{T}_{abc} = (\hat{T}')_{ad}, \quad d = b \times c, \quad (3)$$

tensor \hat{T} is recovered from \hat{T}' by splitting index d of \hat{T}' back into indices b and c . The permutation and reshaping of the indices of a tensor have a straightforward graphical representation; see Fig. 2.

B. Multiplication of two tensors

Given two matrices \hat{R} and \hat{S} with components \hat{R}_{ab} and \hat{S}_{bc} , we can multiply them together to obtain a new matrix \hat{T} , $\hat{T} = \hat{R} \cdot \hat{S}$, with components

$$\hat{T}_{ac} = \sum_b \hat{R}_{ab} \hat{S}_{bc}, \quad (4)$$

by summing over or *contracting* index b . The multiplication of matrices \hat{R} and \hat{S} is represented graphically by connecting together the emerging lines of \hat{R} and \hat{S} corresponding to the contracted index, as shown in Fig. 3(a).

Matrix multiplication can be generalized to tensors. For instance, given tensors \hat{R} and \hat{S} with components \hat{R}_{abcd} and

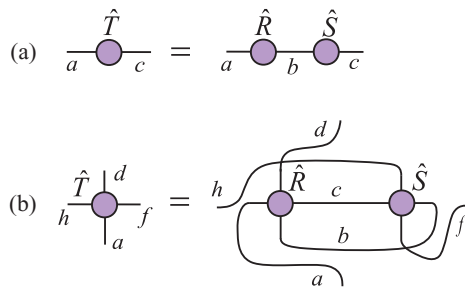


FIG. 3. (Color online) (a) Graphical representation of the matrix multiplication of two matrices \hat{R} and \hat{S} into a new matrix \hat{T} [Eq. (4)]. (b) Graphical representation of an example of the contraction of two tensors \hat{R} and \hat{S} into a new tensor \hat{T} [Eq. (5)].

\hat{S}_{cfbh} , we can define a tensor \hat{T} with components \hat{T}_{hafd} given by

$$\hat{T}_{hafd} = \sum_{bc} \hat{R}_{abcd} \hat{S}_{cfbh}. \quad (5)$$

Again the multiplication of two tensors can be graphically represented by connecting together the lines corresponding to indices that are being contracted [indices b and c in Eq. (5)]; see Fig. 3(b).

The multiplication of two tensors can be broken down into a sequence of elementary steps by transforming the tensors into matrices, multiplying the matrices together, and then transforming the resulting matrix back into a tensor. Next we describe these steps for the contraction given in Eq. (5). They are illustrated in Fig. 4.

(1) *Permute* the indices of tensor \hat{R} in such a way that the indices to be contracted, b and c , appear in the last positions and in a given order, e.g., bc ; similarly, permute the indices of \hat{S} so that the indices to be contracted, again b and c , appear in the first positions and in the same order bc :

$$\begin{aligned} (\hat{R}')_{adbc} &= \hat{R}_{abcd}, \\ (\hat{S}')_{bcfh} &= \hat{S}_{cfbh}. \end{aligned} \quad (6)$$

(2) *Reshape* tensor \hat{R}' into a matrix \hat{R}'' by fusing into a single index u all the indices that are not going to be contracted, $u = a \times d$, and into a single index y all indices to be contracted, $y = b \times c$. Similarly, reshape tensor \hat{S}' into a matrix \hat{S}'' with indices $y = b \times c$ and $w = f \times h$,

$$\begin{aligned} (\hat{R}'')_{uy} &= (\hat{R}')_{adbc}, \\ (\hat{S}'')_{yw} &= (\hat{S}')_{bcfh}. \end{aligned} \quad (7)$$

(3) *Multiply* matrices \hat{R}'' and \hat{S}'' to obtain a matrix \hat{T}'' , with components

$$(\hat{T}'')_{uw} = \sum_y (\hat{R}'')_{uy} (\hat{S}'')_{yw}. \quad (8)$$

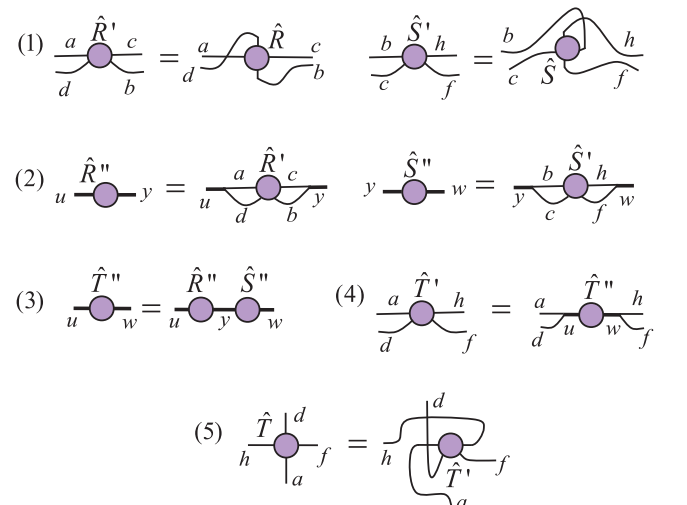


FIG. 4. (Color online) Graphical representations of the five elementary steps (1)–(5) into which one can decompose the contraction of the tensors of Eq. (5).

(4) *Reshape* matrix \hat{T}'' into a tensor \hat{T}' by splitting indices $u = a \times d$ and $w = f \times h$,

$$(\hat{T}')_{adfh} = (\hat{T}'')_{uw}. \quad (9)$$

(5) *Permute* the indices of \hat{T}' into the order in which they appear in \hat{T} ,

$$\hat{T}_{hafd} = (\hat{T}')_{adfh}. \quad (10)$$

We note that breaking down a multiplication of two tensors into elementary steps is not necessary—one can simply implement the contraction of Eq. (5) as a single process. However, it is often more convenient to compose the above elementary steps since, for instance, in this way one can use existing linear algebra libraries for matrix multiplication. In addition, it can be seen that the leading computational cost in multiplying two large tensors is not changed when decomposing the contraction in the above steps. In Sec. IV I this subject will be discussed in more detail for U(1)-invariant tensors.

C. Factorization of a tensor

A matrix \hat{T} can be factorized into the product of two (or more) matrices in one of several canonical forms. For instance, the *singular value decomposition*

$$\hat{T}_{ab} = \sum_{c,d} \hat{U}_{ac} \hat{S}_{cd} \hat{V}_{db} = \sum_c \hat{U}_{ac} s_c \hat{V}_{cb} \quad (11)$$

factorizes \hat{T} into the product of two unitary matrices \hat{U} and \hat{V} , and a diagonal matrix \hat{S} with non-negative diagonal elements $s_c = \hat{S}_{cc}$ known as the *singular values* of \hat{T} ; see Fig. 5(a).

On the other hand, the *eigenvalue* or *spectral decomposition* of a square matrix \hat{T} is of the form

$$\hat{T}_{ab} = \sum_{c,d} \hat{M}_{ac} D_{cd} (\hat{M}^{-1})_{db} = \sum_c \hat{M}_{ac} \lambda_c (\hat{M}^{-1})_{cb}, \quad (12)$$

where \hat{M} is an invertible matrix whose columns encode the eigenvectors $|\lambda_c\rangle$ of \hat{T} ,

$$\hat{T}|\lambda_c\rangle = \lambda_c|\lambda_c\rangle, \quad (13)$$

\hat{M}^{-1} is the inverse of \hat{M} , and \hat{D} is a diagonal matrix, with the eigenvalues $\lambda_c = \hat{D}_{cc}$ on its diagonal. Other useful factorizations include the LU decomposition, the QR decomposition, etc. We refer to any such decomposition generically as a *matrix factorization*.

A tensor \hat{T} with more than two indices can be converted into a matrix in several ways, by specifying how to join its indices into two subsets. After specifying how tensor \hat{T} is to be regarded as a matrix, we can factorize \hat{T} according to any of the above matrix factorizations, as illustrated in Fig. 5(b) for a singular value decomposition. This requires first permuting and reshaping the indices of \hat{T} to form a matrix, then decomposing the latter, and finally restoring the open indices of the resulting matrices into their original form by undoing the reshapes and permutations.

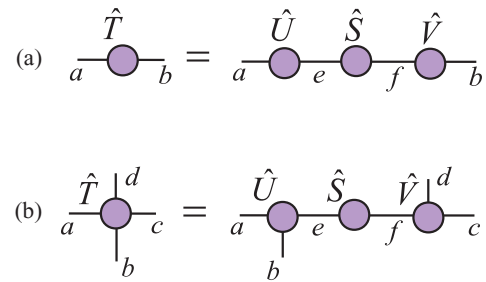


FIG. 5. (Color online) (a) Factorization of a matrix \hat{T} according to a singular value decomposition (11). (b) Factorization of a rank-4 tensor \hat{T} according to one of several possible singular value decompositions.

D. Tensor networks and their manipulation

A *tensor network* \mathcal{N} is a set of tensors whose indices are connected according to a network pattern, e.g., Fig. 6. Given a tensor network \mathcal{N} , a single tensor \hat{T} can be obtained by contracting all the indices that connect the tensors in \mathcal{N} [Fig. 6(b)]. Here, the indices of tensor \hat{T} correspond to the open indices of the tensor network \mathcal{N} . We then say that the network \mathcal{N} is a tensor network decomposition of \hat{T} . One way to obtain \hat{T} from \mathcal{N} is through a sequence of contractions involving two tensors at a time [Fig. 6(c)].

From a tensor network decomposition \mathcal{N} for a tensor \hat{T} , another tensor network decomposition for the same tensor \hat{T} can be obtained in many ways. One possibility is to replace two tensors in \mathcal{N} with the tensor resulting from contracting them together, as is done in each step of Fig. 6(c). Another way is to replace a tensor in \mathcal{N} with a decomposition of that tensor (e.g., with a singular value decomposition). In this paper, we will be concerned with manipulations of a tensor network that, as in the case of multiplying two tensors or decomposing a tensor, can be broken down into a sequence of operations from the following list:

- (1) Permutation of the indices of a tensor, Eq. (1).
- (2) Reshape of the indices of a tensor, Eqs. (2) and (3).
- (3) Multiplication of two matrices, Eq. (4).

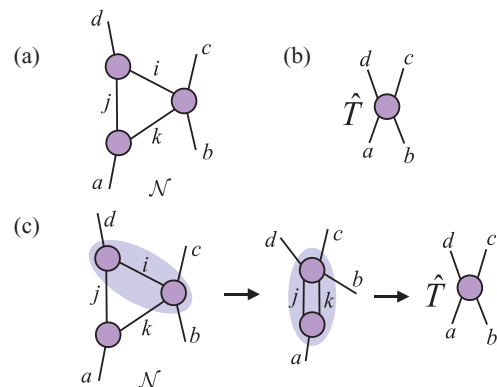


FIG. 6. (Color online) (a) Example of a tensor network \mathcal{N} . (b) Tensor \hat{T} of which the tensor network \mathcal{N} could be a representation. (c) Tensor \hat{T} can be obtained from \mathcal{N} through a sequence of contractions of pairs of tensors. Shading indicates the two tensors to be multiplied together at each step.

(4) Decomposition of a matrix [e.g., singular value decomposition (11) or spectral decomposition (12)].

These operations constitute a set \mathcal{P} of primitive operations for tensor network manipulations (or, at least, for the type of manipulations we will be concerned with). In Sec. IV we will discuss how this set \mathcal{P} of primitive operations can be generalized to tensors that are symmetric under the action of the group $U(1)$.

E. Tensor network states for quantum many-body systems

As mentioned in the Introduction of the paper, tensor networks are used as a means to represent the wave function of certain quantum many-body systems on a lattice. Let us consider a lattice \mathcal{L} made of L sites, each described by a complex vector space \mathbb{V} of dimension d . A generic pure state $|\Psi\rangle \in \mathbb{V}^{\otimes L}$ of \mathcal{L} can always be expanded as

$$|\Psi\rangle = \sum_{i_1, i_2, \dots, i_L} \hat{\Psi}_{i_1 i_2 \dots i_L} |i_1\rangle |i_2\rangle \dots |i_L\rangle, \quad (14)$$

where $i_s = 1, \dots, d$ labels a basis $|i_s\rangle$ of \mathbb{V} for site $s \in \mathcal{L}$. Tensor $\hat{\Psi}$, with components $\hat{\Psi}_{i_1 i_2 \dots i_L}$, contains d^L complex coefficients. This is a number that grows exponentially with the size L of the lattice. Thus the representation of a generic pure state $|\Psi\rangle \in \mathbb{V}^{\otimes L}$ is inefficient. However, it turns out that an efficient representation of certain pure states can be obtained by expressing tensor $\hat{\Psi}$ in terms of a tensor network.

Figure 7 shows several popular tensor network decompositions used to approximately describe the ground states of local Hamiltonians H of lattice models in one or two spatial dimensions. The open indices of each of these tensor networks correspond to the indices i_1, i_2, \dots, i_L of tensor $\hat{\Psi}$. Notice that all the tensor networks of Fig. 7 contain $O(L)$ tensors. If p is the rank of the tensors in one of these tensor networks, and χ is the size of their indices, then the tensor network depends on $O(L\chi^p)$ complex coefficients. For a fixed value of χ this number grows linearly in L , and not exponentially.

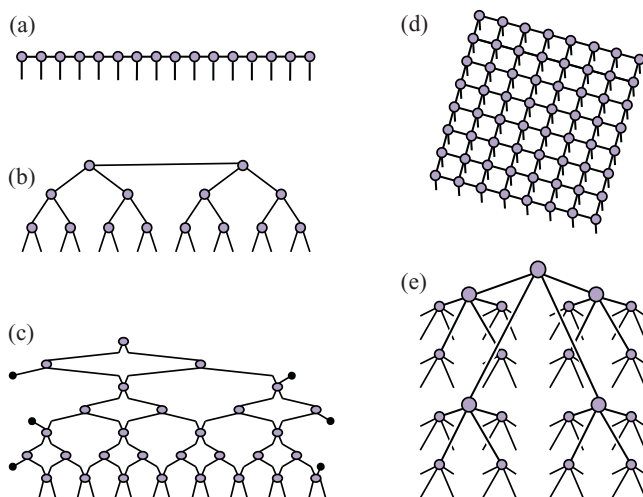


FIG. 7. (Color online) Examples of tensor network states for 1D systems: (a) matrix product state (MPS), (b) tree tensor network (TTN), (c) multiscale entanglement renormalization Ansatz (MERA). Examples of tensor network states for 2D systems: (d) projected entangled-pair state PEPS, (e) 2D TTN (2D MERA not depicted).

It therefore does indeed offer an efficient description of the pure state $|\Psi\rangle \in \mathbb{V}^{\otimes L}$ that it represents. Of course only a subset of pure states can be decomposed in this way. Such states, often referred to as tensor network states, are used as variational Ansätze, with the $O(L\chi^p)$ complex coefficients as the variational parameters.

Given a tensor network state, a variety of algorithms (see, e.g., Refs. 4–50) are used for tasks such as (i) computation of the expectation value $\langle \Psi | \hat{o} | \Psi \rangle$ of a local observable \hat{o} , (ii) optimization of the variational parameters so as to minimize the expectation value of the energy $\langle \Psi | \hat{H} | \Psi \rangle$, or (iii) simulation of time evolution, e.g., $e^{-i\hat{H}t} |\Psi\rangle$. These tasks are accomplished by manipulating tensor networks.

On most occasions, all required manipulations can be reduced to a sequence of primitive operations in the set \mathcal{P} introduced in Sec. IID. Thus in order to adapt the tensor network algorithms of, e.g., Refs. 4–50 to the presence of a symmetry, we only need to modify the set \mathcal{P} of primitive tensor network operations. This will be done in Sec. IV.

F. Tensors as linear maps

A tensor can be used to define a linear map between vector spaces in the following way. First, notice that an index i can be used to label a basis $\{|i\rangle\}$ of a complex vector space $\mathbb{V}^{[i]} \cong \mathbb{C}^{|i|}$ of dimension $|i|$. On the other hand, given a tensor \hat{T} of rank k , we can attach a direction “in” or “out” to each index i_1, i_2, \dots, i_k . This direction divides the indices of \hat{T} into the subset I of incoming indices and the subset O of outgoing indices. We can then build input and output vector spaces given by the tensor product of the spaces of incoming and outgoing indices,

$$\mathbb{V}^{[\text{in}]} = \bigotimes_{i \in I} \mathbb{V}^{[i]}, \quad \mathbb{V}^{[\text{out}]} = \bigotimes_{i \in O} \mathbb{V}^{[i]}, \quad (15)$$

and use tensor \hat{T} to define a linear map between $\mathbb{V}^{[\text{in}]}$ and $\mathbb{V}^{[\text{out}]}$. For instance, if a rank-3 tensor \hat{T}_{abc} has one incoming index $c \in I$ and two outgoing indices $a, b \in O$, then it defines a linear map $\hat{T} : \mathbb{V}^{[c]} \rightarrow \mathbb{V}^{[a]} \otimes \mathbb{V}^{[b]}$ given by

$$\hat{T} = \sum_{a, b, c} \hat{T}_{abc} |a\rangle |b\rangle \langle c|. \quad (16)$$

Graphically, we denote the direction of an index by means of an arrow; see Fig. 8(a).

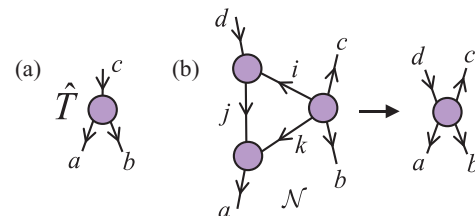


FIG. 8. (Color online) (a) Tensor \hat{T} with one incoming index and two outgoing indices, denoted by incoming and outgoing arrows, respectively [Eq. (16)]. (b) A tensor network \mathcal{N} with directed links can be interpreted as a linear map between incoming and outgoing spaces (of the incoming and outgoing indices) obtained by composing the linear maps associated with each of the tensors in \mathcal{N} .

By decorating the lines of a tensor network \mathcal{N} with arrows [Fig. 8(b)], this can be regarded as a composition of linear maps—namely, one linear map for each tensor in \mathcal{N} . While arrows might be of limited relevance in the absence of a symmetry, they will play an important role when we consider symmetric tensors since they specify how the group acts on each index of a given tensor.

III. REVIEW: REPRESENTATION THEORY OF THE GROUP U(1)

In this section we review basic background material concerning the representation theory of the group U(1). We first consider the action of U(1) on a vector space \mathbb{V} , which decomposes into the direct sum of (possibly degenerate) irreducible representations. We then consider vectors of \mathbb{V} that are symmetric (invariant or covariant) under the action of U(1), as well as linear operators that are U(1) invariant. Then we consider the action of U(1) on the tensor product of two vector spaces, and its generalization to the tensor product of an arbitrary number of vector spaces.

A. Decomposition into direct sum of irreducible representations

Let \mathbb{V} be a finite-dimensional space and let $\varphi \in [0, 2\pi)$ label a set of linear transformations \hat{W}_φ ,

$$\hat{W}_\varphi : \mathbb{V} \rightarrow \mathbb{V}, \quad (17)$$

that are a unitary representation of the group U(1). That is,

$$\hat{W}_\varphi^\dagger \hat{W}_\varphi = \hat{W}_\varphi \hat{W}_\varphi^\dagger = \mathbb{I}, \quad \forall \varphi \in [0, 2\pi), \quad (18)$$

$$\hat{W}_{\varphi_1} \hat{W}_{\varphi_2} = \hat{W}_{\varphi_2} \hat{W}_{\varphi_1} = \hat{W}_{\varphi_1 + \varphi_2 |_{2\pi}}, \quad \forall \varphi_1, \varphi_2 \in [0, 2\pi). \quad (19)$$

Then \mathbb{V} decomposes as the direct sum of (possibly degenerate) one-dimensional irreducible representations (or *irreps*) of U(1),

$$\mathbb{V} \cong \bigoplus_n \mathbb{V}_n, \quad (20)$$

where \mathbb{V}_n is a subspace of dimension d_n , made of d_n copies of an irrep of U(1) with charge $n \in \mathbb{Z}$. We say that irrep n is d_n -fold degenerate and that \mathbb{V}_n is the degeneracy space. For concreteness, in this paper we identify the integer charge n as labeling the number of particles (another frequent identification is with the z component of the spin, in which case semi-integer numbers may be considered). The representation of group U(1) is generated by the particle number operator \hat{n} ,

$$\hat{n} \equiv \sum_n n \hat{P}_n, \quad \hat{P}_n \equiv \sum_{t_n=1}^{d_n} |nt_n\rangle \langle nt_n|, \quad (21)$$

where \hat{P}_n is a projector onto the subspace \mathbb{V}_n of particle number n , and the vectors $|nt_n\rangle$,

$$\hat{n}|nt_n\rangle = n|nt_n\rangle, \quad t_n = 1, \dots, d_n, \quad (22)$$

are an orthonormal basis of \mathbb{V}_n . In terms of \hat{n} , the transformations \hat{W}_φ read

$$\hat{W}_\varphi = e^{-i\hat{n}\varphi}. \quad (23)$$

It then follows from Eq. (22) that

$$\hat{W}_\varphi |nt_n\rangle = e^{-in\varphi} |nt_n\rangle, \quad \forall \varphi \in [0, 2\pi). \quad (24)$$

The dual basis $\{\langle nt_n|\}$ is transformed by the *dual representation* of U(1), with elements \hat{W}_φ^\dagger , as

$$\langle nt_n| \hat{W}_\varphi^\dagger = e^{in\varphi} \langle nt_n|, \quad \forall \varphi \in [0, 2\pi). \quad (25)$$

Example 1. Consider a two-dimensional space \mathbb{V} that decomposes as $\mathbb{V} \cong \mathbb{V}_0 \oplus \mathbb{V}_1$, where the irreps $n = 0$ and $n = 1$ are nondegenerate (i.e., $d_0 = d_1 = 1$). Then the orthogonal vectors $\{|n = 0, t_0 = 1\rangle, |n = 1, t_1 = 1\rangle\}$ form a basis of \mathbb{V} . In column vector notation,

$$\begin{pmatrix} 1 \\ 0 \end{pmatrix} \equiv |n = 0, t_0 = 1\rangle, \quad \begin{pmatrix} 0 \\ 1 \end{pmatrix} \equiv |n = 1, t_1 = 1\rangle, \quad (26)$$

the particle number operator \hat{n} and transformation \hat{W}_φ read

$$\hat{n} \equiv \begin{pmatrix} 0 & 0 \\ 0 & 1 \end{pmatrix}, \quad \hat{W}_\varphi \equiv \begin{pmatrix} 1 & 0 \\ 0 & e^{-i\varphi} \end{pmatrix}. \quad (27)$$

Example 2. Consider a four-dimensional space \mathbb{V} that decomposes as $\mathbb{V} \cong \mathbb{V}_0 \oplus \mathbb{V}_1 \oplus \mathbb{V}_2$, where $d_0 = d_2 = 1$ and $d_1 = 2$, so that now irrep $n = 1$ is twofold degenerate. Let $\{|n = 1, t_1 = 1\rangle, |n = 1, t_1 = 2\rangle\}$ form a basis of \mathbb{V}_1 . In column vector notation,

$$\begin{pmatrix} 1 \\ 0 \\ 0 \\ 0 \end{pmatrix} \equiv |n = 0, t_0 = 1\rangle, \quad \begin{pmatrix} 0 \\ 1 \\ 0 \\ 0 \end{pmatrix} \equiv |n = 1, t_1 = 1\rangle, \quad (28)$$

$$\begin{pmatrix} 0 \\ 0 \\ 1 \\ 0 \end{pmatrix} \equiv |n = 1, t_1 = 2\rangle, \quad \begin{pmatrix} 0 \\ 0 \\ 0 \\ 1 \end{pmatrix} \equiv |n = 2, t_2 = 1\rangle, \quad (29)$$

the particle number operator \hat{n} and transformation \hat{W}_φ read

$$\hat{n} \equiv \begin{pmatrix} 0 & 0 & 0 & 0 \\ 0 & 1 & 0 & 0 \\ 0 & 0 & 1 & 0 \\ 0 & 0 & 0 & 2 \end{pmatrix}, \quad \hat{W}_\varphi \equiv \begin{pmatrix} 1 & 0 & 0 & 0 \\ 0 & e^{-i\varphi} & 0 & 0 \\ 0 & 0 & e^{-i\varphi} & 0 \\ 0 & 0 & 0 & e^{-i2\varphi} \end{pmatrix}. \quad (30)$$

B. Symmetric states and operators

In this work we are interested in states and operators that have a simple transformation rule under the action of U(1). A pure state $|\Psi\rangle \in \mathbb{V}$ is *symmetric* if it transforms as

$$\hat{W}_\varphi |\Psi\rangle = e^{-in\varphi} |\Psi\rangle, \quad \forall \varphi \in [0, 2\pi). \quad (31)$$

The case $n = 0$ corresponds to an *invariant* state, $\hat{W}_\varphi |\Psi\rangle = |\Psi\rangle$, which transforms trivially under U(1), whereas for $n \neq 0$ the state is *covariant*, with $|\Psi\rangle$ being multiplied by a nontrivial phase $e^{-in\varphi}$. Notice that a symmetric state $|\Psi\rangle$ is an eigenstate of \hat{n} : that is, it has a well-defined particle number n . $|\Psi\rangle$ can

thus be expanded in terms of a basis of the relevant subspace \mathbb{V}_n ,

$$\hat{n}|\Psi\rangle = n|\Psi\rangle, \quad |\Psi\rangle = \sum_{t_n=1}^{d_n} (\hat{\Psi}_n)_{t_n} |nt_n\rangle, \quad (32)$$

where we have introduced a charge label n on the state coefficients of $|\Psi\rangle$ so that we can explicitly associate each coefficient $(\hat{\Psi}_n)_{t_n}$ with its corresponding basis vector $|nt_n\rangle$.

A linear operator $\hat{T} : \mathbb{V} \rightarrow \mathbb{V}$ is invariant if it commutes with the generator \hat{n} ,

$$[\hat{T}, \hat{n}] = 0, \quad (33)$$

or equivalently if it commutes with the action of the group,

$$\hat{W}_\varphi \hat{T} \hat{W}_\varphi^\dagger = \hat{T}, \quad \forall \varphi \in [0, 2\pi). \quad (34)$$

It follows that \hat{T} decomposes as (Schur's lemma)

$$\hat{T} = \bigoplus_n \hat{T}_n, \quad (35)$$

where \hat{T}_n is a $d_n \times d_n$ matrix that acts on the subspace \mathbb{V}_n in Eq. (20).

Notice that the operator \hat{T} in Eq. (35) transforms vectors with a well-defined particle number n into vectors with the same particle number. That is, U(1)-invariant operators *conserve particle number*.

Example 1 revisited. In example 1 above, symmetric vectors must be proportional to either $|n=0, t_0=1\rangle$ or $|n=1, t_1=1\rangle$. An invariant operator $\hat{T} = \hat{T}_0 \oplus \hat{T}_1$ is of the form

$$\hat{T} = \begin{pmatrix} \alpha_0 & 0 \\ 0 & \alpha_1 \end{pmatrix}, \quad \alpha_0, \alpha_1 \in \mathbb{C}. \quad (36)$$

Example 2 revisited. In example 2 above, a symmetric vector $|\Psi\rangle$ must be of the form

$$|\Psi\rangle = \begin{pmatrix} \alpha_0 \\ 0 \\ 0 \\ 0 \end{pmatrix}, \quad |\Psi\rangle = \begin{pmatrix} 0 \\ \alpha_1 \\ \beta_1 \\ 0 \end{pmatrix}, \quad \text{or} \quad |\Psi\rangle = \begin{pmatrix} 0 \\ 0 \\ 0 \\ \alpha_2 \end{pmatrix}, \quad (37)$$

where $\alpha_0, \alpha_1, \beta_1, \alpha_2 \in \mathbb{C}$. An invariant operator $\hat{T} = \hat{T}_0 \oplus \hat{T}_1 \oplus \hat{T}_2$ is of the form

$$\hat{T} = \begin{pmatrix} \alpha_0 & 0 & 0 & 0 \\ 0 & \alpha_1 & \beta_1 & 0 \\ 0 & \gamma_1 & \delta_1 & 0 \\ 0 & 0 & 0 & \alpha_2 \end{pmatrix}, \quad (38)$$

where \hat{T}_1 corresponds to the 2×2 central block and $\alpha_0, \alpha_1, \beta_1, \gamma_1, \delta_1, \alpha_2 \in \mathbb{C}$.

The above examples illustrate that the symmetry imposes constraints on vectors and operators. By using an eigenbasis $\{|nt_n\rangle\}$ of the particle number operator \hat{n} , these constraints imply the presence of the zeros in Eqs. (36)–(38). Thus a reduced number of complex coefficients is required in order to describe U(1)-symmetric vectors and operators. As we will discuss in Sec. IV, performing manipulations on

symmetric tensors can also result in a significant reduction in computational costs.

C. Tensor product of two representations

Let $\mathbb{V}^{(A)}$ and $\mathbb{V}^{(B)}$ be two spaces that carry representations of U(1), as generated by particle number operators $\hat{n}^{(A)}$ and $\hat{n}^{(B)}$, and let

$$\mathbb{V}^{(A)} \cong \bigoplus_{n_A} \mathbb{V}_{n_A}^{(A)}, \quad \mathbb{V}^{(B)} \cong \bigoplus_{n_B} \mathbb{V}_{n_B}^{(B)} \quad (39)$$

be their decompositions as a direct sum of (possibly degenerate) irreps. Let us also consider the action of U(1) on the tensor product $\mathbb{V}^{(AB)} \cong \mathbb{V}^{(A)} \otimes \mathbb{V}^{(B)}$ as generated by the *total particle number operator*

$$\hat{n}^{(AB)} \equiv \hat{n}^{(A)} \otimes \mathbb{I} + \mathbb{I} \otimes \hat{n}^{(B)}, \quad (40)$$

that is, implemented by unitary transformations

$$\hat{W}_\varphi^{(AB)} \equiv e^{-i\hat{n}^{(AB)}\varphi}. \quad (41)$$

The space $\mathbb{V}^{(AB)}$ also decomposes as the direct sum of (possibly degenerate) irreps,

$$\mathbb{V}^{(AB)} \cong \bigoplus_{n_{AB}} \mathbb{V}_{n_{AB}}^{(AB)}. \quad (42)$$

Here the subspace $\mathbb{V}_{n_{AB}}^{(AB)}$, with total particle number n_{AB} , corresponds to the direct sum of all products of subspaces $\mathbb{V}_{n_A}^{(A)}$ and $\mathbb{V}_{n_B}^{(B)}$ such that $n_A + n_B = n_{AB}$,

$$\mathbb{V}_{n_{AB}}^{(AB)} \cong \bigoplus_{n_A, n_B | n_A + n_B = n_{AB}} \mathbb{V}_{n_A}^{(A)} \otimes \mathbb{V}_{n_B}^{(B)}. \quad (43)$$

For each subspace $\mathbb{V}_{n_{AB}}^{(AB)}$ in Eq. (42) we introduce a *coupled* basis $\{|n_{AB}t_{n_{AB}}\rangle\}$,

$$\hat{n}^{(AB)}|n_{AB}t_{n_{AB}}\rangle = n_{AB}|n_{AB}t_{n_{AB}}\rangle, \quad (44)$$

where each vector $|n_{AB}t_{n_{AB}}\rangle$ corresponds to the tensor product $|n_{A}t_{n_A}; n_{B}t_{n_B}\rangle \equiv |n_{A}t_{n_A}\rangle \otimes |n_{B}t_{n_B}\rangle$ of a unique pair of vectors $|n_{A}t_{n_A}\rangle$ and $|n_{B}t_{n_B}\rangle$, with $n_A + n_B = n_{AB}$. Let table Υ^{fuse} , with components

$$\Upsilon_{n_A t_{n_A}, n_B t_{n_B} \rightarrow n_{AB} t_{n_{AB}}}^{\text{fuse}} \equiv \langle n_{AB} t_{n_{AB}} | n_{A} t_{n_A}; n_{B} t_{n_B} \rangle, \quad (45)$$

encode this one-to-one correspondence. Notice that each component of Υ^{fuse} is either a 0 or a 1. Then

$$|n_{AB}t_{n_{AB}}\rangle = \sum_{n_A t_{n_A}, n_B t_{n_B}} \Upsilon_{n_A t_{n_A}, n_B t_{n_B} \rightarrow n_{AB} t_{n_{AB}}}^{\text{fuse}} \times |n_A t_{n_A}; n_B t_{n_B}\rangle. \quad (46)$$

For later reference (see the Appendix), we notice that Υ^{fuse} can be decomposed into two pieces. The first piece expresses a basis $\{|n_A t_{n_A}; n_B t_{n_B}\rangle\}$ of $\mathbb{V}^{(AB)}$ in terms of the basis $\{|n_A t_{n_A}\rangle\}$ of $\mathbb{V}^{(A)}$ and the basis $\{|n_B t_{n_B}\rangle\}$ of $\mathbb{V}^{(B)}$. This assignment occurs as in the absence of the symmetry, where one creates a composed index $d = b \times c$ by running, for example, fast over index c and slowly over index b as in Eq. (2). Note that this procedure does not always lead to the set $\{|n_A t_{n_A}; n_B t_{n_B}\rangle\}$ being ordered such that states corresponding to the same total particle number $n_{AB} = n_A + n_B$ are adjacent to each other within the set. This ordering is achieved by the second piece: a permutation of

basis elements that reorganizes them according to their total particle number n_{AB} , so that they are identified in a one-to-one correspondence with the coupled states $\{|n_{AB}t_{n_{AB}}\rangle\}$.

Finally, the product basis can be expressed in terms of the coupled basis

$$|n_A t_{n_A}; n_B t_{n_B}\rangle = \sum_{n_{AB} t_{n_{AB}}} \Upsilon_{n_{AB} t_{n_{AB}} \rightarrow n_A t_{n_A}, n_B t_{n_B}}^{\text{split}} \times |n_{AB} t_{n_{AB}}\rangle, \quad (47)$$

with

$$\Upsilon_{n_{AB} t_{n_{AB}} \rightarrow n_A t_{n_A}, n_B t_{n_B}}^{\text{split}} = \Upsilon_{n_A t_{n_A}, n_B t_{n_B} \rightarrow n_{AB} t_{n_{AB}}}^{\text{fuse}}. \quad (48)$$

Example 3. Consider the case where both $\mathbb{V}^{(A)}$ and $\mathbb{V}^{(B)}$ correspond to the space of example 1, that is, $\mathbb{V}^{(A)} \cong \mathbb{V}_0^{(A)} \oplus \mathbb{V}_1^{(A)}$ and $\mathbb{V}^{(B)} \cong \mathbb{V}_0^{(B)} \oplus \mathbb{V}_1^{(B)}$, where $\mathbb{V}_0^{(A)}$, $\mathbb{V}_1^{(A)}$, $\mathbb{V}_0^{(B)}$, and $\mathbb{V}_1^{(B)}$ all have dimension 1. Then $\mathbb{V}^{(AB)}$ corresponds to the space in example 2, namely

$$\begin{aligned} \mathbb{V}^{(AB)} &\cong \mathbb{V}^{(A)} \otimes \mathbb{V}^{(B)} \\ &\cong (\mathbb{V}_0^{(A)} \oplus \mathbb{V}_1^{(A)}) \otimes (\mathbb{V}_0^{(B)} \oplus \mathbb{V}_1^{(B)}) \\ &\cong \mathbb{V}_0^{(AB)} \oplus \mathbb{V}_1^{(AB)} \oplus \mathbb{V}_2^{(AB)}, \end{aligned} \quad (49)$$

where

$$\mathbb{V}_0^{(AB)} \cong \mathbb{V}_0^{(A)} \otimes \mathbb{V}_0^{(B)}, \quad (50)$$

$$\mathbb{V}_1^{(AB)} \cong (\mathbb{V}_0^{(A)} \otimes \mathbb{V}_1^{(B)}) \oplus (\mathbb{V}_1^{(A)} \otimes \mathbb{V}_0^{(B)}), \quad (51)$$

$$\mathbb{V}_2^{(AB)} \cong \mathbb{V}_1^{(A)} \otimes \mathbb{V}_1^{(B)}. \quad (52)$$

The coupled basis $\{|n_{AB}t_{n_{AB}}\rangle\}$ reads

$$\begin{aligned} |n_{AB} = 0, t_0 = 1\rangle &= |n_A = 0, t_0 = 1\rangle \otimes |n_B = 0, t_0 = 1\rangle, \\ |n_{AB} = 1, t_1 = 1\rangle &= |n_A = 0, t_0 = 1\rangle \otimes |n_B = 1, t_1 = 1\rangle, \\ |n_{AB} = 1, t_1 = 2\rangle &= |n_A = 1, t_1 = 1\rangle \otimes |n_B = 0, t_0 = 1\rangle, \\ |n_{AB} = 2, t_2 = 1\rangle &= |n_A = 1, t_1 = 1\rangle \otimes |n_B = 1, t_1 = 1\rangle, \end{aligned} \quad (53)$$

where we emphasize that the degeneracy index $t_{n_{AB}}$ takes two possible values for $n_{AB} = 1$, i.e., $t_1 \in \{1, 2\}$, since there are two states $|n_A t_{n_A}\rangle \otimes |n_B t_{n_B}\rangle$ with $n_A + n_B = 1$. The components $\Upsilon_{n_A t_{n_A}, n_B t_{n_B} \rightarrow n_{AB} t_{n_{AB}}}^{\text{fuse}}$ of the tensor Υ^{fuse} that encodes this change of basis are all zero except for

$$\Upsilon_{01,01 \rightarrow 01}^{\text{fuse}} = \Upsilon_{01,11 \rightarrow 11}^{\text{fuse}} = \Upsilon_{11,01 \rightarrow 12}^{\text{fuse}} = \Upsilon_{11,11 \rightarrow 21}^{\text{fuse}} = 1.$$

D. Lattice models with U(1) symmetry

The action of U(1) on the threefold tensor product,

$$\mathbb{V}^{(ABC)} \cong \mathbb{V}^{(A)} \otimes \mathbb{V}^{(B)} \otimes \mathbb{V}^{(C)}, \quad (54)$$

as generated by the total particle number operator,

$$\hat{n}^{(ABC)} = \hat{n}^{(A)} \otimes \mathbb{I} \otimes \mathbb{I} + \mathbb{I} \otimes \hat{n}^{(B)} \otimes \mathbb{I} + \mathbb{I} \otimes \mathbb{I} \otimes \hat{n}^{(C)}, \quad (55)$$

induces a decomposition

$$\mathbb{V}^{(ABC)} \cong \bigoplus_{n_{ABC}} \mathbb{V}_{n_{ABC}}^{(ABC)} \quad (56)$$

in terms of irreps $\mathbb{V}_{n_{ABC}}^{(ABC)}$ which we can now relate to $\mathbb{V}_{n_A}^{(A)}$, $\mathbb{V}_{n_B}^{(B)}$, and $\mathbb{V}_{n_C}^{(C)}$. For example, we can consider first the product $\mathbb{V}_{n_{AB}}^{(AB)} \cong \mathbb{V}_{n_A}^{(A)} \otimes \mathbb{V}_{n_B}^{(B)}$ and then the product $\mathbb{V}_{n_{ABC}}^{(ABC)} \cong \mathbb{V}_{n_{AB}}^{(AB)} \otimes \mathbb{V}_{n_C}^{(C)}$, using a different table Υ^{fuse} at each step to relate the coupled basis to the product basis as discussed in the previous section. Similarly we could consider the action of U(1) on four tensor products, and so on.

In particular we will be interested in a lattice \mathcal{L} made of L sites with vector space $\mathbb{V}^{\otimes L}$, where for simplicity we will assume that each site $s \in \mathcal{L}$ is described by the same finite-dimensional vector space \mathbb{V} (see Sec. II E). Given a particle number operator \hat{n} defined on each site, we can consider the action of U(1) generated by the total particle number operator

$$\hat{N} \equiv \sum_{s=1}^L \hat{n}^{(s)}, \quad (57)$$

which corresponds to unitary transformations

$$W_\varphi^{[L]} \equiv e^{-i\hat{N}\varphi} = (e^{-i\hat{n}\varphi})^{\otimes L} = (\hat{W}_\varphi)^{\otimes L}. \quad (58)$$

The tensor product space $\mathbb{V}^{\otimes L}$ decomposes as

$$\mathbb{V}^{\otimes L} \cong \bigoplus_N \mathbb{V}_N \quad (59)$$

and we denote by $\{|Nt_N\rangle\}$ the particle number basis in $\mathbb{V}^{\otimes L}$.

We say that a lattice model is *U(1) symmetric* if its Hamiltonian $\hat{H} : \mathbb{V} \rightarrow \mathbb{V}$ commutes with the action of the group. That is,

$$[\hat{H}, \hat{N}] = 0, \quad (60)$$

or equivalently

$$(\hat{W}_\varphi)^{\otimes L} \hat{H} (\hat{W}_\varphi^\dagger)^{\otimes L} = \hat{H}, \quad \forall \varphi \in [0, 2\pi). \quad (61)$$

One example of a U(1)-symmetric model is the hard-core Bose-Hubbard model, with Hamiltonian

$$\hat{H}_{\text{HCBH}} \equiv \sum_{s=1}^L (\hat{a}_s^\dagger \hat{a}_{s+1} + \hat{a}_s \hat{a}_{s+1}^\dagger + \gamma \hat{n}_s \hat{n}_{s+1}) - \mu \sum_{s=1}^L \hat{n}_s, \quad (62)$$

where we consider periodic boundary conditions (by identifying sites $L+1$ and 1), and \hat{a}_s^\dagger and \hat{a}_s are hard-core bosonic creation and annihilation operators, respectively. In terms of the basis introduced in example 1 these operators are defined as

$$\hat{a} \equiv \begin{pmatrix} 0 & 1 \\ 0 & 0 \end{pmatrix}, \quad \hat{n} \equiv \hat{a}^\dagger \hat{a} = \begin{pmatrix} 0 & 0 \\ 0 & 1 \end{pmatrix}.$$

To see that \hat{H}_{HCBH} commutes with the action of the group, we first observe that for two sites

$$[\hat{a}_1^\dagger \hat{a}_2 + \hat{a}_2^\dagger \hat{a}_1, \hat{n}_1 + \hat{n}_2] = 0, \quad (63)$$

from which it readily follows that $[\hat{H}_{\text{HCBH}}, \hat{N}] = 0$.

Notice that the chemical potential term $-\mu \sum_s \hat{n}_s = -\mu \hat{N}$ also commutes with the rest of the Hamiltonian. The ground state $|\Psi_N^{\text{GS}}\rangle$ of \hat{H}_{HCBH} in a particular subspace \mathbb{V}_N or particle number sector can be turned into the absolute ground state by tuning the chemical potential μ . This fact can be used to find the ground state $|\Psi_N^{\text{GS}}\rangle$ of any particle number sector through an algorithm which can only minimize the expectation value of \hat{H}_{HCBH} . However, we will later see that the use of symmetric tensors in the context of tensor network states will allow us to directly minimize the expectation value of \hat{H}_{HCBH} in a given particle number sector by restricting the search to states

$$|\Psi_N\rangle = \sum_{t_N=1}^{d_N} (\hat{\Psi}_N)_{t_N} |N t_N\rangle \quad (64)$$

with the desired particle number N .

Finally, by making the identifications

$$\hat{n} = \frac{\mathbb{I} - \hat{\sigma}_z}{2}, \quad \hat{a} = \frac{\hat{\sigma}_x + i\hat{\sigma}_y}{2},$$

where $\hat{\sigma}_x, \hat{\sigma}_y, \hat{\sigma}_z$ are the Pauli matrices

$$\hat{\sigma}_x \equiv \begin{pmatrix} 0 & 1 \\ 1 & 0 \end{pmatrix}, \quad \hat{\sigma}_y \equiv \begin{pmatrix} 0 & -i \\ i & 0 \end{pmatrix}, \quad \hat{\sigma}_z \equiv \begin{pmatrix} 1 & 0 \\ 0 & -1 \end{pmatrix}, \quad (65)$$

one can map \hat{H}_{HCBH} to the spin- $\frac{1}{2}$ XXZ quantum spin chain

$$\hat{H}_{XXZ} \equiv \sum_{s=1}^L (\hat{\sigma}_x^{(s)} \hat{\sigma}_x^{(s+1)} + \hat{\sigma}_y^{(s)} \hat{\sigma}_y^{(s+1)} + \Delta \hat{\sigma}_z^{(s)} \hat{\sigma}_z^{(s+1)}), \quad (66)$$

where we have ignored terms proportional to \hat{N} and set $\Delta \equiv \gamma/4$. In particular, for $\Delta = 0$ we obtain the quantum XX spin chain

$$\hat{H}_{XX} \equiv \sum_{s=1}^L (\hat{\sigma}_x^{(s)} \hat{\sigma}_x^{(s+1)} + \hat{\sigma}_y^{(s)} \hat{\sigma}_y^{(s+1)}), \quad (67)$$

and for $\gamma = 1$, the quantum Heisenberg spin chain

$$\hat{H}_{XX} \equiv \sum_{s=1}^L (\hat{\sigma}_x^{(s)} \hat{\sigma}_x^{(s+1)} + \hat{\sigma}_y^{(s)} \hat{\sigma}_y^{(s+1)} + \hat{\sigma}_z^{(s)} \hat{\sigma}_z^{(s+1)}). \quad (68)$$

In Sec. V, the quantum spin models (67) and (68) will be used to benchmark the performance increase resulting from the use of symmetries in tensor networks algorithms.

IV. TENSOR NETWORKS WITH U(1) SYMMETRY

In this section we consider U(1)-symmetric tensors and tensor networks. We explain how to decompose U(1)-symmetric tensors in a compact, canonical form that exploits their symmetry. We then discuss how to adapt the set \mathcal{P} of primitives for tensor network manipulations in order to work in this form. We also analyze how working in the canonical form affects computational costs.

A. U(1)-symmetric tensors

Let \hat{T} be a rank- k tensor with components $\hat{T}_{i_1 i_2 \dots i_k}$. As in Sec. II F, we regard tensor \hat{T} as a linear map between the vector spaces $\mathbb{V}^{[\text{in}]}$ and $\mathbb{V}^{[\text{out}]}$ [Eq. (15)]. This implies that

each index is either an incoming or outgoing index. On each space $\mathbb{V}^{[i_l]}$, associated with index i_l , we introduce a particle number operator $\hat{n}^{(l)}$ that generates a unitary representation of U(1) given by matrices $\hat{W}_\varphi^{(l)} \equiv e^{-i\hat{n}^{(l)}\varphi}$, $\varphi \in [0, 2\pi)$. In the following, we use $\hat{W}_\varphi^{(l)*}$ to denote the complex conjugate of $\hat{W}_\varphi^{(l)}$.

Let us consider the action of U(1) on the space

$$\mathbb{V}^{[i_1]} \otimes \mathbb{V}^{[i_2]} \otimes \dots \otimes \mathbb{V}^{[i_k]} \quad (69)$$

given by

$$\hat{X}_\varphi^{(1)} \otimes \hat{X}_\varphi^{(2)} \otimes \dots \otimes \hat{X}_\varphi^{(k)}, \quad (70)$$

where

$$\hat{X}_\varphi^{(l)} = \begin{cases} \hat{W}_\varphi^{(l)*} & \text{if } i_l \in I, \\ \hat{W}_\varphi^{(l)} & \text{if } i_l \in O. \end{cases} \quad (71)$$

That is, $\hat{X}_\varphi^{(l)}$ acts differently depending on whether index i_l of tensor \hat{T} is an incoming or outgoing index. We then say that tensor \hat{T} , with components $T_{i_1 i_2 \dots i_k}$, is U(1) invariant if it is invariant under the transformation of Eq. (70),

$$\sum_{i_1, i_2, \dots, i_k} (\hat{X}_\varphi^{(1)})_{i_1' i_1} (\hat{X}_\varphi^{(2)})_{i_2' i_2} \dots (\hat{X}_\varphi^{(k)})_{i_k' i_k} \hat{T}_{i_1 i_2 \dots i_k} = \hat{T}_{i_1' i_2' \dots i_k'}, \quad (72)$$

for all $\varphi \in [0, 2\pi)$. This is depicted in Fig. 9.

Example 4. A U(1)-invariant vector $|\Psi\rangle$ —that is, a vector with $\hat{n}|\Psi\rangle = 0$ and components $(\hat{\Psi}_{n=0})_{i_0}$ in the subspace $\mathbb{V}_{n=0}$ which corresponds to vanishing particle number $n = 0$ [cf. Eq. (32)]—fulfills

$$(\hat{\Psi}_{n=0})_{i_0'} = \sum_{i_0} (\hat{W}_\varphi)_{i_0' i_0} (\hat{\Psi}_{n=0})_{i_0}, \quad \forall \varphi \in [0, 2\pi), \quad (73)$$

in accordance with Eq. (31), as shown in Fig. 9(a).

Example 5. A U(1)-invariant matrix \hat{T} (35) fulfills

$$\hat{T}_{a'b'} = \sum_{a,b} (\hat{W}_\varphi)_{a'a} (\hat{W}_\varphi^*)_{b'b} \hat{T}_{ab} \quad (74)$$

$$= \sum_{a,b} (\hat{W}_\varphi)_{a'a} \hat{T}_{ab} (\hat{W}_\varphi^\dagger)_{bb'}, \quad \forall \varphi \in [0, 2\pi), \quad (75)$$

in accordance with Eq. (34) [see Fig. 9(b)].

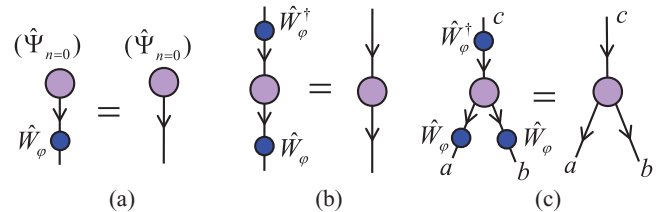


FIG. 9. (Color online) (a) Constraint fulfilled by a U(1)-invariant vector. The only allowed particle number on the single index is $n = 0$. (b) Constraint fulfilled by a U(1)-invariant matrix. It follows from Schur's lemma that the matrix is block diagonal in particle number. (c) Constraint fulfilled by a rank-3 tensor with one incoming index and two outgoing indices.

Example 6. Tensor \hat{T} in Eq. (16), with components \hat{T}_{abc} , where a and b are outgoing indices and c is an incoming index, is U(1) invariant if

$$\hat{T}_{a'b'c'} = \sum_{a,b,c} (\hat{W}_\varphi^{(1)})_{a'a} (\hat{W}_\varphi^{(2)})_{b'b} (\hat{W}_\varphi^{(3)*})_{c'c} \hat{T}_{abc} \quad (76)$$

$$= \sum_{a,b,c} (\hat{W}_\varphi^{(1)})_{a'a} (\hat{W}_\varphi^{(2)})_{b'b} \hat{T}_{abc} (\hat{W}_\varphi^{(3)\dagger})_{cc'} \quad (77)$$

for all $\varphi \in [0, 2\pi)$ [see Fig. 9(c)].

Further, we say that a tensor \hat{Q} with components $\hat{Q}_{i_1 i_2 \dots i_k}$ is U(1) covariant if under the transformation of Eq. (70) it acquires a non trivial phase $e^{-in\varphi}$,

$$\sum_{i_1, i_2, \dots, i_k} (\hat{X}_\varphi^{(1)})_{i_1' i_1} (\hat{X}_\varphi^{(2)})_{i_2' i_2} \dots (\hat{X}_\varphi^{(k)})_{i_k' i_k} \hat{Q}_{i_1 i_2 \dots i_k} = e^{-in\varphi} \hat{Q}_{i_1' i_2' \dots i_k'}, \quad (78)$$

for all $\varphi \in [0, 2\pi)$.

Example 7. A U(1)-covariant vector $|\Psi\rangle$ —that is, one which satisfies $\hat{n}|\Psi\rangle = n|\Psi\rangle$ for some $n \neq 0$, and has nonzero components $(\hat{\Psi}_n)_{i_n}$ only in the relevant subspace \mathbb{V}_n [cf. Eq. (32)]—fulfills

$$\sum_{i_n} (\hat{W}_\varphi)_{i_n' i_n} (\hat{\Psi}_n)_{i_n} = e^{-in\varphi} (\hat{\Psi}_n)_{i_n'}, \quad \forall \varphi \in [0, 2\pi), \quad (79)$$

in accordance with Eq. (31). (See also Fig. 10.)

Notice that we can describe the rank- k covariant tensor \hat{Q} above by a rank- $(k+1)$ invariant tensor \hat{T} with components

$$\hat{T}_{i_1 i_2 \dots i_k i} \equiv \hat{Q}_{i_1 i_2 \dots i_k}, \quad |i| = 1. \quad (80)$$

This is built from \hat{Q} by adding an extra incoming index i , where the index i has a fixed particle number n and no degeneracy (i.e., i is associated to a trivial space $\mathbb{V}^{|i|} \cong \mathbb{C}$). We refer to both *invariant* and *covariant* tensors as *symmetric* tensors. By using the above construction, in this work we will represent all U(1)-symmetric tensors by means of U(1)-invariant tensors. In particular, we represent the nontrivial components $(\hat{\Psi}_n)_{i_n}$ of the covariant vector $|\Psi_n\rangle$ in Eqs. (31) and (32) as an invariant matrix \hat{T} of size $|i_n| \times 1$ with components $\hat{T}_{i_n 1} = (\hat{\Psi}_n)_{i_n}$. Consequently, from now on we will mostly consider only invariant tensors.

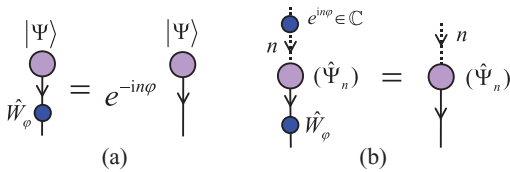


FIG. 10. (Color online) (a) U(1)-covariant vector $|\Psi\rangle$, with some nonvanishing particle number $n \neq 0$. Under the action of U(1) on its index, the covariant vector $|\Psi\rangle$ acquires a phase $e^{-in\varphi}$ [Eq. (79)]. (b) The U(1)-covariant vector $|\Psi\rangle$, with components $(\Psi_n)_{i_n}$, can be represented by a U(1)-invariant matrix \hat{T} with components $\hat{T}_{i i} = (\Psi_n)_{i_1}$, where i is a trivial index ($|i| = 1$) with charge n and is decorated by the opposite arrow to i_1 .

B. Canonical form for U(1)-invariant tensors

Let us now write a tensor \hat{T} in a particle number basis on each factor space in Eq. (69). That is, each index i_1, i_2, \dots, i_k is decomposed into a particle number index n and a degeneracy index t_n , $i_1 = (n_1, t_{n_1}), i_2 = (n_2, t_{n_2}), \dots, i_k = (n_k, t_{n_k})$, and

$$\hat{T}_{i_1 i_2 \dots i_k} \equiv (\hat{T}_{n_1 n_2 \dots n_k})_{t_{n_1} t_{n_2} \dots t_{n_k}}. \quad (81)$$

Here, for each set of particle numbers n_1, n_2, \dots, n_k , we regard $\hat{T}_{n_1 n_2 \dots n_k}$ as a tensor with components $(\hat{T}_{n_1 n_2 \dots n_k})_{t_{n_1} t_{n_2} \dots t_{n_k}}$. Let N_{in} and N_{out} denote the sum of particle numbers corresponding to incoming and outgoing indices,

$$N_{\text{in}} \equiv \sum_{n_l \in I} n_l, \quad N_{\text{out}} \equiv \sum_{n_l \in O} n_l. \quad (82)$$

The condition for a nonvanishing tensor of the form $\hat{T}_{n_1 n_2 \dots n_k}$ to be invariant under U(1), Eq. (70), is simply that the sum of incoming particle numbers equals the sum of outgoing particle numbers. Therefore a U(1)-invariant tensor \hat{T} satisfies

$$\hat{T} = \bigoplus_{n_1, n_2, \dots, n_k} \hat{T}_{n_1 n_2 \dots n_k} \delta_{N_{\text{in}}, N_{\text{out}}}. \quad (83)$$

[We use the direct sum symbol \bigoplus to denote that the different tensors $\hat{T}_{n_1 n_2 \dots n_k}$ are supported on orthonormal subspaces of the tensor product space of Eq. (69).] In components, the above expression reads

$$\hat{T}_{i_1 i_2 \dots i_k} \equiv (\hat{T}_{n_1 n_2 \dots n_k})_{t_{n_1} t_{n_2} \dots t_{n_k}} \delta_{N_{\text{in}}, N_{\text{out}}}. \quad (84)$$

Here, $\delta_{N_{\text{in}}, N_{\text{out}}}$ implements particle number conservation: if $N_{\text{in}} \neq N_{\text{out}}$, then all components of $\hat{T}_{n_1 n_2 \dots n_k}$ must vanish. This generalizes the block structure of U(1)-invariant matrices in Eq. (35) (where \hat{T}_{nn} is denoted \hat{T}_n) to tensors of arbitrary rank k . The canonical decomposition in Eq. (83) is important, in that it allows us to identify the degrees of freedom of tensor \hat{T} that are not determined by the symmetry. Expressing tensor \hat{T} in terms of the tensors $\hat{T}_{n_1 n_2 \dots n_k}$ with $N_{\text{in}} = N_{\text{out}}$ ensures that we store \hat{T} in the most compact way possible.

Notice that the canonical form of Eq. (83) is a particular case of the canonical form presented in Eq. (15) of Ref. 52 for more general (possibly non-Abelian) symmetry groups. There, a symmetric tensor was decomposed into *degeneracy* tensors [analogous to tensors $\hat{T}_{n_1 n_2 \dots n_k}$ in Eq. (83)] and structural tensors [generalizing the term $\delta_{N_{\text{in}}, N_{\text{out}}}$ in Eq. (83)] which can in general be expanded as a trivalent network of Clebsch-Gordan (or coupling) coefficients of the symmetry group. In the case of non-Abelian groups, where some irreps have dimension larger than 1, the structural tensors are highly nontrivial. However, for the group U(1) discussed in this paper (as for any other Abelian group) all irreps are one dimensional and the structural tensors are always reduced to a simple expression such as $\delta_{N_{\text{in}}, N_{\text{out}}}$ in Eq. (83). (Nevertheless, in the Appendix we will resort to a more elaborate decomposition of the structural tensors in order to better exploit the presence of symmetry in those tensor network algorithms based on iterating a fixed sequence of manipulations.)

C. U(1)-symmetric tensor networks

In Sec. II F we saw that a tensor network \mathcal{N} where each line has a direction (represented with an arrow) can be interpreted

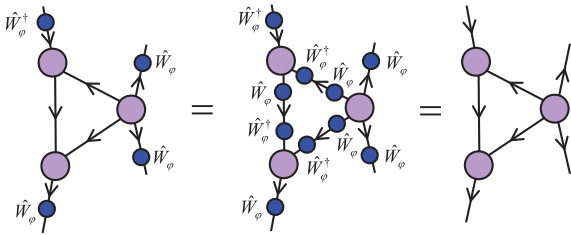


FIG. 11. (Color online) A tensor network \mathcal{N} made of U(1)-invariant tensors represents a U(1)-invariant tensor \hat{T} . This is seen by means of two equalities. The first equality is obtained by inserting resolutions of the identity $\mathbb{I} = \hat{W}_\varphi \hat{W}_\varphi^\dagger$ on each index connecting two tensors in \mathcal{N} . The second equality follows from the fact that each tensor in \mathcal{N} is U(1) invariant.

as a collection of linear maps composed into a single linear map \hat{T} of which \mathcal{N} is a tensor network decomposition. By introducing a particle number operator on the vector space associated to each line of \mathcal{N} , we can define a unitary representation of U(1) on each index of each tensor in \mathcal{N} . Then we say that \mathcal{N} is a U(1)-invariant tensor network if all its tensors are U(1) invariant. Notice that, by construction, if \mathcal{N} is a U(1)-invariant tensor network, then the resulting linear map \hat{T} is also U(1) invariant. This is illustrated in Fig. 11.

More generally, we can consider a U(1)-symmetric tensor network, made of tensors that are U(1) symmetric (that is, either invariant or covariant). Recall, however, that any covariant tensor can be represented as an invariant tensor by adding an extra index (80). Therefore without loss of generality we can restrict our attention to invariant tensor networks.

D. Tensor network states and algorithms with U(1) symmetry

As discussed in Sec. II E, a tensor network \mathcal{N} can be used to describe certain pure states $|\Psi\rangle \in \mathbb{V}^{\otimes L}$ of a lattice \mathcal{L} . If \mathcal{N} is a U(1)-symmetric tensor network then it will describe a pure state $|\Psi\rangle$ that has a well-defined total particle number N . That is, a U(1)-symmetric pure state

$$\hat{N}|\Psi\rangle = N|\Psi\rangle, \quad e^{-i\hat{N}\varphi}|\Psi\rangle = e^{-iN\varphi}|\Psi\rangle. \quad (85)$$

In this way we can obtain a more refined version of popular tensor network states such as MPS, TTN, MERA, PEPS, etc. As a variational *Ansatz*, a symmetric tensor network state is more constrained than a regular tensor network state, and consequently it can represent fewer states $|\Psi\rangle \in \mathbb{V}^{\otimes L}$. However, it also depends on fewer parameters. This implies a more economical description, as well as the possibility of reducing computational costs during its manipulation.

The rest of this section is devoted to explaining how one can achieve a reduction in computational costs. This is based on storing and manipulating U(1)-invariant tensors expressed in the canonical form of Eqs. (83) and (84). We next explain how to adapt the set \mathcal{P} of four primitive operations for the tensor network manipulations discussed in Sec. II D, namely, permutation and reshaping of indices, matrix multiplication, and factorization.

E. Permutation of indices

Given a U(1)-invariant tensor \hat{T} expressed in the canonical form of Eqs. (83) and (84), permuting two of its indices is straightforward. It is achieved by swapping the position of the two particle numbers of $\hat{T}_{n_1 n_2 \dots n_k}$ involved, and also the corresponding degeneracy indices. For instance, if the rank-3 tensor \hat{T} of Eq. (16) is U(1) invariant and has components

$$\hat{T}_{abc} = (\hat{T}_{n_A n_B n_C})_{t_{n_A} t_{n_B} t_{n_C}} \delta_{n_A + n_B, n_C} \quad (86)$$

when expressed in the particle number basis $a = (n_A, t_{n_A})$, $b = (n_B, t_{n_B})$, $c = (n_C, t_{n_C})$, then tensor \hat{T}' of Eq. (1), obtained from \hat{T} by permuting the last two indices, has components

$$(\hat{T}')_{acb} = (\hat{T}'_{n_A n_C n_B})_{t_{n_A} t_{n_C} t_{n_B}} \delta_{n_A + n_B, n_C}, \quad (87)$$

where

$$(\hat{T}'_{n_A n_C n_B})_{t_{n_A} t_{n_C} t_{n_B}} = (\hat{T}_{n_A n_B n_C})_{t_{n_A} t_{n_B} t_{n_C}}. \quad (88)$$

Notice that since we only need to permute the components of those $\hat{T}_{n_A n_B n_C}$ such that $n_A + n_B = n_C$, implementing the permutation of indices requires less computation time than a regular index permutation. This is shown in Fig. 12, corresponding to a permutation of indices using MATLAB.

F. Reshaping of indices

The indices of a U(1)-invariant tensor can be reshaped (fused or split) in a similar manner to those of a regular tensor. However, maintaining the convenient canonical form of Eqs. (83) and (84) requires additional steps. Two adjacent indices can be fused together using the table Υ^{fuse} of Eq. (45), which is a sparse tensor made of 1's and 0's. Similarly an index can be split into two adjacent indices by using its inverse, the sparse tensor Υ^{split} of Eq. (48).

Example 8. Let us consider again the rank-3 tensor \hat{T} of Eq. (16) with components given by Eq. (86), where a and b are outgoing indices and c is an incoming index. We can fuse outgoing index b and incoming index c into an (e.g., incoming) index d , obtaining a new tensor \hat{T}' with components

$$(\hat{T}')_{ad} = (\hat{T}'_{n_A n_D})_{t_{n_A} t_{n_D}} \delta_{n_A, n_D}, \quad (89)$$

where $n_D = -n_B + n_C$. (The sign in front of n_B comes from the fact that d is an incoming index and b is an outgoing index.) The components of \hat{T}' are in one-to-one correspondence with those of \hat{T} and follow from the transformation

$$(\hat{T}'_{n_A n_D})_{t_{n_A} t_{n_D}} = \sum_{n_B, t_{n_B}, n_C, t_{n_C}} (\hat{T}_{n_A n_B n_C})_{t_{n_A} t_{n_B} t_{n_C}} \times \Upsilon_{n_B t_{n_B}, n_C t_{n_C} \rightarrow n_D t_{n_D}}^{\text{fuse}}, \quad (90)$$

where only the case $n_A = n_D$ needs to be considered. To complete the example, let us assume that the index a is described by the vector space $\mathbb{V}^{(A)} \cong \mathbb{V}_0 \oplus \mathbb{V}_1 \oplus \mathbb{V}_2$ with degeneracies $d_0 = 1$, $d_1 = 2$, and $d_2 = 1$; index b is described by a vector space $\mathbb{V}^{(B)} \cong \mathbb{V}_{-1} \oplus \mathbb{V}_0$ without degeneracies, i.e., $d_{-1} = d_0 = 1$; and index c is described by a vector space $\mathbb{V}^{(C)} \cong \mathbb{V}_0 \oplus \mathbb{V}_1$ also without degeneracies, $d_{-1} = d_0 = 1$.

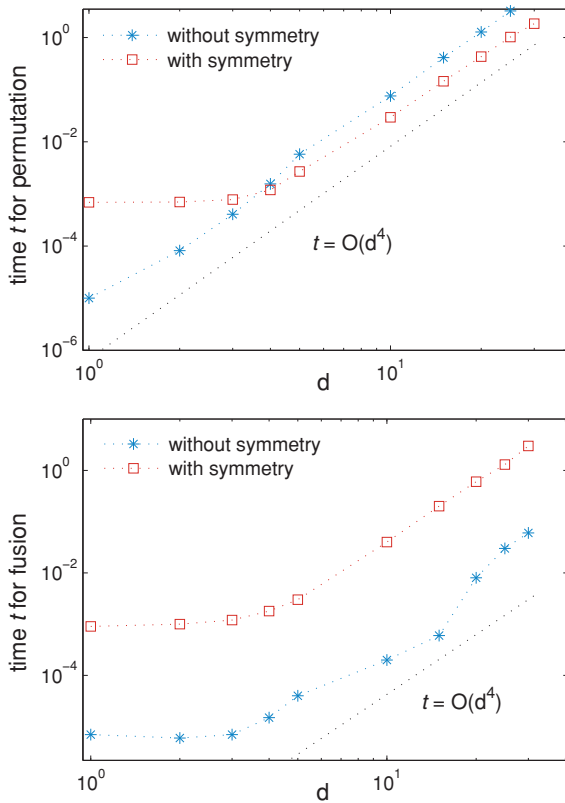


FIG. 12. (Color online) Computation times (in seconds) required to permute and fuse two indices of a rank-4 tensor \hat{T} , as a function of the size of the indices. All four indices of \hat{T} have the same size, $5d$, and therefore the tensor contains $|\hat{T}| = 5^4 d^4$ coefficients. The figures compare the time required to perform these operations using a regular tensor and a U(1)-invariant tensor, where in the second case each index contains five different values of the particle number n (each with degeneracy d) and the canonical form of Eqs. (83) and (84) is used. The upper figure shows the time required to permute two indices: For large d , exploiting the symmetry of a U(1)-invariant tensor by using the canonical form results in shorter computation times. The lower figure shows the time required to fuse two adjacent indices. In this case, maintaining the canonical form requires more computation time. Notice that in both figures the asymptotic cost scales as $O(d^4)$, or the size of \hat{T} , since this is the number of coefficients which need to be rearranged. We note that the fixed-cost overheads associated with symmetric manipulations could potentially vary substantially with choice of programming language, compiler, and machine architecture. The results given here show the performance of the authors' MATLAB implementation of U(1) symmetry.

Then $\mathbb{V}^{(D)} \cong \mathbb{V}^{(B)} \otimes \mathbb{V}^{(C)}$ (and in this example, also $\mathbb{V}^{(D)} \cong \mathbb{V}^{(A)}$) and Eq. (90) amounts to

$$\begin{aligned} (\hat{T}'_{00})_{11} &= (\hat{T}_{000})_{111}, & (\hat{T}'_{11})_{11} &= (\hat{T}_{101})_{111}, \\ (\hat{T}'_{11})_{12} &= (\hat{T}_{101})_{211}, & (\hat{T}'_{11})_{21} &= (\hat{T}_{1(-1)0})_{111}, \\ (\hat{T}'_{11})_{22} &= (\hat{T}_{1(-1)0})_{211}, & (\hat{T}'_{22})_{11} &= (\hat{T}_{2(-1)1})_{111}, \end{aligned}$$

where we notice that tensor \hat{T}' is a matrix as in Eq. (38). Similarly, we can split incoming index d of tensor \hat{T}' back into

outgoing index b and incoming index c of tensor \hat{T} according to

$$\begin{aligned} (\hat{T}_{n_A n_B n_C})_{t_{n_A} t_{n_B} t_{n_C}} &= \sum_{n_D, t_{n_D}} (\hat{T}'_{n_A n_D})_{t_{n_A} t_{n_D}} \\ &\quad \times \Upsilon_{n_D t_{n_D} \rightarrow n_B t_{n_B}, n_C t_{n_C}}^{\text{split}}, \end{aligned} \quad (91)$$

which, again, is nontrivial only for $-n_B + n_C = n_D$ and $n_A + n_B = n_C$.

This example illustrates that fusing and splitting indices while maintaining the canonical form of Eqs. (83) and (84) requires more work than reshaping regular indices. Indeed, after taking indices b and c into $d = b \times c$ by listing all pairs of values $b \times c$, we still need to reorganize the resulting basis elements according to their particle number n_D . Although this can be done by following the simple table given by Υ^{fuse} , it may add significantly to the overall computational cost associated with reshaping a tensor. For instance, Fig. 12 shows that fusing indices of invariant tensors can be more expensive than fusing indices of regular tensors.

G. Multiplication of two matrices

By permuting and reshaping the indices of a U(1)-invariant tensor, we can convert it into a U(1)-invariant matrix $\hat{T} = \bigoplus_{nn'} \hat{T}_{nn'} \delta_{n,n'}$, or simply

$$\hat{T} = \bigoplus_n \hat{T}_n, \quad (92)$$

where $\hat{T}_n \equiv \hat{T}_{nn}$. In components, matrix \hat{T} reads

$$(\hat{T})_{ab} = (\hat{T}_n)_{t_n t'_n}, \quad (93)$$

where $a = (n, t_n)$ and $b = (n, t'_n)$. In particular, similar to the discussion in Sec. II B for regular tensors, the multiplication of two tensors invariant under the action of U(1) can be reduced to the multiplication of two U(1)-invariant matrices.

Let \hat{R} and \hat{S} be two U(1)-invariant matrices, with canonical forms

$$\hat{R} = \bigoplus_n \hat{R}_n, \quad \hat{S} = \bigoplus_n \hat{S}_n. \quad (94)$$

Their product $\hat{T} = \hat{R} \cdot \hat{S}$, Eq. (4), is then another matrix \hat{T} which is also block diagonal,

$$\hat{T} = \bigoplus_n \hat{T}_n, \quad (95)$$

such that each block \hat{T}_n is obtained by multiplying the corresponding blocks \hat{R}_n and \hat{S}_n ,

$$\hat{T}_n = \hat{R}_n \cdot \hat{S}_n. \quad (96)$$

Equations (92) and (96) make evident the potential reduction of computational costs that can be achieved by manipulating U(1)-invariant matrices in their canonical form. First, a reduction in memory space follows from only having to store the diagonal blocks in Eq. (92). Second, a reduction in computational time is implied by only having to multiply these blocks in Eq. (96). This is illustrated in the following example.

Example 9. Consider a U(1)-invariant matrix \hat{T} which is a linear map in a space \mathbb{V} that decomposes into q irreps \mathbb{V}_n , each

of which has the same degeneracy $d_n = d$. That is, \hat{T} is a square matrix of dimensions $dq \times dq$, with the block-diagonal form of Eq. (92). Since there are q blocks \hat{T}_n and each block has size $d \times d$, the U(1)-invariant matrix \hat{T} contains qd^2 coefficients. For comparison, a regular matrix of the same size contains q^2d^2 coefficients, a number greater by a factor of q .

Let us now consider multiplying two such matrices. We use an algorithm that requires $O(l^3)$ computational time to multiply two matrices of size $l \times l$. The cost of performing q multiplications of $d \times d$ blocks in Eq. (96) scales as $O(qd^3)$. In contrast, the cost of multiplying two regular matrices of the same size scales as $O(q^3d^3)$, requiring q^2 times more computation time. Figure 13 shows a comparison of computation times when multiplying two matrices for both U(1)-symmetric and regular matrices.

H. Factorization of a matrix

The factorization of a U(1)-invariant matrix \hat{T} [Eq. (92)] can also benefit from the block-diagonal structure. Consider, for instance, the singular value decomposition $\hat{T} = \hat{U}\hat{S}\hat{V}$ of Eq. (11). In this case we can obtain the matrices

$$\hat{U} = \bigoplus_n \hat{U}_n, \quad \hat{S} = \bigoplus_n \hat{S}_n, \quad \hat{V} = \bigoplus_n \hat{V}_n \quad (97)$$

by performing the singular value decomposition of each block \hat{T}_n independently,

$$\hat{T}_n = \hat{U}_n \hat{S}_n \hat{V}_n. \quad (98)$$

The computational savings are analogous to those described in example 9 above for the multiplication of matrices. Figure 13 also shows a comparison of computation times required to perform a singular value decomposition on U(1)-invariant and regular matrices using MATLAB.

I. Discussion

In this section we have seen that U(1)-invariant tensors can be written in the canonical form of Eqs. (83) and (84), and that this canonical form is of interest because it offers a compact description in terms of only those coefficients which are not constrained by the symmetry. We have also seen that maintaining the canonical form during tensor manipulations adds some computational overhead when reshaping (fusing or splitting) indices, but reduces computation time when permuting indices (for sufficiently large tensors) and when multiplying or factorizing matrices (for sufficiently large matrix sizes).

The cost of reshaping and permuting indices is proportional to the size $|\hat{T}|$ of the tensors, whereas the cost of multiplying and factorizing matrices is a larger power of the matrix size, for example, $|\hat{T}|^{3/2}$. The use of the canonical form when manipulating large tensors therefore frequently results in an overall reduction in computation time, making it a very attractive option in the context of tensor network algorithms. This is exemplified in the next section, where we apply the MERA to study the ground state of quantum spin models with a U(1) symmetry.

On the other hand, however, the cost of maintaining invariant tensors in the canonical form becomes more relevant

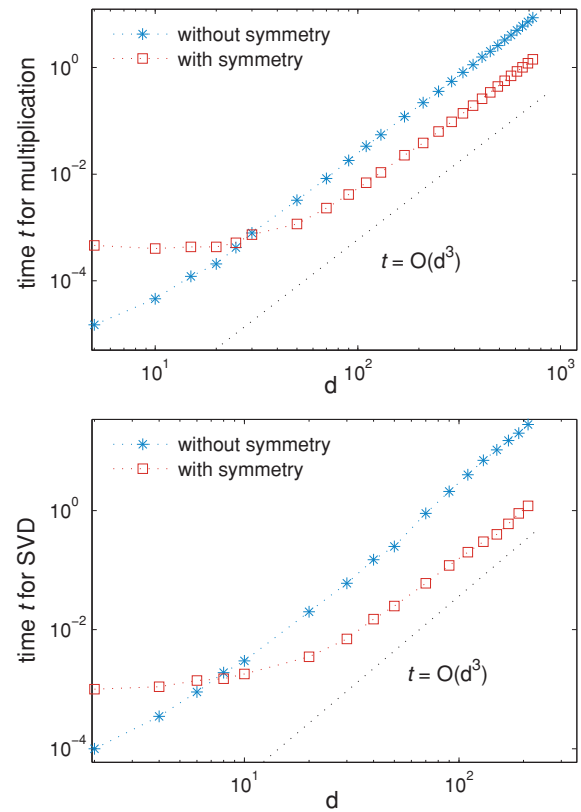


FIG. 13. (Color online) Computation times (in seconds) required to multiply two matrices (upper panel) and to perform a singular value decomposition (lower panel) as a function of the size of the indices. Matrices of size $5d \times 5d$ are considered. The figures compare the time required to perform these operations using regular matrices and U(1)-invariant matrices, where for the U(1)-invariant matrices each index contains five different values of the particle number n , each with degeneracy d , and the canonical form of Eqs. (92) and (93) is used. That is, each matrix decomposes into five blocks of size $d \times d$. For large d , exploiting the block-diagonal form of U(1)-invariant matrices results in shorter computation time both for multiplication and for singular value decomposition. The asymptotic cost scales with d as $O(d^3)$, while the size of the matrices grows as $O(d^2)$. We note that the fixed-cost overheads associated with symmetric manipulations could potentially vary substantially with choice of programming language, compiler, and machine architecture. The results given here show the performance of the authors' MATLAB implementation of U(1) symmetry.

when dealing with smaller tensors. In the next section we will also see that in some situations, this additional cost may significantly reduce, or even offset, the benefits of using the canonical form. In this event, and in the specific context of algorithms where the same tensor manipulations are iterated many times, it is possible to significantly decrease the additional cost by *precomputing* the parts of the tensor manipulations that are repeated on each iteration. Precomputation schemes are described in more detail in the Appendix. Their performance is illustrated in the next section.

V. TENSOR NETWORK ALGORITHMS WITH U(1) SYMMETRY: A PRACTICAL EXAMPLE

In previous sections we have described a strategy to incorporate a U(1) symmetry into tensors, tensor networks, and their manipulations. To further illustrate how the strategy works in practice, in this section we demonstrate its use in the context of the multiscale entanglement renormalization *Ansatz*, or MERA, and present numerical results from our reference implementation of the U(1) symmetry in MATLAB.

A. Multiscale entanglement renormalization *Ansatz*

Figure 14 shows a MERA that represent states $|\Psi\rangle \in \mathbb{V}^{\otimes L}$ of a lattice \mathcal{L} made of $L = 18$ sites (see Sec. II E). Recall that the MERA is made of layers of isometric tensors, known as disentanglers \hat{u} and isometries \hat{w} , that implement a coarse-graining transformation. In this particular scheme, isometries map three sites into one and the coarse-graining transformation reduces the $L = 18$ sites of \mathcal{L} into two sites using two layers of tensors. A collection of states on these two sites is then encoded in a top tensor \hat{t} , whose upper index $a = 1, 2, \dots, \chi_{\text{top}}$ is used to label χ_{top} states $|\Psi_a\rangle \in \mathbb{V}^{\otimes L}$. This particular arrangement of tensors corresponds to the 3:1 MERA described in Ref. 18.

In this section we will consider a MERA analogous to that of Fig. 14 but with Q layers of disentanglers and isometries, which we will use to describe states on a lattice \mathcal{L} made of 2×3^Q sites. We will use this variational *Ansatz* to obtain an approximation to the ground state and first excited states of two quantum spin chains that have a global internal U(1) symmetry, namely the spin-1/2 quantum XX chain of Eq. (67) and the spin-1/2 antiferromagnetic quantum Heisenberg chain of Eq. (68). Each spin-1/2 degree of freedom of the chain is described by a vector space spanned by two orthonormal states $\{|\downarrow\rangle, |\uparrow\rangle\}$. Here we will represent them by the states $\{|0\rangle, |1\rangle\}$ corresponding to zero and one particles, as in example 1 of Sec. III A. For computational convenience, we will consider a lattice \mathcal{L} where each site contains two spins, or states, $\{|\downarrow\downarrow\rangle, |\downarrow\uparrow\rangle, |\uparrow\downarrow\rangle, |\uparrow\uparrow\rangle\}$. Therefore each site of \mathcal{L} is described by a space $\mathbb{V} \cong \mathbb{V}_0 \oplus \mathbb{V}_1 \oplus \mathbb{V}_2$, where $d_0 = d_2 = 1$ and $d_1 = 2$, as in example 2 of Sec. III A. Thus a lattice \mathcal{L} made of L sites corresponds to a chain of $2L$ spins. In such a system, the total particle number N ranges from 0 to $2L$. (Equivalently, the z component of the total spin S_z ranges from $-L$ to L , with $S_z = N - L$.)

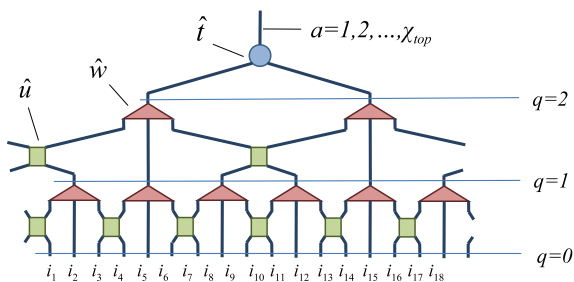


FIG. 14. (Color online) MERA for a system of $L = 2 \times 3^2 = 18$ sites, made of two layers of disentanglers \hat{u} and isometries \hat{w} , and a top tensor \hat{t} .

B. MERA with U(1) symmetry

A U(1)-invariant version of the MERA, or U(1) MERA for short, is obtained by simply considering U(1)-invariant versions of all of the isometric tensors, namely the disentanglers \hat{u} , isometries \hat{w} , and the top tensor \hat{t} . This requires assigning a particle number operator to each index of the MERA. Each open index of the first layer of disentanglers corresponds to one site of \mathcal{L} . The particle number operator on any such index is therefore given by the quantum spin model under consideration. We can characterize the particle number operator by two vectors, \vec{n} and \vec{d} : a list of the different values the particle number takes and the degeneracy associated with each such particle number, respectively. In the case of the vector space \mathbb{V} for each site of \mathcal{L} described above, $\vec{n} = \{0, 1, 2\}$ and $\vec{d} = \{1, 2, 1\}$. For the open index of the tensor \hat{t} at the very top of the MERA, the assignment of charges is also straightforward. For instance, to find an approximation to the ground state and first seven excited states of the quantum spin model with particle number N , we choose $\vec{n} = \{N\}$ and $\vec{d} = \{8\}$. (In particular, a vanishing S_z corresponds to $N = L$.)

For each of the remaining indices of the MERA, the assignment of the pair (\vec{n}, \vec{d}) needs careful consideration and a final choice may only be possible after numerically testing several options and selecting the one which produces the lowest expectation value of the energy. Table I shows the assignment of particle numbers and degeneracies made to represent the ground state and several excited states in a system of $L = 2 \times 3^3 = 54$ sites (that is, 108 spins) with total particle number $N = L = 54$ (or $S_z = 0$). Notice that at level q of the MERA ($q = 1, 2, 3$), each index effectively corresponds to a block of $n_q \equiv 3^q$ sites of \mathcal{L} . Therefore having exactly n_q particles in a block of n_q sites corresponds to a density of one particle per site of \mathcal{L} . The assigned particle numbers of Table I, namely, $[n_q - 2, n_q - 1, n_q, n_q + 1, n_q + 2]$ for level q , then correspond to allowing for fluctuations of up to two particles with respect to the average density. The sum of corresponding degeneracies $\vec{d} = \{d_{n_q-2}, d_{n_q-1}, d_{n_q}, d_{n_q+1}, d_{n_q+2}\}$ gives the bond dimension χ , which in the example is $\chi = 13$.

In order to find an approximation to the ground state of either \hat{H}_{XX} or \hat{H}_{XXX} in Eqs. (67) and (68), we set $\chi_{\text{top}} = 1$ and optimize the tensors in the MERA so as to minimize the expectation value

$$\langle \Psi | \hat{H} | \Psi \rangle, \quad (99)$$

where $|\Psi\rangle \in \mathbb{V}^{\otimes L}$ is the pure state represented by the MERA and \hat{H} is the relevant Hamiltonian. In order to find an

TABLE I. Example of particle number assignment in a U(1) MERA for $L = 54$ sites (or 108 spins). The total bond dimension is $\chi = 1 + 3 + 5 + 3 + 1 = 13$. The value of χ_{top} is set as described in the text.

Level q	Particle numbers \vec{n}	Degeneracies \vec{d}
top	$\{N = 54\}$	$\{\chi_{\text{top}}\}$
3	$\{25, 26, 27, 28, 29\}$	$\{1, 3, 5, 3, 1\}$
2	$\{7, 8, 9, 10, 11\}$	$\{1, 3, 5, 3, 1\}$
1	$\{1, 2, 3, 4, 5\}$	$\{1, 3, 5, 3, 1\}$
0	$\{0, 1, 2\}$	$\{1, 2, 1\}$

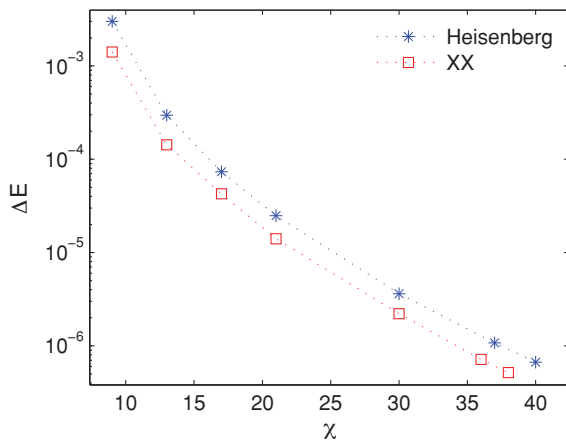


FIG. 15. (Color online) Error in ground-state energy ΔE as a function of χ for the XX and Heisenberg models with $2L = 108$ spins and periodic boundary conditions, in the particle number sector $N = L$ (or $S_z = 0$). The error is calculated with respect to the exact solutions, and is seen to decay exponentially with χ .

approximation to the $\chi_{\text{top}} > 1$ eigenstates of \hat{H} with lowest energies, we optimize the tensors in the MERA so as to minimize the expectation value

$$\sum_{a=1}^{\chi_{\text{top}}} \langle \Psi_a | \hat{H} | \Psi_a \rangle, \quad \langle \Psi_a | \Psi_{a'} \rangle = \delta_{aa'}. \quad (100)$$

The optimization is carried out using the MERA algorithm described in Ref. 18, which requires contracting tensor networks (by sequentially multiplying pairs of tensors) and performing singular value decompositions. In the present example, all of these operations will be performed exploiting the U(1) symmetry.

Figure 15 shows the error in the ground-state energy as a function of the bond dimension χ , for assignments of degeneracies similar to those in Table II. The error is seen to decay exponentially with increasing χ , indicating increasingly accurate approximations to the ground state.

TABLE II. Number of coefficients required to specify the tensors of a MERA for $L = 54$ as a function of the bond dimension χ , decomposed according to a degeneracy vector \vec{d} . A comparison is made between regular tensors and U(1)-invariant tensors.

χ	Degeneracy \vec{d}	No. of coefficients (regular)	No. of coefficients (symmetric)	Ratio
4	[0,1,2,1,0]	1552	426	3.6 : 1
8	[0,2,4,2,0]	17216	4714	3.7 : 1
13	[1,3,5,3,1]	115501	21969	5.3 : 1
17	[1,4,7,4,1]	335717	68469	5.0 : 1
21	[1,5,9,5,1]	779965	166901	4.7 : 1
30	[2,7,12,7,2]	3243076	639794	5.1 : 1

C. Exploiting the symmetry

We now discuss some of the advantages of using the U(1) MERA.

1. Selection of particle number sector

An important advantage of the U(1) MERA is that it exactly preserves the U(1) symmetry. In other words, the states resulting from a numerical optimization are exact eigenvectors of the total particle number operator \hat{N} [Eq. (57)]. In addition, the total particle number N can be preselected at the onset of optimization by specifying it in the open index of the top tensor \hat{t} .

Figure 16 shows the energy gap between the ground state and two excited states of an XX chain with $2L$ spins (or L sites), for $N = L$ particles ($S_z = 0$). One is the first excited state which also has $N = L$ particles. The other is the ground state in the sector with $N = L + 1$ particles. The two energy gaps are seen to decay with the system size as L^{-1} . The ability to preselect a given particle number N means that only two optimizations were required: one MERA optimization for $N = L$ with $\chi_{\text{top}} = 2$ in order to obtain an approximation to the ground state and first excited state of \hat{H}_{XX} in that particle number sector; and one MERA optimization for $N = L + 1$ with $\chi_{\text{top}} = 1$ in order to obtain an approximation to the ground state of \hat{H}_{XX} in the particle number sector $N = L + 1$.

Similar results can be obtained with the regular MERA. For instance, one can obtain an approximation to the ground state of a given particle number sector by adding a chemical potential term $-\mu \sum_s \hat{n}^{(s)}$ to the Hamiltonian and carefully tuning the chemical potential term μ until the expectation value of the particle number \hat{N} is the desired one. However, the regular MERA cannot guarantee that the states obtained in this way are exact eigenvectors of \hat{N} . Instead the resulting states are likely to have particle number fluctuations.

Figure 17 shows the low-energy spectrum of the Heisenberg model \hat{H}_{XX} for a periodic system of $L = 54$ sites (or

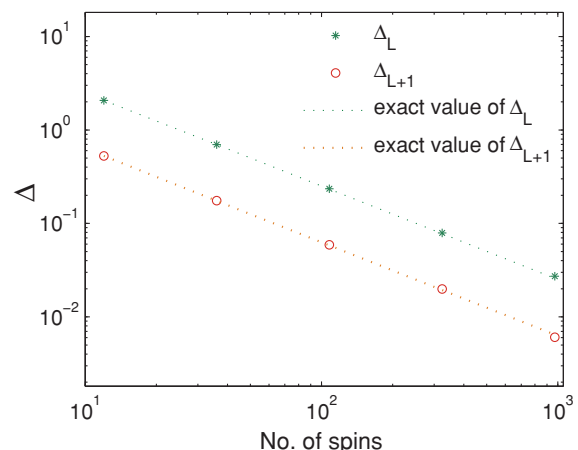


FIG. 16. (Color online) Decay of energy gaps Δ with system size L in the XX model. The upper line corresponds to the energy gap Δ_L between the ground state and the first excited state in the $N = L$ particle number (or $S_z = 0$) sector. The lower line corresponds to the energy gap Δ_{L+1} between the ground states of the $N = L$ and $N = L + 1$ particle number sectors.

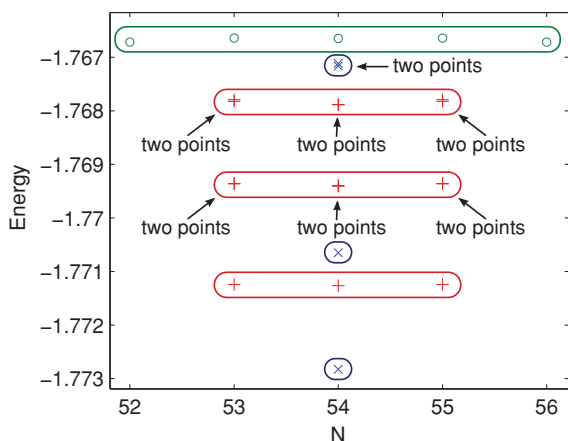


FIG. 17. (Color online) Low-energy spectrum of \hat{H}_{XXX} with $L = 54$ sites ($= 108$ spins). Depicted states have spins of zero (\times , blue loops), one ($+$, red loops), or two (\circ , green loop), and total number of particles (N) between 52 and 56. Note that the second and third spin-1 triplets are twofold degenerate.

108 spins), including the ground state and several excited states both in the particle sector $N = 54$ (or $S_z = 0$), and in neighboring particle sectors. Recall that \hat{H}_{XXX} is actually invariant under a global internal $SU(2)$ symmetry, of which particle number is a $U(1)$ subgroup. Correspondingly the spectrum is organized according to irreps of $SU(2)$, namely singlets (total spin 0), triplets (total spin 1), quintuplets (total spin 2), etc. Again, using the $U(1)$ MERA, the five particle number sectors $N = 52, 53, 54, 55$, and 56 can be addressed with independent computations. This implies, for instance, that in order to find the gap between the first and fourth singlets, we can simply set $N = 54$ and $\chi_{\text{top}} = 9$ on the open index of the top tensor \hat{t} , to accommodate the first four spin-0 states and five spin-1 states in the $N = 54$ sector, as seen in Fig. 17. In order to capture the fourth singlet using the regular MERA, we would need to consider at least $\chi_{\text{top}} = 19$ (at a larger computational cost and possibly lower accuracy), since this state has only the 19th lowest energy overall.

2. Reduction of computational costs

The use of $U(1)$ -invariant tensors in the MERA also results in a reduction of computational costs. First, $U(1)$ -invariant tensors, when written in the canonical form of Eqs. (83) and (84), are block diagonal and therefore require less storage space. Table II compares the number of MERA coefficients that need to be stored in the regular and symmetric case, for different choices of particle number assignments relevant to the present examples.

Second, the computation time required to manipulate tensors is also reduced when using $U(1)$ -invariant tensors in the canonical form. Figure 18 shows the computation time required for one iteration of the energy minimization algorithm of Ref. 18 (during which all tensors in the MERA are updated once), as a function of the total bond dimension χ . The plot compares the time required using regular tensors and $U(1)$ -invariant tensors. For $U(1)$ -invariant tensors, we display the time per iteration for three different levels of

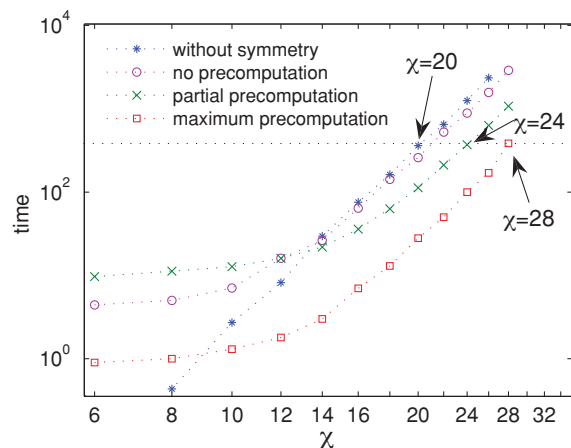


FIG. 18. (Color online) Computation time (in seconds) for one iteration of the MERA energy minimization algorithm, as a function of the bond dimension χ . For sufficiently large χ , exploiting the $U(1)$ symmetry leads to reductions in computation time. The horizontal line on this graph shows that this reduction in computation time equates to the ability to evaluate MERAs with a higher bond dimension χ : For the same cost per iteration incurred when optimizing a standard MERA in MATLAB with bond dimension $\chi = 20$, one may choose instead to optimize a $U(1)$ -symmetric MERA with partial precomputation and $\chi = 24$, or with full precomputation and $\chi = 28$.

precomputation, as described in the Appendix. The figure shows that for sufficiently large χ , using $U(1)$ -invariant tensors leads to a shorter time per iteration of the optimization algorithm.

In the authors' reference implementation (written in MATLAB), using the symmetry without precomputation is seen to only reduce the computation time by about a factor of 2 for the largest χ under consideration. This is because maintaining the canonical form for $U(1)$ -invariant tensors still imposes a significant overhead for the values of χ considered. In contrast, when using precomputation we obtained times shorter by a factor of 10 or more.

The magnitude of the overhead imposed by maintaining the canonical form will depend on factors such as programming language and machine architecture, but in general more significant gains can be obtained by making full use of precomputation. This option, however, requires a significant amount of additional memory (see the Appendix), and a more convenient middle ground can be obtained by using a partial precomputation scheme.

VI. CONCLUSIONS

In this paper we have provided a detailed explanation of how a global internal Abelian symmetry may be incorporated into any tensor network algorithm. Following Ref. 52 we considered tensor networks constructed from tensors which were invariant under the action of the internal symmetry, and showed how each tensor may be decomposed according to a canonical form into *degeneracy* tensors (which contain all the degrees of freedom that are not affected by the symmetry) and *structural* tensors (which are completely determined by the symmetry). We then introduced a set of primitive operations

TABLE III. Fusion rules for the group \mathbb{Z}_3 : Outcomes of evaluating $a \times a'$.

		a		
		0	1	2
a'	0	0	1	2
	1	1	2	0
	2	2	0	1

\mathcal{P} which may be used to carry out tensor network algorithms using *Ansätze* such as MPS, PEPS, and MERA, and showed how each of these operations can be implemented in such a way that the canonical form is both preserved and exploited for computational gain.

We then demonstrated the implementation of this decomposition for tensors with an internal U(1) symmetry, and computed multiple benchmarks demonstrating the computational costs and speedups inherent in this approach. We found that although maintaining the canonical form imposed additional costs when combining or splitting tensor indices, for simulations of a sufficiently large scale these costs can be offset by the gains made when performing permutations, matrix multiplications, and matrix decompositions.

Finally, we implemented the MERA on a quantum spin chain with U(1) symmetry. We showed that exploitation of this symmetry can lead to a decrease in the computational cost by a factor of between 10 and 20. These gains may be used either to reduce overall computation time or to permit substantial increases in the MERA bond dimension χ , and consequently in the accuracy of the results obtained.

Although in this paper we have focused on an example which is a continuous Abelian group, the formalism presented here may equally well be applied to a finite Abelian group. In particular let us consider a cyclic group Z_q , $q \in \mathbb{Z}^+$.⁷⁵ As in the case of U(1), the Hilbert space decomposes under the action of the group into a direct sum of one-dimensional irreps which are each characterized by an integer charge a , and consequently most of the analysis presented in this paper remains unchanged. In particular, matrices which are invariant under the action of the group will be block diagonal in the basis labeled by charge according to Eq. (35), and symmetric tensors enjoy the canonical decomposition stated in Eqs. (83) and (84). The only objects which need modification are the fusion and splitting maps, which need to be altered so that they encode the fusion rules for Z_q instead for U(1). For a cyclic group Z_q , the fusion of two charges a and a' gives rise to a charge a'' according to $a'' = (a + a')|_q$ where $|_q$ indicates that the addition is performed modulo q . For example, Z_3 has charges $a = 0, 1, 2$, and the fusion rules for Z_3 take the form $a \times a' \rightarrow a''$ where the value of a'' is given in Table III.

More generally, a generic Abelian group will be characterized by a set of charges (a_1, a_2, a_3, \dots) . When fusing two such sets of charges (a_1, a_2, a_3, \dots) and $(a'_1, a'_2, a'_3, \dots)$, each charge a_i is combined with its counterpart a'_i according to the fusion rule of the relevant subgroup. Once again, this behavior may be encoded in a single fusion map Υ^{fuse} and its inverse Υ^{split} .

The formalism presented in this paper is therefore directly applicable to any Abelian group.

ACKNOWLEDGMENTS

The authors thank Ian P. McCulloch for fruitful discussions. Support from the Australian Research Council (Grants No. FF0668731, No. DP0878830, and No. DP1092513, and APA scholarship) is acknowledged.

APPENDIX: USE OF PRECOMPUTATION IN ITERATIVE ALGORITHMS

We have seen that the use of the canonical form given in Eqs. (83) and (84) to represent U(1)-invariant tensors can potentially lead to substantial reductions in memory requirements and in calculation time. We also pointed out, however, that there is an additional cost in maintaining an invariant tensor in its canonical form, and that this is associated with the reshaping (fusing and/or splitting) of its indices. In some situations this additional cost may significantly reduce, or even offset, the benefits of using the canonical form.

In this Appendix we investigate techniques for reducing this additional cost in the context of iterative tensor network algorithms. Many of the algorithms discussed in Sec. II E are iterative algorithms, repeating the same sequence of tensor network manipulations many times over. Examples include algorithms which compute tensor network approximations to the ground state by minimizing the expectation value of the energy or by simulating evolution in imaginary time, with each iteration yielding an increasingly accurate approximation to the ground state of the system.

The goal of this Appendix is to identify calculations which depend only on the symmetry group, and are independent of the variational coefficients of such algorithms. Where these calculations are repeated in each iteration of the algorithm, we can effectively eliminate the associated computational cost by performing them only once, either during or prior to the first iteration of the algorithm, and then storing and reusing these *precomputed* results in subsequent iterations. We will illustrate this procedure by considering the precomputation of a series of operations applied to a single tensor \hat{T} .

To do this, we begin by revisiting the fusion and splitting tables of Sec. III C and introducing a graphical representation of these objects. We then introduce a convenient decomposition of a symmetric tensor into a matrix accompanied by multiple fusion and/or splitting tensors, and linear maps Γ that map one such decomposition into another. These linear maps are independent of the coefficients of the tensor being reorganized, and consequently they are precisely the objects which can be precomputed in order to quicken an iterative algorithm at the expense of additional memory cost. Finally we describe two specific precomputation schemes, differing in what is precomputed and in how the precomputed data are utilized during the execution of the algorithm, in order to illustrate the tradeoff between the amount of memory needed to store the precomputation data and the associated computational speedup which may be obtained. In practice, the nature of the specific implementation employed will depend on available computational resources.

1. Diagrammatic notation of fusing and splitting tensors

In describing how we can precompute repeated manipulations of this tensor \hat{T} , we will find it useful to employ diagrammatic representations of the fusion and splitting tables Υ^{fuse} and Υ^{split} introduced in Sec. III C. These tables implement a linear map between a pair of indices and their fusion product, and thus can be understood as trivalent tensors having two input legs and one output leg (or vice versa) in accordance with Sec. II F. We choose to represent them graphically as shown in Fig. 19(a), where the arrow within the circle always points toward the coupled index. The linear maps Υ^{fuse} and Υ^{split} are unitary, and consequently we impose that the tensors of Fig. 19(a) must satisfy the identities given in Fig. 19(b), corresponding to unitarity under the action of the conjugation operation employed in diagrammatic tensor network notation (vertical reflection of a tensor and the complex conjugation of its components, typically denoted \dagger). Our notation also reflects the property, first noted in Sec. III C, that Υ^{fuse} and Υ^{split} may be decomposed into two pieces [Fig. 19(c)]. For the fusion tensor, we identify the first piece (represented by a circle containing an arrow) with the creation of a composed index using the manner we would employ in the absence of symmetry (2). The second piece, represented by the small square, permutes the basis elements of the composed index, reorganizing them according to total particle number. The two components of the splitting tensor are then uniquely defined by consistency with the process of conjugation for the diagrammatic representation of tensors, and with the unitarity condition of Fig. 19(b).

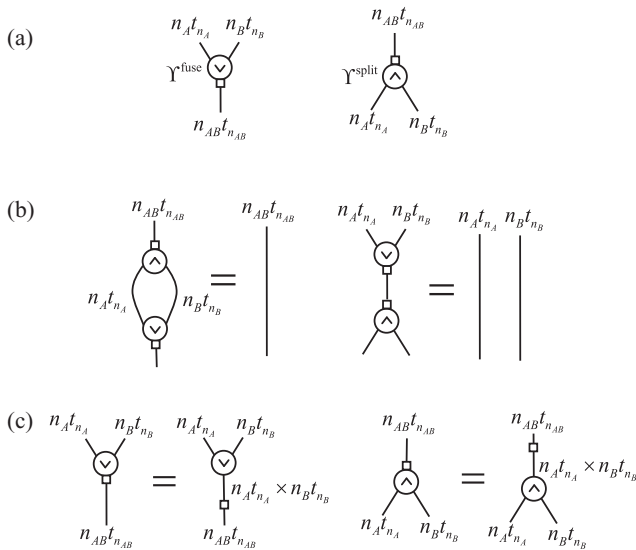


FIG. 19. (a) Graphical representation of the fusion tensor Υ^{fuse} and the splitting tensor Υ^{split} . (b) The tensors Υ^{fuse} and Υ^{split} are unitary, and thus yield the identity when contracted pairwise as shown. (c) A fusion tensor decomposed into two parts. The first part (indicated by a circle with an arrow) performs the tensor product of input irreps, $n_A t_A \times n_B t_B$. The result is an index that labels pairs $(n_A t_A, n_B t_B)$. The second part (indicated by a rectangle) is a permutation that associates each pair $(n_A t_A, n_B t_B)$ with a unique $(n_{AB} t_{n_{AB}})$, corresponding to a vector in the coupled basis of $\mathbb{V}^{(AB)}$.

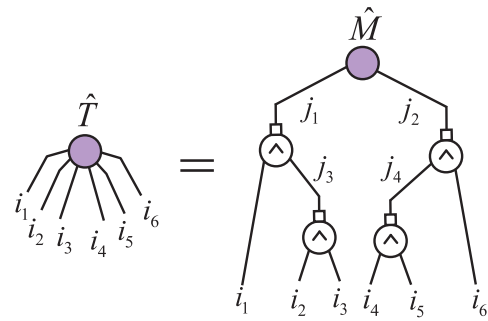


FIG. 20. (Color online) Binary tree decomposition of a symmetric tensor \hat{T} having components $\hat{T}_{i_1 i_2 i_3 i_4 i_5 i_6}$. The tree \mathcal{T} is comprised of a matrix \hat{M} as the root node, four splitting tensors as internal nodes, and i_1, i_2, \dots, i_6 as its leaf indices. No incoming or outgoing arrows are indicated on the indices in the figure, as the decomposition is valid for any such assignment of directional arrows.

These requirements have an important consequence. Suppose the first part of Υ^{fuse} implements $b \times c \rightarrow d$ by iterating rapidly over the values of b and more slowly over the values of c , and b lies clockwise of c on the graphical representation of Υ^{fuse} . This then means that on the graphical representation of Υ^{split} which implements $d \rightarrow b \times c$, index b must lie counterclockwise of c . It is therefore vitally important to distinguish between the splitting tensor and a rotated depiction of the fusing tensor. To this end we require that when using this diagrammatic notation, all tensors (with the exception of the fusion and splitting tensors) must be drawn with only downward-going legs, as seen, for example, in Fig. 20, though the legs are still free to carry either incoming or outgoing arrows as before.

2. Tree decomposition

We find it convenient to decompose a rank- k , U(1)-invariant tensor \hat{T} , having components $\hat{T}_{i_1 i_2 \dots i_k}$, as a binary tree tensor network \mathcal{T} consisting of a matrix \hat{M} which we will call the *root node*, and of $k - 2$ splitting tensors Υ^{split} as branching *internal nodes*, with the *leaf* indices of tree \mathcal{T} corresponding to the indices $\{i_1, i_2, \dots, i_k\}$ of tensor \hat{T} . We refer to decomposition \mathcal{T} as a tree decomposition of \hat{T} . Figure 20 shows an example of tree decomposition for a rank-6 tensor. It is of the form

$$\hat{T}_{i_1 i_2 i_3 i_4 i_5 i_6} = \sum_{j_1, j_2, j_3, j_4} \hat{M}_{j_1 j_2} \Upsilon_{j_1 \rightarrow i_1, j_3}^{\text{split}} \Upsilon_{j_2 \rightarrow j_4, i_6}^{\text{split}} \times \Upsilon_{j_3 \rightarrow i_2, i_3}^{\text{split}} \Upsilon_{j_4 \rightarrow i_4, i_5}^{\text{split}}, \quad (\text{A1})$$

where $\{j_1, j_2, j_3, j_4\}$ are the internal indices of the tree. The same tensor \hat{T} may be decomposed as a tree in many different ways, corresponding to different choices of the fusion tree. As an example we show two different but equivalent decompositions of a rank-4 tensor in Fig. 21. Different choices $\mathcal{T}_1, \mathcal{T}_2, \dots$ of tree decomposition for tensor \hat{T} will lead to different matrix representations $\hat{M}_1, \hat{M}_2, \dots$ of the same tensor. Finally, Fig. 22 shows how to obtain the tree decompositions from $\hat{T}_{i_1 i_2 i_3 i_4}$ by introducing an appropriate resolution of the identity, constructed from pairs of fusion operators Υ^{fuse} and splitting operators Υ^{split} in accordance with Fig. 19(b).

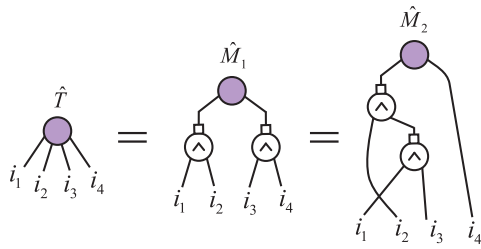


FIG. 21. (Color online) Two possible tree decompositions of a rank-4 tensor \hat{T} . Different choices $\mathcal{T}_1, \mathcal{T}_2, \dots$ of tree decomposition for tensor \hat{T} lead to different matrices $\hat{M}_1, \hat{M}_2, \dots$ for the same tensor.

The representation of a tensor \hat{T} by means of a tree decomposition is particularly useful because many tensor network algorithms may be understood as a sequence of operations carried out on tensors reduced to matrix form. For example, consider tensor network algorithms such as MPS, MERA, and PEPS. When tensors are updated in these algorithms, the new tensor is typically created as a matrix, to which operations from the primitive set \mathcal{P} of Sec. II D are then applied. When they are decomposed or contracted with other tensors, this may once again take place with the tensor in matrix form. Any such matrix form may always be understood as the matrix component of an appropriate tree decomposition \mathcal{T} of tensor \hat{T} , where the sequence of operations reshaping tensor \hat{T} to matrix \hat{M} corresponds to the contents of the shaded area in Fig. 22.

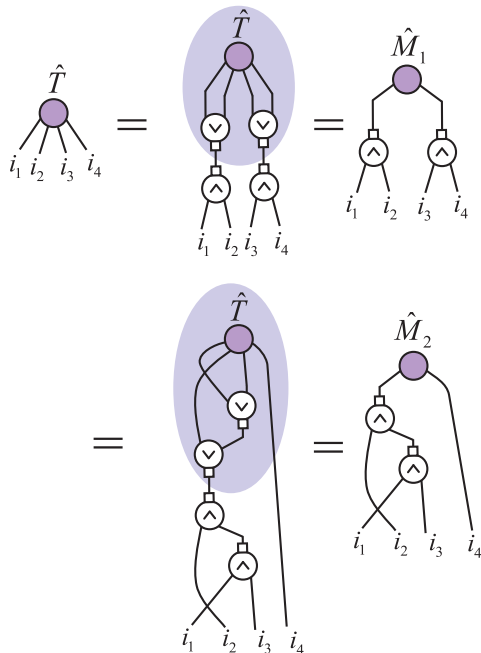


FIG. 22. (Color online) Tree decompositions of tensor \hat{T} are obtained by contracting the tensor with an appropriate resolution of the identity on its indices, selected according to the desired choice of the fusion tree \mathcal{T} . In each instance, evaluation of the contents of the shaded region yields the appropriate matrix \hat{M} .

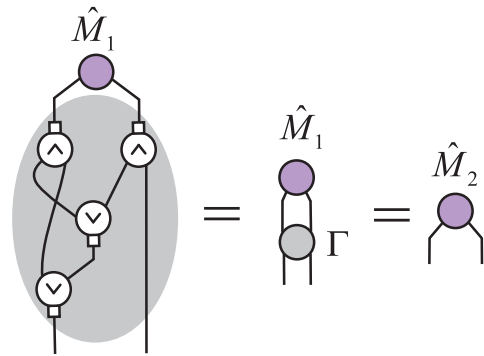


FIG. 23. (Color online) A matrix \hat{M}_1 can be reorganized into another matrix \hat{M}_2 by means of fusion tensors, splitting tensors, and the permutation of indices. These operations define a one-to-one linear map Γ that acts to reorganize the coefficients of \hat{M}_1 . Γ does not depend on the coefficients of \hat{M}_1 , but solely on the sequence of operations performed.

3. Mapping between tree decompositions

Suppose now that we have a tensor \hat{T} in matrix form \hat{M}_1 , which is associated with a particular choice of tree decomposition \mathcal{T}_1 , and we wish to transform it into another matrix form \hat{M}_2 , corresponding to another tree decomposition \mathcal{T}_2 . As indicated, this process may frequently arise during the application of many common tensor network algorithms. The new matrix \hat{M}_2 can be obtained from \hat{M}_1 by means of a series of reshaping (splitting/fusing) and permuting operations, as indicated in Fig. 23, and this series of operations may be understood as defining a map Γ :

$$\hat{M}_2 = \Gamma(\hat{M}_1). \tag{A2}$$

The map Γ is a linear map which depends only on the tree structure of \mathcal{T}_1 and \mathcal{T}_2 , and is independent of the coefficients of \hat{M}_1 . Moreover, Γ is unitary, and it follows from the construction of fusing and splitting tensors and the behavior of permutation of indices (which serves to relocate the coefficients of a tensor) that Γ simply reorganizes the coefficients of \hat{M}_1 into the coefficients of \hat{M}_2 in a one-to-one fashion.

Therefore one way to compute the matrix \hat{M}_2 from matrix \hat{M}_1 is by first computing the linear map Γ , which is independent of the specific coefficients in tensor \hat{T} , and by then applying it to \hat{M}_1 .

4. Precomputation schemes for iterative tensor network algorithms

The observation that the map Γ is independent of the specific coefficients in \hat{M}_1 is particularly useful in the context of iterative tensor network algorithms. It implies that, although the coefficients in \hat{M}_1 will change from iteration to iteration, the linear map Γ in Eq. (A2) remains unchanged. It is therefore possible to calculate the map Γ once, during the first iteration of the simulation, and then to store it in memory and reuse it during subsequent iterations. We refer to such a strategy as a *precomputation scheme*. Figure 24 contrasts the program flow of a generic iterative tensor network algorithm with and without precomputation of the transformations Γ .

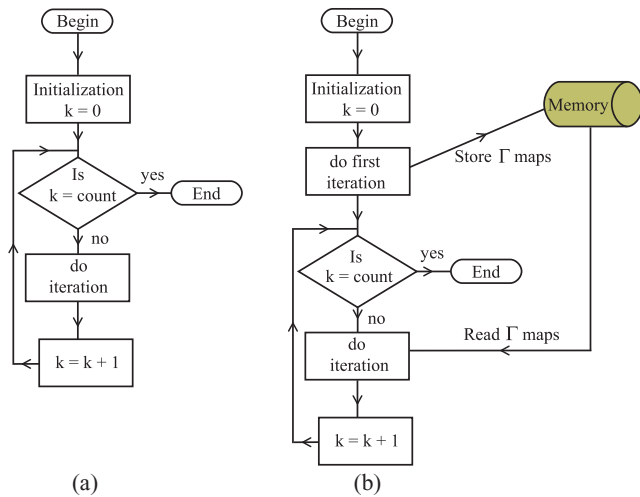


FIG. 24. (Color online) Flow diagram for the execution of a predetermined number of iterations of a generic iterative tensor network algorithm, (a) without any precomputation and (b) with precomputation of the operations Γ .

Using such a precomputation scheme, a significant speedup of simulations can be obtained, at the price of storing potentially large amounts of precomputed data (as a single iteration of the algorithm may require the application of many different transformations Γ). Therefore a tradeoff necessarily exists between the amount of speedup that can be obtained and the memory requirement that this entails. In this section we describe two different precomputation schemes. The first one fully precomputes and stores all maps Γ , and is relatively straightforward to implement. This results in the maximal increase in simulation speed, but implementation requires a large amount of memory. The second scheme only partially precomputes the maps Γ , resulting in a moderate speedup of simulations, but with memory requirements which are also similarly more modest.

a. Maximal precomputation scheme

As noted in Sec. III of this Appendix, applying the map Γ to a matrix \hat{M}_1 simply reorganizes its coefficients to produce the matrix \hat{M}_2 . Moreover, if the indices of matrices \hat{M}_1 and \hat{M}_2 are fused to yield vectors \hat{V}_1 and \hat{V}_2 then the map Γ may be understood as a permutation matrix, and this in turn may be concisely represented as a string of integers $\Gamma = \gamma_1, \dots, \gamma_{|\hat{M}_1|}$ such that entry i of $\hat{V}_2 = \Gamma \hat{V}_1$ is given by entry γ_i of vector \hat{V}_1 . Because all of the elements from which Γ is composed are sparse, unitary, and composed entirely of 0's and 1's, the permutation to which Γ corresponds may be calculated at a total cost of only $O(|\hat{M}_1|)$, where $|\hat{M}_1|$ counts only the elements of \hat{M}_1 which are not fixed to be zero by the symmetry constraints of Eq. (83). In essence, for each element of the vector \hat{V}_1 one identifies the corresponding number and degeneracy indices $(n_i^{\hat{M}_1}, t_i^{\hat{M}_1})$ on each leg $i \in \{1, 2\}$ of matrix \hat{M}_1 . One can then read down the figure, applying each table Υ^{fuse} or Υ^{split} in turn to identify the corresponding labels (n', t') on the intermediate legs, until finally the corresponding labels on the indices of \hat{M}_2 are obtained. There is then a further 1:1 mapping from each set of labels $(n_1^{\hat{M}_2}, t_1^{\hat{M}_2})$, $(n_2^{\hat{M}_2}, t_2^{\hat{M}_2})$ on \hat{M}_2

to the corresponding entry in \hat{V}_2 , completing the definition of Γ as a map from \hat{V}_1 to \hat{V}_2 .

Storing the map Γ for a transformation such as the one shown in Fig. 23 imposes a memory cost of $O(|\hat{M}_1|)$. The application of this map also incurs a computational cost of $O(|\hat{M}_1|)$, but computational overhead is saved in not having to reconstruct the map Γ on every iteration of the algorithm.

b. Partial precomputation scheme

The $O(|\hat{M}_1|)$ memory cost incurred in the previous scheme can be significant for large matrices. However, we may reduce this cost by replacing the single permutation Γ employed in that scheme with multiple smaller operations which may also be precomputed. In this approach \hat{M}_1 is retained in matrix form rather than being reshaped into a vector, and we precompute permutations to be performed on its rows and columns.

First, we decompose all the fusion and splitting tensors into two pieces in accordance with Fig. 19(c). Next, we recognize that any permutations applied to one or more legs of a fusion or splitting tensor may always be written as a single permutation applied to the coupled index [Fig. 25(a)]. We use this to replace all permutations on the intermediate indices of the diagram with equivalent permutations acting only on the indices of \hat{M}_1 and the open indices, as shown for a simple example in Fig. 25(b). The residual fusion and splitting operations, depicted by just a circle enclosing an arrow, then simply carry out fusion and splitting of indices as would be performed in the absence of symmetry (2), (3). These operations are typically far faster than their symmetric counterparts as they do not need to sort the entries of their output indices according to particle number.

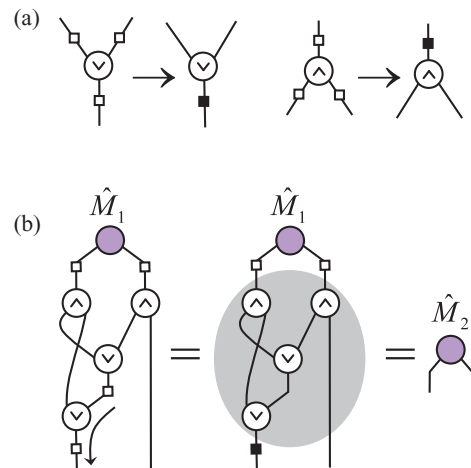


FIG. 25. (Color online) (a) Permutations applied to one or more legs of a fusion or splitting tensor can be replaced by an appropriate permutation on the coupled index. This process can be used to replace all permutations applied on internal indices of a diagram such as Fig. 23 with net permutations on the indices of \hat{M}_1 and on the open indices of the network, as in shown in (b). The residual fusion and splitting operations, depicted as an arrow in a circle, simply perform the basic tensor product operation and its inverse, Eqs. (2) and (3), as described in Fig. 19(c) and Sec. I of this Appendix.

In subsequent iterations, the matrix \hat{M}_2 is obtained from \hat{M}_1 by consecutively

(1) permuting the rows and columns of \hat{M}_1 using the precomputed net permutations which act on the legs of \hat{M}_1 ;

(2) performing any elementary (nonsymmetric) splitting, permuting of indices, and fusing operations, as described by the gray-shaded region in Fig. 25(b);

(3) permuting the rows and columns of the resulting matrix, using the precomputed net permutations which act on the open legs of Fig. 25(b).

When matrix \hat{M}_1 is defined compactly, as in Eq. (83), so that elements which are identically zero by symmetry are not explicitly stored, a tensor \hat{T} is constructed from multiple blocks identified by U(1) charge labels on their indices [$\hat{T}_{n_1 n_2 \dots n_k}$ in Eq. (83)]. Under these conditions the elementary splitting, fusing, and permutation operations of

step (2) above are applied to each individual block, but some additional computational overhead is incurred in determining the necessary rearrangements of these blocks arising out of the actions performed. This rearrangement may be computed on the fly, or may also be precomputed as a mapping between the arrangement of blocks in \hat{M}_1 and that in \hat{M}_2 .

The memory required to store the precomputation data in this scheme is dominated by the size of the net permutations collected on the matrix indices, and is therefore of $O(\sqrt{|\hat{M}_1|})$. The overall cost of obtaining \hat{M}_2 from \hat{M}_1 is once again of $O(|\hat{M}_1|)$, but is in general higher than the previous scheme as this cost now involves two complete permutations of the matrix coefficients, as well as a reorganization of the block structure of \hat{M}_1 which may possibly be computed at runtime. Nevertheless, in situations where memory constraints are significant, partial precomputation schemes of this sort may be preferred.

¹M. Fannes, B. Nachtergaele, and R. Werner, *Commun. Math. Phys.* **144**, 443 (1992).
²S. Ostlund and S. Rommer, *Phys. Rev. Lett.* **75**, 3537 (1995).
³D. Perez-Garcia, F. Verstraete, M. M. Wolf, and J. I. Cirac, *Quantum Inf. Comput.* **7**, 401 (2007).
⁴K. G. Wilson, *Rev. Mod. Phys.* **47**, 773 (1975).
⁵S. R. White, *Phys. Rev. Lett.* **69**, 2863 (1992).
⁶S. R. White, *Phys. Rev. B* **48**, 10345 (1993).
⁷U. Schollwöck, *Rev. Mod. Phys.* **77**, 259 (2005).
⁸I. P. McCulloch, e-print arXiv:0804.2509v1 (unpublished).
⁹G. Vidal, *Phys. Rev. Lett.* **91**, 147902 (2003).
¹⁰G. Vidal, *Phys. Rev. Lett.* **93**, 040502 (2004).
¹¹G. Vidal, *Phys. Rev. Lett.* **98**, 070201 (2007).
¹²A. J. Daley, C. Kollath, U. Schollwöck, and G. Vidal, *J. Stat. Mech.: Theor. Exp.* (2004) P04005.
¹³S. R. White and A. E. Feiguin, *Phys. Rev. Lett.* **93**, 076401 (2004).
¹⁴U. Schollwöck, *J. Phys. Soc. Jpn. S* **74**, 246 (2005).
¹⁵Y. Y. Shi, L.-M. Duan, and G. Vidal, *Phys. Rev. A* **74**, 022320 (2006).
¹⁶G. Vidal, *Phys. Rev. Lett.* **99**, 220405 (2007).
¹⁷G. Vidal, *Phys. Rev. Lett.* **101**, 110501 (2008).
¹⁸G. Evenbly and G. Vidal, *Phys. Rev. B* **79**, 144108 (2009).
¹⁹V. Giovannetti, S. Montangero, and R. Fazio, *Phys. Rev. Lett.* **101**, 180503 (2008).
²⁰R. N. C. Pfeifer, G. Evenbly, and G. Vidal, *Phys. Rev. A* **79**, 040301(R) (2009).
²¹G. Vidal, in *Understanding Quantum Phase Transitions*, edited by L. D. Carr (Taylor & Francis, Boca Raton, 2010).
²²F. Verstraete and J. I. Cirac, e-print arXiv:cond-mat/0407066v1 (unpublished).
²³G. Sierra and M. A. Martín-Delgado, in *Proceedings of the Workshop on the Exact Renormalization Group, Faro (Portugal)* (World Scientific 1998).
²⁴T. Nishino and K. Okunishi, *J. Phys. Soc. Jpn.* **67**, 3066 (1998).
²⁵Y. Nishio, N. Maeshima, A. Gendiar, and T. Nishino, e-print arXiv:cond-mat/0401115v1 (unpublished).
²⁶V. Murg, F. Verstraete, and J. I. Cirac, *Phys. Rev. A* **75**, 033605 (2007).
²⁷J. Jordan, R. Orus, G. Vidal, F. Verstraete, and J. I. Cirac, *Phys. Rev. Lett.* **101**, 250602 (2008).
²⁸Z.-C. Gu, M. Levin, and X.-G. Wen, *Phys. Rev. B* **78**, 205116 (2008).
²⁹H. C. Jiang, Z. Y. Weng, and T. Xiang, *Phys. Rev. Lett.* **101**, 090603 (2008).
³⁰Z. Y. Xie, H. C. Jiang, Q. N. Chen, Z. Y. Weng, and T. Xiang, *Phys. Rev. Lett.* **103**, 160601 (2009).
³¹V. Murg, F. Verstraete, and J. I. Cirac, *Phys. Rev. B* **79**, 195119 (2009).
³²L. Tagliacozzo, G. Evenbly, and G. Vidal, *Phys. Rev. B* **80**, 235127 (2009).
³³V. Murg, O. Legeza, R. M. Noack, and F. Verstraete, *Phys. Rev. B* **82**, 205105 (2010).
³⁴G. Evenbly and G. Vidal, *Phys. Rev. B* **81**, 235102 (2010).
³⁵G. Evenbly and G. Vidal, *New J. Phys.* **12**, 025007 (2010).
³⁶M. Aguado and G. Vidal, *Phys. Rev. Lett.* **100**, 070404 (2008).
³⁷L. Cincio, J. Dziarmaga, and M. M. Rams, *Phys. Rev. Lett.* **100**, 240603 (2008).
³⁸G. Evenbly and G. Vidal, *Phys. Rev. Lett.* **102**, 180406 (2009).
³⁹R. König, B. W. Reichardt, and G. Vidal, *Phys. Rev. B* **79**, 195123 (2009).
⁴⁰G. Evenbly and G. Vidal, *Phys. Rev. Lett.* **104**, 187203 (2010).
⁴¹P. Corboz, G. Evenbly, F. Verstraete, and G. Vidal, *Phys. Rev. A* **81**, 010303(R) (2010).
⁴²C. V. Kraus, N. Schuch, F. Verstraete, and J. I. Cirac, *Phys. Rev. A* **81**, 052338 (2010).
⁴³C. Pineda, T. Barthel, and J. Eisert, *Phys. Rev. A* **81**, 050303(R) (2010).
⁴⁴P. Corboz and G. Vidal, *Phys. Rev. B* **80**, 165129 (2009).
⁴⁵T. Barthel, C. Pineda, and J. Eisert, *Phys. Rev. A* **80**, 042333 (2009).
⁴⁶Q.-Q. Shi, S.-H. Li, J.-H. Zhao, and H.-Q. Zhou, e-print arXiv:0907.5520v1 (unpublished).
⁴⁷S.-H. Li, Q.-Q. Shi, and H.-Q. Zhou, e-print arXiv:1001.3343v1 (unpublished).
⁴⁸P. Corboz, R. Orus, B. Bauer, and G. Vidal, *Phys. Rev. B* **81**, 165104 (2010).
⁴⁹I. Pizorn and F. Verstraete, *Phys. Rev. B* **81**, 245110 (2010).
⁵⁰Z.-C. Gu, F. Verstraete, and X.-G. Wen, e-print arXiv:1004.2563v1 (unpublished).
⁵¹J. F. Cornwell, *Group Theory in Physics* (Academic, San Diego, 1997).

- ⁵²S. Singh, R. N. C. Pfeifer, and G. Vidal, *Phys. Rev. A* **82**, 050301 (2010).
- ⁵³S. Singh and G. Vidal (unpublished).
- ⁵⁴S. Ramasesha, S. K. Pati, H. R. Krishnamurthy, Z. Shuai, and J. L. Bredas, *Phys. Rev. B* **54**, 7598 (1996).
- ⁵⁵G. Sierra and T. Nishino, *Nucl. Phys. B* **495**, 505 (1997).
- ⁵⁶W. Tatsuaki, *Phys. Rev. E* **61**, 3199 (2000).
- ⁵⁷I. P. McCulloch and M. Gulacsi, *Europhys. Lett.* **57**, 852 (2002).
- ⁵⁸S. Bergkvist, I. P. McCulloch, and A. Rosengren, *Phys. Rev. A* **74**, 053419 (2006).
- ⁵⁹S. Pittel and N. Sandulescu, *Phys. Rev. C* **73**, 014301 (2006).
- ⁶⁰I. McCulloch, *J. Stat. Mech.: Theor. Exp.* (2007) P10014.
- ⁶¹D. Perez-Garcia, M. M. Wolf, M. Sanz, F. Verstraete, and J. I. Cirac, *Phys. Rev. Lett.* **100**, 167202 (2008).
- ⁶²M. Sanz, M. M. Wolf, D. Perez-Garcia, and J. I. Cirac, *Phys. Rev. A* **79**, 042308 (2009).
- ⁶³A. J. Daley, S. R. Clark, D. Jaksch, and P. Zoller, *Phys. Rev. A* **72**, 043618 (2005).
- ⁶⁴I. Danshita, J. E. Williams, C. A. R. Sá de Melo, and C. W. Clark, *Phys. Rev. A* **76**, 043606 (2007).
- ⁶⁵D. Muth, B. Schmidt, and M. Fleischhauer, *New J. Phys.* **12**, 083065 (2010).
- ⁶⁶R. V. Mishmash, I. Danshita, C. W. Clark, and L. D. Carr, *Phys. Rev. A* **80**, 053612 (2009).
- ⁶⁷S. Singh, H.-Q. Zhou, and G. Vidal, *New J. Phys.* **12**, 033029 (2010).
- ⁶⁸Z. Cai, L. Wang, X. C. Xie, and Y. Wang, *Phys. Rev. A* **81**, 043602 (2010).
- ⁶⁹D. Perez-Garcia, M. Sanz, C. E. Gonzalez-Guillen, M. M. Wolf, and J. I. Cirac, *New J. Phys.* **12**, 025010 (2010).
- ⁷⁰H. H. Zhao, Z. Y. Xie, Q. N. Chen, Z. C. Wei, J. W. Cai, and T. Xiang, *Phys. Rev. B* **81**, 174411 (2010).
- ⁷¹N. Schuch, I. Cirac, and D. Perez-Garcia, *Ann. Phys.* **325**, 2153 (2010).
- ⁷²B. Swingle and X.-G. Wen, e-print [arXiv:1001.4517v1](https://arxiv.org/abs/1001.4517v1) (unpublished).
- ⁷³X. Chen, B. Zeng, Z.-C. Gu, I. L. Chuang, and X.-G. Wen, *Phys. Rev. B* **82**, 165119 (2010).
- ⁷⁴L. Tagliacozzo and G. Vidal, e-print [arXiv:1007.4145v1](https://arxiv.org/abs/1007.4145v1) (unpublished).
- ⁷⁵The fundamental theorem of Abelian groups states that every finite Abelian group may be expressed as a direct sum of cyclic subgroups of prime-power order.

Implementation of non-Abelian symmetries

I

In this and the following chapter we will address the implementation of global non-Abelian symmetries into tensor network algorithms. We consider the specific context of an internal $SU(2)$ symmetry, that gives rise to spin isotropy. This is an extremely important symmetry that appears amply in lattice spin models.

In this chapter we will focus on the conceptual aspects of incorporating the symmetry. The theoretic formalism developed in Chapter 3 will be adapted to the specific case of $SU(2)$ symmetry. We consider tensors that are invariant under the action of $SU(2)$. The structural tensors, that are part of the canonical decomposition, are highly non-trivial (and are given in terms of the Clebsch-Gordan coefficients). However, the key advantage of the canonical decomposition is that it allows tensor manipulations, such as reshape or permutation of indices, to be broken into an independent manipulation of degeneracy tensors and of structural tensors.

In the context of numerical simulations the canonical decomposition leads to a computational gain. Computational cost is incurred only when manipulating degeneracy tensors. On the other hand, structural tensors are manipulated *algebraically* by exploiting properties of the Clebsch-Gordan coefficients. Manipulations of the structural tensors reduce to evaluating a spin network. This process involves integrating over the degrees of free-

dom associated with spin projection, which are therefore suppressed in the outcome of the tensor manipulation, as is expected in a spin isotropic description.

In Chapter 6 we will describe a specific implementation scheme of elementary manipulations of $SU(2)$ -invariant tensors. We will address several concerns that are of importance in the practical implementations of the symmetry.

5.1 Preparatory Review: Tensor network formalism

In this section we review the basic formalism of tensors and tensor networks. Even though we do not make any explicit reference to symmetry here, our formalism is directed towards $SU(2)$ -invariant tensors.

We begin by recalling the basic notion of a tensor. A *tensor* \hat{T} is a multidimensional array of complex numbers $\hat{T}_{i_1 i_2 \dots i_k}$. The *rank* of a tensor is the number k of indices. The *size* of an index i , denoted $|i|$, is the number of values that the index takes, $i \in 1, 2, \dots, |i|$. The *size* of a tensor \hat{T} , denoted $|\hat{T}|$, is the number of complex numbers it contains, namely, $|\hat{T}| = |i_1| \times |i_2| \times \dots \times |i_k|$.

5.1.1 Tensors as linear maps

For the purpose of this thesis we regard a rank- k tensor as a linear map. To this end, we first equip each index i_l , $l = 1, 2, \dots, k$, of the tensor with a direction: ‘in’ or ‘out’, that is, either incoming into the tensor or outgoing from the tensor respectively. We denote by \vec{D} the directions associated with the indices of tensor \hat{T} , namely, $\vec{D}(l) = \text{‘in’}$ if i_l is an incoming index and $\vec{D}(l) = \text{‘out’}$ if i_l is outgoing.

Let us also use index i of the tensor to label a basis $|i\rangle$ of a complex vector space $\mathbb{V}^{[i]} \cong \mathbb{C}^{|i|}$ of dimension $|i|$. Then a rank-one ($k = 1$) tensor with an outgoing index i represents a vector in $\mathbb{V}^{[i]}$, a rank-two ($k = 2$) tensor \hat{T} with one incoming index a and one outgoing index b represents a matrix and so on.

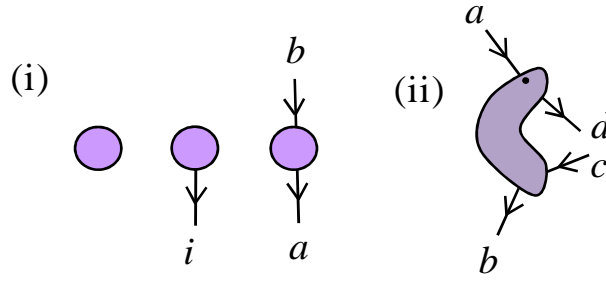


Figure 5.1 – Graphical representation of tensors by means of a shape e.g. circle or a “blob” with emanating lines corresponding to indices of the tensor. Indices may be incoming or outgoing as indicated by arrows. (i) Graphical representations of tensors with rank 0, 1 and 2, corresponding to a complex number $c \in \mathbb{C}$, a vector $|v\rangle \in \mathbb{C}^{[i]}$ and a matrix $\hat{M} \in \mathbb{C}^{|a| \times |b|}$. (ii) Graphical representation of a tensor \hat{T} with components \hat{T}_{abcd} with directions $\vec{D} = \{\text{‘in’}, \text{‘out’}, \text{‘in’}, \text{‘out’}\}$. Notice that the indices emerge in a counterclockwise order, perpendicular to the boundary of the blob; the first index is identified by the presence of a dot within the blob close to the index. All arrows in a tensor diagram point downwards, that may be interpreted as choosing a metaphorical “time” that flows downwards.

A tensor can be unambiguously regarded as a linear map from a vector space to complex numbers \mathbb{C} . For instance, a vector can be regarded as a linear map from $\mathbb{V}^{[i]}$ to \mathbb{C} , a matrix \hat{T} can be regarded as a linear map from $(\mathbb{V}^{[a]})^* \otimes \mathbb{V}^{[b]}$ to \mathbb{C} where $(\mathbb{V}^{[a]})^*$ is the dual of vector space $\mathbb{V}^{[a]}$ etc. More generally, we can use a rank- k tensor \hat{T} to define a linear map from the tensor product of k vector spaces to \mathbb{C} in the following way. Define a set $\mathbb{W}^{[i_l]}$, $l = 1, 2, \dots, k$, of k spaces where

$$\mathbb{W}^{[i_l]} = \begin{cases} \mathbb{V}^{[i_l]} & \text{if } \vec{D}(l) = \text{‘out’}, \\ (\mathbb{V}^{[i_l]})^* & \text{if } \vec{D}(l) = \text{‘in’}, \end{cases} \quad (5.1)$$

where the $(\mathbb{V}^{[i_l]})^*$ is the dual of vector space $\mathbb{V}^{[i_l]}$. Then tensor \hat{T} can be regarded as a linear map from the product space $\bigotimes_l \mathbb{W}^{[i_l]}$ to \mathbb{C} ,

$$\hat{T} : \bigotimes_l \mathbb{W}^{[i_l]} \rightarrow \mathbb{C}. \quad (5.2)$$

We will find this viewpoint of tensors useful for subsequent generalization to $SU(2)$ -invariant tensors.

It is convenient to use a graphical representation of tensors, as illustrated in Fig. 1, where

a tensor is depicted as a “blob” (or by a shape e.g., circle, square etc.) and each of its indices is represented by a line emerging *perpendicular* from the boundary of the blob. In order to specify which index corresponds to which emerging line, we follow the prescription that the lines corresponding to indices $\{i_1, i_2, \dots, i_k\}$ emerge in counterclockwise order. The first index corresponds to the line emerging closest to a mark (black dot) inside the boundary of the blob (or the first line encountered while proceeding counterclockwise from nine o'clock in case the tensor is depicted as a circle without a mark). The direction of an index is depicted by attaching an arrow to the line corresponding to the index. We follow a convention that all arrows in a diagram point downwards.

5.1.2 Elementary manipulations of a tensor

A tensor can be transformed into another tensor in several elementary ways. These include, *reversing* the direction of one or several of its indices, *permuting* its indices, and/or *reshaping* its indices.

Reversing the direction of an index corresponds to mapping the vector space that is associated with the index to its dual. For example, in

$$(\hat{T}')_{\bar{a}b} = \hat{T}_{ab}, \quad (5.3)$$

if index a is associated to a vector space $\mathbb{V}^{[a]}$, then index \bar{a} that is obtained by reversing the direction of a is associated with the dual space $(\mathbb{V}^{[a]})^*$. Since all arrows in a diagram point downwards, reversing the direction of an index i is depicted [Fig. 5.2(i)] by ‘bending’ the line corresponding to i upwards if it is an outgoing index or downwards if it is an incoming index. Since tensor \hat{T}' is components wise equal to tensor \hat{T} arrows appear to be irrelevant in the absence of the symmetry. However, arrows will play an important role when we consider $SU(2)$ -invariant tensors since they specify how the group acts on each index of a given tensor.

A *permutation* of indices corresponds to creating a new tensor \hat{T}' from \hat{T} by simply changing the order in which the indices appear, e.g.

$$(\hat{T}')_{bac} = \hat{T}_{abc}. \quad (5.4)$$

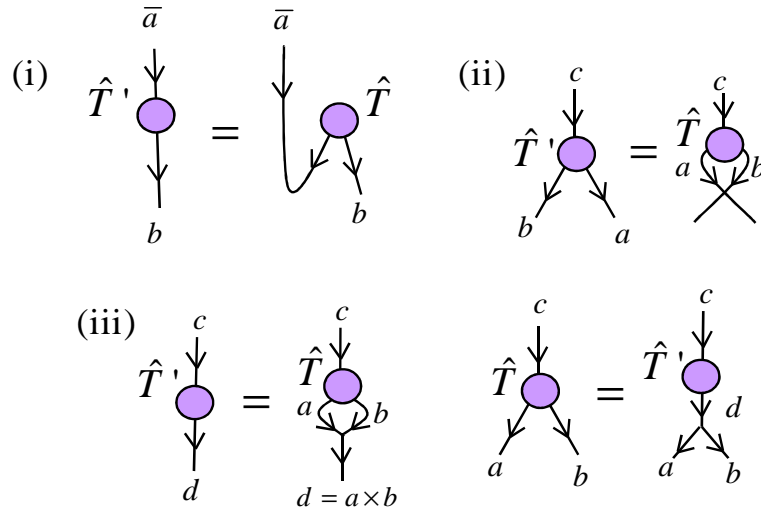


Figure 5.2 – Transformations of a tensor: (i) Reversing direction of an index, Eq. (5.3). (ii) Permutation of indices, Eq. (5.4). (iii) Fusion of indices a and b into $d = a \times b$, Eq. (5.5); splitting of index $d = a \times b$ into a and b , Eq. (5.6).

Permutation of indices is depicted by intercrossing indices, as illustrated in Fig. 5.2(ii). Note that when the permutation involves the first index of the tensor the mark, that indicates the first index, is also shifted to a new location within the blob. It is useful to note that an arbitrary permutation of the indices can be broken into a sequence of *swaps* of adjacent indices wherein the position of two indices are interchanged at a time.

Last but not the least, a tensor \hat{T} can be *reshaped* into a new tensor \hat{T}' by ‘fusing’ two adjacent indices into a single index and/or ‘splitting’ an index into two indices. For instance, in

$$(\hat{T}')_{dc} = \hat{T}_{abc}, \quad d = a \times b, \quad (5.5)$$

tensor \hat{T}' is obtained from tensor \hat{T} by fusing indices $a \in \{1, \dots, |a|\}$ and $b \in \{1, \dots, |b|\}$ together into a single index d of size $|d| = |a| \cdot |b|$ that runs over all pairs of values of a and b , i.e. $d \in \{(1, 1), (1, 2), \dots, (|a|, |b| - 1), (|a|, |b|)\}$, whereas in

$$\hat{T}_{abc} = (\hat{T}')_{dc}, \quad d = a \times b, \quad (5.6)$$

tensor \hat{T} is recovered from \hat{T}' by splitting index d of \hat{T}' back into indices a and b . Reshape of the indices is depicted as shown in Fig. 5.2(iii).

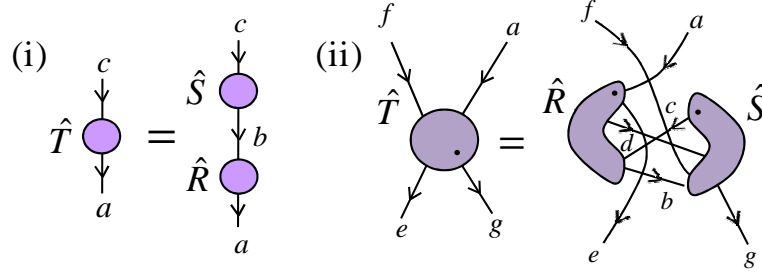


Figure 5.3 – (i) Graphical representation of the matrix multiplication of two matrices \hat{R} and \hat{S} into a new matrix \hat{T} , Eq. (5.7). (ii) Graphical representation of an example of the multiplication of two tensors \hat{R} and \hat{S} into a new tensor \hat{T} , Eq. (5.8).

5.1.3 Multiplication of two tensors

Given two matrices \hat{R} and \hat{S} with components \hat{R}_{ab} and \hat{S}_{bc} , we can multiply them together to obtain a new matrix \hat{T} , $\hat{T} = \hat{R} \cdot \hat{S}$, with components

$$\hat{T}_{ac} = \sum_b \hat{R}_{ab} \hat{S}_{bc}, \quad (5.7)$$

by summing over or *contracting* index b . The multiplication of matrices \hat{R} and \hat{S} is represented graphically by connecting together the emerging lines of \hat{R} and \hat{S} corresponding to the contracted index, as shown in Fig. 5.3(i).

Matrix multiplication can be generalized to tensors, such that, an incoming index of one tensor is identified and contracted with an outgoing index of another. For instance, given tensor \hat{R} with components \hat{R}_{abcde} and directions {'in', 'out', 'in', 'out', 'out'}, and tensor \hat{S} with components \hat{S}_{cdfbg} and directions {'out', 'in', 'in', 'in', 'out'}, we can define a tensor \hat{T} with components \hat{T}_{gafe} that are given by,

$$\hat{T}_{gafe} = \sum_{bcd} \hat{R}_{abcde} \hat{S}_{cdfbg}. \quad (5.8)$$

Note that each of the indices b, c and d , that are contracted, is incoming into one tensor and outgoing from the other. The multiplication is represented graphically by connecting together the lines emerging from \hat{R} and \hat{S} corresponding to each of these indices, as shown in Fig. 5.3(ii).

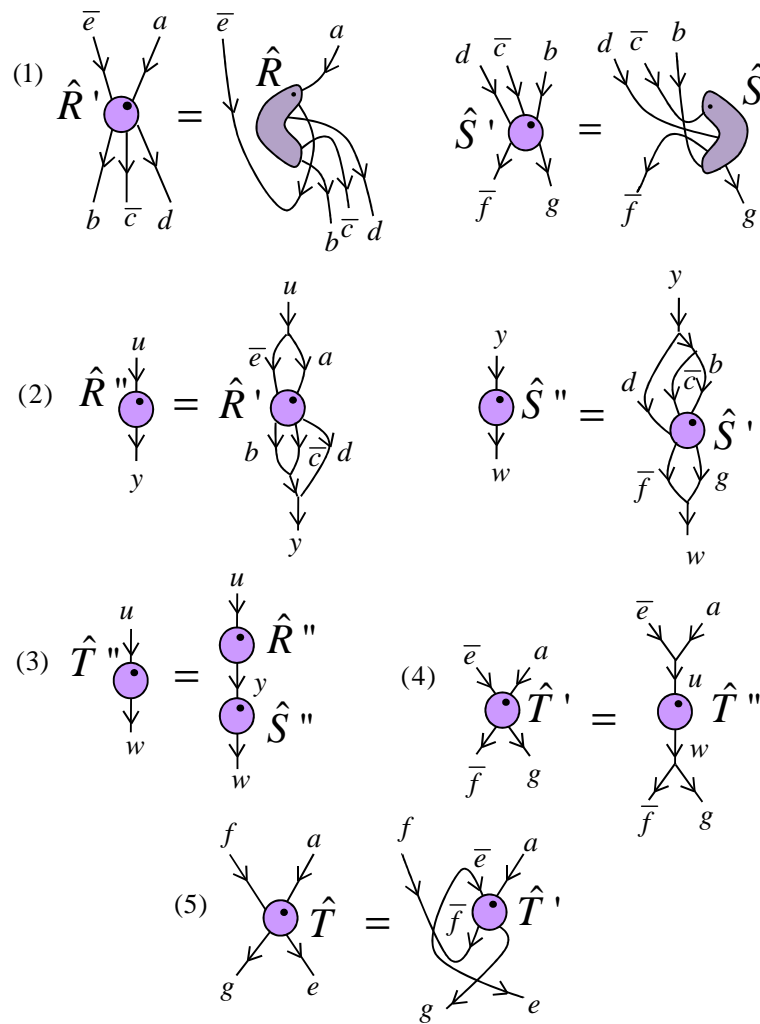


Figure 5.4 – Graphical representations of the five elementary steps 1-5 into which one can decompose the multiplication of the tensors of Eq. (5.8).

Multiplication of two tensors can be broken down into a sequence of elementary steps by transforming the tensors into matrices, multiplying the matrices together, and then transforming the resulting matrix back into a tensor. Next we describe these steps for the contraction given in Eq. (5.8). They are illustrated in Fig. 5.4.

1. *Reverse* and *Permute* the indices of tensor \hat{R} in such a way that the indices b, c and d that are contracted appear in the last positions as *outgoing* indices and in a given order, e.g. $\bar{b}\bar{c}\bar{d}$, and the remaining indices a and e appear in the first positions as *incoming* indices; similarly reverse and permute the indices of \hat{S} so that the indices

b, c and d appear in the first positions as *incoming* indices and in the same order, $\bar{b}\bar{c}\bar{d}$, and the remaining indices \bar{f} and g appear in the last positions as *outgoing* indices,

$$\begin{aligned}(\hat{R}')_{a\bar{e} \bar{b}cd} &= (\hat{R})_{abcde}, \\ (\hat{S}')_{\bar{b}\bar{c}\bar{d} \bar{f}g} &= (\hat{S})_{cdfbg}.\end{aligned}\tag{5.9}$$

2. *Reshape* tensor \hat{R}' into a matrix \hat{R}'' by fusing into a single index u all the indices that are not contracted, $u = a \times \bar{e}$, and into a single index y all indices that are contracted, $y = b \times \bar{c} \times d$; similarly reshape tensor \hat{S}' into a matrix \hat{S}'' with indices $\bar{y} = \bar{b} \times \bar{c} \times d$ and $w = \bar{f} \times g$ (indices b, c and d are required to be fused according to the *same* fusion sequence in the two tensors. A possible fusion sequence may involve, for example, first fusing b and c and then fusing the resulting index with d),

$$\begin{aligned}(\hat{R}'')_{uy} &= (\hat{R}')_{a\bar{e}b\bar{c}d}, \\ (\hat{S}'')_{\bar{y}w} &= (\hat{S}')_{\bar{b}\bar{c}\bar{d}\bar{f}g}.\end{aligned}\tag{5.10}$$

3. *Multiply* matrices \hat{R}'' and \hat{S}'' to obtain a matrix \hat{T}'' with components

$$(\hat{T}'')_{uw} = \sum_y (\hat{R}'')_{uy} (\hat{S}'')_{\bar{y}w}.\tag{5.11}$$

4. *Reshape* matrix \hat{T}'' into a tensor \hat{T}' by splitting indices $u = a \times \bar{e}$ and $w = \bar{f} \times g$,

$$(\hat{T}')_{ae\bar{f}g} = (\hat{T}'')_{uw}.\tag{5.12}$$

5. *Reverse* and *Permute* indices of tensor \hat{T}' in the order in which they appear in \hat{T} ,

$$\hat{T}_{afge} = (\hat{T}')_{a\bar{e}\bar{f}g}.\tag{5.13}$$

The contraction of Eq. (5.8) can be implemented at once, without breaking the multiplication down into elementary steps. However, it is often more convenient to compose the above elementary steps since, for instance, in this way one can use existing linear algebra libraries for matrix multiplication. In addition, it can be seen that the leading computational cost in multiplying two large tensors is not changed when decomposing the contraction in the above steps.

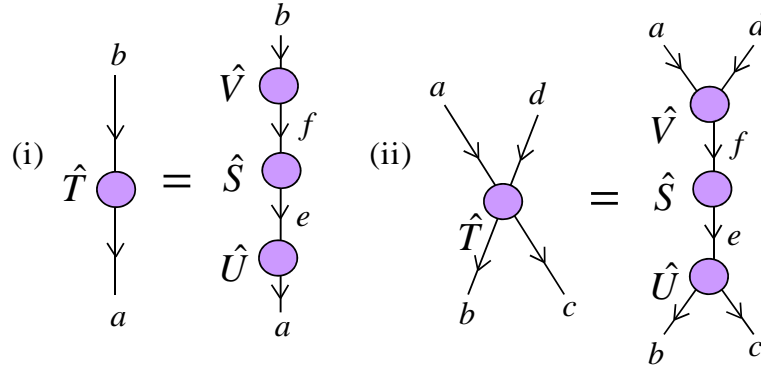


Figure 5.5 – (i) Factorization of a matrix \hat{T} according to a singular value decomposition, Eq. (5.14). (ii) Factorization of a rank-4 tensor \hat{T} according to one of several possible singular value decompositions.

5.1.4 Factorization of a tensor

A matrix \hat{T} can be factorized into the product of two (or more) matrices in one of several canonical forms. For instance, the *singular value decomposition*

$$\hat{T}_{ab} = \sum_{c,d} \hat{U}_{ac} \hat{S}_{cd} \hat{V}_{db} = \sum_c \hat{U}_{ac} s_c \hat{V}_{cb} \quad (5.14)$$

factorizes \hat{T} into the product of two unitary matrices \hat{U} and \hat{V} , and a diagonal matrix \hat{S} with non-negative diagonal elements $s_c = \hat{S}_{cc}$ known as the *singular values* of \hat{T} [Fig. 5.5(i)]. On the other hand, the *eigenvalue* or *spectral decomposition* of a square matrix \hat{T} is of the form

$$\hat{T}_{ab} = \sum_{c,d} \hat{M}_{ac} D_{cd} (\hat{M}^{-1})_{db} = \sum_c \hat{M}_{ac} \lambda_c (\hat{M}^{-1})_{cb} \quad (5.15)$$

where \hat{M} is an invertible matrix whose columns encode the eigenvectors $|\lambda_c\rangle$ of \hat{T} ,

$$\hat{T}|\lambda_c\rangle = \lambda_c|\lambda_c\rangle, \quad (5.16)$$

\hat{M}^{-1} is the inverse of \hat{M} , and \hat{D} is a diagonal matrix, with the eigenvalues $\lambda_c = \hat{D}_{cc}$ on its diagonal. Other useful factorizations include the LU decomposition, the QR decomposition, etc. We refer to any such decomposition generically as a *matrix factorization*.

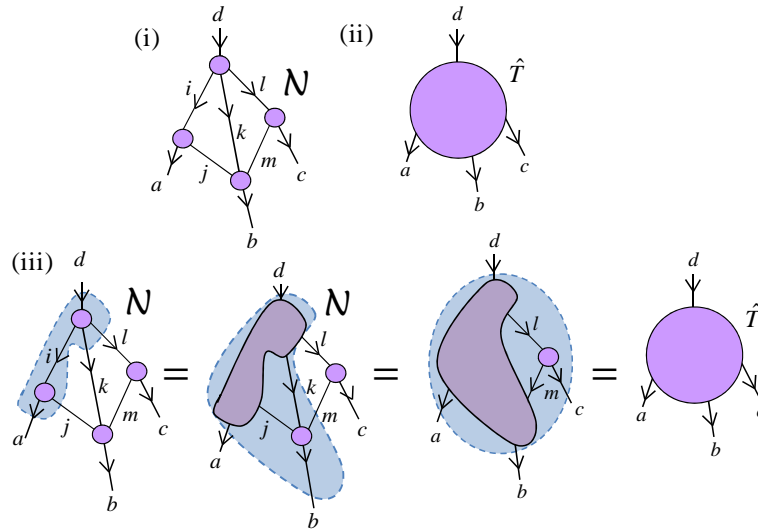


Figure 5.6 – (i) Example of a tensor network \mathcal{N} . (ii) Tensor \hat{T} of which the tensor network \mathcal{N} could be a representation. (iii) Tensor \hat{T} can be obtained from \mathcal{N} through a sequence of contractions of pairs of tensors. Shading indicates the two tensors to be multiplied together at each step. The product tensor is depicted by a blob that covers the two tensors that are multiplied.

A tensor \hat{T} with more than two indices can be converted into a matrix in several ways by specifying how to join its indices into two subsets. After specifying how tensor \hat{T} is to be regarded as a matrix, we can factorize \hat{T} according to any of the above matrix factorizations, as illustrated in Fig. 5.5(ii) for a singular value decomposition. This requires first reversing directions, permuting and reshaping the indices of \hat{T} to form a matrix, then decomposing the latter, and finally restoring the open indices of the resulting matrices into their original form by undoing the reshapes, permutations and reversal of directions.

5.1.5 Tensor networks and their manipulation

A *tensor network* \mathcal{N} is a set of tensors whose indices are connected according to a network pattern, e.g. Fig. 5.6.

Given a tensor network \mathcal{N} , a single tensor \hat{T} can be obtained by contracting all the indices that connect the tensors in \mathcal{N} [Fig. 5.6(ii)]. Here, the indices of tensor \hat{T} correspond to

the open indices of the tensor network \mathcal{N} . We then say that the tensor network \mathcal{N} is a tensor network decomposition of \hat{T} . One way to obtain \hat{T} from \mathcal{N} is through a sequence of contractions involving two tensors at a time [Fig. 5.6(iii)]. Notice how a tensor that is obtained by contracting a region of a tensor network is conveniently depicted by a blob or shape that covers that region.

From a tensor network decomposition \mathcal{N} for a tensor \hat{T} , another tensor network decomposition for the same tensor \hat{T} can be obtained in many ways. One possibility is to replace two tensors in \mathcal{N} with the tensor resulting from contracting them together, as is done in each step of Fig. 5.6(iii). Another way is to replace a tensor in \mathcal{N} with a decomposition of that tensor (e.g. with a singular value decomposition). In this thesis, we will be concerned with manipulations of a tensor network that, as in the case of multiplying two tensors or decomposing a tensor, can be broken down into a sequence of operations from the following list:

1. Reversal of direction of indices of a tensor, Eq. (5.3).
2. Permutation of the indices of a tensor, Eq. (5.4).
3. Reshape of the indices of a tensor, Eqs. (5.5)-(5.6).
4. Multiplication of two matrices, Eq. (5.7).
5. Factorization of a matrix (e.g. singular value decomposition Eq. (5.14) or spectral decomposition Eq. (5.15)).

These operations constitute a set \mathcal{P} of *primitive* operations for tensor network manipulations (or, at least, for the type of manipulations we will be concerned with). In Sec. 5.6 (and again in Chapter 6) we discuss how this set \mathcal{P} of primitive operations can be generalized to tensors that are invariant under the action of the group $SU(2)$.

Next we review basic background material concerning the representation theory of the group $SU(2)$ without reference to tensor network states and algorithms. This review is distributed over Sections 5.2, 5.3 and 5.4. We refer the reader to (Cornwell, 1997) and Chapters 3 and 4 of (Sakurai, 1994) for additional supporting material for these sections.

5.2 Representations of the group SU(2)

In this section we consider the action of SU(2) on a vector space that is an irreducible representation of the group, and then more generally on a vector space \mathbb{V} that is a reducible representation, namely, \mathbb{V} decomposes as a direct sum of (possibly degenerate) irreducible representations. We also characterize vectors belonging to \mathbb{V} and linear operators acting on \mathbb{V} that are invariant under the action of SU(2).

Let \mathbb{V} be a finite dimensional vector space on which SU(2) acts *unitarily* by means of transformations $\hat{W}_{\mathbf{r}} : \mathbb{V} \rightarrow \mathbb{V}$,

$$\hat{W}_{\mathbf{r}} \equiv e^{i\mathbf{r}\cdot\mathbf{J}} = e^{i(r_x\hat{J}_x+r_y\hat{J}_y+r_z\hat{J}_z)}. \quad (5.17)$$

Here $\mathbf{r} \equiv (r_x, r_y, r_z) \in \mathbb{R}^3$ parameterizes the group elements and $\mathbf{J} \equiv (\hat{J}_x, \hat{J}_y, \hat{J}_z)$; \hat{J}_x , \hat{J}_y and \hat{J}_z are traceless hermitian operators that are said to *generate* the representation $\hat{W}_{\mathbf{r}}$ of SU(2). These operators close the lie algebra $\mathfrak{su}(2)$, namely,

$$[\hat{J}_\alpha, \hat{J}_\beta] = i \sum_{\gamma=x,y,z} \epsilon_{\alpha\beta\gamma} \hat{J}_\gamma, \quad \alpha, \beta = x, y, z, \quad (5.18)$$

where $\epsilon_{\alpha\beta\gamma}$ is the Levi-Civita symbol. The operators \hat{J}_x , \hat{J}_y and \hat{J}_z are associated, for example, with the projection of angular momentum or spin along the three spatial directions x , y and z , respectively.

It follows that,

$$[\mathbf{J}^2, \hat{J}_\alpha] = 0, \quad \mathbf{J}^2 = \sum_{\alpha=x,y,z} \hat{J}_\alpha^2. \quad (5.19)$$

5.2.1 Irreducible representations

Let vector space \mathbb{V} transform as an irreducible representation (or irrep) of SU(2) with spin j . Here j can take values $0, \frac{1}{2}, 1, \frac{3}{2}, 2, \dots$ and \mathbb{V} has dimension $2j + 1$. We choose an orthonormal basis $|jm_j\rangle$, the *spin basis*, in \mathbb{V} that is a simultaneous eigenbasis of the

operators \mathbf{J}^2 and \hat{J}_z ,

$$\begin{aligned}\mathbf{J}^2|jm_j\rangle &= j(j+1)|jm_j\rangle, \\ \hat{J}_z|jm_j\rangle &= m_j|jm_j\rangle.\end{aligned}\tag{5.20}$$

Here m_j is the magnitude of the spin projection along the z direction and can assume values in the range $\{-j, -j+1, \dots, j\}$. In this basis, the action of the operators \hat{J}_x and \hat{J}_y on the space \mathbb{V} is conveniently described in terms of the raising operator $\hat{J}_+ = \hat{J}_x + i\hat{J}_y$ and the lowering operator $\hat{J}_- = \hat{J}_x - i\hat{J}_y$ as

$$\hat{J}_\pm|jm_j\rangle = \sqrt{j(j+1) - m_j(m_j \pm 1)}|j, (m_j \pm 1)\rangle.\tag{5.21}$$

The operator \mathbf{J}^2 can be written as

$$\mathbf{J}^2 = j(j+1)\hat{I}_{2j+1},\tag{5.22}$$

where \hat{I}_{2j+1} is the Identity acting on the irrep j .

Example 1: Consider that vector space \mathbb{V} is a spin $j = 0$ irrep of SU(2). Then \mathbb{V} has dimension one, $\mathbb{V} \cong \mathbb{C}$. The operators \hat{J}_α are trivial, $\hat{J}_x = \hat{J}_y = \hat{J}_z = (0)$. ■

Example 2: Consider a two-dimensional vector space \mathbb{V} that transforms as an irrep $j = \frac{1}{2}$. Then the orthogonal vectors (in column vector notation)

$$\begin{pmatrix} 1 \\ 0 \end{pmatrix} \equiv |j = \frac{1}{2}, m_{\frac{1}{2}} = -\frac{1}{2}\rangle, \quad \begin{pmatrix} 0 \\ 1 \end{pmatrix} \equiv |j = \frac{1}{2}, m_{\frac{1}{2}} = \frac{1}{2}\rangle,\tag{5.23}$$

form a basis of \mathbb{V} . In this basis the operators $\hat{J}_x, \hat{J}_y, \hat{J}_z$ and \mathbf{J}^2 read as

$$\hat{J}_x \equiv \begin{pmatrix} 0 & \frac{1}{2} \\ \frac{1}{2} & 0 \end{pmatrix}, \quad \hat{J}_y \equiv \begin{pmatrix} 0 & -\frac{i}{2} \\ \frac{i}{2} & 0 \end{pmatrix}, \quad \hat{J}_z \equiv \begin{pmatrix} -\frac{1}{2} & 0 \\ 0 & \frac{1}{2} \end{pmatrix}, \quad \mathbf{J}^2 \equiv \begin{pmatrix} \frac{3}{4} & 0 \\ 0 & \frac{3}{4} \end{pmatrix}.\tag{5.24}$$

In terms of Pauli matrices $\hat{\sigma}_\alpha$ we have

$$\hat{J}_\alpha = \frac{\hat{\sigma}_\alpha}{2}, \quad \alpha = x, y, z. \quad \blacksquare\tag{5.25}$$

Example 3: Also consider a three-dimensional vector space \mathbb{V} that transforms as an

irrep $j = 1$. The orthogonal vectors

$$\begin{pmatrix} 1 \\ 0 \\ 0 \end{pmatrix} \equiv |j=1, m_1=-1\rangle, \quad \begin{pmatrix} 0 \\ 1 \\ 0 \end{pmatrix} \equiv |j=1, m_1=0\rangle, \quad \begin{pmatrix} 0 \\ 0 \\ 1 \end{pmatrix} \equiv |j=1, m_1=1\rangle, \quad (5.26)$$

form a basis of \mathbb{V} . In this basis, operators $\hat{J}_x, \hat{J}_y, \hat{J}_z$ and \mathbf{J}^2 read as

$$\begin{aligned} \hat{J}_x &\equiv \begin{pmatrix} 0 & \frac{1}{\sqrt{2}} & 0 \\ \frac{1}{\sqrt{2}} & 0 & \frac{1}{\sqrt{2}} \\ 0 & \frac{1}{\sqrt{2}} & 0 \end{pmatrix}, \quad \hat{J}_y \equiv \begin{pmatrix} 0 & \frac{i}{\sqrt{2}} & 0 \\ -\frac{i}{\sqrt{2}} & 0 & \frac{i}{\sqrt{2}} \\ 0 & -\frac{i}{\sqrt{2}} & 0 \end{pmatrix}, \\ \hat{J}_z &\equiv \begin{pmatrix} -1 & 0 & 0 \\ 0 & 0 & 0 \\ 0 & 0 & 1 \end{pmatrix}, \quad \mathbf{J}^2 \equiv \begin{pmatrix} 2 & 0 & 0 \\ 0 & 2 & 0 \\ 0 & 0 & 2 \end{pmatrix}. \quad \blacksquare \end{aligned} \quad (5.27)$$

5.2.2 Reducible representations

More generally, $SU(2)$ can act on the vector space \mathbb{V} reducibly, in that, \mathbb{V} may decompose as the direct sum of irreps of $SU(2)$,

$$\begin{aligned} \mathbb{V} &\cong \bigoplus_j d_j \mathbb{V}_j \\ &\cong \bigoplus_j (\mathbb{D}_j \otimes \mathbb{V}_j). \end{aligned} \quad (5.28)$$

Here space \mathbb{V}_j accommodates a spin j irrep of $SU(2)$ and d_j is the number of times \mathbb{V}_j occurs in \mathbb{V} . The decomposition can also be re-written in terms of a d_j -dimensional space \mathbb{D}_j . We say that irrep j is d_j -fold degenerate and that \mathbb{D}_j is the degeneracy space. The total dimension of space \mathbb{V} is given by $\sum_j d_j(2j+1)$.

Let $t_j = 1, 2, \dots, d_j$ label an orthonormal basis $|jt_j\rangle$ in the space \mathbb{D}_j . Then a natural choice of basis of the space \mathbb{V} is the set of orthonormal vectors $|jt_j m_j\rangle \equiv |jt_j\rangle \otimes |jm_j\rangle$, where j assumes various values that occur in the direct sum decomposition, Eq. (5.28).

In this basis the action of $SU(2)$ on \mathbb{V} is given by

$$\hat{W}_{\mathbf{r}} \equiv \bigoplus_j \left(\hat{I}_{d_j} \otimes \hat{W}_{\mathbf{r},j} \right), \quad (5.29)$$

as generated by the operators

$$\hat{J}_\alpha \equiv \bigoplus_j \left(\hat{I}_{d_j} \otimes \hat{J}_{\alpha,j} \right), \quad \alpha = x, y, z. \quad (5.30)$$

Here \hat{I}_{d_j} is a $d_j \times d_j$ Identity and operators $\hat{J}_{\alpha,j}$ generate the irreducible representation $\hat{W}_{\mathbf{r},j}$ on space \mathbb{V}_j .

The operator \mathbf{J}^2 takes the form

$$\mathbf{J}^2 \equiv \bigoplus_j j(j+1) \left(\hat{I}_{d_j} \otimes \hat{I}_{2j+1} \right). \quad (5.31)$$

Example 4: Let vector space \mathbb{V} transform as an irrep $j = \frac{1}{2}$ with a finite degeneracy $d_{\frac{1}{2}} = 3$. The space \mathbb{V} decomposes as $\mathbb{V} \cong \mathbb{D}_{\frac{1}{2}} \otimes \mathbb{V}_{\frac{1}{2}}$ where $\mathbb{D}_{\frac{1}{2}}$ is a three-dimensional degeneracy space and $\mathbb{V}_{\frac{1}{2}}$ corresponds to the space of Example 1.

The total dimension of space \mathbb{V} is $d_{\frac{1}{2}}(2j+1) = 6$. The vectors

$$\begin{pmatrix} 1 \\ 0 \\ 0 \end{pmatrix} \equiv |j = \frac{1}{2}, t_0 = 1\rangle, \quad \begin{pmatrix} 0 \\ 1 \\ 0 \end{pmatrix} \equiv |j = \frac{1}{2}, t_0 = 2\rangle, \quad \begin{pmatrix} 0 \\ 0 \\ 1 \end{pmatrix} \equiv |j = \frac{1}{2}, t_0 = 3\rangle. \quad (5.32)$$

form a basis of $\mathbb{D}_{\frac{1}{2}}$. A basis of \mathbb{V} can be obtained as the product of the the basis (5.32) of $\mathbb{D}_{\frac{1}{2}}$ and the basis (5.23) of $\mathbb{V}_{\frac{1}{2}}$. In this basis of the operators \hat{J}_α take the form of Eq. (5.30).

For instance,

$$\hat{J}_x \equiv \begin{pmatrix} 1 & 0 & 0 \\ 0 & 1 & 0 \\ 0 & 0 & 1 \end{pmatrix} \otimes \begin{pmatrix} 0 & \frac{1}{2} \\ \frac{1}{2} & 0 \end{pmatrix} = \begin{pmatrix} 0 & \frac{1}{2} & 0 & 0 & 0 & 0 \\ \frac{1}{2} & 0 & 0 & 0 & 0 & 0 \\ 0 & 0 & 0 & \frac{1}{2} & 0 & 0 \\ 0 & 0 & \frac{1}{2} & 0 & 0 & 0 \\ 0 & 0 & 0 & 0 & 0 & \frac{1}{2} \\ 0 & 0 & 0 & 0 & \frac{1}{2} & 0 \end{pmatrix} \quad (5.33)$$

Similarly, operators \hat{J}_y and \hat{J}_z read as

$$\hat{J}_y \equiv \begin{pmatrix} 0 & \frac{i}{2} & 0 & 0 & 0 & 0 \\ -\frac{i}{2} & 0 & 0 & 0 & 0 & 0 \\ 0 & 0 & 0 & \frac{i}{2} & 0 & 0 \\ 0 & 0 & -\frac{i}{2} & 0 & 0 & 0 \\ 0 & 0 & 0 & 0 & 0 & \frac{i}{2} \\ 0 & 0 & 0 & 0 & -\frac{i}{2} & 0 \end{pmatrix},$$

$$\hat{J}_z \equiv \begin{pmatrix} -\frac{1}{2} & 0 & 0 & 0 & 0 & 0 \\ 0 & \frac{1}{2} & 0 & 0 & 0 & 0 \\ 0 & 0 & -\frac{1}{2} & 0 & 0 & 0 \\ 0 & 0 & 0 & \frac{1}{2} & 0 & 0 \\ 0 & 0 & 0 & 0 & -\frac{1}{2} & 0 \\ 0 & 0 & 0 & 0 & 0 & \frac{1}{2} \end{pmatrix}. \quad (5.34)$$

The operator \mathbf{J}^2 reads

$$\mathbf{J}^2 \equiv \frac{1}{2}(\frac{1}{2} + 1)\hat{I}_3 \otimes \hat{I}_2 \equiv \begin{pmatrix} \frac{3}{4} & 0 & 0 & 0 & 0 & 0 \\ 0 & \frac{3}{4} & 0 & 0 & 0 & 0 \\ 0 & 0 & \frac{3}{4} & 0 & 0 & 0 \\ 0 & 0 & 0 & \frac{3}{4} & 0 & 0 \\ 0 & 0 & 0 & 0 & \frac{3}{4} & 0 \\ 0 & 0 & 0 & 0 & 0 & \frac{3}{4} \end{pmatrix}. \blacksquare \quad (5.35)$$

Example 5: Consider a five-dimensional Hilbert space \mathbb{V} that decomposes into two different irreps $j = 0$ and $j = 1$ with degeneracy dimensions $d_0 = 2$ and $d_1 = 1$ so that irrep $j = 0$ is two-fold degenerate. The space \mathbb{V} decomposes as $\mathbb{V} \cong (\mathbb{D}_0 \otimes \mathbb{V}_0) \oplus (\mathbb{D}_1 \otimes \mathbb{V}_1)$, where \mathbb{D}_0 is the two-dimensional degeneracy space of irrep $j = 0$ and \mathbb{D}_1 is the one-dimensional degeneracy space of irrep $j = 1$.

The orthogonal vectors

$$\begin{aligned}
 \begin{pmatrix} 1 \\ 0 \\ 0 \\ 0 \\ 0 \end{pmatrix} &\equiv |j = 0, t_0 = 1, m_0 = 0\rangle, \\
 \begin{pmatrix} 0 \\ 1 \\ 0 \\ 0 \\ 0 \end{pmatrix} &\equiv |j = 0, t_0 = 2, m_0 = 0\rangle, \\
 \begin{pmatrix} 0 \\ 0 \\ 1 \\ 0 \\ 0 \end{pmatrix} &\equiv |j = 1, t_1 = 1, m_1 = -1\rangle, \\
 \begin{pmatrix} 0 \\ 0 \\ 0 \\ 1 \\ 0 \end{pmatrix} &\equiv |j = 1, t_1 = 1, m_1 = 0\rangle, \\
 \begin{pmatrix} 0 \\ 0 \\ 0 \\ 0 \\ 1 \end{pmatrix} &\equiv |j = 1, t_1 = 1, m_1 = 1\rangle.
 \end{aligned} \tag{5.36}$$

form a basis of \mathbb{V} . In this basis, the operators \hat{J}_α take the form

$$\hat{J}_\alpha = (\hat{I}_{d_0} \otimes \hat{J}_{\alpha,0}) \oplus (\hat{I}_{d_1} \otimes \hat{J}_{\alpha,1}), \quad \alpha = x, y, z, \tag{5.37}$$

where $\hat{J}_{\alpha,0}$ and $\hat{J}_{\alpha,1}$ are the generators of irrep $j = 0$ (Examples 1) and irrep $j = 1$

(Examples 3) respectively. Operators \hat{J}_α and \mathbf{J}^2 read as

$$\begin{aligned}
\hat{J}_x &\equiv \begin{pmatrix} 0 & 0 & 0 & 0 & 0 \\ 0 & 0 & 0 & 0 & 0 \\ 0 & 0 & 0 & \frac{1}{\sqrt{2}} & 0 \\ 0 & 0 & \frac{1}{\sqrt{2}} & 0 & \frac{1}{\sqrt{2}} \\ 0 & 0 & 0 & \frac{1}{\sqrt{2}} & 0 \end{pmatrix}, \\
\hat{J}_y &\equiv \begin{pmatrix} 0 & 0 & 0 & 0 & 0 \\ 0 & 0 & 0 & 0 & 0 \\ 0 & 0 & 0 & \frac{i}{\sqrt{2}} & 0 \\ 0 & 0 & -\frac{i}{\sqrt{2}} & 0 & \frac{i}{\sqrt{2}} \\ 0 & 0 & 0 & -\frac{i}{\sqrt{2}} & 0 \end{pmatrix}, \\
\hat{J}_z &\equiv \begin{pmatrix} 0 & 0 & 0 & 0 & 0 \\ 0 & 0 & 0 & 0 & 0 \\ 0 & 0 & -1 & 0 & 0 \\ 0 & 0 & 0 & 0 & 0 \\ 0 & 0 & 0 & 0 & 1 \end{pmatrix}, \\
\mathbf{J}^2 &\equiv \begin{pmatrix} 0 & 0 & 0 & 0 & 0 \\ 0 & 0 & 0 & 0 & 0 \\ 0 & 0 & 2 & 0 & 0 \\ 0 & 0 & 0 & 2 & 0 \\ 0 & 0 & 0 & 0 & 2 \end{pmatrix}. \blacksquare
\end{aligned} \tag{5.38}$$

5.2.3 SU(2)-invariant states and operators

We are interested in states and operators that have a simple transformation rule under the action of SU(2).

A pure state $|\Psi\rangle \in \mathbb{V}$ with a well defined spin j belongs to the subspace $\mathbb{D}_j \otimes \mathbb{V}_j$. In the spin basis $|jt_j m_j\rangle$ the state $|\Psi\rangle$ can be expanded as

$$|\Psi\rangle = \sum_{t_j m_j} (\Psi_j)_{t_j m_j} |jt_j m_j\rangle, \tag{5.39}$$

Under the action of SU(2), $|\Psi\rangle$ transforms to another pure state $|\Psi'\rangle$, $|\Psi'\rangle = \hat{W}_{\mathbf{r}}|\Psi\rangle$, within the same subspace $\mathbb{D}_j \otimes \mathbb{V}_j$. The components $(\Psi'_j)_{t'_j m'_j}$ of $|\Psi'\rangle$ are related to those of $|\Psi\rangle$ as

$$(\Psi'_j)_{t'_j m'_j} = \sum_{t_j m_j} (W_{r,j})_{t'_j m'_j t_j m_j} (\Psi_j)_{t_j m_j}. \quad (5.40)$$

In case of vanishing spin $j = 0$, the state $|\Psi\rangle$ transforms trivially under the action of SU(2), $\hat{W}_{r,j=0} \equiv 1$. In this case Eq. (5.40) reduces to,

$$\hat{W}_{\mathbf{r}}|\Psi\rangle = |\Psi\rangle, \quad \forall \mathbf{r} \in \mathbb{R}^3. \quad (5.41)$$

That is, $|\Psi\rangle$ remains *invariant* under the action of SU(2). Equivalently, it is annihilated by the action of generators,

$$\hat{J}_{\alpha}|\Psi\rangle = 0, \quad \alpha = x, y, z. \quad (5.42)$$

An SU(2)-invariant state $|\Psi\rangle$ can be expanded in the basis $|j = 0, t_0, m_0 = 0\rangle$ of the spin $j = 0$ subspace, $\mathbb{D}_0 \otimes \mathbb{V}_0$,

$$|\Psi\rangle = \sum_{t_0} (\Psi_0)_{t_0} |j = 0, t_0, m_0 = 0\rangle, \quad (5.43)$$

where we have used $(\Psi_0)_{t_0}$ as a shorthand for $(\Psi_{j=0})_{t_0, m_0=0}$.

A linear operator $\hat{T} : \mathbb{V} \rightarrow \mathbb{V}$ is SU(2)-invariant if it commutes with the action of the group,

$$[\hat{T}, \hat{W}_{\mathbf{r}}] = 0, \quad \forall \mathbf{r} \in \mathbb{R}^3, \quad (5.44)$$

or equivalently, if it commutes with the generators \hat{J}_{α} ,

$$[\hat{T}, \hat{J}_{\alpha}] = 0, \quad \alpha = x, y, z. \quad (5.45)$$

Notice that the operator \mathbf{J}^2 is SU(2)-invariant, Eq. (5.19).

An SU(2)-invariant operator \hat{T} decomposes as

$$\hat{T} = \bigoplus_j \left(\hat{T}_j \otimes \hat{I}_{2j+1} \right),$$

$$\text{(Schur's Lemma)} \quad (5.46)$$

where \hat{T}_j is a $d_j \times d_j$ matrix that acts on the degeneracy space \mathbb{D}_j . This decomposition implies, for instance, that operator \hat{T} transforms states with a well defined spin j [such as $|\Psi\rangle$ of Eq. (5.39)] into states with the same spin j . Thus, $SU(2)$ -invariant operators *conserve* spin.

Example 2 revisited: A generic state $|\Psi\rangle \in \mathbb{V}_{\frac{1}{2}}$ has the form,

$$|\Psi\rangle = \begin{pmatrix} (\Psi_{j=\frac{1}{2}})_{m_{\frac{1}{2}}=-\frac{1}{2}} \\ (\Psi_{j=\frac{1}{2}})_{m_{\frac{1}{2}}=\frac{1}{2}} \end{pmatrix} \in \mathbb{C}^2. \quad (5.47)$$

and is an eigenstate of $\mathbf{J}_{\frac{1}{2}}^2$ with eigenvalue $\frac{3}{4}$.

According to Schur's lemma, an $SU(2)$ -invariant operator \hat{T} acting on $\mathbb{V}_{\frac{1}{2}}$ must be proportional to the Identity,

$$\hat{T} = (T_{j=\frac{1}{2}}) \begin{pmatrix} 1 & 0 \\ 0 & 1 \end{pmatrix}, \quad T_{j=\frac{1}{2}} \in \mathbb{C}. \quad \blacksquare \quad (5.48)$$

Example 4 revisited: A generic state $|\Psi\rangle$ in the vector space $\mathbb{V} \cong 3\mathbb{V}_{\frac{1}{2}}$ of Example 3 has the form

$$|\Psi\rangle = \begin{pmatrix} (\Psi_{j=\frac{1}{2}})_{t_{\frac{1}{2}}=1, m_{\frac{1}{2}}=-\frac{1}{2}} \\ (\Psi_{j=\frac{1}{2}})_{t_{\frac{1}{2}}=1, m_{\frac{1}{2}}=\frac{1}{2}} \\ (\Psi_{j=\frac{1}{2}})_{t_{\frac{1}{2}}=2, m_{\frac{1}{2}}=-\frac{1}{2}} \\ (\Psi_{j=\frac{1}{2}})_{t_{\frac{1}{2}}=2, m_{\frac{1}{2}}=\frac{1}{2}} \\ (\Psi_{j=\frac{1}{2}})_{t_{\frac{1}{2}}=3, m_{\frac{1}{2}}=-\frac{1}{2}} \\ (\Psi_{j=\frac{1}{2}})_{t_{\frac{1}{2}}=3, m_{\frac{1}{2}}=\frac{1}{2}} \end{pmatrix} \in \mathbb{C}^6. \quad (5.49)$$

Similar to the previous example, $|\Psi\rangle$ is an eigenstate of $\mathbf{J}_{\frac{1}{2}}^2$ with eigenvalue $\frac{3}{4}$.

An SU(2)-invariant operator $\hat{T} : \mathbb{V} \rightarrow \mathbb{V}$ must be of the form

$$\begin{aligned} \hat{T} &= \begin{pmatrix} T_{11} & T_{12} & T_{13} \\ T_{21} & T_{22} & T_{23} \\ T_{31} & T_{32} & T_{33} \end{pmatrix} \otimes \begin{pmatrix} 1 & 0 \\ 0 & 1 \end{pmatrix} \\ &= \begin{pmatrix} T_{11} & 0 & T_{12} & 0 & T_{13} & 0 \\ 0 & T_{11} & 0 & T_{12} & 0 & T_{13} \\ T_{21} & 0 & T_{22} & 0 & T_{23} & 0 \\ 0 & T_{21} & 0 & T_{22} & 0 & T_{23} \\ T_{31} & 0 & T_{32} & 0 & T_{33} & 0 \\ 0 & T_{31} & 0 & T_{32} & 0 & T_{33} \end{pmatrix}, \end{aligned} \quad (5.50)$$

where we have used T_{ij} as a shorthand for $(T_{\frac{1}{2}})_{ij} \in \mathbb{C}$. Notice that \mathbf{J}^2 in Eq. (5.35) has this form. ■

Example 5 revisited: A generic state $|\Psi\rangle \in \mathbb{V}$, $\mathbb{V} \cong 2\mathbb{V}_0 \oplus \mathbb{V}_1$ has the form

$$|\Psi\rangle = \begin{pmatrix} (\Psi_0)_{1,0} \\ (\Psi_0)_{2,0} \\ (\Psi_1)_{1,-1} \\ (\Psi_1)_{1,0} \\ (\Psi_1)_{1,1} \end{pmatrix} \in \mathbb{C}^5. \quad (5.51)$$

(For simplicity we have omitted explicit labels in the subscripts.) In contrast to the previous two examples, a generic state $|\Psi\rangle \in \mathbb{V}$ is not an eigenstate of \mathbf{J}^2 , that is, $|\Psi\rangle$ is generally not a state with a well defined spin j .

An SU(2)-invariant vector $|\Psi\rangle$ has the form

$$|\Psi\rangle = \begin{pmatrix} (\Psi_0)_{1,0} \\ (\Psi_0)_{2,0} \\ 0 \\ 0 \\ 0 \end{pmatrix}, \quad (5.52)$$

with non-trivial components only in the spin $j = 0$ subspace. Notice that this state is annihilated by the action of the operators \hat{J}_α [Eq. (5.38)] in accordance with Eq. (5.42).

A state with a well defined spin $j = 1$ must be of the form

$$|\Psi_1\rangle = \begin{pmatrix} 0 \\ 0 \\ (\Psi_1)_{1,-1} \\ (\Psi_1)_{1,0} \\ (\Psi_1)_{1,1} \end{pmatrix} \in \mathbb{C}^5, \quad (5.53)$$

with non-trivial components only in the spin $j = 1$ subspace.

An SU(2)-invariant operator \hat{T} e.g. \mathbf{J}^2 in Eq. (5.38) has the form

$$\begin{aligned} \hat{T} &= \begin{pmatrix} (T_0)_{11} & (T_0)_{12} \\ (T_0)_{21} & (T_0)_{22} \end{pmatrix} \otimes (1) \oplus \left((T_1)_{11} \right) \otimes \begin{pmatrix} 1 & 0 & 0 \\ 0 & 1 & 0 \\ 0 & 0 & 1 \end{pmatrix} \\ &= \begin{pmatrix} (T_0)_{11} & (T_0)_{12} & 0 & 0 & 0 \\ (T_0)_{21} & (T_0)_{22} & 0 & 0 & 0 \\ 0 & 0 & (T_1)_{11} & 0 & 0 \\ 0 & 0 & 0 & (T_1)_{11} & 0 \\ 0 & 0 & 0 & 0 & (T_1)_{11} \end{pmatrix}, \end{aligned} \quad (5.54)$$

where $(T_0)_{11}, (T_0)_{12}, (T_0)_{21}, (T_0)_{22}, (T_1)_{11} \in \mathbb{C}$. ■

Notice that the SU(2)-invariant vector in Eq. (5.52) and the SU(2)-invariant matrices in Eqs. (5.48),(5.50) and (5.54) have a *sparse* structure. In particular, the non-trivial components of an SU(2)-invariant matrix \hat{T} are organized into blocks \hat{T}_j . This block structure can be exploited for computational gain. An SU(2)-invariant matrix can be stored compactly by storing the degeneracy blocks \hat{T}_j , while matrix multiplication and matrix factorizations can be performed block-wise [Sec. 5.6] resulting in a significant speedup [Fig. 5.26] for these operations.

5.3 Tensor product of representations

So far we have described the action of $SU(2)$ on a single vector space. Let us now consider the action of $SU(2)$ on a space \mathbb{V} that is a tensor product of L vector spaces,

$$\mathbb{V} \equiv \bigotimes_{l=1}^L \mathbb{V}^{(l)}, \quad (5.55)$$

where each vector space $\mathbb{V}^{(l)}$, $l = 1, 2, \dots, L$, transforms as a finite dimensional representation of $SU(2)$ as generated by spin operators $\hat{J}_\alpha^{(l)}$, $\alpha = x, y, z$. We consider the action of $SU(2)$ on the space \mathbb{V} that is generated by the *total* spin operators,

$$\hat{J}_\alpha \equiv \sum_{l=1}^L \hat{J}_\alpha^{(l)}, \quad \alpha = x, y, z, \quad (5.56)$$

(each term in the sum acts as $\hat{J}_\alpha^{(l)}$ on site l and the Identity on the remaining sites) and which corresponds to the unitary transformations,

$$\hat{W}_{\mathbf{r}} \equiv e^{i\mathbf{r} \cdot \mathbf{J}} = \bigotimes_{l=1}^L e^{i\mathbf{r} \cdot \mathbf{J}^{(l)}} = \bigotimes_{l=1}^L \hat{W}_{\mathbf{r}}^{(l)}. \quad (5.57)$$

As an example consider two vector spaces $\mathbb{V}^{(A)}$ and $\mathbb{V}^{(B)}$ on which the action of $SU(2)$ is generated by spin operators $\hat{J}_\alpha^{(A)}$ and $\hat{J}_\alpha^{(B)}$ respectively. We can then consider the action of the group on the product space $\mathbb{V}^{(AB)} \cong \mathbb{V}^{(A)} \otimes \mathbb{V}^{(B)}$ as generated by the total spin operators $\hat{J}_\alpha^{(AB)}$, $\alpha = x, y, z$, that are given by

$$\hat{J}_\alpha^{(AB)} \equiv \hat{J}_\alpha^{(A)} \otimes \hat{I} + \hat{I} \otimes \hat{J}_\alpha^{(B)}. \quad (5.58)$$

Similarly, we can consider the action of $SU(2)$ on the product of three vector spaces, $\mathbb{V}^{(A)}$, $\mathbb{V}^{(B)}$ and $\mathbb{V}^{(C)}$, that is generated by spin operators $\hat{J}_\alpha^{(ABC)}$, $\alpha = x, y, z$,

$$\hat{J}_\alpha^{(ABC)} \equiv \hat{J}_\alpha^{(A)} \otimes \hat{I} \otimes \hat{I} + \hat{I} \otimes \hat{J}_\alpha^{(B)} \otimes \hat{I} + \hat{I} \otimes \hat{I} \otimes \hat{J}_\alpha^{(C)}, \quad (5.59)$$

where $\hat{J}_\alpha^{(A)}$, $\hat{J}_\alpha^{(B)}$ and $\hat{J}_\alpha^{(C)}$ are the spin operators that act on the three vector spaces.

A basis of \mathbb{V} can be obtained in terms of the spin basis of each vector space in the product, Eq. 5.55. However, it is convenient to introduce a *coupled* basis: the simultaneous

eigenbasis of the *total* spin operators \hat{J}_z and \mathbf{J}^2 . In the coupled basis SU(2)-invariant states $|\Psi\rangle \in \mathbb{V}$,

$$|\Psi\rangle = \hat{W}_{\mathbf{r}}|\Psi\rangle, \quad \forall \mathbf{r} \in \mathbb{R}^3, \quad (5.60)$$

and SU(2)-invariant operators $\hat{T} : \mathbb{V} \rightarrow \mathbb{V}$,

$$[\hat{T}, \hat{W}_{\mathbf{r}}] = \hat{T}, \quad \forall \mathbf{r} \in \mathbb{R}^3, \quad (5.61)$$

have a sparse structure, namely, $|\Psi\rangle$ has non-trivial components only in the spin zero sector of \mathbb{V} while \hat{T} is block-diagonal [Eq. (5.46)].

In the remainder of the section we focus on the tensor product of *two* representations. We first discuss the case where the two sites transform as irreducible representations and then the more general case of reducible representations. The tensor product of several representations can then be analyzed by considering a sequence of pairwise products.

5.3.1 Tensor product of two irreducible representations

Let vector spaces $\mathbb{V}^{(A)}$ and $\mathbb{V}^{(B)}$ transform as irreps j_A and j_B respectively. The space $\mathbb{V}^{(AB)}$ is, in general, reducible and decomposes as

$$\mathbb{V}^{(AB)} \cong \bigoplus_{j_{AB}} \mathbb{V}_{j_{AB}}^{(AB)}, \quad (5.62)$$

where the total spin j_{AB} assumes all values in the range

$$\boxed{j_{AB} : \{|j_A - j_B|, |j_A - j_B| + 1, \dots, j_A + j_B\}.}$$

(Fusion rules)

(5.63)

Let $|j_A m_A\rangle \in \mathbb{V}^{(A)}$ and $|j_B m_B\rangle \in \mathbb{V}^{(B)}$ denote the spin basis of the respective vector spaces. Then the vectors

$$|j_A m_{j_A}; j_B m_{j_B}\rangle \equiv |j_A m_{j_A}\rangle \otimes |j_B m_{j_B}\rangle \quad (5.64)$$

form a basis of $\mathbb{V}^{(AB)}$. Introduce a coupled basis $|j_{AB} m_{j_{AB}}\rangle \in \mathbb{V}^{(AB)}$ that fulfills

$$\begin{aligned} \mathbf{J}^{2(AB)} |j_{AB} m_{j_{AB}}\rangle &= j_{AB}(j_{AB} + 1) |j_{AB} m_{j_{AB}}\rangle, \\ \hat{J}_z^{(AB)} |j_{AB} m_{j_{AB}}\rangle &= m_{j_{AB}} |j_{AB} m_{j_{AB}}\rangle. \end{aligned} \quad (5.65)$$

The coupled basis is related to the product basis (5.64) by means of the transformation

$$\boxed{|j_{AB}m_{j_{AB}}\rangle = \sum_{m_{j_A}m_{j_B}} C_{j_A m_{j_A}, j_B m_{j_B} \rightarrow j_{AB} m_{j_{AB}}}^{\text{fuse}} |j_A m_{j_A}; j_B m_{j_B}\rangle.} \quad (5.66)$$

Here

$$C_{j_A m_{j_A}, j_B m_{j_B} \rightarrow j_{AB} m_{j_{AB}}}^{\text{fuse}} \equiv \langle j_A m_{j_A}; j_B m_{j_B} | j_{AB} m_{j_{AB}} \rangle \quad (5.67)$$

are the *Clebsch-Gordan coefficients*, which vanish unless j_A, j_B and j_{AB} are compatible, that is, j_A, j_B and j_{AB} fulfill

$$|j_A - j_B| \leq j_{AB} \leq j_A + j_B, \quad (5.68)$$

and m_{j_A}, m_{j_B} and $m_{j_{AB}}$ fulfill

$$m_{j_{AB}} = m_{j_A} + m_{j_B}. \quad (5.69)$$

The product basis can be expressed in terms of the coupled basis as

$$\boxed{|j_A m_{j_A}; j_B m_{j_B}\rangle = \sum_{m_{j_{AB}}} C_{j_{AB} m_{j_{AB}} \rightarrow j_A m_{j_A}, j_B m_{j_B}}^{\text{split}} |j_{AB} m_{j_{AB}}\rangle,} \quad (5.70)$$

where

$$C_{j_{AB} m_{j_{AB}} \rightarrow j_A m_{j_A}, j_B m_{j_B}}^{\text{split}} \equiv C_{j_A m_{j_A}, j_B m_{j_B} \rightarrow j_{AB} m_{j_{AB}}}^{\text{fuse}}. \quad (5.71)$$

We graphically represent tensors C^{fuse} and C^{split} differently from usual tensors, as shown in Fig. 5.7(i).

Tensor $C_{j_A m_{j_A}, j_B m_{j_B} \rightarrow j_{AB} m_{j_{AB}}}^{\text{fuse}}$ is depicted by means of two incoming lines and one outgoing line that emerge from a point. The outgoing line corresponds to the spin index $(j_{AB}, m_{j_{AB}})$. The incoming lines that are encountered first and second when proceeding *clockwise* from the outgoing line correspond to the spin indices (j_A, m_{j_A}) and (j_B, m_{j_B}) respectively.

Analogously, tensor $C_{j_{AB} m_{j_{AB}} \rightarrow j_A m_{j_A}, j_B m_{j_B}}^{\text{split}}$ is depicted by means of one incoming line and two outgoing lines that emerge from a point. The spin index $(j_{AB}, m_{j_{AB}})$ corresponds to the incoming line in this case while spin indices (j_A, m_{j_A}) and (j_B, m_{j_B}) correspond to the outgoing lines in the order in which they are encountered when proceeding *counterclockwise* from the incoming line.

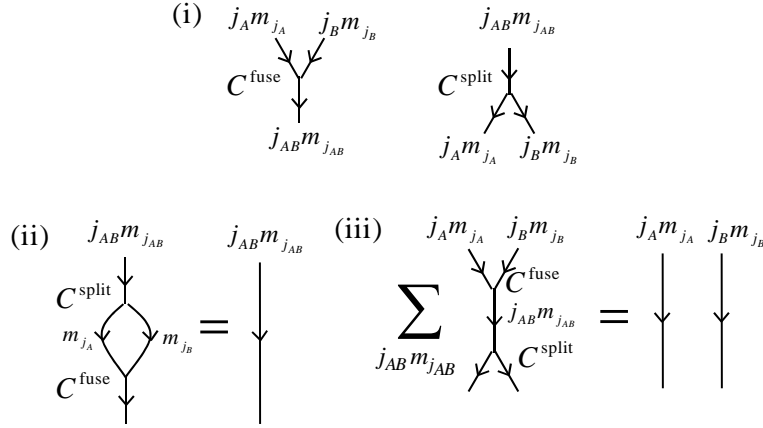


Figure 5.7 – (i) The graphical representation of the Clebsch-Gordan tensors: C^{fuse} and C^{split} . (ii) Tensors C^{fuse} and C^{split} are isometries and thus yield the Identity when contracted pairwise either as (i) or (ii), Eq. (5.72).

Tensor C^{fuse} and tensor C^{split} fulfill the orthogonality identities,

$$\begin{aligned}
\sum_{m_{j_A} m_{j_B}} C^{\text{split}}_{j_{AB} m_{j_{AB}} \rightarrow j_A m_{j_A} j_B m_{j_B}} \cdot C^{\text{fuse}}_{j_A m_{j_A} j_B m_{j_B} \rightarrow j_{AB} m_{j_{AB}}} &= \delta_{j_{AB} j'_{AB}} \delta_{m_{j_{AB}} m_{j'_{AB}}} \\
\sum_{j_{AB} m_{j_{AB}}} C^{\text{fuse}}_{j_A m_{j_A} j_B m_{j_B} \rightarrow j_{AB} m_{j_{AB}}} \cdot C^{\text{split}}_{j_{AB} m_{j_{AB}} \rightarrow j'_A m_{j'_A} j'_B m_{j'_B}} &= \delta_{j_A j'_A} \delta_{m_{j_A} m_{j'_A}} \delta_{j_B j'_B} \delta_{m_{j_B} m_{j'_B}}
\end{aligned} \tag{5.72}$$

The special graphical representations for these tensors allows one to depict the above identities in an intuitive way, as shown in Fig. 5.7.(ii)-(iii).

Example 6: Let both vector spaces $\mathbb{V}^{(A)}$ and $\mathbb{V}^{(B)}$ transform as a spin $\frac{1}{2}$ irrep, $j_A = j_B = \frac{1}{2}$ (Example 2). The space $\mathbb{V}^{(AB)}$ decomposes into a direct sum of irreps,

$$\mathbb{V}^{(AB)} \cong \mathbb{V}^{(A)} \otimes \mathbb{V}^{(B)} \cong \mathbb{V}_0^{(AB)} \oplus \mathbb{V}_1^{(AB)}. \tag{5.73}$$

A basis can be introduced in $\mathbb{V}^{(AB)}$ in terms of the spin basis [Eq. (5.23)] of $\mathbb{V}^{(A)}$ and of $\mathbb{V}^{(B)}$. The coupled basis of $\mathbb{V}^{(AB)}$,

$$\begin{aligned}
&|j_{AB} = 0, m_{j_{AB}} = 0\rangle, \\
&|j_{AB} = 1, m_{j_{AB}} = -1\rangle, |j_{AB} = 1, m_{j_{AB}} = 0\rangle, |j_{AB} = 1, m_{j_{AB}} = 1\rangle,
\end{aligned}$$

is related to the product basis by means of the Clebsch-Gordan coefficients,

$$\begin{aligned} |j_{AB} = 0, m_{AB} = 0\rangle &= C_{\frac{1}{2}, \frac{-1}{2}, \frac{1}{2}, \frac{1}{2} \rightarrow 00}^{\text{fuse}} |j_A = \frac{1}{2}, m_A = \frac{-1}{2}; j_B = \frac{1}{2}, m_B = \frac{1}{2}\rangle \\ &+ C_{\frac{1}{2}, \frac{1}{2}, \frac{1}{2}, \frac{-1}{2} \rightarrow 00}^{\text{fuse}} |j_A = \frac{1}{2}, m_A = \frac{1}{2}; j_B = \frac{1}{2}, m_B = \frac{-1}{2}\rangle \end{aligned} \quad (5.74)$$

$$|j_{AB} = 1, m_{AB} = -1\rangle = C_{\frac{1}{2}, \frac{-1}{2}, \frac{1}{2}, \frac{-1}{2} \rightarrow 1-1}^{\text{fuse}} |j_A = \frac{1}{2}, m_A = \frac{-1}{2}; j_B = \frac{1}{2}, m_B = \frac{-1}{2}\rangle \quad (5.75)$$

$$\begin{aligned} |j_{AB} = 1, m_{AB} = 0\rangle &= C_{\frac{1}{2}, \frac{1}{2}, \frac{1}{2}, \frac{-1}{2} \rightarrow 10}^{\text{fuse}} |j_A = \frac{1}{2}, m_A = \frac{1}{2}; j_B = \frac{1}{2}, m_B = \frac{-1}{2}\rangle \\ &+ C_{\frac{1}{2}, \frac{-1}{2}, \frac{1}{2}, \frac{1}{2} \rightarrow 10}^{\text{fuse}} |j_A = \frac{1}{2}, m_A = \frac{-1}{2}; j_B = \frac{1}{2}, m_B = \frac{1}{2}\rangle \end{aligned} \quad (5.76)$$

$$|j_{AB} = 1, m_{AB} = 1\rangle = C_{\frac{1}{2}, \frac{1}{2}, \frac{1}{2}, \frac{1}{2} \rightarrow 11}^{\text{fuse}} |j_A = \frac{1}{2}, m_A = \frac{1}{2}; j_B = \frac{1}{2}, m_B = \frac{1}{2}\rangle. \quad (5.77)$$

For completeness, we list below the numerical value of the Clebsch-Gordan coefficients that appear in Eqs. (5.74)-(5.77),

$$\begin{aligned} C_{\frac{1}{2}, \frac{1}{2}, \frac{1}{2}, \frac{-1}{2} \rightarrow 00}^{\text{fuse}} &= \frac{1}{\sqrt{2}}, & C_{\frac{1}{2}, \frac{-1}{2}, \frac{1}{2}, \frac{1}{2} \rightarrow 00}^{\text{fuse}} &= \frac{-1}{\sqrt{2}}, & C_{\frac{1}{2}, \frac{-1}{2}, \frac{1}{2}, \frac{-1}{2} \rightarrow 1-1}^{\text{fuse}} &= 1, \\ C_{\frac{1}{2}, \frac{1}{2}, \frac{1}{2}, \frac{-1}{2} \rightarrow 10}^{\text{fuse}} &= \frac{1}{\sqrt{2}}, & C_{\frac{1}{2}, \frac{-1}{2}, \frac{1}{2}, \frac{1}{2} \rightarrow 10}^{\text{fuse}} &= \frac{1}{\sqrt{2}}, & C_{\frac{1}{2}, \frac{1}{2}, \frac{1}{2}, \frac{1}{2} \rightarrow 11}^{\text{fuse}} &= 1. \blacksquare \end{aligned}$$

5.3.2 Tensor product of two reducible representations

Let us now consider that vector spaces $\mathbb{V}^{(A)}$ and $\mathbb{V}^{(B)}$ transform reducibly under the action of $\text{SU}(2)$. We have

$$\mathbb{V}^{(A)} \cong \bigoplus_{j_A} \left(\mathbb{D}_{j_A}^{(A)} \otimes \mathbb{V}_{j_A}^{(A)} \right), \quad \mathbb{V}^{(B)} \cong \bigoplus_{j_B} \left(\mathbb{D}_{j_B}^{(B)} \otimes \mathbb{V}_{j_B}^{(B)} \right). \quad (5.78)$$

The space $\mathbb{V}^{(AB)}$ decomposes into a direct sum of irreps,

$$\mathbb{V}^{(AB)} \cong \bigoplus_{j_{AB}} d_{j_{AB}} \mathbb{V}_{j_{AB}}^{(AB)} \cong \bigoplus_{j_{AB}} \left(\mathbb{D}_{j_{AB}}^{(AB)} \otimes \mathbb{V}_{j_{AB}}^{(AB)} \right), \quad (5.79)$$

where the total spin j_{AB} takes all values that are compatible with *any* pair of irreps j_A and j_B .

Let $|j_A t_{j_A} m_{j_A}\rangle$ and $|j_B t_{j_B} m_{j_B}\rangle$ denote the spin basis of $\mathbb{V}^{(A)}$ and $\mathbb{V}^{(B)}$ respectively. We introduce a coupled basis $|j_{AB} t_{j_{AB}} m_{j_{AB}}\rangle \in \mathbb{V}^{(AB)}$ that fulfills,

$$\begin{aligned} \mathbf{J}^{2(AB)} |j_{AB} t_{j_{AB}} m_{j_{AB}}\rangle &= j_{AB}(j_{AB} + 1) |j_{AB} t_{j_{AB}} m_{j_{AB}}\rangle, \\ \hat{j}_z^{(AB)} |j_{AB} t_{j_{AB}} m_{j_{AB}}\rangle &= m_{j_{AB}} |j_{AB} t_{j_{AB}} m_{j_{AB}}\rangle. \end{aligned} \quad (5.80)$$

and which is related to the product basis,

$$|j_{At_{j_A}} m_{j_A}; j_{Bt_{j_B}} m_{j_B}\rangle \equiv |j_{At_{j_A}} m_{j_A}\rangle \otimes |j_{Bt_{j_B}} m_{j_B}\rangle,$$

by means of a transformation,

$$\boxed{|j_{ABt_{j_{AB}}} m_{j_{AB}}\rangle = \sum_{t_{j_A} t_{j_B}} \sum_{m_{j_A} m_{j_B}} \Upsilon_{j_{At_{j_A}} m_{j_A}; j_{Bt_{j_B}} m_{j_B} \rightarrow j_{ABt_{j_{AB}}} m_{j_{AB}}}^{\text{fuse}} |j_{At_{j_A}} m_{j_A}; j_{Bt_{j_B}} m_{j_B}\rangle.} \quad (5.81)$$

The components $\Upsilon_{j_{At_{j_A}} m_{j_A}; j_{Bt_{j_B}} m_{j_B} \rightarrow j_{ABt_{j_{AB}}} m_{j_{AB}}}^{\text{fuse}}$ can be expressed in terms of the Clebsch-Gordan coefficients as

$$\boxed{\Upsilon_{j_{At_{j_A}} m_{j_A}; j_{Bt_{j_B}} m_{j_B} \rightarrow j_{ABt_{j_{AB}}} m_{j_{AB}}}^{\text{fuse}} = X_{j_{At_{j_A}}; j_{Bt_{j_B}} \rightarrow j_{ABt_{j_{AB}}}}^{\text{fuse}} C_{j_{Am_{j_A}}; j_{Bm_{j_B}} \rightarrow j_{ABm_{j_{AB}}}}^{\text{fuse}}.} \quad (5.82)$$

Let us explain how this expression is obtained. From the definition, Eq. (5.81), we have

$$\Upsilon_{j_{At_{j_A}} m_{j_A}; j_{Bt_{j_B}} m_{j_B} \rightarrow j_{ABt_{j_{AB}}} m_{j_{AB}}}^{\text{fuse}} \equiv \langle j_{ABt_{j_{AB}}} m_{j_{AB}} | j_{At_{j_A}} m_{j_A}; j_{Bt_{j_B}} m_{j_B} \rangle. \quad (5.83)$$

According to the direct sum decomposition, Eq. (5.79), each vector $|j_{ABt_{j_{AB}}} m_{j_{AB}}\rangle$ belongs to the subspace $\mathbb{D}_{j_{AB}}^{(AB)} \otimes \mathbb{V}_{j_{AB}}^{(AB)}$ where it factorizes as

$$|j_{ABt_{j_{AB}}} m_{j_{AB}}\rangle = |j_{ABt_{j_{AB}}}\rangle \otimes |j_{ABm_{j_{AB}}}\rangle. \quad (5.84)$$

Similarly, we can factorize vectors $|j_{At_{j_A}} m_{j_A}\rangle$ and $|j_{Bt_{j_B}} m_{j_B}\rangle$. The expression Eq. (5.82) can then be obtained by substituting these factorizations into Eq. (5.83) and re-arranging the terms as shown below,

$$\begin{aligned} \Upsilon_{j_{At_{j_A}} m_{j_A}; j_{Bt_{j_B}} m_{j_B} \rightarrow j_{ABt_{j_{AB}}} m_{j_{AB}}}^{\text{fuse}} &= \langle j_{ABt_{j_{AB}}} | j_{At_{j_A}}; j_{Bt_{j_B}} \rangle \langle j_{ABm_{j_{AB}}} | j_{Am_{j_A}}; j_{Bm_{j_B}} \rangle, \\ &= X_{j_{At_{j_A}}; j_{Bt_{j_B}} \rightarrow j_{ABt_{j_{AB}}}}^{\text{fuse}} C_{j_{Am_{j_A}}; j_{Bm_{j_B}} \rightarrow j_{ABm_{j_{AB}}}}^{\text{fuse}}, \end{aligned}$$

where $|j_{At_{j_A}}; j_{Bt_{j_B}}\rangle \equiv |j_{At_{j_A}}\rangle \otimes |j_{Bt_{j_B}}\rangle$.

Here X^{fuse} is a one to one map that relates vectors $|j_{ABt_{j_{AB}}}\rangle \in \mathbb{D}_{j_{AB}}^{(AB)}$ to the vectors $|j_{At_{j_A}}; j_{Bt_{j_B}}\rangle \in \mathbb{D}_{j_{AB}}^{(AB)}$. It can be regarded as a rank-3 tensor such that each component of X^{fuse} is either a zero or a one. We have,

$$X_{j_{At_{j_A}}; j_{Bt_{j_B}} \rightarrow j_{ABt_{j_{AB}}}}^{\text{fuse}} = \begin{cases} 1 & \text{if } |j_{ABt_{j_{AB}}}\rangle = |j_{At_{j_A}}; j_{Bt_{j_B}}\rangle, \\ 0 & \text{otherwise.} \end{cases} \quad (5.85)$$

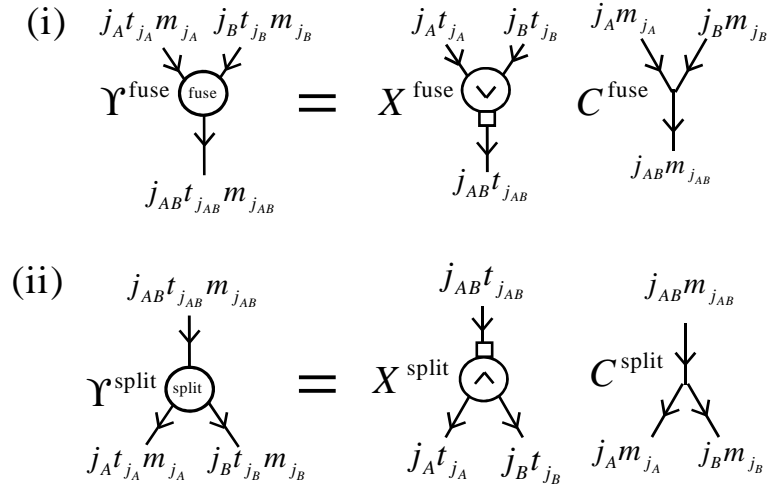


Figure 5.8 – The graphical representations of (i) the fusing tensor Υ^{fuse} and (ii) the splitting tensor. For fixed values of j_A, j_B and j_{AB} each of these tensors factorizes into a X and a C tensor.

The product basis can, in turn, be expressed in terms of the coupled basis,

$$\boxed{|j_A t_{j_A} m_{j_A}; j_B t_{j_B} m_{j_B}\rangle = \sum_{t_{j_{AB}}} \sum_{m_{j_{AB}}} \Upsilon_{j_{AB} t_{j_{AB}} m_{j_{AB}} \rightarrow j_A t_{j_A} m_{j_A} j_B t_{j_B} m_{j_B}}^{\text{split}} |j_{AB} t_{j_{AB}} m_{j_{AB}}\rangle,} \quad (5.86)$$

where

$$\boxed{\Upsilon_{j_{AB} t_{j_{AB}} m_{j_{AB}} \rightarrow j_A t_{j_A} m_{j_A} j_B t_{j_B} m_{j_B}}^{\text{split}} = X_{j_{AB} t_{j_{AB}} \rightarrow j_A t_{j_A} j_B t_{j_B}}^{\text{split}} \cdot C_{j_{AB} m_{j_{AB}} \rightarrow j_A m_{j_A} j_B m_{j_B}}^{\text{split}},} \quad (5.87)$$

and

$$X_{j_{AB} t_{j_{AB}} \rightarrow j_A t_{j_A} j_B t_{j_B}}^{\text{split}} \equiv X_{j_A t_{j_A} j_B t_{j_B} \rightarrow j_{AB} t_{j_{AB}}}^{\text{fuse}}. \quad (5.88)$$

We refer to the tensors Υ^{fuse} and Υ^{split} as the *fusing* tensor and the *splitting* tensor respectively, since they will play an instrumental role in fusing and splitting indices of an SU(2)-invariant tensor. The special graphical representation of these tensors and their decomposition into X and C tensors is shown in Fig. 5.8. Tensors $X_{j_A t_{j_A} j_B t_{j_B} \rightarrow j_{AB} t_{j_{AB}}}^{\text{fuse}}$ and $X_{j_{AB} t_{j_{AB}} \rightarrow j_A t_{j_A} j_B t_{j_B}}^{\text{split}}$ are graphically represented by means of a circle enclosing an arrow head and three lines emerging from the circle corresponding to the three indices of the tensors. The three lines in the diagrams of X^{fuse} and X^{split} correspond to the degeneracy

indices $(j_A, t_{j_A}), (j_B, t_{j_B})$ and $(j_{AB}, t_{j_{AB}})$ by using the same assignment rules that were introduced for tensors C^{fuse} and C^{split} respectively. Other features of the graphical representation include an arrow head that is placed within the circle to indicate the direction of the fusion and a small rectangle, placed on the line carrying the coupled spins, that represents a permutation of basis elements.

We notice that tensor X^{fuse} can be decomposed into two pieces. The first piece (depicted as the circle enclosing an arrow head) expresses a basis $\{|j_A t_{j_A}; j_B t_{j_B} \equiv |j_A t_{j_A} \rangle \otimes |j_B t_{j_B} \rangle\}$ of $\mathbb{D}^{(AB)}$ as the direct product of the basis $\{|j_A t_{j_A}\}$ of $\mathbb{D}^{(A)}$ and the basis $\{|j_B t_{j_B}\}$ of $\mathbb{D}^{(B)}$. Note that this procedure does not always lead to the set $\{|j_A t_{j_A}; j_B t_{j_B}\}$ being ordered such that states corresponding to the same total spin j_{AB} are adjacent to each other within the set. However, we require that the basis associated to an index be maintained as such (this ensures, for example, that an $SU(2)$ -invariant matrix is block diagonal when expressed in such a basis). This ordering is achieved by means of the second piece (depicted as the small rectangle): a permutation of basis states $\{|j_A t_{j_A}; j_B t_{j_B}\}$ that reorganizes them according to their total spin j_{AB} , so that they are identified in an one-to-one correspondence with the coupled states $\{|j_{AB} t_{j_{AB}}\}$. In particular, this description of the tensors X^{fuse} and X^{split} can be exploited to multiply together several such tensors, such as in Fig. 5.12(iv), in a fast way.

By construction, a resolution of Identity can be obtained in terms of tensor Υ^{fuse} and tensor Υ^{split} , as shown in Fig. 5.8(ii)-(iii).

Example 7: Let vector spaces $\mathbb{V}^{(A)}$ and $\mathbb{V}^{(B)}$ correspond to the vector space of Example 4, that is,

$$\begin{aligned}\mathbb{V}^{(A)} &\cong 3\mathbb{V}_{\frac{1}{2}}^{(A)} \cong \mathbb{D}_{\frac{1}{2}}^{(A)} \otimes \mathbb{V}_{\frac{1}{2}}^{(A)}, \\ \mathbb{V}^{(B)} &\cong 3\mathbb{V}_{\frac{1}{2}}^{(B)} \cong \mathbb{D}_{\frac{1}{2}}^{(B)} \otimes \mathbb{V}_{\frac{1}{2}}^{(B)}.\end{aligned}\tag{5.89}$$

The space $\mathbb{V}^{(AB)}$ decomposes as

$$\mathbb{V}^{(AB)} \cong \left(\mathbb{D}_0^{(AB)} \otimes \mathbb{V}_0^{(AB)}\right) \oplus \left(\mathbb{D}_1^{(AB)} \otimes \mathbb{V}_1^{(AB)}\right),\tag{5.90}$$

where,

$$\mathbb{V}_{\frac{1}{2}}^{(A)} \otimes \mathbb{V}_{\frac{1}{2}}^{(B)} \cong (\mathbb{V}_0^{(AB)} \oplus \mathbb{V}_1^{(AB)}),\tag{5.91}$$

and

$$\mathbb{D}_0^{(AB)} \cong \mathbb{D}_{\frac{1}{2}}^{(A)} \otimes \mathbb{D}_{\frac{1}{2}}^{(B)}, \quad (5.92)$$

$$\mathbb{D}_1^{(AB)} \cong \mathbb{D}_{\frac{1}{2}}^{(A)} \otimes \mathbb{D}_{\frac{1}{2}}^{(B)}. \quad (5.93)$$

Recall that the basis of the l.h.s. and r.h.s. of Eq. (5.91) are related by the transformations Eqs. (5.74)-(5.77). Let us now consider how the basis of the l.h.s. and r.h.s. of Eq. (5.92) and of Eq. (5.93) are related. In Eq. (5.92), for instance, the vectors

$$|j_{AB} = 0, t_{j_{AB}}\rangle \in \mathbb{D}_0^{(AB)}, \quad t_{j_{AB}} = 1, 2, \dots, 9,$$

are related to the vectors

$$|j_A = \frac{1}{2}, t_{j_A}; j_B = \frac{1}{2}, t_{j_B}\rangle, \in \mathbb{D}_0^{(AB)} \quad t_{j_A}, t_{j_B} = 1, 2, 3,$$

in straightforward way by associating the vectors in a one to one fashion in the order in which they appear in the respective basis. For example, the change of basis maps the vector

$$|j_{AB} = 0, t_{j_{AB}} = 1\rangle \text{ to } |j_A = \frac{1}{2}, t_{j_A} = 1; j_B = \frac{1}{2}, t_{j_B} = 1\rangle$$

and the vector

$$|j_{AB} = 0, t_{j_{AB}} = 2\rangle \text{ to } |j_A = \frac{1}{2}, t_{j_A} = 2; j_B = \frac{1}{2}, t_{j_B} = 1\rangle$$

and so on. The basis of the l.h.s. and r.h.s. of Eq. (5.93) are related in a similar way. This one to one mapping can be encoded into $X_{j_A t_{j_A}, j_B t_{j_B} \rightarrow j_{AB} t_{j_{AB}}}^{\text{fuse}}$ by setting the numerical value of the following components equal to one,

$$\begin{aligned} X_{\frac{1}{2}1, \frac{1}{2}1 \rightarrow 01}^{\text{fuse}}, & \quad X_{\frac{1}{2}1, \frac{1}{2}2 \rightarrow 02}^{\text{fuse}}, & \quad X_{\frac{1}{2}1, \frac{1}{2}3 \rightarrow 03}^{\text{fuse}}, \\ X_{\frac{1}{2}2, \frac{1}{2}1 \rightarrow 01}^{\text{fuse}}, & \quad X_{\frac{1}{2}2, \frac{1}{2}2 \rightarrow 02}^{\text{fuse}}, & \quad X_{\frac{1}{2}2, \frac{1}{2}3 \rightarrow 03}^{\text{fuse}}, \\ X_{\frac{1}{2}3, \frac{1}{2}1 \rightarrow 01}^{\text{fuse}}, & \quad X_{\frac{1}{2}3, \frac{1}{2}2 \rightarrow 02}^{\text{fuse}}, & \quad X_{\frac{1}{2}3, \frac{1}{2}3 \rightarrow 03}^{\text{fuse}}, \end{aligned}$$

and

$$\begin{aligned} X_{\frac{1}{2}1, \frac{1}{2}1 \rightarrow 11}^{\text{fuse}}, & \quad X_{\frac{1}{2}1, \frac{1}{2}2 \rightarrow 12}^{\text{fuse}}, & \quad X_{\frac{1}{2}1, \frac{1}{2}3 \rightarrow 13}^{\text{fuse}}, \\ X_{\frac{1}{2}2, \frac{1}{2}1 \rightarrow 11}^{\text{fuse}}, & \quad X_{\frac{1}{2}2, \frac{1}{2}2 \rightarrow 12}^{\text{fuse}}, & \quad X_{\frac{1}{2}2, \frac{1}{2}3 \rightarrow 13}^{\text{fuse}}, \\ X_{\frac{1}{2}3, \frac{1}{2}1 \rightarrow 11}^{\text{fuse}}, & \quad X_{\frac{1}{2}3, \frac{1}{2}2 \rightarrow 12}^{\text{fuse}}, & \quad X_{\frac{1}{2}3, \frac{1}{2}3 \rightarrow 13}^{\text{fuse}}. \blacksquare \end{aligned}$$

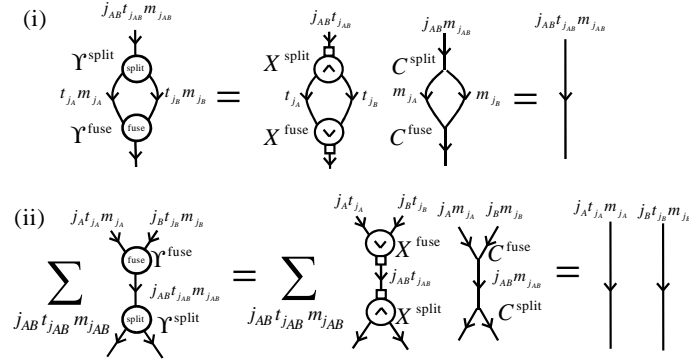


Figure 5.9 – Tensors Υ^{fuse} and Υ^{split} are unitary and thus yield the Identity when contracted pairwise either as (i) or (ii).

Example 8: As another example of the change of basis X^{fuse} , consider that $\mathbb{V}^{(A)}$ and $\mathbb{V}^{(B)}$ correspond to the vector spaces of Example 3 and Example 5 respectively. That is,

$$\begin{aligned} \mathbb{V}^{(A)} &\cong \mathbb{V}_1^{(A)} \cong (\mathbb{D}_1^{(A)} \otimes \mathbb{V}_1^{(A)}), \\ \mathbb{V}^{(B)} &\cong 2\mathbb{V}_0^{(B)} \oplus \mathbb{V}_1^{(B)} \cong (\mathbb{D}_0^{(B)} \otimes \mathbb{V}_0^{(B)}) \oplus (\mathbb{D}_1^{(B)} \otimes \mathbb{V}_1^{(B)}). \end{aligned} \quad (5.94)$$

The space $\mathbb{V}^{(AB)}$ decomposes as

$$\mathbb{V}^{(AB)} \cong (\mathbb{D}_0^{(AB)} \otimes \mathbb{V}_0^{(AB)}) \oplus (\mathbb{D}_1^{(AB)} \otimes \mathbb{V}_1^{(AB)}) \oplus (\mathbb{D}_2^{(AB)} \otimes \mathbb{V}_2^{(AB)}), \quad (5.95)$$

where

$$\mathbb{D}_0^{(AB)} \cong \mathbb{D}_1^{(A)} \otimes \mathbb{D}_1^{(B)} \quad (5.96)$$

$$\mathbb{D}_1^{(AB)} \cong (\mathbb{D}_0^{(A)} \otimes \mathbb{D}_1^{(B)}) \oplus (\mathbb{D}_1^{(A)} \otimes \mathbb{D}_0^{(B)}) \quad (5.97)$$

$$\mathbb{D}_2^{(AB)} \cong \mathbb{D}_1^{(A)} \otimes \mathbb{D}_1^{(B)}. \quad (5.98)$$

The transformation that relates the bases of l.h.s. and r.h.s. of Eq. (5.96) and of Eq. 5.98) is straightforward, we set

$$X_{01,11 \rightarrow 01}^{\text{fuse}} = X_{11,11 \rightarrow 21}^{\text{fuse}} = 1.$$

The basis of the l.h.s. and r.h.s. of Eq. (5.97) can be related by mapping the three vectors

$$|j_{AB} = 1, t_{j_{AB}} = 1, 2, 3\rangle \in \mathbb{D}_1^{(AB)},$$

in a one to one manner, to the two vectors

$$|j_A = 1, t_{j_A} = 1; j_B = 0, t_{j_B} = 1, 2\rangle \in (\mathbb{D}_0^{(A)} \otimes \mathbb{D}_1^{(B)}),$$

and the vector

$$|j_A = 0, t_{j_A} = 1; j_B = 1, t_{j_B} = 1\rangle \in (\mathbb{D}_1^{(A)} \otimes \mathbb{D}_0^{(B)}).$$

This is encoded into X^{fuse} by setting

$$X_{02,11 \rightarrow 12}^{\text{fuse}} = X_{11,11 \rightarrow 01}^{\text{fuse}} = X_{11,11 \rightarrow 13}^{\text{fuse}} = 1. \blacksquare$$

5.4 Review: Fusion trees

When considering the tensor product of more than two representations one can obtain several coupled bases of the product space. These correspond to taking the product of the vector spaces according to different sequences of pairwise products. The spaces are linearly ordered in a given way and we only consider a pairwise product of ‘adjacent’ spaces in this linear ordering. For example, when considering the tensor product of three representations,

$$\mathbb{V}^{(ABC)} \cong \mathbb{V}^{(A)} \otimes \mathbb{V}^{(B)} \otimes \mathbb{V}^{(C)}, \quad (5.99)$$

one can consider either the pairwise products

$$\begin{aligned} \mathbb{V}^{(D)} &\cong \mathbb{V}^{(A)} \otimes \mathbb{V}^{(B)}, \\ \mathbb{V}^{(ABC)} &\cong \mathbb{V}^{(D)} \otimes \mathbb{V}^{(C)}, \end{aligned} \quad (5.100)$$

or the pairwise products

$$\begin{aligned} \mathbb{V}^{(E)} &\cong \mathbb{V}^{(B)} \otimes \mathbb{V}^{(C)}, \\ \mathbb{V}^{(ABC)} &\cong \mathbb{V}^{(A)} \otimes \mathbb{V}^{(E)}. \end{aligned} \quad (5.101)$$

Considering the tensor product one way or the other leads to two different coupled bases in $\mathbb{V}^{(ABC)}$.

More generally, there exist several choices of a coupled basis in the tensor product of L representations, Eqs. (5.55)-(5.57). A useful way to specify a particular sequence of pairwise products is by means of a *fusion tree*.

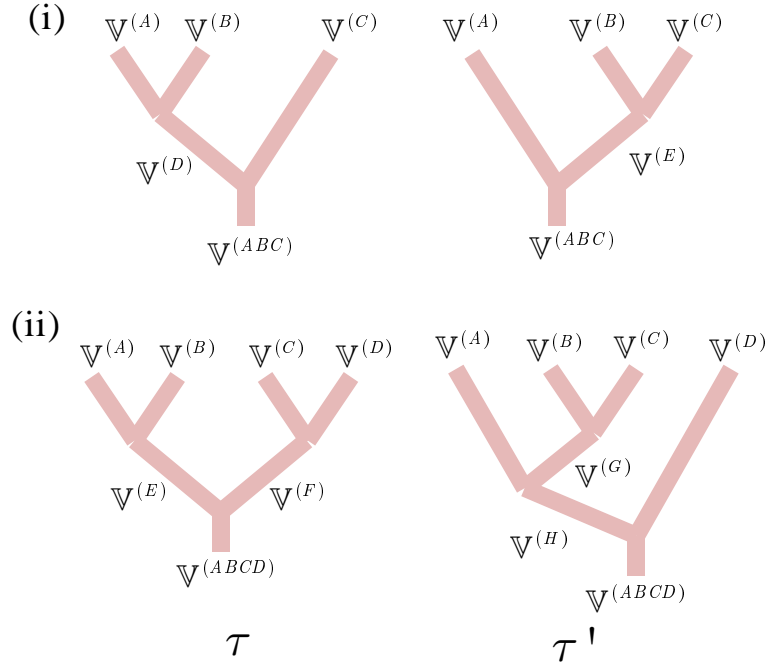


Figure 5.10 – Examples of two fusion trees τ and τ' that describe two different ways of considering the tensor product of (i) three vector spaces $\mathbb{V}^{(A)}$, $\mathbb{V}^{(B)}$ and $\mathbb{V}^{(C)}$ and (ii) four vector spaces $\mathbb{V}^{(A)}$, $\mathbb{V}^{(B)}$, $\mathbb{V}^{(C)}$ and $\mathbb{V}^{(D)}$. Fusion proceeds from top to bottom.

A fusion tree, denoted τ , is a *directed* trivalent tree such that each node of the tree represents the tensor product of two incoming spaces into the outgoing space. The tree has a total of $L + 1$ open links which correspond to the L vector spaces $\mathbb{V}^{(1)}$, $\mathbb{V}^{(2)}$, \dots , $\mathbb{V}^{(L)}$ and the product space \mathbb{V} . The internal links correspond to the intermediate product spaces that appear in a sequence of pairwise products. Figure 5.10 illustrates two different fusion trees τ and τ' that correspond to two different ways of considering the tensor product of three and of four representations. The sequence of fusions proceeds from top to bottom. A fusion tree can also be specified as a list of fusions. For example, the fusion trees τ and τ' depicted in Fig. 5.10(i) can be specified as

$$\begin{aligned}\tau &\equiv \{A, B \rightarrow D; D, C \rightarrow (ABC)\}, \\ \tau' &\equiv \{B, C \rightarrow E; A, E \rightarrow (ABC)\}.\end{aligned}$$

Fusion trees play an important role in our discussion. In the present context, a fusion tree characterizes a coupled basis of a tensor product space. In Sec. 5.5 fusion trees are

also used to characterize different canonical decompositions of an $SU(2)$ -invariant tensor.

In the remainder of the section we consider coupled bases that are labeled by different fusion trees. We define the unitary transformation that relates two such coupled bases. This transformation is important since it also relates two different canonical decompositions of an $SU(2)$ -invariant tensor, as discussed in Sec. 5.5. For purpose of illustration, we first characterize the coupled basis in the simple case of the tensor product of three representations before proceeding to the generic case of L representations.

5.4.1 Tensor product of three irreps

Let vector spaces $\mathbb{V}^{(A)}, \mathbb{V}^{(B)}$ and $\mathbb{V}^{(C)}$ transform as irreps j_A, j_B and j_C respectively. The space $\mathbb{V}^{(ABC)}$ is in general reducible, and may contain several copies of an irrep j_{ABC} . Let us first consider the sequence (5.100) of tensor products corresponding to a fusion tree τ . The vector spaces $\mathbb{V}^{(D)}$ and $\mathbb{V}^{(ABC)}$ decompose as

$$\mathbb{V}^{(D)} \cong \bigoplus_{j_D} \mathbb{V}_{j_D}^{(D)}, \quad (5.102)$$

and

$$\mathbb{V}^{(ABC)} \cong \bigoplus_{j_{ABC}, j_D} \mathbb{V}_{j_{ABC}, j_D}^{(ABC)}. \quad (5.103)$$

Notice that we can use the values of j_D that appear on the r.h.s. of Eq. (5.102) to label different copies of j_{ABC} that appear on the r.h.s. of Eq. (5.103). Thus, a coupled basis of $\mathbb{V}^{(ABC)}$ can be labeled as $|j_{ABC} m_{j_{ABC}}; \tau; j_D\rangle$.

Let $(\hat{Q}_{j_A j_B j_C j_{ABC}}^{j_D})_{m_{j_A} m_{j_B} m_{j_C} m_{j_{ABC}}}$ denote the transformation from the product basis $|j_A m_{j_A}\rangle \otimes |j_B m_{j_B}\rangle \otimes |j_C m_{j_C}\rangle$ to the coupled basis $|j_{ABC} m_{j_{ABC}}; \tau; j_D\rangle$. This change of basis can be expressed in terms of Clebsch-Gordan coefficients as

$$(\hat{Q}_{j_A j_B j_C j_{ABC}}^{j_D})_{m_{j_A} m_{j_B} m_{j_C} m_{j_{ABC}}} \equiv \sum_{m_{j_D}} C_{j_A m_{j_A}, j_B m_{j_B} \rightarrow j_D m_{j_D}}^{\text{fuse}} \cdot C_{j_D m_{j_D}, j_C m_{j_C} \rightarrow j_{ABC} m_{j_{ABC}}}^{\text{fuse}}, \quad (5.104)$$

where $C_{j_A m_{j_A}, j_B m_{j_B} \rightarrow j_D m_{j_D}}^{\text{fuse}}$ relates the basis $|j_A, m_{j_A}\rangle \otimes |j_B, m_{j_B}\rangle$ to the intermediate basis $|j_D m_{j_D}\rangle$, and $C_{j_D m_{j_D}, j_C m_{j_C} \rightarrow j_{ABC} m_{j_{ABC}}}^{\text{fuse}}$ relates this intermediate basis to the coupled basis $|j_{ABC} m_{j_{ABC}}; \tau; j_D\rangle$.

$$\begin{aligned}
\text{(i)} \quad & \begin{array}{c} j_A \quad j_B \quad j_C \\ \swarrow \quad \downarrow \quad \searrow \\ j_D \quad \hat{Q} \\ \downarrow \\ j_{ABC} \end{array} = \sum_{j_E} \hat{F}_{j_A j_B j_C j_{ABC}}^{j_D j_E} \begin{array}{c} j_A \quad j_B \quad j_C \\ \swarrow \quad \downarrow \quad \searrow \\ \hat{Q}' \quad j_E \\ \downarrow \\ j_{ABC} \end{array} \\
\text{(ii)} \quad & \begin{array}{c} j_{ABC} \\ \downarrow \\ \begin{array}{c} j_A \quad j_B \\ \swarrow \quad \searrow \\ j_D \quad j_C \end{array} \\ \downarrow \\ j_{ABC} \end{array} = \hat{F}_{j_A j_B j_C j_{ABC}}^{j_D j_E} \begin{array}{c} j_{ABC} \\ \downarrow \\ j_{ABC} \end{array}
\end{aligned}$$

Figure 5.11 – (i) In the tensor product of three irreps, two coupled bases that are labeled by fusion trees τ (5.100) and τ' (5.101) are related to one another by means of the recoupling coefficients $\hat{F}_{j_A j_B j_C j_{ABC}}^{j_D j_E}$. (ii) A recoupling coefficient is given as the ‘scalar product’ of \hat{Q} and \hat{Q}' .

Alternatively, we can first consider the tensor product $\mathbb{V}^{(B)} \otimes \mathbb{V}^{(C)}$ (corresponding to the sequence (5.101) of tensor products characterized by another fusion tree τ'),

$$\mathbb{V}^{(E)} \cong \mathbb{V}^{(B)} \otimes \mathbb{V}^{(C)} \cong \bigoplus_{j_E} \mathbb{V}_{j_E}^{(E)}, \quad (5.105)$$

and use irrep j_E to label another coupled basis $|j_{ABC} m_{j_{ABC}}; \tau'; j_E\rangle$ of $\mathbb{V}^{(ABC)}$. Denote by $(\hat{Q}_{j_A j_B j_C j_{ABC}}^{j_E})_{m_{j_A} m_{j_B} m_{j_C} m_{j_{ABC}}}$ the change of basis to this new coupled basis. In terms of Clebsch-Gordan coefficients we have

$$(\hat{Q}_{j_A j_B j_C j_{ABC}}^{j_E})_{m_{j_A} m_{j_B} m_{j_C} m_{j_{ABC}}} \equiv \sum_{m_{j_E}} C_{j_B m_{j_B}, j_C m_{j_C} \rightarrow j_E m_{j_E}}^{\text{fuse}} \cdot C_{j_A m_{j_A}, j_E m_{j_E} \rightarrow j_{ABC} m_{j_{ABC}}}^{\text{fuse}}. \quad (5.106)$$

The two coupled bases $|j_{ABC} m_{j_{ABC}}; \tau; j_D\rangle$ and $|j_{ABC} m_{j_{ABC}}; \tau'; j_E\rangle$ are related by a transformation that is given by a rank-6 tensor \hat{F} with components $\hat{F}_{j_A j_B j_C j_{ABC}}^{j_D j_E}$,

$$\boxed{\hat{Q}_{j_A j_B j_C j_{ABC}}^{j_E} = \sum_{j_D} \hat{F}_{j_A j_B j_C j_{ABC}}^{j_D j_E} \hat{Q}_{j_A j_B j_C j_{ABC}}^{j_D}} \quad (5.107)$$

Here $\hat{F}_{j_A j_B j_C j_{ABC}}^{j_D j_E}$ are the *recoupling coefficients* (Cornwell, 1997) of SU(2). By using Eqs. (5.104) and (5.106), the recoupling coefficients can be explicitly expressed in terms of Clebsch-Gordan coefficients,

$$\hat{F}_{j_A j_B j_C j_{ABC}}^{j_D j_E} \equiv \frac{1}{2j_{ABC} + 1} \times \sum_{\mathbf{m}} \left(C_{j_A m_{j_A}, j_B m_{j_B} \rightarrow j_D m_{j_D}}^{\text{fuse}} C_{j_D m_{j_D}, j_C m_{j_C} \rightarrow j_{ABC} m_{j_{ABC}}}^{\text{fuse}} C_{j_B m_{j_B}, j_C m_{j_C} \rightarrow j_E m_{j_E}}^{\text{fuse}} C_{j_D m_{j_D}, j_C m_{j_C} \rightarrow j_{ABC} m_{j_{ABC}}}^{\text{fuse}} \right), \quad (5.108)$$

where $\mathbf{m} \equiv \{m_{j_D}, m_{j_E}, m_{j_A}, m_{j_B}, m_{j_C}, m_{j_{ABC}}\}$. Notice that, since the m 's are summed over, the recoupling coefficients depend only on the j 's. Also recall that the recoupling coefficients are proportional to the 6-j symbols of the group,

$$\hat{F}_{j_A j_B j_C j_{ABC}}^{j_D j_E} = \alpha \begin{Bmatrix} j_A & j_B & j_D \\ j_C & j_{ABC} & j_E \end{Bmatrix}, \quad (5.109)$$

where

$$\alpha \equiv (-1)^{(j_A + j_B + j_C + j_{ABC})} \sqrt{(2j_D + 1)(2j_E + 1)}. \quad (5.110)$$

5.4.2 Tensor product of three reducible representations

Consider the action of SU(2) on the space $\mathbb{V}^{(ABC)}$,

$$\mathbb{V}^{(ABC)} \cong \mathbb{V}^{(A)} \otimes \mathbb{V}^{(B)} \otimes \mathbb{V}^{(C)},$$

where $\mathbb{V}^{(A)}$, $\mathbb{V}^{(B)}$ and $\mathbb{V}^{(C)}$ are reducible representations of SU(2). It induces a decomposition

$$\mathbb{V}^{(ABC)} \cong \bigoplus_{j_{ABC}} \left(\mathbb{D}_{j_{ABC}}^{(ABC)} \otimes \mathbb{V}_{j_{ABC}}^{(ABC)} \right), \quad (5.111)$$

where j_{ABC} takes all values that are compatible with any j_A, j_B and j_C .

Extending the argument for irreps, we can relate the coupled basis of $\mathbb{V}^{(ABC)}$ to the product basis by first considering the sequence (5.100) of tensor products and using two Υ^{fuse} tensors

$$\Upsilon_{A,B \rightarrow D}^{\text{fuse}}, \quad \Upsilon_{D,C \rightarrow (ABC)}^{\text{fuse}} \quad (5.112)$$

to relate at each step the coupled basis with the product basis. Alternatively, we can consider the sequence (5.101) of tensor products and use the different set of fusing tensors

$$\Upsilon_{B,C \rightarrow E}^{\text{fuse}}, \quad \Upsilon_{A,E \rightarrow (ABC)}^{\text{fuse}} \quad (5.113)$$

to relate the product basis to the coupled basis at each step. The respective change of basis transformation for the two cases is depicted in Fig. 5.12(i).

The two coupled bases, so obtained, are related by means of a matrix $\hat{\Gamma}$ that decomposes, according to Schur's Lemma [Eq. (5.46)] as

$$\hat{\Gamma} = \bigoplus_{j_{ABC}} (\hat{D}_{j_{ABC}} \otimes \hat{I}_{j_{ABC}}), \quad (5.114)$$

where the components of $\hat{D}_{j_{ABC}}$ can be expressed in terms of recoupling coefficients. This decomposition can be derived as follows.

The matrix $\hat{\Gamma}$ is obtained by contracting the tensor network made of tensors Υ^{fuse} and tensors Υ^{split} that is shown in Fig. 5.12(ii). This contraction can be performed piecewise [Fig. 5.12(iii)]. For fixed values of j 's on all links the tensor network factorizes into two pieces since each constituent tensor Υ^{fuse} and tensor Υ^{split} factorizes into a X and a C tensor. The tensor network made of C tensors equates [Fig 5.11(ii)] the Identity times the recoupling coefficient $\hat{F}_{j_A j_B j_C j_{ABC}}^{j_E}$. The matrix $\hat{D}_{j_{ABC}}$ in Eq. (5.114) is then defined as

$$\hat{D}_{j_{ABC}} \equiv \sum_{j_A j_B j_C j_D j_E} \hat{F}_{j_A j_B j_C j_{ABC}}^{j_E} \hat{D}_{j_A j_B j_C j_{ABC}}^{j_E}, \quad (5.115)$$

where $\hat{D}_{j_A j_B j_C j_{ABC}}^{j_E}$ denotes the matrix that is obtained by contracting together the X tensors. Here the sum is over all values of j_A, j_B, j_C, j_D , and j_E that are compatible with a given value of j_{ABC} .

5.4.3 Tensor product of L irreps

In a similar way, we can consider the tensor product of four irreps; different choices of a coupled basis, corresponding to different fusion trees, are related by the $9 - j$ symbols and so on.

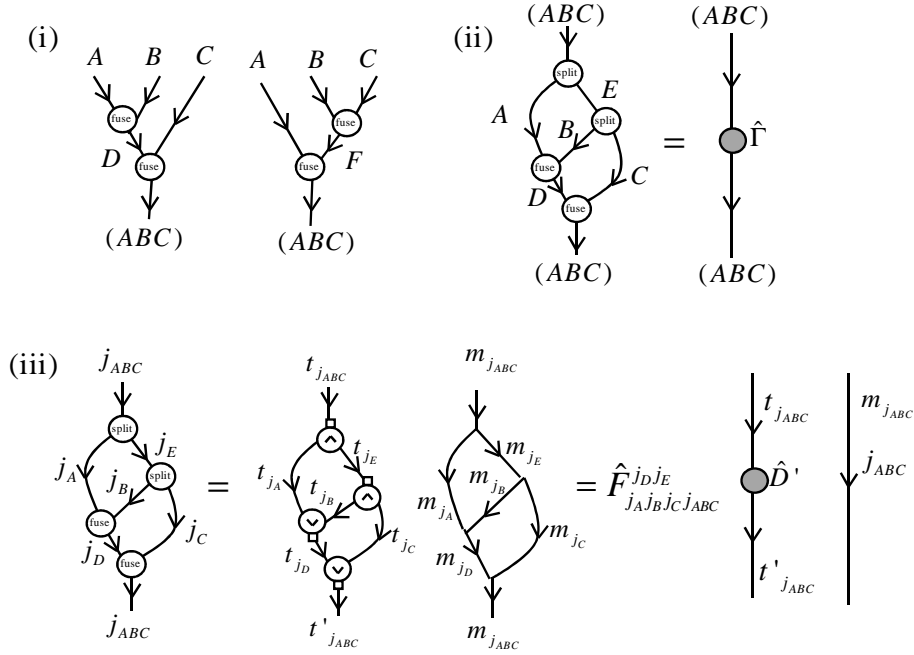


Figure 5.12 – (i) The change of basis from the product basis to two different coupled bases in the fusion of three reducible representations is given in terms of two fusing tensors. (ii) The two coupled basis are related by means of the matrix $\hat{\Gamma}$ [Eq. (5.114)] that is obtained by contracting a tensor network made of tensors Υ^{fuse} and tensors Υ^{split} . (iii) The components of $\hat{\Gamma}$ are given in terms of recoupling coefficients. This can be seen by performing the contraction piecewise. For fixed values of spins $j_A, j_B, j_C, j_{ABC}, j_D$ and j_E the tensor network decomposes into a tensor network made of X tensors and a spin network. The former is contracted to obtain a matrix \hat{D}' whereas the latter can be replaced by the Identity $\hat{I}_{2j_{ABC}+1}$ and a recoupling coefficient [Fig. 5.11(ii)].

More generally, let us consider the tensor product of L representations, Eq. (5.55), where each space $\mathbb{V}^{(l)}$ ($l = 1, 2, \dots, L$) transforms as an irrep j_l . A coupled basis can be labeled by a fusion tree τ and the set of intermediate irreps $j_{e_1}, j_{e_2}, \dots, j_{e_Z}$ that are assigned to the internal links of τ . We denote by

$$|jm_j; \tau; j_{e_1} \dots j_{e_Z}\rangle \in \mathbb{V} \quad (5.116)$$

such a basis. By attaching the appropriate Clebsch-Gordan tensor C^{fuse} to each node of τ and contracting the resulting tree tensor network we can obtain tensors

$$\hat{Q}_{j_1 \dots j_L}^{j_{e_1} \dots j_{e_Z}}(\tau), \quad (5.117)$$

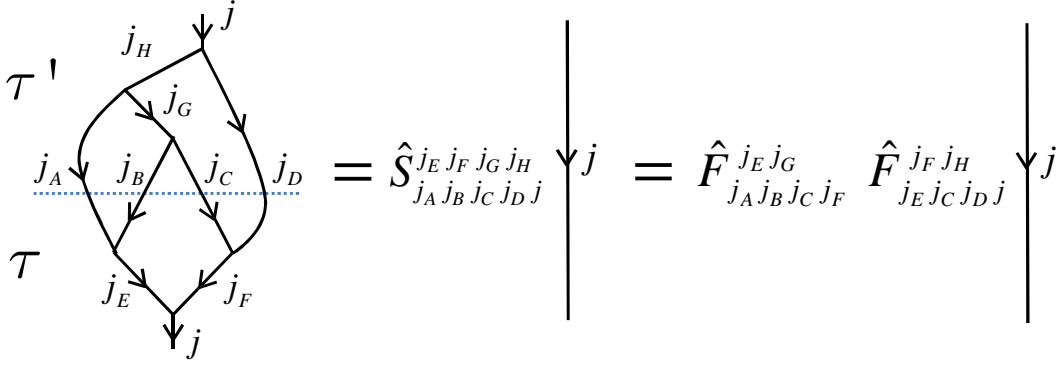


Figure 5.13 – The spin network that relates two coupled bases labeled by fusion trees τ and τ' . The spin network is proportional to the Identity, the proportionality factor is the coefficient $\hat{S}_{j_A j_B j_C j_D j}^{j_E j_F j_G j_H}$, which can be shown to be the product of two recoupling coefficients.

that mediate the change from the product basis to this coupled basis.

Another coupled basis $|jm_j; \tau'; j_{f_1} \dots j_{f_z}\rangle$ corresponding to a different fusion tree τ' is related to the basis (5.116) by the transformation

$$\hat{Q}_{j_1 \dots j_L}^{j_{f_1} \dots j_{f_z}}(\tau') = \sum_{j_{f_1} \dots j_{f_z}} \hat{S}_{j_1 \dots j_L}^{j_{e_1} \dots j_{e_z} j_{f_1} \dots j_{f_z}}(\tau, \tau') \hat{Q}_{j_1 \dots j_L}^{j_{e_1} \dots j_{e_z}}(\tau), \quad (5.118)$$

where the coefficients $\hat{S}_{j_1 \dots j_k}^{j_{e_1} \dots j_{e_z} j_{f_1} \dots j_{f_z}}(\tau, \tau')$ can be expressed in terms of the recoupling coefficients [Eq. (5.107)].

As an example, consider two different ways of coupling four spins j_A, j_B, j_C and j_D according to the fusion trees τ and τ' that are shown in Fig. 5.10(ii). The two coupled bases are related by coefficients $\hat{S}_{j_A j_B j_C j_D j}^{j_E j_F j_G j_H}(\tau, \tau')$ that are defined according to the equality depicted in Fig. 5.13. Note that the tensor network made of Clebsch-Gordan tensors, shown in Fig. 5.13, is an instance of a *spin network*. In this case, the spin network has two open links and can therefore be regarded as an $SU(2)$ -invariant operator. The equality in the figure then simply depicts that the spin network is proportional to the Identity. The numerical value of the coefficient $\hat{S}_{j_A j_B j_C j_D j}^{j_E j_F j_G j_H}(\tau, \tau')$ can be calculated without contracting the spin network, but by instead following a procedure called *evaluating* a spin network. Section 5.7 illustrates with simple examples the procedure to evaluate a spin network corresponding to a generic coefficient $\hat{S}_{j_1 \dots j_k}^{j_{e_1} \dots j_{e_z} j_{f_1} \dots j_{f_z}}(\tau, \tau')$. For instance, it is shown that

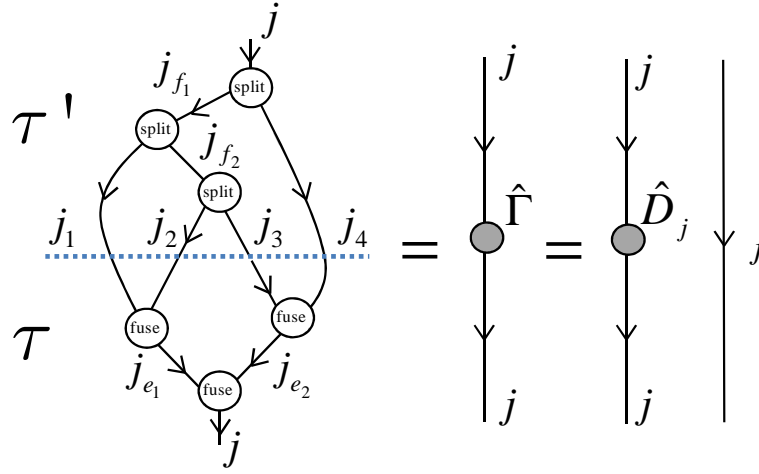


Figure 5.14 – The transformation $\hat{\Gamma}$ that relates two different coupled bases, labeled by fusion trees τ and τ' , when fusing four reducible representations. Matrix $\hat{\Gamma}$ decomposes into a degeneracy matrix \hat{D}_j and the Identity.

$\hat{S}_{j_A j_B j_C j_D}^{j_E j_F j_G j_H}(\tau, \tau')$ can be expressed in terms of two recoupling coefficients,

$$\hat{S}_{j_A j_B j_C j_D}^{j_E j_F j_G j_H}(\tau, \tau') = \hat{F}_{j_A j_B j_C j_F}^{j_E j_G} \hat{F}_{j_E j_C j_D j}^{j_F j_H}. \quad (5.119)$$

5.4.4 Tensor product of L reducible representations

Finally, consider the tensor product of L reducible representations. A coupled basis, labeled by a given fusion tree, is related to the product basis by means of a transformation that is obtained by attaching a tensor Υ^{fuse} to each node of the fusion tree, and contracting the resulting tree tensor network.

Two different choices of a coupled basis, corresponding to two different fusion trees τ and τ' , are related by a matrix $\hat{\Gamma}(\tau, \tau')$. The matrix $\hat{\Gamma}(\tau, \tau')$ is a generalization of the matrix with the same name that appears Eq. (5.114). This matrix is obtained by contracting a tensor network [e.g. Fig. 5.14] made of tensors Υ^{fuse} and tensors Υ^{split} .

For a fixed value of the total spin j , matrix $\hat{\Gamma}(\tau, \tau')$ decomposes in terms of degeneracy matrices \hat{D}_j . The components of the latter can be expressed in terms of recoupling

coefficients by generalizing Eq. (5.115). We obtain,

$$\hat{D}_j = \sum \hat{S}_{j_1 \dots j_k}^{j_{e_1} \dots j_{e_z}, j'_{e_1} \dots j'_{e_z}} \hat{D}_{j_1, \dots, j_k, j}^{j_{e_1}, \dots, j_{e_z}}, \quad (5.120)$$

where the sum runs over all spin labels but excluding j .

5.5 Block structure of SU(2)-invariant tensors

In this section we consider tensors that are invariant under the action of the symmetry. We explain how such tensors decompose into a compact canonical form which exploits their symmetry. The canonical form can be understood as a block structure in the tensor components. In Sec. 5.6 we then adapt the set \mathcal{P} of primitive tensor network manipulations to work in this form. With the formalism of SU(2)-invariant tensors at hand we then consider tensor network decompositions made of SU(2)-invariant tensors in Sec. 6.1.

5.5.1 SU(2)-invariant tensors

Consider a rank- k tensor \hat{T} with indices $\{i_1, i_2, \dots, i_k\}$ and directions \vec{D} . Each index i_l is associated with a vector space $\mathbb{V}^{(l)}$ on which SU(2) acts by means of transformations $\hat{W}_{\mathbf{r}}^{(l)}$.

Also consider the action of SU(2) on the space $\mathbb{V} \equiv \bigotimes_{l=1}^k \mathbb{V}^{(l)}$ given by

$$\hat{Y}_{\mathbf{r}}^{(1)} \otimes \hat{Y}_{\mathbf{r}}^{(2)} \otimes \dots \otimes \hat{Y}_{\mathbf{r}}^{(k)}, \quad (5.121)$$

where

$$\hat{Y}_{\mathbf{r}}^{(l)} = \begin{cases} \hat{W}_{\mathbf{r}}^{(l)*} & \text{if } \vec{D}^{(l)} = \text{'in'}, \\ \hat{W}_{\mathbf{r}}^{(l)} & \text{if } \vec{D}^{(l)} = \text{'out'}. \end{cases} \quad (5.122)$$

($\hat{W}_{\mathbf{r}}^{(l)*}$ denotes the complex conjugate of $\hat{W}_{\mathbf{r}}^{(l)}$.) That is, $\hat{Y}_{\mathbf{r}}^{(l)}$ acts differently depending on whether index i_l is an incoming or outgoing index. We then say that tensor \hat{T} is SU(2) *invariant* if it is invariant under the transformation of Eq. (5.121). In components we have

$$\sum_{i_1, i_2, \dots, i_k} \left(\hat{Y}_{\mathbf{r}}^{(1)} \right)_{i'_1 i_1} \left(\hat{Y}_{\mathbf{r}}^{(2)} \right)_{i'_2 i_2} \dots \left(\hat{Y}_{\mathbf{r}}^{(k)} \right)_{i'_k i_k} \hat{T}_{i_1 i_2 \dots i_k} = \hat{T}_{i'_1 i'_2 \dots i'_k}, \quad (5.123)$$

for all $\mathbf{r} \in \mathbb{R}^3$.

In the remainder of this section we explore the consequences of the constraints in Eq. (5.123). The main result is as follows. By writing each index i_l of the tensor in a spin basis, $i_l = (j_l, t_{j_l}, m_{j_l})$, the tensor is revealed to have a block structure, namely, the non-trivial components are organized into blocks that are supported on orthogonal subspaces. For a given value of spin j_l , the index i_l splits into a *degeneracy index* (j_l, t_{j_l}) and a *spin index* (j_l, m_{j_l}) . An SU(2)-invariant tensor \hat{T} decomposes into a set of *degeneracy tensors*, denoted by \hat{P} and carrying all the degeneracy indices, and a set of *structural tensors*, denoted \hat{Q} , carrying all the spin indices. The degeneracy tensors contain all the degrees of freedom and correspond to the ‘blocks’ alluded above. On the other hand, the structural tensors are completely determined by the symmetry since they can be factorized into a trivalent tree tensor network made of Clebsch-Gordan coefficients. Examples of structural tensors include Eq. (5.117), however, a structural tensor may not generally decompose according to a fusion tree. We refer to the decomposition (\hat{P}, \hat{Q}) as the *canonical decomposition* or the *canonical form* of tensor \hat{T} . The main benefit of the canonical form lies in the fact that \hat{T} can be specified compactly by means of only the degeneracy tensors.

In the ensuing discussion we describe the canonical decomposition of SU(2)-invariant tensors on a case by case basis. We explicitly describe the canonical form of SU(2)-invariant tensors with one to three indices. The canonical form in these cases is unique up to overall numerical factors. On the other hand, an SU(2)-invariant tensor with four or more indices can be decomposed in several equivalent ways. We illustrate this with examples without resorting to a complete theoretical characterization of the canonical form in all cases. A more rigorous characterization is developed Chapter 6 where we consider a special canonical form of SU(2)-invariant tensors, namely, tree decompositions. A tree decomposition corresponds to decomposing *both* the degeneracy tensors and the structural tensors according to a *fusion tree*. We find this decomposition more convenient from an implementation point of view. In Chapter 6, we also describe how to construct a tree decomposition for any SU(2)-invariant tensor, how two different tree decompositions of the same tensor are related to one another, and how primitive tensor manipulations are adapted to tree decompositions.

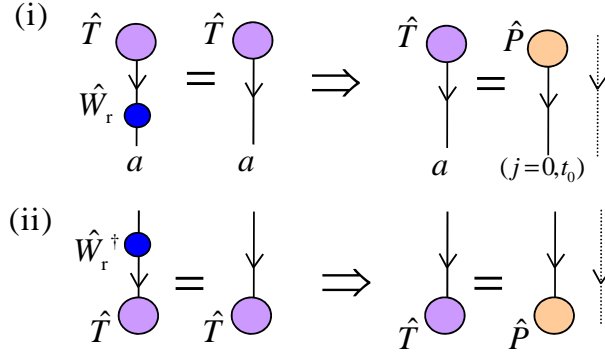


Figure 5.15 – Implication of the symmetry constraints fulfilled by a rank-1 SU(2)-invariant tensor with (i) an outgoing index, and (ii) an incoming index. The only allowed spin on the one index is $j = 0$.

5.5.2 One index

An SU(2)-invariant tensor \hat{T} with an outgoing index a fulfills the constraint [Fig. 5.15(i)]

$$(\Psi)_{a'} = \sum_a (\hat{W}_{\mathbf{r}})_{a'a} (\Psi)_a, \quad (5.124)$$

where $\hat{W}_{\mathbf{r}}$ is the representation of SU(2) on the vector space associated to index a .

Let us now write index a in the spin basis $a = (j, t_j, m_j) = (0, t_0, 0)$. Then we have

$$\hat{T}_a = (\hat{P})_{t_0}, \quad (5.125)$$

where $(\hat{P})_{t_0}$, shorthand for $(\hat{T}_{j_a=0})_{t_0, m_0=0}$, encodes the non-trivial components of \hat{T} . Since the only relevant irrep on the one index is $j = 0$ the structural tensors are trivial. Therefore, tensor \hat{T} can be stored compactly as \hat{P} .

On the other hand, an SU(2)-invariant tensor \hat{T} with an incoming index a fulfills

$$(\Psi)_{a'} = \sum_a (\hat{W}_{\mathbf{r}}^*)_{a'a} (\Psi)_a, \quad (5.126)$$

or equivalently

$$(\Psi)_{a'} = \sum_a (\Psi)_a (\hat{W}_{\mathbf{r}}^\dagger)_{a'a}, \quad (5.127)$$

where $\hat{W}_{\mathbf{r}}^*$ and $\hat{W}_{\mathbf{r}}^\dagger$ are the complex conjugate and adjoint of $\hat{W}_{\mathbf{r}}$ respectively. The canonical form of \hat{T} is the same as that stated as Eq. (5.125).

5.5.3 Two indices

An SU(2)-invariant matrix \hat{T} , possibly rectangular, with indices a and b fulfills [Fig. 5.16(i)]

$$\begin{aligned}\hat{T}_{a'b'} &= \sum_{ab} \left(\hat{W}_{\mathbf{r}}^{(A)*} \right)_{a'a} \left(\hat{W}_{\mathbf{r}}^{(B)} \right)_{b'b} \hat{T}_{ab}, \\ &= \sum_{ab} \left(\hat{W}_{\mathbf{r}}^{(B)} \right)_{b'b} \hat{T}_{ab} \left(\hat{W}_{\mathbf{r}}^{(A)\dagger} \right)_{aa'},\end{aligned}\quad (5.128)$$

where $\hat{W}_{\mathbf{r}}^{(A)}$ and $\hat{W}_{\mathbf{r}}^{(B)}$ are the representations of SU(2) on the vector space associated to index $a = (j_a, m_{j_a}, t_{j_a})$ and $b = (j_b, m_{j_b}, t_{j_b})$ respectively. Schur's Lemma establishes that the matrix \hat{T} decomposes as

$$(\hat{T})_{ab} = (\hat{P}_{j_a j_b})_{t_{j_a} t_{j_b}} \delta_{j_a j_b} \delta_{m_{j_a} m_{j_b}}, \quad (5.129)$$

which can also be written in a block-diagonal form,

$$\begin{aligned}\hat{T} &= \bigoplus_j \hat{T}_j, \\ &= \bigoplus_j (\hat{P}_j \otimes \hat{I}_j).\end{aligned}\quad (5.130)$$

Here the sum is over all values j of spin j_a that are equal to a value of spin j_b .

A rank-2 SU(2)-invariant tensor \hat{T} with both incoming indices a and b is associated with fusing spins j_a and j_b into a total spin 0. It fulfills [Fig. 5.16(ii)]

$$\begin{aligned}\hat{T}_{a'b'} &= \sum_{ab} \left(\hat{W}_{\mathbf{r}}^{(A)*} \right)_{a'a} \left(\hat{W}_{\mathbf{r}}^{(B)*} \right)_{b'b} \hat{T}_{ab}, \\ &= \sum_{ab} \hat{T}_{ab} \left(\hat{W}_{\mathbf{r}}^{(A)\dagger} \right)_{aa'} \left(\hat{W}_{\mathbf{r}}^{(B)\dagger} \right)_{bb'}\end{aligned}\quad (5.131)$$

and decomposes as

$$(\hat{T})_{ab} = (\hat{P}_{j_a j_b})_{t_{j_a} t_{j_b}} C_{j_a m_{j_a}, j_b m_{j_b} \rightarrow 00}^{\text{fuse}}. \quad (5.132)$$

Similarly, a rank-2 SU(2)-invariant tensor with both outgoing indices a and b fulfills [Fig. 5.16(iii)]

$$\hat{T}_{a'b'} = \sum_{ab} \left(\hat{W}_{\mathbf{r}}^{(A)} \right)_{a'a} \left(\hat{W}_{\mathbf{r}}^{(B)} \right)_{b'b} \hat{T}_{ab}, \quad (5.133)$$

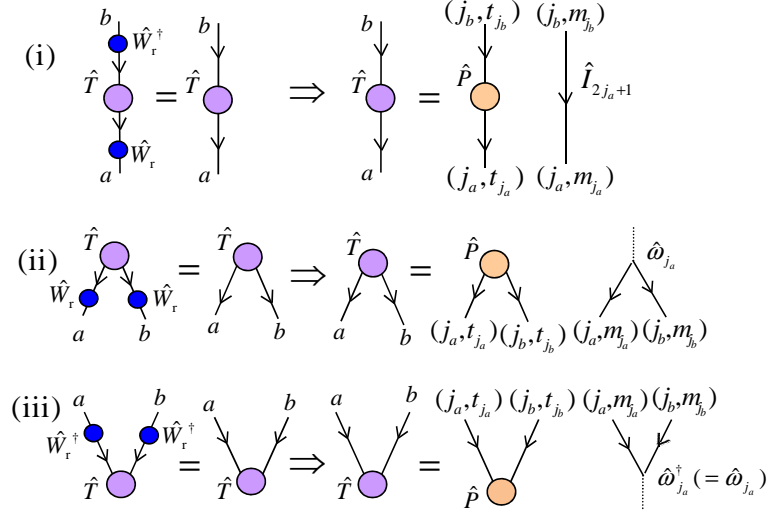


Figure 5.16 – Implication of the symmetry constraints fulfilled by rank-2 $SU(2)$ -invariant tensors as resulting in the decomposition of the tensors into degeneracy tensors \hat{P} and structural tensors.

and decomposes as

$$(\hat{T})_{ab} = (\hat{P}_{j_a j_b})_{t_{j_a} t_{j_b}} C_{00 \rightarrow j_a m_{j_a}, j_b m_{j_b}}^{\text{split}}. \quad (5.134)$$

Both incoming (or both outgoing) spins j_a and j_b are compatible with the total spin 0 only for values j of spin j_a such that $j_a = j_b = j$ and for values m of m_a such that $m_{j_a} = -m_{j_b} = m$. Therefore, we can recast the canonical decompositions of Eqs. (5.132)-(5.134) in a block-diagonal form,

$$\begin{aligned} \hat{T} &= \bigoplus_j \hat{T}_j, \\ &= \bigoplus_j \left(\hat{P}_j \otimes \hat{\omega}_j \right), \end{aligned} \quad (5.135)$$

where $\hat{\omega}_j$ is a $(2j+1) \times (2j+1)$ reverse diagonal matrix with diagonal components

$$(\hat{\omega}_j)_{m, -m} \equiv C_{j m, j -m \rightarrow 00}^{\text{fuse}} = C_{00 \rightarrow j m, j -m}^{\text{split}} = \frac{(-1)^{j-m}}{\sqrt{2j+1}}. \quad (5.136)$$

To summarize, the canonical form of a rank-2 $SU(2)$ -invariant tensor reads

$$\hat{T} = \bigoplus_j \left(\hat{P}_j \otimes \hat{Q}_j \right). \quad (5.137)$$

Here \hat{P}_j contains the degrees of freedom of \hat{T} that are not fixed by the symmetry, namely, \hat{P}_j transforms trivially under the action of the SU(2), Eq. (5.29). On the other hand \hat{Q}_j is determined by the symmetry according to the directions \vec{D} of indices a and b ,

$$\hat{Q}_j = \hat{I}_j \quad \text{if } \vec{D} = \{\text{'in'}, \text{'out'}\} \text{ or } \{\text{'out'}, \text{'in'}\}, \quad (5.138)$$

$$= \hat{\omega}_j \quad \text{if } \vec{D} = \{\text{'in'}, \text{'in'}\} \text{ or } \{\text{'out'}, \text{'out'}\}, \quad (5.139)$$

Thus, a rank-2 SU(2)-invariant tensor \hat{T} can be stored compactly as

$$\{\{a = (j_a, t_{j_a}, m_{j_a}), b = (j_b, t_{j_b}, m_{j_b})\}, \vec{D}, \{\hat{P}_j\}\}. \quad (5.140)$$

Example 10: Consider a rank-2 SU(2)-invariant tensor \hat{T} with both outgoing indices and with each index associated to the vector space \mathbb{V} of Example 8, $\mathbb{V} \equiv \mathbb{V}_0 \oplus 3\mathbb{V}_1 \oplus \mathbb{V}_2$. Tensor \hat{T} has the canonical form

$$\hat{T} \equiv (\hat{P}_0 \otimes \hat{\omega}_0) \oplus (\hat{P}_1 \otimes \hat{\omega}_1) \oplus (\hat{P}_2 \otimes \hat{\omega}_2), \quad (5.141)$$

where

$$\begin{aligned} \hat{\omega}_0 &\equiv 1, \\ \hat{\omega}_1 &\equiv \begin{pmatrix} 0 & 0 & \frac{1}{\sqrt{3}} \\ 0 & -\frac{1}{\sqrt{3}} & 0 \\ \frac{1}{\sqrt{3}} & 0 & 0 \end{pmatrix}, \\ \hat{\omega}_2 &\equiv \begin{pmatrix} 0 & 0 & 0 & 0 & \frac{1}{\sqrt{5}} \\ 0 & 0 & 0 & -\frac{1}{\sqrt{5}} & 0 \\ 0 & 0 & \frac{1}{\sqrt{5}} & 0 & 0 \\ 0 & -\frac{1}{\sqrt{5}} & 0 & 0 & 0 \\ \frac{1}{\sqrt{5}} & 0 & 0 & 0 & 0 \end{pmatrix}. \end{aligned} \quad (5.142)$$

The total number of complex coefficients contained in tensor \hat{T} is $|\hat{T}| = 15 \times 15 = 225$. However, the tensor can be stored compactly as

$$\{\{a, b\}, \{\text{'out'}, \text{'out'}\}, \{\hat{P}_0, \hat{P}_1, \hat{P}_2\}\},$$

where the total number of complex coefficients that are contained in tensors \hat{P}_0, \hat{P}_1 and \hat{P}_2 is

$$|\hat{P}_0| + |\hat{P}_1| + |\hat{P}_2| = 1 \times 1 + 3 \times 3 + 1 \times 1 = 11. \quad (5.143)$$

Therefore, by exploiting the symmetry the number of coefficients that need to be stored is twenty times smaller. ■

5.5.4 Three indices

Consider a rank-3 SU(2)-invariant tensor \hat{T} with incoming indices a and b and outgoing index c . It fulfills [Fig. 5.17(i)]

$$\begin{aligned} \hat{T}_{a'b'c'} &= \sum_{abc} \left(\hat{W}_{\mathbf{r}}^{(A)*} \right)_{a'a} \left(\hat{W}_{\mathbf{r}}^{(B)*} \right)_{b'b} \left(\hat{W}_{\mathbf{r}}^{(C)} \right)_{c'c} \hat{T}_{abc}, \\ &= \sum_{abc} \left(\hat{W}_{\mathbf{r}}^{(C)} \right)_{c'c} \hat{T}_{abc} \left(\hat{W}_{\mathbf{r}}^{(A)\dagger} \right)_{aa'} \left(\hat{W}_{\mathbf{r}}^{(B)\dagger} \right)_{bb'}, \end{aligned} \quad (5.144)$$

where $\hat{W}_{\mathbf{r}}^{(A)}, \hat{W}_{\mathbf{r}}^{(B)}$ and $\hat{W}_{\mathbf{r}}^{(C)}$ are the representations of SU(2) on indices $a = (j_a, m_{j_a}, t_{j_a}), b = (j_b, m_{j_b}, t_{j_b})$ and $c = (j_c, m_{j_c}, t_{j_c})$ respectively. The *Wigner-Eckart theorem* establishes that \hat{T} decomposes as

$$(\hat{T})_{abc} = (\hat{P}_{j_a j_b j_c})_{t_{j_a} t_{j_b} t_{j_c}} C_{j_a m_{j_a}, j_b m_{j_b} \rightarrow j_c m_{j_c}}^{\text{fuse}}. \quad (5.145)$$

That is, for compatible values of the spins j_a, j_b and j_c , tensor \hat{T} factorizes into tensor $\hat{P}_{j_a j_b j_c}$ containing degrees of freedom and a Clebsch-Gordan tensor that mediates the fusion of spins j_a and j_b into spin j_c .

An SU(2)-invariant tensor \hat{T} with another combination of incoming and outgoing indices has a canonical decomposition that differs in the Clebsch-Gordan coefficients. For example, if \hat{T} is an SU(2)-invariant tensor with incoming indices b and outgoing indices a and c then it fulfills

$$\begin{aligned} \hat{T}_{a'b'c'} &= \sum_{abc} \left(\hat{W}_{\mathbf{r}}^{(A)} \right)_{a'a} \left(\hat{W}_{\mathbf{r}}^{(B)*} \right)_{b'b} \left(\hat{W}_{\mathbf{r}}^{(C)} \right)_{c'c} \hat{T}_{abc}, \\ &= \sum_{abc} \left(\hat{W}_{\mathbf{r}}^{(A)} \right)_{a'a} \left(\hat{W}_{\mathbf{r}}^{(C)} \right)_{c'c} \hat{T}_{abc} \left(\hat{W}_{\mathbf{r}}^{(B)\dagger} \right)_{bb'}, \end{aligned} \quad (5.146)$$

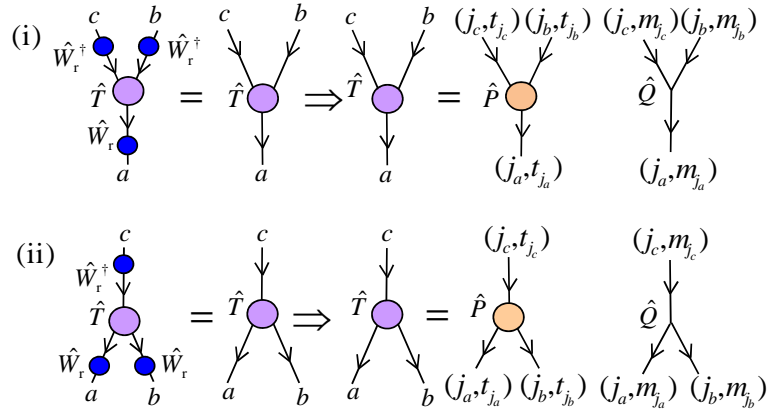


Figure 5.17 – Examples of the constraints fulfilled by rank-3 SU(2)-invariant tensors and their implication as resulting in the decomposition of the tensors into degeneracy tensors \hat{P} and a Clebsch-Gordan tensors.

and decomposes as

$$(\hat{T})_{abc} = (\hat{P}_{j_a j_b j_c})_{t_{j_a} t_{j_b} t_{j_c}} C_{j_b m_{j_b} \rightarrow j_a m_{j_a} j_c m_{j_c}}^{\text{split}}. \quad (5.147)$$

More generally, a rank-3 SU(2)-invariant tensor with any combination of incoming and outgoing indices decomposes as

$$(\hat{T})_{abc} = (\hat{P}_{j_a j_b j_c})_{t_{j_a} t_{j_b} t_{j_c}} (\hat{Q}_{j_a j_b j_c})_{m_{j_a} m_{j_b} m_{j_c}}. \quad (5.148)$$

(Wigner Eckart Theorem)

The block structure can be made more explicit by recasting Eq. (5.148) as

$$\begin{aligned} \hat{T} &\equiv \bigoplus_{j_a j_b j_c} \hat{T}_{j_a j_b j_c}, \\ &\equiv \bigoplus_{j_a j_b j_c} \left(\hat{P}_{j_a j_b j_c} \otimes \hat{Q}_{j_a j_b j_c} \right), \end{aligned} \quad (5.149)$$

where we use the direct sum symbol \bigoplus to denote that the different tensors $\hat{T}_{j_a j_b j_c}$ are supported on orthonormal subspaces of the tensor product of the spaces associated with indices a, b and c , and where the direct sum runs over all compatible values of j_a, j_b and

j_c . The components $(\hat{Q}_{j_a j_b j_c})_{m_{j_a} m_{j_b} m_{j_c}}$ are determined by the directions \vec{D} of the indices,

$$C_{j_a m_{j_a}, j_b m_{j_b} \rightarrow j_c m_{j_c}}^{\text{fuse}} \quad \text{if } \vec{D} = \{\text{'in'}, \text{'in'}, \text{'out'}\}, \quad (5.150)$$

$$C_{j_a m_{j_a}, j_c m_{j_c} \rightarrow j_b m_{j_b}}^{\text{fuse}} \quad \text{if } \vec{D} = \{\text{'in'}, \text{'out'}, \text{'in'}\}, \quad (5.151)$$

$$C_{j_a m_{j_a}, j_c m_{j_c} \rightarrow j_b m_{j_b}}^{\text{fuse}} \quad \text{if } \vec{D} = \{\text{'out'}, \text{'in'}, \text{'in'}\}, \quad (5.152)$$

$$C_{j_b m_{j_b} \rightarrow j_a m_{j_a}, j_b m_{j_b}}^{\text{split}} \quad \text{if } \vec{D} = \{\text{'out'}, \text{'in'}, \text{'out'}\}, \quad (5.153)$$

$$C_{j_c m_{j_c} \rightarrow j_a m_{j_a}, j_b m_{j_b}}^{\text{split}} \quad \text{if } \vec{D} = \{\text{'out'}, \text{'out'}, \text{'in'}\}, \quad (5.154)$$

$$C_{j_a m_{j_a} \rightarrow j_b m_{j_b}, j_c m_{j_c}}^{\text{split}} \quad \text{if } \vec{D} = \{\text{'in'}, \text{'out'}, \text{'out'}\}, \quad (5.155)$$

$$\beta C_{j_a m_{j_a} \rightarrow j_b m_{j_b}, j_c m_{j_c}}^{\text{split}} \quad \text{if } \vec{D} = \{\text{'out'}, \text{'out'}, \text{'out'}\}, \quad (5.156)$$

$$\beta C_{j_a m_{j_a}, j_b m_{j_b} \rightarrow j_c m_{j_c}}^{\text{fuse}} \quad \text{if } \vec{D} = \{\text{'in'}, \text{'in'}, \text{'in'}\}, \quad (5.157)$$

where $\beta = (-1)^{j_a - j_b + m_c} \sqrt{2j_c + 1}$.

To summarize, a rank-3 $\text{SU}(2)$ -invariant tensor \hat{T} can be stored in the most compact way as

$$\{\{a, b, c\}, \vec{D}, \{\hat{P}_{j_a j_b j_c}\}\}, \quad (5.158)$$

where the indices a, b and c are specified in the spin basis,

$$a = (j_a, t_{j_a}, m_{j_a}), \quad b = (j_b, t_{j_b}, m_{j_b}), \quad c = (j_c, t_{j_c}, m_{j_c}). \quad (5.159)$$

Example 11: Consider a rank-3 $\text{SU}(2)$ -invariant tensor \hat{T} such that each index, a, b and c , is associated to the vector space \mathbb{V} of Example 8. Tensor \hat{T} can be stored by storing the degeneracy tensors,

$$\begin{aligned} & \hat{P}_{0,0,0}, \quad \hat{P}_{0,1,1}, \quad \hat{P}_{0,2,2}, \quad \hat{P}_{1,0,1}, \quad \hat{P}_{1,1,0}, \quad \hat{P}_{1,1,1}, \quad \hat{P}_{1,1,2}, \\ & \hat{P}_{1,2,1}, \quad \hat{P}_{1,2,2}, \quad \hat{P}_{2,0,2}, \quad \hat{P}_{2,1,1}, \quad \hat{P}_{2,2,0}, \quad \hat{P}_{2,2,1}, \quad \hat{P}_{2,2,2}, \end{aligned}$$

corresponding to all compatible values of j_a, j_b and j_c .

The total number of complex coefficients that are contained in the degeneracy tensors is $\sum_{j_a j_b j_c} |\hat{P}_{j_a j_b j_c}| = 45$, whereas $|\hat{T}| = |a| \times |b| \times |c| = 15^3 = 3375$ components; the reduction in the number of coefficients is seventy-five times, much greater than that computed for rank-2 tensors in Example 10. In general, the sparsity of $\text{SU}(2)$ -invariant tensors increases with increasing number of indices. ■

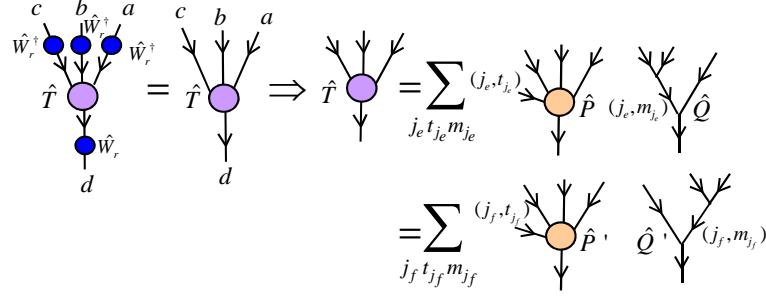


Figure 5.18 – Two equivalent canonical decompositions of a rank-4 SU(2)-invariant tensor corresponding to two different ways of fusing the three incoming indices into the outgoing index.

5.5.5 Four indices

A rank-4 SU(2)-invariant tensor may be decomposed in several ways in terms of degenerate tensors and structural tensors in correspondence with the existence of different fusion trees for four spins.

Consider a rank-4 SU(2)-invariant tensor \hat{T} with incoming indices $a = (j_a, t_{j_a}, m_{j_a})$, $b = (j_b, t_{j_b}, m_{j_b})$ and $c = (j_c, t_{j_c}, m_{j_c})$ and outgoing index $d = (j_d, t_{j_d}, m_{j_d})$. It fulfills

$$\hat{T}_{a'b'c'd'} = \sum_{abcd} \left(\hat{W}_{\mathbf{r}}^{(D)} \right)_{d'd} \hat{T}_{abcd} \left(\hat{W}_{\mathbf{r}}^{(A)} \right)_{aa'}^\dagger \left(\hat{W}_{\mathbf{r}}^{(B)} \right)_{bb'}^\dagger \left(\hat{W}_{\mathbf{r}}^{(C)} \right)_{cc'}^\dagger \quad (5.160)$$

where $\hat{W}_{\mathbf{r}}^{(A)}$, $\hat{W}_{\mathbf{r}}^{(B)}$, $\hat{W}_{\mathbf{r}}^{(C)}$ and $\hat{W}_{\mathbf{r}}^{(D)}$ are the representations of SU(2) on the indices a, b, c and d respectively. Tensor \hat{T} decomposes as

$$(T)_{abcd} = \sum_{j_e} (\hat{P}_{j_a j_b j_c j_d}^{j_e})_{t_{j_a} t_{j_b} t_{j_c} t_{j_d}} \cdot (\hat{Q}_{j_a j_b j_c j_d}^{j_e})_{m_{j_a} m_{j_b} m_{j_c} m_{j_d}}, \quad (5.161)$$

where the sum is over all values of the intermediate spin j_e .

The coefficients $(\hat{Q}_{j_a j_b j_c j_d}^{j_e})_{m_{j_a} m_{j_b} m_{j_c} m_{j_d}}$ [Eq. (5.104)] mediate the fusion of the spins j_a, j_b and j_c into a total spin j_d according to a fusion tree, for example, first fusing j_a and j_b and then fusing the resulting spin with j_c .

Alternatively, tensor \hat{T} can be decomposed as

$$(T)_{abcd} = \sum_{j_f} (\hat{P}'_{j_a j_b j_c j_d}{}^{j_f})_{t_{j_a} t_{j_b} t_{j_c} t_{j_d}} \cdot (\hat{Q}'_{j_a j_b j_c j_d}{}^{j_f})_{m_{j_a} m_{j_b} m_{j_c} m_{j_d}}, \quad (5.162)$$

in terms of different structural coefficients $(\hat{Q}_{j_a j_b j_c j_d}^{j_f})_{m_{j_a} m_{j_b} m_{j_c} m_{j_d}}$ [Eq. (5.106)] that are associated with fusing the spins according to a different fusion tree, namely, fusing spin j_a with the spin obtained by first fusing j_b and j_c .

Since Eqs. (5.161) and (5.162) represent the same tensor \hat{T} , the tensors \hat{P} and \hat{P}' are related by

$$\hat{P}'_{j_a j_b j_c j_d}{}^{j_f} = \sum_{j_e} \hat{F}_{j_a j_b j_c j_d}^{j_e j_f} \hat{P}_{j_a j_b j_c j_d}{}^{j_e}, \quad (5.163)$$

where $\hat{F}_{j_a j_b j_c j_d}^{j_e j_f}$ are the recoupling coefficients [Eq. 5.107].

5.5.6 k indices

Finally, consider a rank- k SU(2)-invariant tensor \hat{T} with all *outgoing* indices and which fulfills Eq. (5.123). By writing each index in a spin basis, $i_l = (j_l, t_{j_l}, m_{j_l})$, tensor \hat{T} can be decomposed as

$$(\hat{T})_{i_1 \dots i_k} \equiv \sum_{j_{e_1} \dots j_{e_l}} \left(\hat{P}_{j_1 \dots j_k}^{j_{e_1} \dots j_{e_l}} \right)_{t_{j_1} \dots t_{j_k}} \cdot \left(\hat{Q}_{j_1 \dots j_k}^{j_{e_1} \dots j_{e_l}} \right)_{m_{j_1} \dots m_{j_k}}. \quad (5.164)$$

Here tensor $\hat{Q}_{j_1 \dots j_k}^{j_{e_1} \dots j_{e_l}}$ [Eq. (5.117)] is a transformation characterized by a fusion tree τ whose internal links are decorated by the spins $\{j_{e_1}, \dots, j_{e_l}\}$. Another canonical form of the tensor \hat{T} ,

$$(\hat{T})_{i_1 \dots i_k} \equiv \sum_{j'_{e_1} \dots j'_{e_l}} \left(\hat{P}'_{j_1 \dots j_k}^{j'_{e_1} \dots j'_{e_l}} \right)_{t_{j_1} \dots t_{j_k}} \cdot \left(\hat{Q}'_{j_1 \dots j_k}^{j'_{e_1} \dots j'_{e_l}} \right)_{m_{j_1} \dots m_{j_k}}, \quad (5.165)$$

comprises of different degeneracy tensors $\hat{P}'_{j_1 \dots j_k}^{j'_{e_1} \dots j'_{e_l}}$ and different structural tensors $\hat{Q}'_{j_1 \dots j_k}^{j'_{e_1} \dots j'_{e_l}}$ where the latter is a transformation characterized by another fusion tree τ' .

The two canonical forms, Eq. (5.164) and (5.165), are related as

$$\hat{P}'_{j_1 \dots j_k}^{j'_{e_1} \dots j'_{e_l}} = \sum_{j_{e_1} \dots j_{e_l}} \hat{S}_{j_1 \dots j_k}^{j_{e_1} \dots j_{e_l} j'_{e_1} \dots j'_{e_l}}(\tau, \tau') \hat{P}_{j_1 \dots j_k}^{j_{e_1} \dots j_{e_l}}, \quad (5.166)$$

where the coefficients $\hat{S}_{j_1 \dots j_k}^{j_{e_1} \dots j_{e_l} j'_{e_1} \dots j'_{e_l}}(\tau, \tau')$ are those which appear in Eq. (5.118).

Thus tensor \hat{T} can be compactly stored as

$$\{\{i_1, i_2, \dots, i_k\}, \tau, \vec{D}, \{\hat{P}_{j_1 \dots j_k}^{j_{e_1} \dots j_{e_l}}\}\}. \quad (5.167)$$

For an arbitrary combination of incoming and outgoing indices of the tensor, the canonical decomposition is characterized by intermediate spins $j_{e_1} \dots j_{e_l}$ that are assigned to the links of a trivalent tree that is more general than the fusion tree. Furthermore, two canonical decompositions are related by means of more generic spin networks than those considered (See Section 5.7) for evaluating the coefficients $\hat{S}_{j_1 \dots j_k}^{j_{e_1} \dots j_{e_l} j'_{e_1} \dots j'_{e_l}}(\boldsymbol{\tau}, \boldsymbol{\tau}')$. A rigorous result is presented in Chapter 6 where we describe the generic transformation that relates two tree decompositions of an SU(2)-invariant tensor.

5.6 Manipulations of SU(2)-invariant tensors

In this section we consider manipulations of SU(2)-invariant tensors that belong to the set \mathcal{P} [Sec. 5.1.5] of primitives: reversal of indices, permutation of indices, reshaping of indices and matrix operations (matrix multiplication and matrix factorizations). We will adapt these manipulations to the presence of the symmetry by implementing them in such a way that the canonical form is maintained.

Our approach will be to describe the basic transformations that are instrumental in implementing the symmetric version of these manipulations and demonstrate their use with simple examples. A more rigorous treatment of adapting the primitive tensor manipulations for SU(2)-invariant tensors is presented in Chapter 6. The basic transformations are symmetry preserving and can be described by means of special SU(2)-invariant tensors. Consequently, a symmetric manipulation decomposes into the manipulation of the degeneracy tensors and the manipulation of the structural tensors. Computational cost is incurred only by the manipulation of degeneracy tensors. On the other hand, the manipulation of structural tensors can be performed *algebraically* by applying relevant properties of Clebsch-Gordan coefficients. This fact is responsible for obtaining computational speedup from exploiting the symmetry.

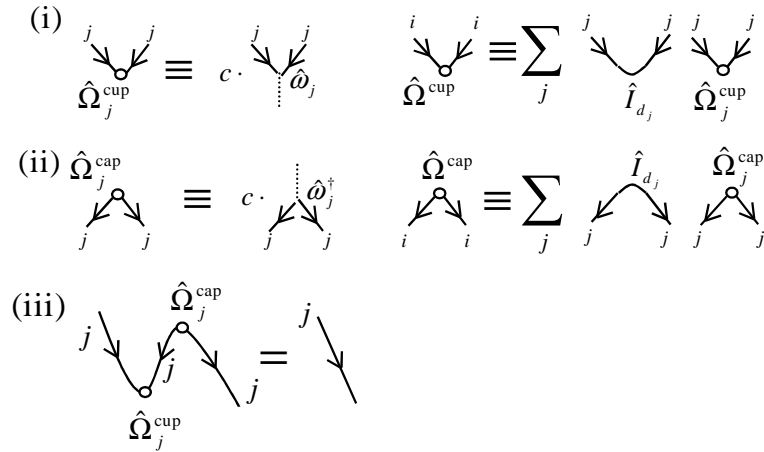


Figure 5.19 – (i) Graphical representation of the cup tensor. For simplicity, we choose the same graphical representation for a cup tensor applied to an index that carries a single spin j as well as for one that is applied on an index i that carries several spins j (possibly with degeneracy d_j). ($c = 2j + 1$ is a normalization constant.) (ii) The analogous graphical representation of the cap tensor. (iii) Multiplying together a cup tensor and a cap tensor yields the Identity.

5.6.1 Reversal of indices

An index $i = (j, t_j, m_j)$ of an $SU(2)$ -invariant tensor can be reversed by means of the ‘cup’ and ‘cap’ transformations. The cup transformation is given by a rank-2 $SU(2)$ -invariant tensor $\hat{\Omega}^{\text{cup}}$ with both *incoming* indices. It can be used to reverse an *outgoing* index. Analogously, the cap transformation is given by a rank-2 $SU(2)$ -invariant tensor $\hat{\Omega}^{\text{cap}}$ with both *outgoing* indices and can be used to reverse an *incoming* index.

In the canonical form, the cup and cap tensors read as block-diagonal matrices,

$$\hat{\Omega}^{\text{cup}} \equiv \bigoplus_j (\hat{I}_{d_j} \otimes \hat{\Omega}_j^{\text{cup}}), \quad (5.168)$$

$$\hat{\Omega}^{\text{cap}} \equiv \bigoplus_j (\hat{I}_{d_j} \otimes \hat{\Omega}_j^{\text{cap}}), \quad (5.169)$$

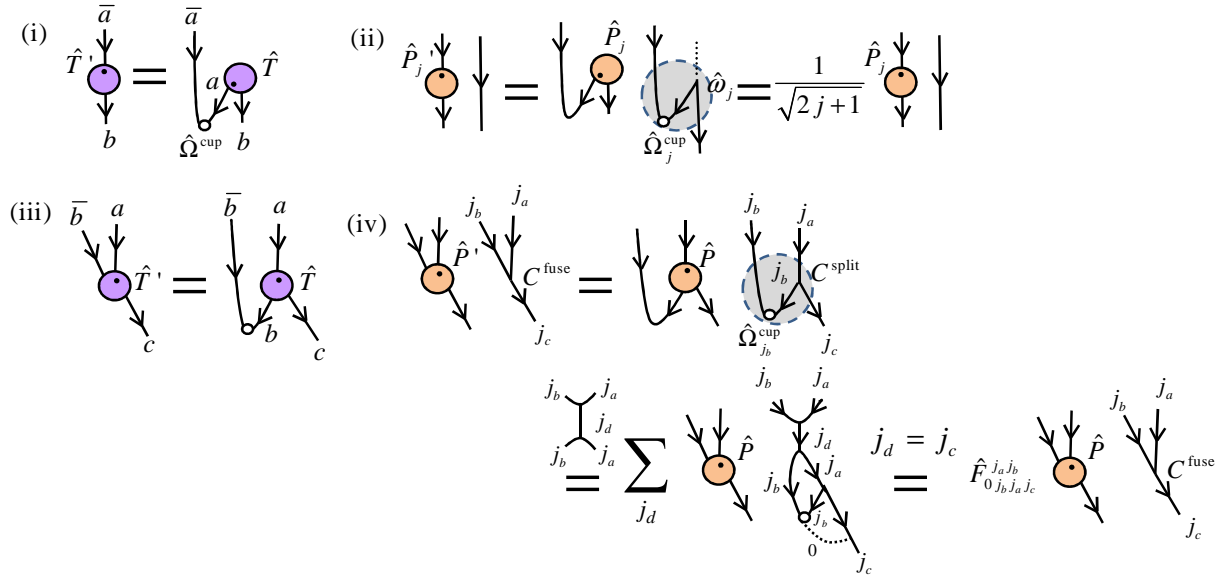


Figure 5.20 – Reversing an index of an SU(2)-invariant tensor by means of a cup tensor. (i) Reversing an index of an SU(2)-invariant tensor \hat{T} with two outgoing indices to obtain a matrix \hat{T}' . (ii) The reversal in (i) as performed on the canonical form of \hat{T} . The degeneracy index can be reversed without affecting the components of the degeneracy tensor \hat{P} . The reversal of the spin index equates to replacing the shaded region with a Clebsch-Gordan tensor and a numerical factor $\frac{1}{\sqrt{2j+1}}$, which is absorbed into \hat{P} to obtain \hat{P}' . (iii) Reversing an index of a rank-3 SU(2)-invariant tensor. (iv) The reversal in (iii) as performed on the canonical form of \hat{T} . The reversal of the spin index equates to replacing the shaded region with a Clebsch-Gordan tensor and a recoupling coefficient $\hat{F}_{0j_bj_a j_c}^{j_d}$. The recoupling coefficient appears as a result of introducing a resolution of Identity [Fig. 5.7(iii)] on the spins j_b and j_a and then simplifying the resulting diagram by applying the equality in Fig. 5.11(ii).

where $d_j = |t_j|$ and where

$$\hat{\Omega}_j^{\text{cup}} \equiv \sqrt{2j+1} \hat{\omega}_j, \quad (5.170)$$

$$\hat{\Omega}_j^{\text{cap}} \equiv (-1)^{2j} \sqrt{2j+1} \hat{\omega}_j. \quad (5.171)$$

Here $\hat{\omega}_j$ is the tensor defined in Eq. (5.136). By definition, the cup transformation inverts the action of the cap transformation and vice-versa,

$$\hat{\Omega}_j^{\text{cup}} \hat{\Omega}_j^{\text{cap}} = \hat{\Omega}_j^{\text{cap}} \hat{\Omega}_j^{\text{cup}} = \hat{I}_{2j+1}. \quad (5.172)$$

Reversal of index i of tensor \hat{T} can be decomposed into the reversal of the degeneracy index

(j, t_j) of the degeneracy tensors and reversal of the spin index (j, m_j) of the structural tensors. Reversal of the degeneracy index is trivial since the cup and cap transformations act as the Identity \hat{I}_{d_j} on it whereas the reversal of the spin index is mediated by transformations $\hat{\Omega}_j^{\text{cup}}$ and $\hat{\Omega}_j^{\text{cap}}$.

Figure 5.19(i)-(ii) introduces a graphical representation of the cup and cap tensors. The cup tensor is depicted as a small circle with two incoming lines (forming a ‘cup’) whereas a cap tensor is depicted as a small circle with two outgoing lines (forming a ‘cap’) (Baez; Biamonte et al., 2010).

Next, we illustrate how an outgoing index of a tensor can be reversed by means of the cup transformation. A cap transformation can be used to reverse an incoming index in an analogous way.

Example 12: Consider a rank-2 SU(2)-invariant tensor \hat{T} with outgoing indices $a = (j_a, t_{j_a}, m_{j_a})$ and $b = (j_b, t_{j_b}, m_{j_b})$ and which is given in the canonical form,

$$\{\{a, b\}, \{\text{‘out’}, \text{‘out’}\}, \{\hat{P}_j\}\}, \quad (5.173)$$

where j assumes all values of j_a that are equal to a value of j_b . Consider reversing index a of \hat{T} as shown in Fig. 5.20(i). The resulting tensor (or matrix) \hat{T}' is obtained by multiplying tensor \hat{T} with a cup by contracting a . We follow the convention that multiplying with a cup corresponds to bending index a upwards from the *left* in the graphical representation. The same index can be bent upwards from the right by multiplying with the *transpose* of the cup.

The resulting matrix \hat{T}' has the canonical form

$$\{\{a, b\}, \{\text{‘in’}, \text{‘out’}\}, \{\hat{P}'_j\}\}, \quad (5.174)$$

where

$$\hat{P}'_j = \frac{\hat{P}_j}{\sqrt{2j+1}}. \quad (5.175)$$

In order to explain this expression consider Fig. 5.20(ii) where the reversal is depicted as it is performed on the canonical form of \hat{T} . Reversal of the spin index equates to replacing

the shaded region by a straight line. This corresponds to applying the following algebraic identity

$$\hat{\Omega}_j^{\text{cup}} \hat{\omega}_j = \frac{\hat{I}_{2j+1}}{\sqrt{2j+1}}. \quad (5.176)$$

The factor $\frac{1}{\sqrt{2j+1}}$ is absorbed into the degeneracy tensor \hat{P}_j , Eq. (5.175), to obtain the final canonical form. ■

Example 13: Consider a rank-3 SU(2)-invariant tensor \hat{T} which is given in the canonical form,

$$\{\{a, b, c\}, \{\text{'in'}, \text{'out'}, \text{'out'}\}, \{\hat{P}_{j_a j_b j_c}\}\}. \quad (5.177)$$

Consider reversing index b of tensor \hat{T} as shown in Fig. 5.20(iii) by multiplying \hat{T} with a cup such that b is contracted. The canonical form of \hat{T}' reads

$$\{\{a, b, c\}, \{\text{'in'}, \text{'in'}, \text{'out'}\}, \{\hat{P}'_{j_a j_b j_c}\}\}, \quad (5.178)$$

where

$$\boxed{\hat{P}'_{j_a j_b j_c} = \hat{F}_{0 j_b j_a j_c}^{j_a j_b} \hat{P}_{j_a j_b j_c}}. \quad (5.179)$$

The recoupling coefficient $\hat{F}_{0 j_b j_a j_c}^{j_a j_b}$ appears due to the reversal of the spin index (j_b, m_{j_b}) , as shown in Fig. 5.20(iv). The Clebsch-Gordan tensor and the cup within the shaded region are replaced with another Clebsch-Gordan tensor and a recoupling coefficient. This is achieved by applying a resolution of Identity on spins j_a and j_b and simplifying the resulting diagram by applying the equality shown in Fig. 5.11(ii). ■

The procedure of reversing the spin index illustrated in Example 13 can be applied to reverse a spin index of a generic rank- k SU(2)-invariant tensor. Recall that a structural tensor is maintained as a trivalent tree of Clebsch-Gordan tensors. Reversal of the spin index corresponds to multiplying a cup with a Clebsch-Gordan tensor within this tree. Then, as in Example 13, we proceed by replacing the Clebsch-Gordan tensor and the cup by another Clebsch-Gordan tensor and a recoupling coefficient. The recoupling coefficient is absorbed into the degeneracy tensor to obtain the canonical form of the resulting tensor. In this way we can reverse an index of a generic rank- k SU(2)-invariant tensor.

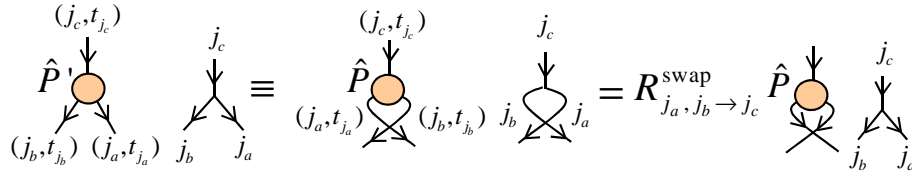


Figure 5.21 – Permutation of indices [Fig. 5.2(ii)] as performed on the canonical form of a rank-3 SU(2)-invariant tensor. The permutation decomposes into permutation of the degeneracy indices and permutation of the spin indices. The latter equates to replacing the Clebsch-Gordan tensor and a ‘cross’ with a Clebsch-Gordan tensor and a numerical factor

$$R_{j_a, j_b \rightarrow j_c}^{\text{swap}}.$$

5.6.2 Permutation of indices

Let us focus on the swap of two adjacent indices of an SU(2)-invariant tensor. As mentioned in Sec. 5.1.2 an arbitrary permutation of indices can be applied as a sequence of a number of such swaps.

Consider the swap e.g. Eq. (5.4) of two adjacent indices of a rank-3 SU(2)-invariant tensor \hat{T} that is given in the canonical form,

$$\{\{a, b, c\}, \{\text{‘in’}, \text{‘in’}, \text{‘out’}\}, \{\hat{P}_{j_a j_b j_c}\}\}.$$

Then tensor \hat{T}' that is obtained as result of swapping indices a and b has the canonical form

$$\{\{b, a, c\}, \{\text{‘in’}, \text{‘in’}, \text{‘out’}\}, \{\hat{P}'_{j_b j_a j_c}\}\},$$

where

$$\hat{P}'_{j_b j_a j_c} = R_{j_a, j_b \rightarrow j_c}^{\text{swap}} \hat{P}_{j_a j_b j_c}. \quad (5.180)$$

Here \hat{R}^{swap} is a rank-3 SU(2)-invariant tensor with components $R_{j_a, j_b \rightarrow j_c}^{\text{swap}}$,

$$R_{j_a, j_b \rightarrow j_c}^{\text{swap}} \equiv (-1)^{j_a + j_b - j_c}, \quad (5.181)$$

which mediates the swap of the spin indices (j_a, m_{j_a}) and (j_b, m_{j_b}) that fuse into index (j_c, m_{j_c}) , see Fig. 5.21. That is,

$$C_{j_b m_{j_b}, j_a m_{j_a} \rightarrow j_c m_{j_c}}^{\text{fuse}} = R_{j_a, j_b \rightarrow j_c}^{\text{swap}} C_{j_a m_{j_a}, j_b m_{j_b} \rightarrow j_c m_{j_c}}^{\text{fuse}}. \quad (5.182)$$

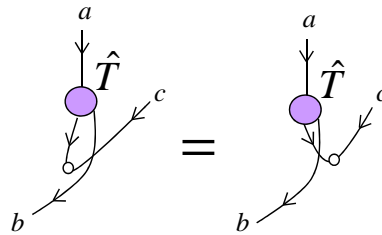


Figure 5.22 – Illustration of the property that reversal of indices “commutes” with a permutation of them.

(The same tensor $R_{j_a, j_b \rightarrow j_c}^{\text{swap}}$ also relates, in a similar way, tensor $C_{j_c m_{j_c} \rightarrow j_b m_{j_b}, j_a m_{j_a}}^{\text{split}}$ and tensor $C_{j_c m_{j_c} \rightarrow j_a m_{j_a}, j_b m_{j_b}}^{\text{split}}$.)

When swapping two adjacent indices of a generic rank- k tensor the degeneracy tensors \hat{P} and \hat{P}' are also related directly by the swap tensor \hat{R}^{swap} , such as in Eq. (5.180), if we work in a canonical form in which the indices that are swapped belong to the *same* node of the trivalent tree that characterizes the canonical form.

Notice how the canonical form of an SU(2)-invariant tensor facilitates a computational speedup for permutation of indices: permuting indices of the tensor is reduced to permuting indices of the much smaller degeneracy tensors. Figure 5.25 illustrates the computational speedup corresponding to a permutation of indices performed using our reference implementation MATLAB. In this implementation permutation of several indices is performed without necessarily breaking the permutation into swaps, see Sec. 6.0.4 in Chapter 6.

One can also consider manipulations that involve both reversing indices and permuting them. In this context it is useful to note that these manipulations “commute” with one another, as illustrated in Fig. 5.22.

5.6.3 Reshape of indices

The transformation that implements the reshape of indices of an SU(2)-invariant tensor depends on the directions of the indices. We analyze three distinct cases. First, we

consider fusion of two outgoing indices into an outgoing index and splitting of an outgoing index into two outgoing indices. Second, we consider the analogous reshape of incoming indices. And third, we consider the fusion of an incoming index with an outgoing index.

Let us consider the fusion e.g. Eq. (5.5) of two outgoing indices of an $SU(2)$ -invariant tensor \hat{T} . In order to obtain the reshaped tensor \hat{T}' in a canonical form it is required that the fused index be maintained in the spin basis. However, the direct product of indices $d = a \times b$ may result in an index that does not label a spin basis. Therefore, we fuse indices by multiplying \hat{T} with the fusing tensor $\Upsilon_{a,b \rightarrow d}^{\text{fuse}}$ such that indices a and b are contracted [Fig. (5.23(i))],

$$\hat{T}'_{dc} \equiv \sum_{ab} \hat{T}_{abc} \Upsilon_{a,b \rightarrow d}^{\text{fuse}}, \quad (5.183)$$

or in the canonical form [Fig. 5.23(ii)] ,

$$\hat{P}'_{jadc} = \sum_{j_a j_b} \sum_{t_{j_a} t_{j_b}} X_{j_a t_{j_a}, j_b t_{j_b} \rightarrow j_d t_{j_d}}^{\text{fuse}} \hat{P}_{j_a j_b j_c}. \quad (5.184)$$

Notice that the fusion of the spin indices, here, is straightforward. We proceed by multiplying with tensor C^{fuse} and replacing the resulting ‘loop’ in the figure with a straight line [Fig. 5.7(ii)]. The fusion of two adjacent indices of a generic rank- k $SU(2)$ -invariant tensor follows a straightforward generalization of Eq. (5.186). By working in a canonical form that is characterized by a trivalent tree in which the two indices belong to the same node, the fusion of the spin indices involves a simple loop elimination, similar to the one illustrated in Fig. 5.23(ii).

The original tensor \hat{T} can be recovered from \hat{T}' by splitting the index d back into indices a and b . This is achieved by multiplying tensor \hat{T}' with the splitting tensor $\Upsilon_{d \rightarrow a,b}^{\text{split}}$ such that d is contracted [Fig. 5.23(iii)],

$$\hat{T}_{abc} \equiv \sum_d \hat{T}'_{dc} \Upsilon_{d \rightarrow a,b}^{\text{split}}, \quad (5.185)$$

or in the canonical form [Fig. 5.23(iv)],

$$\hat{P}'_{jadc} = \sum_{j_a j_b} \sum_{t_{j_a} t_{j_b}} X_{j_a t_{j_a}, j_b t_{j_b} \rightarrow j_d t_{j_d}}^{\text{fuse}} \hat{P}_{j_a j_b j_c}. \quad (5.186)$$

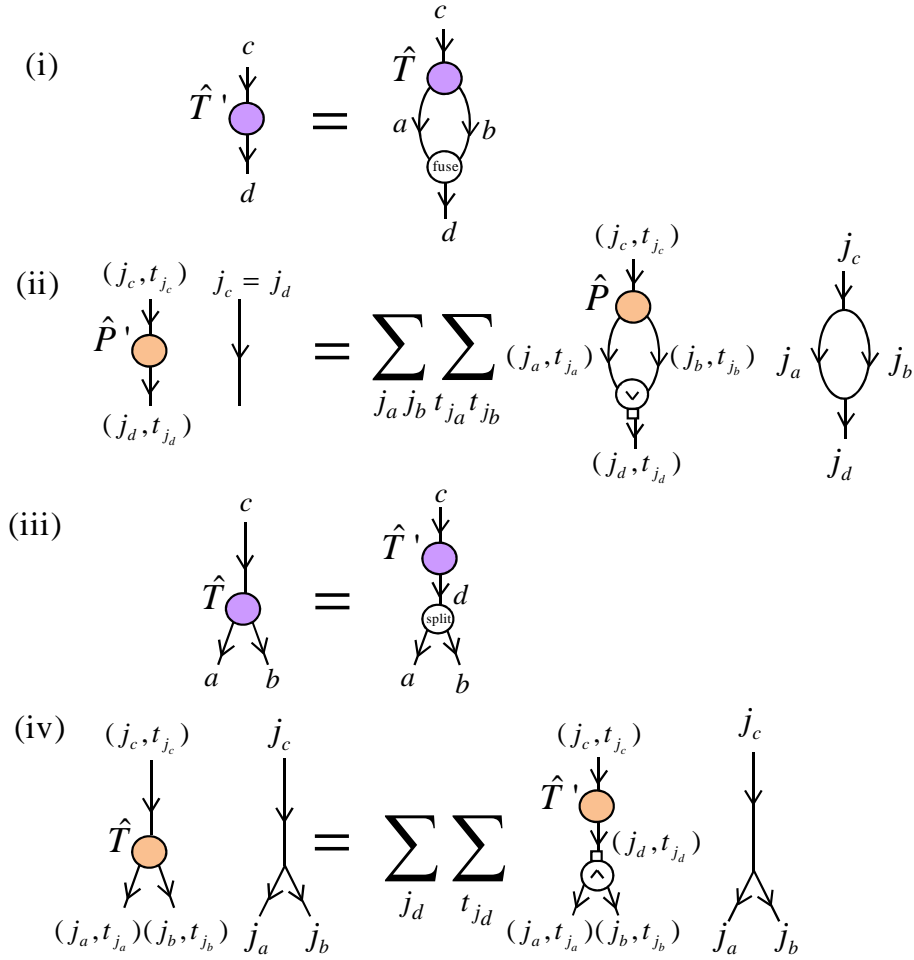


Figure 5.23 – (i) Fusion of two outgoing indices of an SU(2)-invariant tensor by means of the fusing tensor Υ^{fuse} . (ii) Fusion in the canonical form of the tensor decomposes into the fusion of the degeneracy indices using tensor X^{fuse} , and the fusion of the spin indices using tensor C^{fuse} . The latter can be performed for free since the loop can directly be replaced with a straight line [Fig. 5.7(ii)]. (iii) Splitting of an outgoing index into two indices by means of the splitting tensor Υ^{split} . (iv) Splitting the index in the canonical form of the tensor.

Notice that the sum in Eq. (5.186) implies that a reshaped tensor $\hat{P}'_{j_a j_b j_c}$ involves a linear combination of several tensors $\hat{P}_{j_a j_b j_c}$. Thus, performing the fusion in the canonical form requires more work than reshaping regular indices which is a simple rearrangement of the tensor components. As a result, fusing indices of SU(2)-invariant tensors can be more expensive than fusing indices of regular tensors, as illustrated in Fig. 5.25 for a reshaping done in MATLAB.

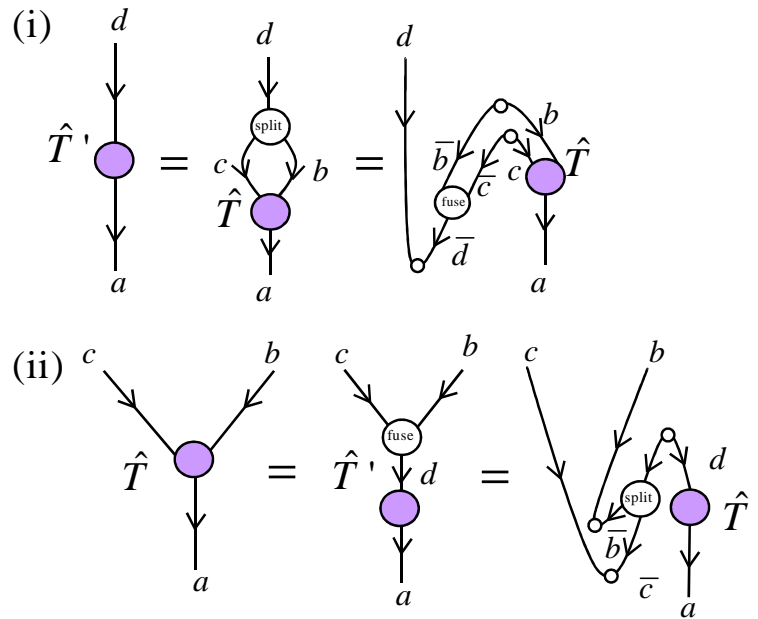


Figure 5.24 – (i) Fusion of two incoming indices into an incoming index, and (ii) splitting an incoming index into two incoming indices can be performed in one of two way.

Next, let us consider fusing two incoming indices into a single incoming index. This can be done in one of two equivalent ways. The first involves multiplying the tensor with a *splitting tensor* by contracting the two incoming indices. Equivalently, if one prefers to use the *fusing tensor*, one can reverse the two indices, multiply with the fusing tensor, and finally reverse the fused index. The two approaches are depicted in Fig. 5.24(i). The fused index can be split back into the original indices by reverting the fusion. In the first approach this is done by multiplying with a fusing tensor while in the second approach this is done by multiplying with a splitting tensor and then reversing the two indices [Fig. 5.24(ii)].

Finally, consider the fusion of an incoming index with an outgoing index to produce, say, an outgoing index. This can be achieved by reversing the incoming index and then fusing the indices by means of a fusing tensor. The fused index should be split in a consistent manner by reverting this fusion procedure.

5.6.4 Multiplication of two matrices

Let \hat{M} and \hat{N} be two SU(2)-invariant matrices given in the canonical form

$$\hat{M} = \bigoplus_j (\hat{M}_j \otimes \hat{I}_{2j+1}), \quad \hat{N} = \bigoplus_j (\hat{N}_j \otimes \hat{I}_{2j+1}). \quad (5.187)$$

Then the SU(2)-invariant matrix $\hat{T} = \hat{M}\hat{N}$ obtained by multiplying together matrices \hat{M} and \hat{N} has the canonical form

$$\hat{T} = \bigoplus_j (\hat{T}_j \otimes \hat{I}_{2j+1}), \quad (5.188)$$

where \hat{T}_j is obtained by multiplying matrices \hat{M}_j and \hat{N}_j ,

$$\hat{T}_j = \hat{M}_j \hat{N}_j. \quad (5.189)$$

Clearly, computational gain is obtained as a result of performing the multiplication $\hat{T} = \hat{M}\hat{N}$ block-wise. This is illustrated by the following example.

Example 13 : (Computational gain from blockwise multiplication) Consider vector space \mathbb{V} that decomposes as $\mathbb{V} \cong \bigoplus_j d_j \mathbb{V}_j$ where j assumes values $1, \dots, q$ and let $d_j = d, \forall j$. The dimension of the space \mathbb{V} is dp where $p = \sum_{j=1}^q (2j+1) = q^2 + q$.

Consider an SU(2)-invariant matrix $\hat{T} : \mathbb{V} \rightarrow \mathbb{V}$. Since there are q blocks \hat{T}_j and each block has size $d \times d$, the SU(2)-invariant matrix \hat{T} contains qd^2 coefficients. For comparison, a regular matrix of the same size contains $d^2 p^2$ coefficients, a number greater by a factor of $O(q^3)$.

Let us now consider multiplying two such matrices. We use an algorithm that requires $O(l^3)$ computational time to multiply two matrices of size $l \times l$. The cost of performing q multiplications of $d \times d$ blocks in Eq. 5.189 scales as $O(qd^3)$. In contrast the cost of multiplying two regular matrices of the same size scales as $O(d^3 p^3)$, requiring $O(q^5)$ times more computational time. Figure 5.26 shows a comparison of the computation times when multiplying two matrices for both SU(2)-invariant and regular matrices. ■

5.6.5 Factorization of a matrix

The factorization of an $SU(2)$ -invariant matrix \hat{T} can also benefit from the block-diagonal structure. Consider, for instance, the singular value decomposition (SVD), $\hat{T} = \hat{U}\hat{S}\hat{V}$, where \hat{U} and \hat{V} are unitary matrices and \hat{S} is a diagonal matrix with non-negative components. If \hat{T} has the canonical form

$$\hat{T} = \bigoplus_j (\hat{T}_j \otimes \hat{I}_{2j+1}), \quad (5.190)$$

we can obtain the $SU(2)$ -invariant matrices

$$\begin{aligned} \hat{U} &= \bigoplus_j (\hat{U}_j \otimes \hat{I}_{2j+1}), \\ \hat{S} &= \bigoplus_j (\hat{S}_j \otimes \hat{I}_{2j+1}), \\ \hat{V} &= \bigoplus_j (\hat{V}_j \otimes \hat{I}_{2j+1}), \end{aligned}$$

by performing SVD of each degeneracy matrix \hat{T}_j independently,

$$\hat{T}_j = \hat{U}_j \hat{S}_j \hat{V}_j. \quad (5.191)$$

A different factorization of \hat{T} , such as spectral decomposition or polar decomposition, can be obtained by the analogous factorization of the blocks \hat{T}_j . The computational savings are analogous to those described in Example 13 for the multiplication of matrices. Figure 5.26 shows a comparison of computation times required to perform a singular value decomposition on $SU(2)$ -invariant and regular matrices using MATLAB.

5.7 Supplement: Examples of evaluating a spin network

Let us consider a spin network $\mathcal{S}(\boldsymbol{\tau}, \boldsymbol{\tau}')$ that is constructed by means of two fusion trees $\boldsymbol{\tau}$ and $\boldsymbol{\tau}'$ in the following way. First obtain a tree tensor network \mathcal{T} by attaching a tensor C^{fuse} to each node the fusion tree $\boldsymbol{\tau}$. A tensor C^{fuse} mediates the fusion of the incoming

spins into the outgoing spin. Next, obtain the *splitting tree* that is dual to τ' . A splitting tree is obtained by reversing the direction of all links of a fusion tree. In the graphical representation this corresponds to a horizontal reflection of the fusion tree. Then obtain a tree tensor network \mathcal{T}' by attaching to each node of the splitting tree a tensor C^{split} that mediates the splitting of the incoming spin into outgoing spins. The spin network $\mathcal{S}(\tau, \tau')$ is obtained by connecting the open links of the two tree tensor networks: \mathcal{T} and \mathcal{T}' .

Since the spin network $\mathcal{S}(\tau, \tau')$ has two open links it can be contracted to obtain an SU(2)-invariant matrix, which according to Schur's lemma is proportional to the Identity. An important property of $\mathcal{S}(\tau, \tau')$ is that this proportionality factor can be *evaluated* algebraically without contracting the spin network. This property can be exploited to suppress the potentially high cost of contracting spin networks in numerical simulations.

The spin network $\mathcal{S}(\tau, \tau')$ can be evaluated in terms of the values of basic spin networks that are shown in Fig. 5.7(ii) and Fig. 5.11(ii). The first step of the evaluation procedure generally involves expressing the spin network as a composition of these basic spin networks. This can be achieved by applying, possibly several times, a resolution of Identity, Fig. 5.7(i), on appropriate links of the spin network. Then one proceeds by recursively applying the equalities in Fig. 5.7(ii) and Fig. 5.11(ii) to regions of the spin network, eventually replacing the spin network with a straight line and an overall numerical factor. Figure 5.27(i) illustrates these steps for the simple case of evaluating the spin network of Fig. 5.13 in terms of two recoupling coefficients.

We can also consider spin networks that have intercrossing lines such as those which appear when applying permuting indices of an SU(2)-invariant tensor. Such a spin network can be evaluated in terms of recoupling coefficients *and* swap factors, as illustrated in Fig. 5.27(ii).

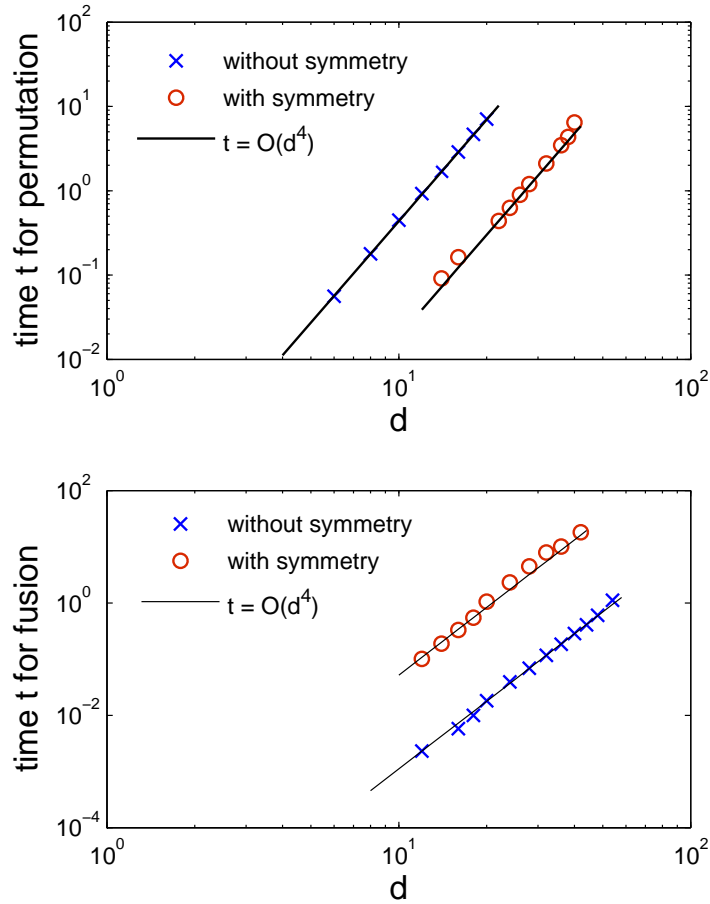


Figure 5.25 – Computation times (in seconds) required to permute indices of a rank-four tensor \hat{T} , as a function of the size of the indices. All four indices of \hat{T} have the same size $9d$, and therefore the tensor contains $|\hat{T}| = 9^4 d^4$ coefficients. The figures compare the time required to perform these operations using a regular tensor and an $SU(2)$ -invariant tensor, where in the second case each index contains three different values of spin $j = 0, 1, 2$, each with degeneracy d , and the canonical form of Eq. (5.161) is used. The upper figure shows the time required to permute two indices: For large d , exploiting the symmetry of an $SU(2)$ -invariant tensor by using the canonical form results in shorter computation times. The lower figure shows the time required to fuse two adjacent indices. In this case, maintaining the canonical form requires more computation time. Notice that in both figures the asymptotic cost scales as $O(d^4)$, or the size of \hat{T} , since this is the number of coefficients which need to be rearranged. We note that the fixed-cost overheads associated with symmetric manipulations could potentially vary substantially with choice of programming language, compiler, and machine architecture. The results given here show the performance of our MATLAB implementation of $SU(2)$ symmetry.

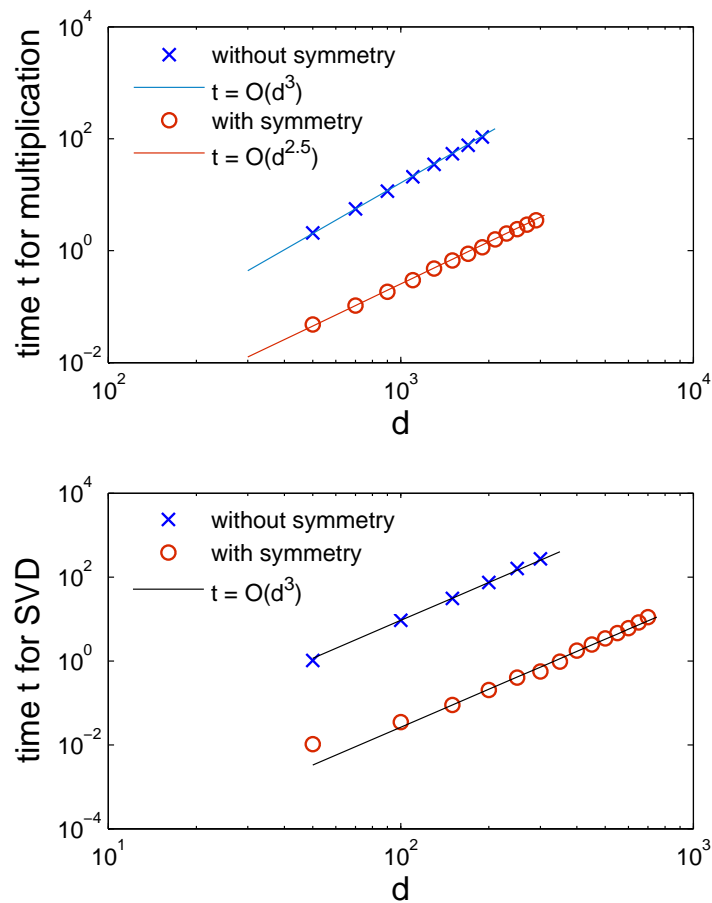


Figure 5.26 – Computation times (in seconds) required to multiply two matrices (upper panel) and to perform a singular value decomposition (lower panel), as a function of the size of the indices. Matrices of size $9d \times 9d$ are considered. The figures compare the time required to perform these operations using regular matrices and $SU(2)$ -invariant matrices, where for the $SU(2)$ matrices each index contains three different values of the spin $j = 0, 1, 2$, each with degeneracy d , and the canonical form of Eq. (5.137) is used. That is, each matrix decomposes into three blocks of size $d \times d$. For large d , exploiting the block diagonal form of $SU(2)$ -invariant matrices results in shorter computation time for both multiplication and singular value decomposition. The asymptotic cost scales with d as $O(d^3)$, while the size of the matrices grows as $O(d^2)$. (For matrix multiplication, a tighter bound of $O(d^{2.5})$ for the scaling of computational cost with d is seen in this example.) We note that the fixed-cost overheads associated with symmetric manipulations could potentially vary substantially with choice of programming language, compiler, and machine architecture. The results given here show the performance of our MATLAB implementation of $SU(2)$ symmetry.

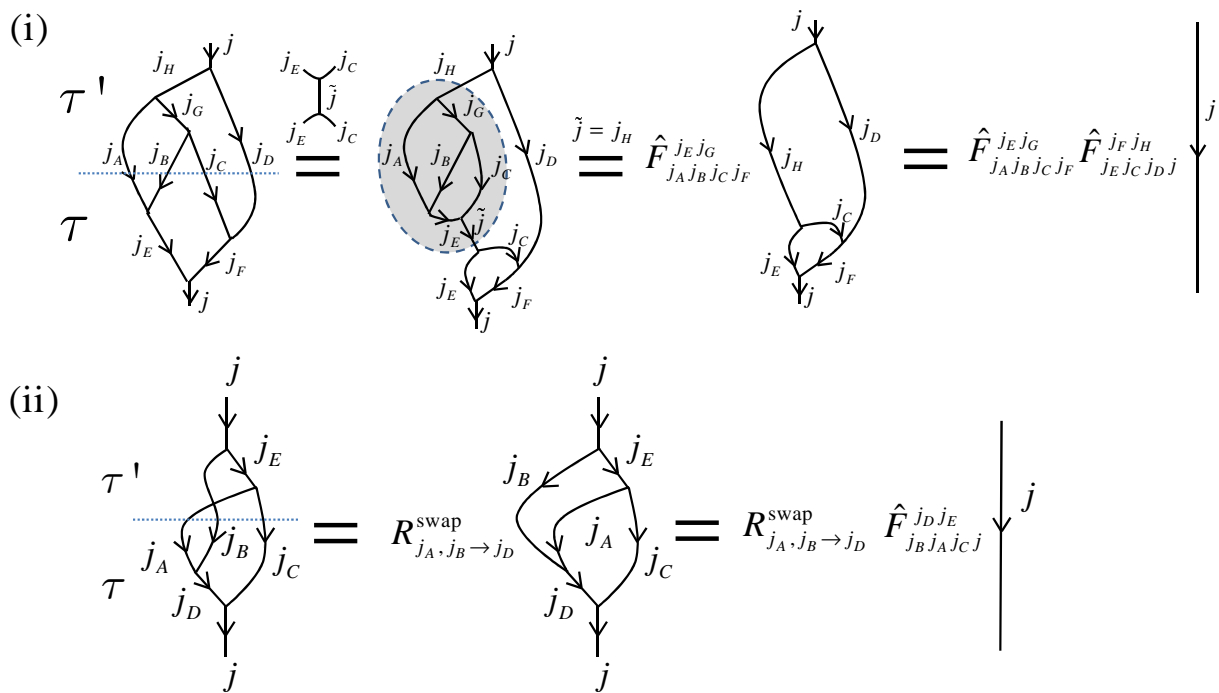


Figure 5.27 – Illustration of evaluating a spin network.

Implementation of non-Abelian symmetries

II

In this chapter we will describe a specific scheme for implementing non-Abelian symmetries. Our implementation is based on a special canonical form, the *tree decomposition*, of symmetric tensors.

A tree decomposition of a symmetric tensor corresponds to representing and storing the tensor as a tree tensor network made of two parts: (i) a symmetric *vector* and (ii) possibly several *splitting tensors* Υ^{split} . We describe how to implement the tensor manipulations within the set \mathcal{P} of primitive operations based on tree decompositions. In a tree decomposition, reshape and permutation of indices take a very simple form. In order to obtain the vector of the output tensor, one needs to simply multiply the vector of the initial tree decomposition with a matrix $\hat{\Gamma}$ [Fig 5.13(ii)] that depends only on the permutation or reshape.

This approach offers several advantages. Reshapes and permutations can be performed without breaking them into pairwise fusions and swaps, as was described in the previous chapter. More importantly, one can precompute (that is, compute before running the algorithm) the matrices $\hat{\Gamma}$ since these do not depend on the actual components of the tensor being manipulated. This is of special advantage in the case of iterative algorithms, where by pre-computing these matrices one also eliminates the cost of evaluating spin networks at runtime, thus substantially reducing the computational costs.

6.0.1 Tree decompositions of SU(2)-invariant tensors

Consider a rank- k SU(2)-invariant tensor \hat{T} with indices $\{i_1, i_2, \dots, i_k\}$ and directions \vec{D} . Let us apply the following transformations on tensor \hat{T} to obtain a vector. First reverse all incoming indices of \hat{T} to obtain another tensor \hat{T}' . Then fuse the indices of \hat{T}' according to a given fusion tree τ to obtain an SU(2)-invariant vector \hat{v} . This gives rise to a decomposition of tensor \hat{T} in terms of the vector \hat{v} , a set of splitting tensors that revert the fusion sequence τ , and a set of cup tensors that reverse the split indices that are identified with the incoming indices of \hat{T} . We refer to such a decomposition as a *tree decomposition* of \hat{T} and denote it as $\mathcal{D}(\hat{T})$. It is completely specified by the following list of elements:

$$\mathcal{D}(\hat{T}) \equiv (\{i_1, i_2, \dots, i_k\}, \vec{D}, \tau, \hat{v}). \quad (6.1)$$

Here the fusion tree τ determines the splitting tensors that are part of the decomposition while the directions \vec{D} indicate the presence or absence of a cup tensor on the open indices of the tree decomposition.

A tree decomposition of a rank-6 SU(2)-invariant tensor is shown in Fig. 6.1. The tree decomposition in the diagram can be specified as,

$$\mathcal{D}(\hat{T}) \equiv (\{i_1, i_2, i_3, i_4, i_5, i_6\}, \{\text{'in'}, \text{'out'}, \text{'out'}, \text{'in-R'}, \text{'out'}, \text{'out'}\}, \tau, \hat{v}), \quad (6.2)$$

where

$$\tau : \{i_4, i_5 \rightarrow i_e; \quad i_2, i_3 \rightarrow i_c; \quad i_e, i_6 \rightarrow i_c; \quad i_1, i_d \rightarrow i_b; i_b, i_c \rightarrow i_a\}.$$

In the graphical representation of a tree decomposition $\mathcal{D}(\hat{T})$ the vector \hat{v} appears at the top of the tree, the ‘body’ of the tree comprises of splitting tensors that are connected according to the fusion tree τ and the indices $\{i_1, i_2, \dots, i_6\}$ are associated, from left to right, to the open lines at the bottom of the tree. Some open indices are bent upwards by attaching cup tensors. A value $\vec{D}(l) = \text{'in'}$ indicates a cup tensor is attached to index i_l while $\vec{D}(l) = \text{'out'}$ indicates its absence. We additionally denote by $\vec{D}(l) = \text{'in-R'}$ that the transpose of a cup tensor is attached to index i_l . In the graphical representation, the values $\vec{D}(l) = \text{'in'}$ or $\vec{D}(l) = \text{'in-R'}$ correspond to bending the index i_l upwards from the left or from the right respectively.

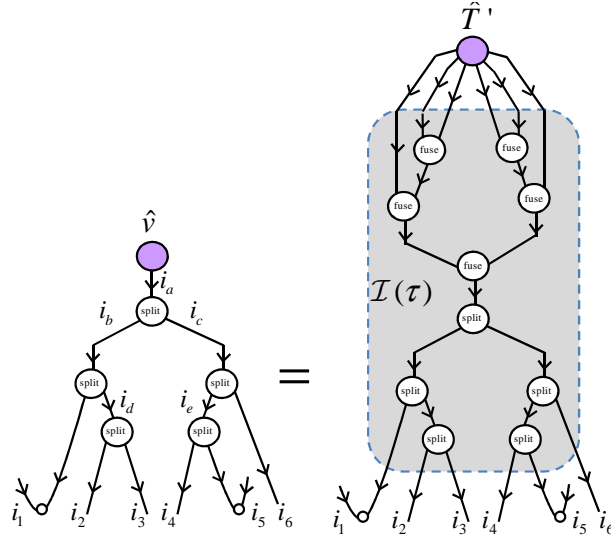


Figure 6.1 – A tree decomposition $\mathcal{D}(\hat{T})$ of a rank-6 $SU(2)$ -invariant tensor \hat{T} with indices $\{i_1, i_2, \dots, i_6\}$. (All internal indices are summed over.) The tree decomposition consists of an $SU(2)$ -invariant vector \hat{v} , a set of splitting tensors and cup tensors that are attached to the incoming indices of \hat{T} . The tree decomposition is obtained by applying a resolution of Identity $\mathcal{I}(\tau)$ on the tensor. The fusing and splitting tensors that constitute $\mathcal{I}(\tau)$ are connected together according to the fusion tree τ .

The vector \hat{v} is obtained by applying an resolution of Identity, denoted $\mathcal{I}(\tau)$, on tensor \hat{T}' , as shown on the r.h.s. of Fig. 6.1. The resolution of Identity $\mathcal{I}(\tau)$ is given by a tensor network made of a set of fusing tensors, that fuse the indices of \hat{T}' according to the fusion tree τ , and the corresponding set of splitting tensors that inverts the fusion. The vector \hat{v} is obtained by contracting \hat{T}' with the fusing tensors.

We emphasize that the cup tensors are stored *as part* of the tree decomposition without consuming them into the tree. This is done to simplify reshape and permutation of indices of a tree decomposition since these operations can be performed without noticing the cup tensors. For instance, in order to permute the open indices of a tree decomposition one may proceed by detaching any cup tensors from the tree, permuting the indices and re-attaching the cup tensors to the updated tree, a direct application of the commutation property depicted in Fig. 5.22. On the other hand, manipulations that involve summing over an index that is attached to a cup tensor are an exception. For example, when

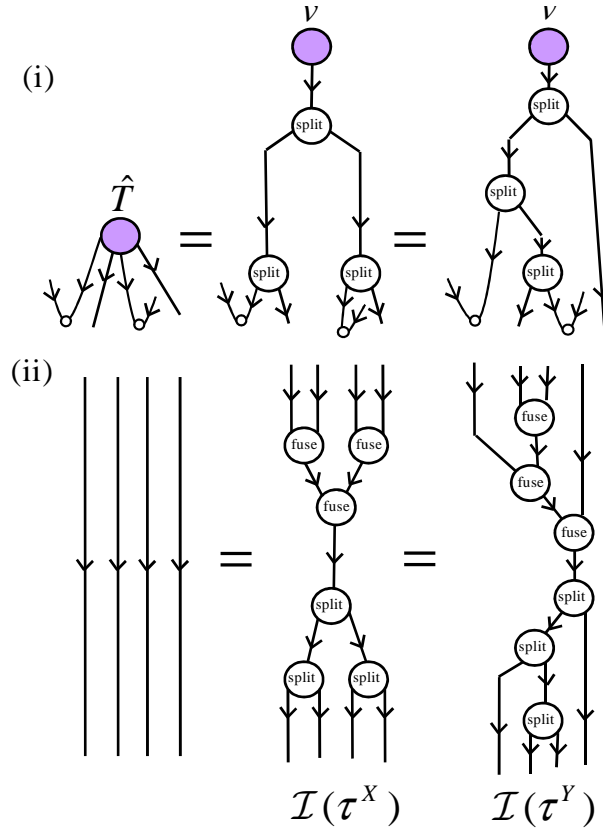


Figure 6.2 – (i) Two different, but equivalent, tree decompositions $\mathcal{D}^X(\hat{T})$ and $\mathcal{D}^Y(\hat{T})$ of a rank-4 SU(2)-invariant tensor \hat{T} . The two decompositions are characterized by different fusion trees τ^X and τ^Y . (ii) Tree decompositions $\mathcal{D}^X(\hat{T})$ and $\mathcal{D}^Y(\hat{T})$ are obtained by applying the resolutions of Identity $\mathcal{I}(\tau^X)$ and $\mathcal{I}(\tau^Y)$ on \hat{T} .

multiplying two SU(2)-invariant matrices, each given as a tree decomposition, the cup tensor has to be properly considered to obtain the resultant matrix. This is discussed in Sec. 6.0.6.

6.0.2 Mapping between tree decompositions

The same tensor \hat{T} may be expressed in different tree decompositions corresponding to different choices of the fusion tree. Two different fusion trees τ^X and τ^Y lead to two different tree decompositions $\mathcal{D}^X(\hat{T})$ and $\mathcal{D}^Y(\hat{T})$ of the same tensor \hat{T} . As an example we show two different but equivalent tree decompositions of a rank-4 tensor in Fig. 6.2(i).

The two decompositions

$$(\{i_1, i_2, i_3, i_4\}, \vec{D}, \boldsymbol{\tau}^X, \hat{v}^X) \text{ and } (\{i_1, i_2, i_3, i_4\}, \vec{D}, \boldsymbol{\tau}^Y, \hat{v}^Y),$$

are obtained by applying on the tensor the resolutions of Identity $\mathcal{I}(\boldsymbol{\tau}^X)$ and $\mathcal{I}(\boldsymbol{\tau}^Y)$ respectively that are separately depicted in Fig. 6.2(ii).

Suppose now that we have a tensor \hat{T} in a tree decomposition $\mathcal{D}^X(\hat{T})$ and we wish to transform it into another tree decomposition $\mathcal{D}^Y(\hat{T})$. We find it convenient to obtain the vector $\hat{v}^Y \in \mathcal{D}^Y(\hat{T})$ in steps, as shown in Fig. 6.3. First detach all cup tensors from $\mathcal{D}^X(\hat{T})$ and apply the resolution of Identity $\mathcal{I}(\boldsymbol{\tau}^Y)$ on the open indices of the tree. Then contract the splitting tensors in $\mathcal{D}^X(\hat{T})$ and the fusing tensors in $\mathcal{D}^Y(\hat{T})$ to obtain a matrix $\hat{\Gamma}(\boldsymbol{\tau}^X, \boldsymbol{\tau}^Y)$. The new vector \hat{v}^Y can be obtained by multiplying \hat{v}^X with the matrix $\hat{\Gamma}(\boldsymbol{\tau}^X, \boldsymbol{\tau}^Y)$,

$$\hat{v}^Y = \hat{\Gamma}(\boldsymbol{\tau}^X, \boldsymbol{\tau}^Y)\hat{v}^X. \quad (6.3)$$

Thus, the matrix $\hat{\Gamma}(\boldsymbol{\tau}^X, \boldsymbol{\tau}^Y)$ can be used to map from one tree decomposition of an $SU(2)$ -invariant tensor into another tree decomposition of the same tensor. Recall that the components of $\hat{\Gamma}(\boldsymbol{\tau}^X, \boldsymbol{\tau}^Y)$ can be expressed in terms of recoupling coefficients [Fig. 5.14, Eq. (5.120)].

To summarize the above procedure we define a template routine `NEWTREE` that takes as input a tree decomposition $\mathcal{D}^X(\hat{T})$ and a fusion tree $\boldsymbol{\tau}^Y$ and returns the tree decomposition

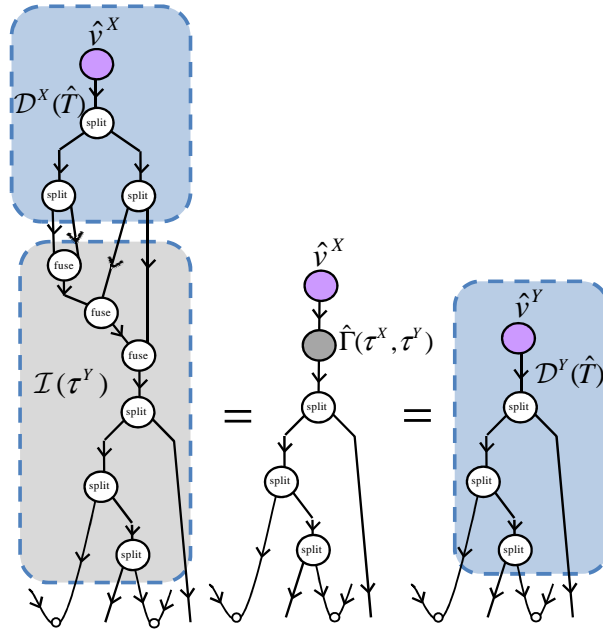


Figure 6.3 – Mapping a tree decomposition $\mathcal{D}^X(\hat{T})$ of an $SU(2)$ -invariant tensor \hat{T} to another tree decomposition $\mathcal{D}^Y(\hat{T})$ by applying a resolution of Identity $\mathcal{I}(\tau^Y)$ to $\mathcal{D}^X(\hat{T})$. We obtain an intermediate matrix $\hat{\Gamma}(\tau^X, \tau^Y)$ by contracting together the splitting tensors in $\mathcal{D}^X(\hat{T})$ and the fusing tensors in $\mathcal{I}(\tau^Y)$ and then multiply it with vector \hat{v}^X to obtain vector \hat{v}^Y .

$\mathcal{D}^Y(\hat{T})$ of the tensor. The routine reads

NEWTREE

Input:

$$\mathcal{D}^X(\hat{T}) := (\{i_1, i_2, \dots, i_k\}, \vec{D}, \tau^X, \hat{v}^X)$$

$$\tau^Y$$

Output:

$$\mathcal{D}^Y(\hat{T}) := (\{i_1, i_2, \dots, i_k\}, \vec{D}, \tau^Y, \hat{v}^Y)$$

Compute $\hat{\Gamma}(\tau^X, \tau^Y)$

$$\hat{v}^Y = \hat{\Gamma}(\tau^X, \tau^Y)\hat{v}^X$$

$$\mathcal{D}^Y(\hat{T}) := (\{i_1, i_2, \dots, i_k\}, \vec{D}, \tau^Y, \hat{v}^Y)$$

return($\mathcal{D}^Y(\hat{T})$).

(6.4)

(where $:=$ denotes ‘stored as’.)

Recall that the matrix $\hat{\Gamma}$ is sparse [Eq. (5.115)]. It can be shown that the matrix-vector multiplication, Eq. (6.3), can be performed with a cost that is $O(|\hat{v}|)$ by means of sparse multiplication.

Next we describe how manipulations in the set \mathcal{P} of primitive tensor manipulations [Sec. 5.1.5] are performed on tree decompositions. Consider an $SU(2)$ -invariant tensor \hat{T} that has been given as a tree decomposition $\mathcal{D}(\hat{T})$,

$$\mathcal{D}(\hat{T}) \equiv (\{i_1, i_2, \dots, i_k\}, \vec{D}, \boldsymbol{\tau}, \hat{v}).$$

Let \hat{T}' denote the $SU(2)$ -invariant tensor that is obtained from tensor \hat{T} as a result of a manipulation in \mathcal{P} . Also, let $\mathcal{D}(\hat{T}')$ denote a tree decomposition of \hat{T}' ,

$$\mathcal{D}(\hat{T}') \equiv (\{i'_1, i'_2, \dots, i'_m\}, \vec{D}', \boldsymbol{\tau}', \hat{v}').$$

We will describe how the components of vector \hat{v}' are determined systematically in terms of components of the vector \hat{v} .

6.0.3 Reversal of indices

Reversal of an index of a tree decomposition is trivial since the cup tensors are stored as part of the tree decomposition. It corresponds to attaching a cup (or its transpose) to the corresponding open index of the tree in case the index is outgoing or detaching the cup from the index in case it is incoming. This simple procedure is summarized in the following template routine which describes reversal of possibly several indices of tensor \hat{T} according to new directions \vec{D}' provided as input. No computation is involved in the

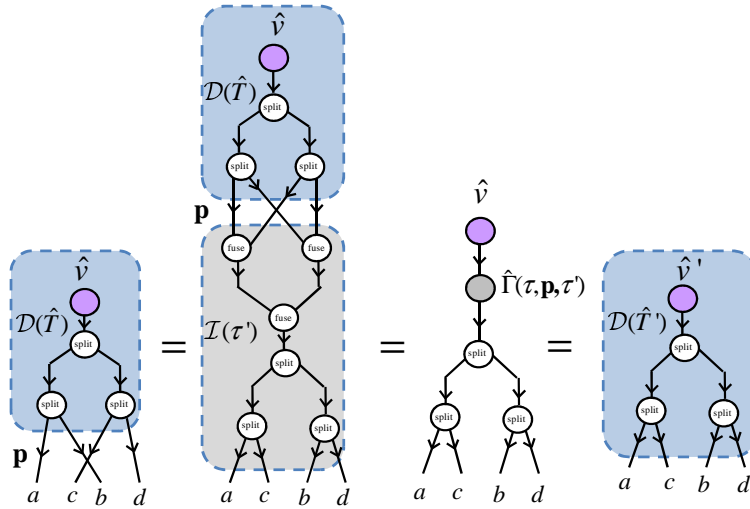


Figure 6.4 – Permuting indices of a rank-4 $SU(2)$ -invariant tensor \hat{T} given in a tree decomposition. The “crossings” in the diagram can be absorbed into the tree by applying a resolution of Identity $\mathcal{I}(\tau')$ (for a given fusion tree τ'). An intermediate matrix $\hat{\Gamma}(\tau, \mathbf{p}, \tau')$ is obtained by contracting together the splitting tensors in $\mathcal{D}(\hat{T})$, the permutation \mathbf{p} and the fusing tensors in $\mathcal{I}(\tau')$. The matrix is multiplied with the vector \hat{v} to determine the updated vector \hat{v}' .

procedure. Only information pertaining to the directions of indices is updated,

REVERSE

Input:

$$\mathcal{D}(\hat{T}) := (\{i_1, i_2, \dots, i_k\}, \vec{D}, \tau, \hat{v})$$

$$\vec{D}'$$

Output:

$$\mathcal{D}(\hat{T}') := (\{i_1, i_2, \dots, i_k\}, \vec{D}', \tau, \hat{v})$$

$$\mathcal{D}(\hat{T}') := (\{i_1, i_2, \dots, i_k\}, \vec{D}', \tau, \hat{v})$$

return($\mathcal{D}(\hat{T}')$)

(6.5)

6.0.4 Permutation of indices

The procedure to permute indices of a tree decomposition is illustrated in Fig. 6.4(i). We consider a rank-4 $SU(2)$ -invariant tensor with indices $\{a, b, c, d\}$ and apply a permutation \mathbf{p} ,

$$\{a, c, b, d\} = \mathbf{p}(\{a, b, c, d\}).$$

The permutation is depicted by intercrossing index a and index c of the tree. This crossing can be ‘absorbed’ into the tree by applying the resolution of Identity $\mathcal{I}(\boldsymbol{\tau}')$ on the tree. In order to determine the vector \hat{v}' we contract the splitting tensors in $\mathcal{D}(\hat{T})$ and the fusing tensors in $\mathcal{I}(\boldsymbol{\tau}')$ to obtain a matrix $\hat{\Gamma}(\boldsymbol{\tau}, \mathbf{p}, \boldsymbol{\tau}')$, which is then multiplied with the initial vector \hat{v} ,

$$\hat{v}' = \hat{\Gamma}(\boldsymbol{\tau}, \mathbf{p}, \boldsymbol{\tau}')\hat{v}. \quad (6.6)$$

Clearly, the above procedure can be employed to apply any permutation \mathbf{p} on the indices of a rank- k $SU(2)$ -invariant tensor. Matrix $\hat{\Gamma}(\boldsymbol{\tau}, \mathbf{p}, \boldsymbol{\tau}')$ is a generalization of matrix $\hat{\Gamma}(\boldsymbol{\tau}, \boldsymbol{\tau}')$ [e.g. Fig. 5.14] in that it additionally includes a permutation of indices. The latter can then be seen as a special instance of $\hat{\Gamma}(\boldsymbol{\tau}, \mathbf{p}, \boldsymbol{\tau}')$ with a trivial permutation of indices. The components of the degeneracy part \hat{D} of matrix $\hat{\Gamma}(\boldsymbol{\tau}, \mathbf{p}, \boldsymbol{\tau}')$ are given by Eq. (5.120) where coefficients $\hat{S}_{j_1 \dots j_k}^{j_{e_1} \dots j_{e_z}, j'_{e_1} \dots j'_{e_z}}$ can be expressed in terms of recoupling coefficients *and* swap factors (see Sec. 5.7).

Finally, note that the cup tensors do not play any role in the permutation since reversal of indices commutes with a permutation of them [Fig. 5.22]. In practice, all cup tensors can be detached from the tree before applying the permutation and then re-attached to the updated tree.

The procedure to permute indices of a tree decomposition is summarized in the following

template routine:

PERMUTE

Input:

$$\hat{T} := (\{i_1, i_2, \dots, i_k\}, \vec{D}, \boldsymbol{\tau}, \hat{v})$$

$\boldsymbol{\tau}'$

\mathbf{p}

Output:

$$\mathcal{D}(\hat{T}') := (\{i'_1, i'_2, \dots, i'_k\}, \vec{D}', \boldsymbol{\tau}', \hat{v}')$$

—

Compute $\hat{\Gamma}(\boldsymbol{\tau}, \mathbf{p}, \boldsymbol{\tau}')$

$$\hat{v}' = \hat{\Gamma}(\boldsymbol{\tau}, \mathbf{p}, \boldsymbol{\tau}')\hat{v}$$

$$\{i'_1, i'_2, \dots, i'_k\} = \mathbf{p}(\{i_1, i_2, \dots, i_k\})$$

$$\hat{T}' := (\{i'_1, i'_2, \dots, i'_k\}, \vec{D}', \boldsymbol{\tau}', \hat{v}')$$

$$\mathbf{return}(\mathcal{D}(\hat{T}')) \tag{6.7}$$

6.0.5 Reshape of indices

Consider fusing a pair of adjacent indices i_l and i_{l+1} of the tree decomposition $\mathcal{D}(\hat{T})$. Let us suppose that indices i_l and i_{l+1} do not carry cup tensors and also that they belong to the same node in $\mathcal{D}(\hat{T})$. Indices i_l and i_{l+1} can be fused into an index i by applying the tensor $\Upsilon_{i_l, i_{l+1} \rightarrow i}^{\text{fuse}}$ and using the equality shown in Fig. 5.9(i) to immediately obtain the tree decomposition $\mathcal{D}(\hat{T}')$. This is illustrated in Fig. 6.5(i). Note that the final vector \hat{v}' is the same as the initial vector \hat{v} . The updated fusion tree $\boldsymbol{\tau}'$ can be obtained from $\boldsymbol{\tau}$ by deleting the node $\{i_l, i_{l+1} \rightarrow i\}$ from $\boldsymbol{\tau}$. We denote this as,

$$\boldsymbol{\tau}' = \boldsymbol{\tau} - \{i_l, i_{l+1} \rightarrow i_m\}.$$

The original tree decomposition may be recovered from $\mathcal{D}(\hat{T}')$ by splitting index i back into indices i_l and i_{l+1} . This operation is again straightforward since it does not involve a computation of vector components, as illustrated in Fig. 6.5(ii). The original fusion tree

τ is recovered by concatenating a node to τ' ,

$$\tau \equiv \tau' \cup \{i \rightarrow i_l, i_{l+1}\}. \quad (6.8)$$

Now let us consider fusing indices i_l and i_{l+1} that *do not* belong to the same node of $\mathcal{D}(\hat{T})$. In this case one can first map $\mathcal{D}(\hat{T})$ into another tree decomposition $\tilde{\mathcal{D}}(\hat{T})$ in which indices i_l and i_{l+1} belong to the same node and then proceed with the fusion on the tree $\mathcal{D}(\hat{T})$ as described above. This can be done by applying the procedure NEWTREE (6.4) with inputs $\tilde{\mathcal{D}}(\hat{T})$ and the desired fusion tree.

Consider the template routine FUSE that fuses indices according to a set of *disjoint* fusion trees τ_1, τ_2, \dots where each fusion tree specifies fusion of a subset of adjacent indices $\{i_m, i_{m+1}\}, \{i_n, i_{n+1}, i_{n+2}\}, \dots$:

FUSE

Input args:

$$\mathcal{D}(\hat{T}) := (\{i_1, i_2, \dots, i_k\}, \vec{D}, \tau, \hat{v})$$

$$\{\tau_1, \tau_2, \dots\}$$

$$\text{Final indices: } \{i'_1, i'_2, \dots, i'_l\}$$

$$\text{Fusion tree of final tensor: } \tau'$$

Output args:

$$\mathcal{D}(\hat{T}') := (\{i'_1, i'_2, \dots, i'_l\}, \vec{D}, \tau', \hat{v}')$$

$$\tau'' = \tau' \cup \tau_1 \cup \tau_2 \cup \dots$$

$$\mathcal{D}''(\hat{T}) = \text{NEWTREE}(\mathcal{D}(\hat{T}), \tau'')$$

$$\hat{v}' = \hat{v}''$$

$$\mathcal{D}(\hat{T}') := (\{i'_1, i'_2, \dots, i'_l\}, \tau', \hat{v}')$$

$$\text{return}(\mathcal{D}(\hat{T}')) \quad (6.9)$$

Notice that here we essentially apply the total fusion at once by concatenating the input fusion trees τ_1, τ_2, \dots into a single tree and then applying the procedure NEWTREE. Consequently, the fusion is carried out by means of a single matrix-vector multiplication.

Furthermore, the computational cost incurred by the procedure is dominated by the cost of this step. As mentioned previously, this cost is $O(|\hat{v}|)$.

Also consider the following routine to split indices $\{i'_1, i'_2, \dots\}$ of a tree decomposition $\mathcal{D}(\hat{T}')$ (typically the output of FUSE) by reversing the fusion sequence encoded in fusion trees τ_1, τ_2, \dots :

SPLIT

Input args:

$$\mathcal{D}(\hat{T}') := (\{i'_1, i'_2, \dots, i'_l\}, \vec{D}, \tau', \hat{v}')$$

$$\text{Final indices: } \{i_1, i_2, \dots, i_k\}$$

$$\tau_1, \tau_2, \dots$$

Output args:

$$\mathcal{D}(\hat{T}) := (\{i_1, i_2, \dots, i_k\}, \vec{D}, \tau, \hat{v})$$

$$\tau = \tau' \cup \tau_1 \cup \tau_2 \cup \dots$$

$$\hat{v} = \hat{v}'$$

$$\hat{T} := (\{i_1, i_2, \dots, i_k\}, \tau, \hat{v})$$

$$\mathbf{return}(\hat{T}) \tag{6.10}$$

Note that no computation of vector components is involved in this procedure.

Let us now describe how to reshape indices that may carry cup tensors. First consider the fusion of indices each of which carries a cup tensor. We proceed by detaching the cup tensors from the indices, applying the procedure FUSE and finally attaching a cup tensor to each of the fused indices. Analogously, an index that carries a cup tensor may be split into two indices, by detaching the cup tensor, applying the procedure SPLIT and attaching a cup tensor to each of two indices so obtained.

Finally, consider the fusion of an index that carries a cup tensor with an index that does not carry a cup tensor. The fusion proceeds by detaching the cup tensor and then applying the procedure FUSE on the indices. The fusion is to be reversed in a consistent manner

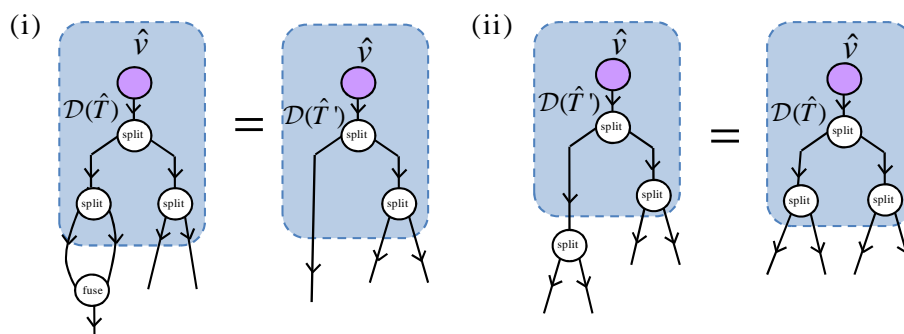


Figure 6.5 – (i) Fusion of two adjacent indices that belong to the same node of the tree decomposition proceeds by simply deleting the node to obtain the updated tree decomposition. (ii) Splitting an index corresponds to concatenating a new node to the tree decomposition.

by first applying the procedure SPLIT on the fused index and then attaching a cup tensor to the originally incoming index.

6.0.6 Matrix multiplication and factorizations

Let us consider how matrix operations are performed on tree decompositions. Two $SU(2)$ -invariant matrices, each given as a tree decomposition, may be multiplied together by first obtaining the matrices in a block-diagonal form (from the respective tree decompositions), performing a block-wise multiplication (Sec. 5.6.4) and recasting the resulting block-diagonal matrix into a tree decomposition.

An $SU(2)$ -invariant matrix may be factorized e.g. singular value decomposed in a similar way. One proceeds by obtaining the matrix in a block-diagonal form, performing block-wise factorization (Sec. 5.6.5), and recasting each of the factor block-diagonal matrices into a tree decomposition.

In the remainder of the section we explain how a block-diagonal form is obtained from a tree decomposition and vice-versa.

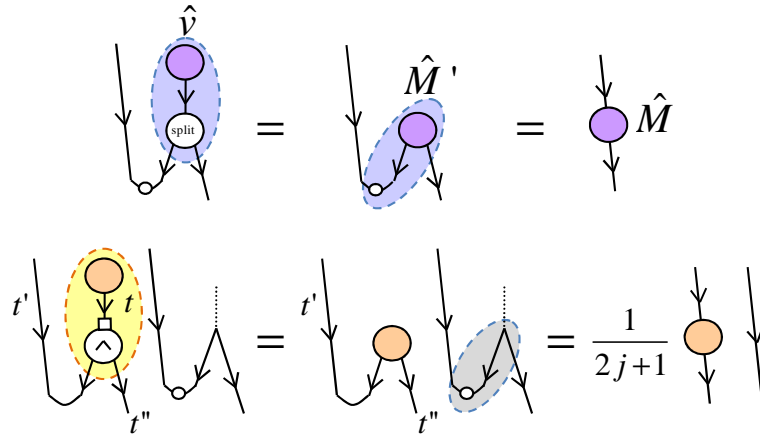


Figure 6.6 – The block-diagonal form of an $SU(2)$ -invariant matrix is obtained from its tree decomposition by performing two multiplications. At each step the tensors within the shaded region are multiplied together. The same steps are also shown in the canonical form.

Block-diagonal matrix from the tree decomposition

Consider a tree decomposition $\mathcal{D}(\hat{T})$ of an $SU(2)$ -invariant matrix \hat{T} . The decomposition $\mathcal{D}(\hat{T})$ comprises of a vector \hat{v} , a splitting tensor Υ^{split} and a cup tensor $\hat{\Omega}^{\text{cup}}$. We wish to obtain, from $\mathcal{D}(\hat{T})$, the corresponding block diagonal matrix,

$$\hat{T} = \bigoplus_j (\hat{T}_j \otimes \hat{I}_{2j+1}). \quad (6.11)$$

This can be achieved by multiplying together the vector, the splitting tensor and the cup tensor. We perform this multiplication in two simple steps as shown in Fig. 6.6. We first multiply \hat{v} with Υ^{split} to obtain an intermediate $SU(2)$ -invariant tensor \hat{T}' that takes the canonical form,

$$\hat{T}'_j = \bigoplus_j (\hat{T}'_j \otimes \hat{\omega}_j), \quad (6.12)$$

where the components $(\hat{T}'_j)_{t't''}$ of \hat{T}'_j are given by

$$(\hat{T}'_j)_{t't''} = \sum_t \hat{v}_t X_{0t \rightarrow jt', jt''}^{\text{split}}. \quad (6.13)$$

We then multiply (algebraically) tensor \hat{T}' with the cup tensor to obtain the block-diagonal matrix \hat{T} to obtain

$$\hat{T}_j = \frac{1}{2j+1} \hat{T}'_j. \quad (6.14)$$

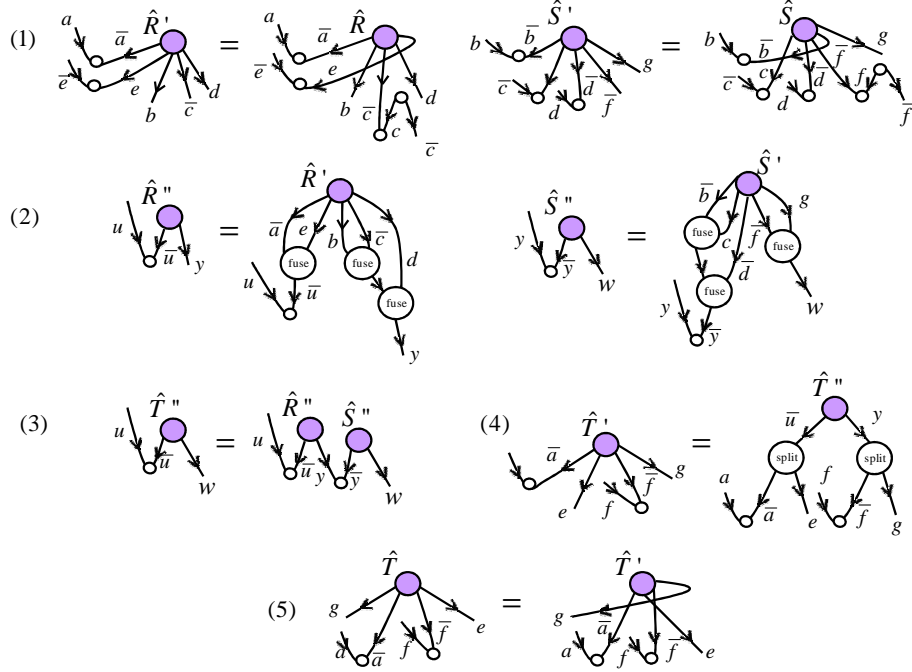


Figure 6.7 – The five steps of tensor multiplication [Fig. 5.4] as adapted to the presence of the symmetry. For simplicity, the tree decompositions are not explicitly shown; the circle representing a tensor masks the tree decomposition of the tensor.

Tree decomposition from the block-diagonal matrix

The tree decomposition $\mathcal{D}(\hat{T})$ can be obtained from the block-diagonal form (6.11) in a straightforward manner by reverting the previous procedure. We first multiply \hat{T} with a cap tensor to obtain tensor \hat{T}' . Once again, the outcome of this multiplication follows algebraically. We obtain

$$(\hat{T}'_j)_{\nu\nu'} = (2j + 1)(\hat{T}_j)_{\nu\nu'}. \tag{6.15}$$

We then fuse the indices of \hat{T}' to obtain a vector \hat{v} ,

$$\hat{v}_t = \sum_j \sum_{\nu\nu'} (\hat{T}'_j)_{\nu\nu'} X_{j\nu',j\nu' \rightarrow 0t}^{\text{fuse}}. \tag{6.16}$$

The tree decomposition $\mathcal{D}(\hat{T})$ comprises of vector \hat{v} , the splitting tensor X^{split} that reverts the fusion in Eq. (6.16) and a cup tensor.

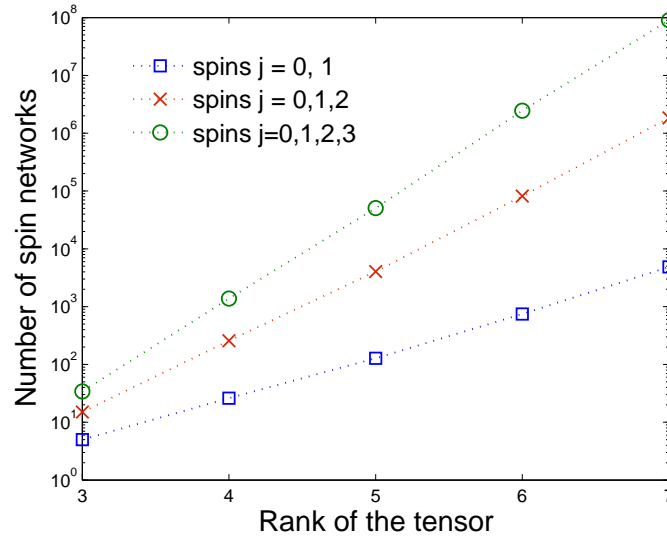


Figure 6.8 – The number of spin networks to be evaluated when permuting or reshaping an $SU(2)$ -invariant tensor, as a function of the number of indices of the tensor and the number of different spins j assigned to each index of the tensor. The plot shows the increase in the number of spin networks that are evaluated when reshaping tensors with increasing number of indices. It also illustrates the corresponding increase that results from increasing the number of different values of spin j that are assigned to the indices of the tensor. (Note that the number of spin networks does not depend on the degeneracy dimension of a spin j .) Consequently, the cost of reshaping tensors with a large number of indices may potentially become significant.

6.0.7 Multiplication of two tensors

We can now consider the multiplication of two $SU(2)$ -invariant tensors by breaking it into a sequence of five elementary steps consisting of reversals, permutes, reshapes and matrix multiplication, as was exemplified in Sec. 5.1.3 and Fig. 5.4. Here the elementary steps are performed on the tree decompositions of tensors. Figure 6.7 illustrates the five steps of the tensor multiplication, Eq. (5.8), as adapted to tree decompositions. For simplicity, we have not shown the tree decompositions in the figure and the circle that depicts a tensor can be imagined to mask the tree decomposition of the tensor.

6.0.8 Discussion on computational performance

The core of obtaining computational gain from exploiting the symmetry lies in block-wise matrix operations [Fig. 5.26] while permutation and reshape of indices are applied mainly to obtain block-diagonal matrices from tensors. As has been illustrated in Fig. 5.25 the cost of reshaping, for instance, $SU(2)$ -invariant tensors can be significantly larger than that incurred in reshaping regular tensors, and in some case can lead to a severe degradation of the overall gain obtained by exploiting the symmetry. Let us analyze the cost associated to reshape and permutation of indices of an $SU(2)$ -invariant tensor.

We have described that by working on tree decompositions reshape and permutation of indices equates to multiplying a matrix $\hat{\Gamma}$ with a vector. The computation of $\hat{\Gamma}$ may be costly since it generally involve evaluating many spin networks, see Fig. 6.8. Consequently, the cost of reshaping or permuting tensors with a large number of indices may become significant. This is more so the case for *iterative* algorithms where a fixed set of manipulations repeat many times. For example, one may optimize tensors iteratively in a variational algorithm such that the components of the tensor are updated in the current iteration and used as an input to the subsequent iteration. Note that each iteration involves evaluating a large number of spin networks, albeit the *same* spin networks are evaluated in each iteration. This fact can be exploited to *pre-compute* the transformations $\hat{\Gamma}$ once, say in the first iteration of the algorithm, and storing them in memory for *reuse* in subsequent iterations. By precomputation of these matrices the cost of evaluating many spin networks is suppressed from the runtime costs.

In our MATLAB implementation the use of such a precomputation scheme resulted in a significant speed-up of simulations at the cost of storing additional amounts of precomputed data. In the passing we also remark that since all computations have been reduced to matrix operations, computational performance can also be potentially enhanced by parallelizing and vectorizing the underlying matrix operations.

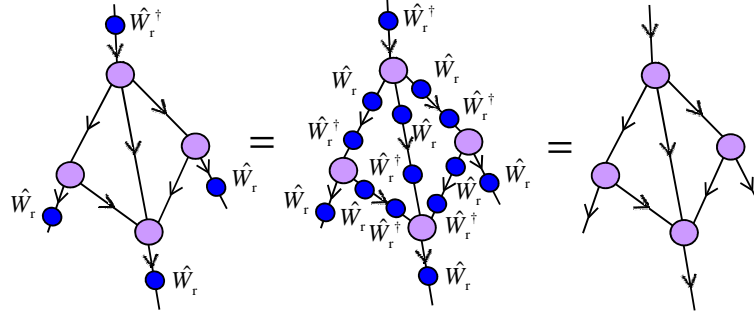


Figure 6.9 – A tensor network \mathcal{N} made of $SU(2)$ -invariant tensors represents an $SU(2)$ -invariant tensor \hat{T} . This is seen by means of two equalities. The first equality is obtained by inserting resolutions of the Identity $\hat{I} = \hat{W}_r \hat{W}_r^\dagger$ on each index connecting two tensors in \mathcal{N} . The second equality follows from the fact that each tensor in \mathcal{N} is $SU(2)$ -invariant.

6.1 Tensor networks with $SU(2)$ symmetry: A practical demonstration

Consider a lattice \mathcal{L} made of L sites where each site l is described by a vector space $\mathbb{V}^{(l)}$ that transforms as a finite dimensional representation of $SU(2)$. The vector space $\mathbb{V}^{(\mathcal{L})}$ of the lattice is given as

$$\mathbb{V}^{(\mathcal{L})} \equiv \bigotimes_l \mathbb{V}^{(l)}. \quad (6.17)$$

Consider a state $|\Psi\rangle \in \mathbb{V}^{(\mathcal{L})}$ that is invariant, Eq. 5.60, under the action of $SU(2)$ on the vector space $\mathbb{V}^{(\mathcal{L})}$. We describe $|\Psi\rangle$ by means of a tensor network made of $SU(2)$ -invariant tensors.

It readily follows that the tensor obtained by contracting such a tensor network is $SU(2)$ -invariant, as illustrated in Fig. 6.9.

On the one hand, by storing each constituent tensor of the tensor network in a canonical form we can ensure a compact tensor network description of $|\Psi\rangle$. On the other, computational speedup can be obtained by exploiting the sparse canonical form of the tensors when performing manipulations of individual tensors in a tensor network algorithm.

In the remainder of the section we illustrate the implementation of $SU(2)$ symmetry in

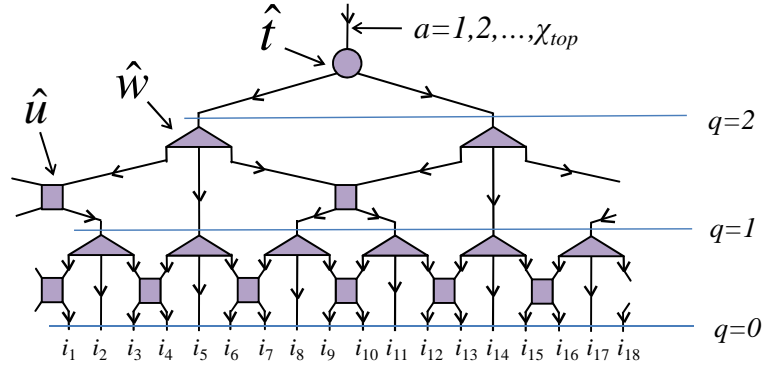


Figure 6.10 – MERA for a system of $L = 2 \times 3^2 = 18$ sites, made of two layers of disentanglers \hat{u} and isometries \hat{w} , and a top tensor \hat{t} .

tensor network algorithms with practical examples. We do so in the context of the Multi-scale Entanglement Renormalization Ansatz, or MERA, and present numerical results from our reference implementation of SU(2) symmetry in MATLAB.

6.1.1 Multi-scale entanglement renormalization ansatz

Figure 6.10 shows a MERA that represent states $|\Psi\rangle \in \mathbb{V}^{\mathcal{L}}$ of a lattice \mathcal{L} made of $L = 18$ sites. Recall that the MERA is made of layers of isometric tensors, known as disentanglers \hat{u} and isometries \hat{w} , that implement a coarse-graining transformation. In this particular scheme, isometries map three sites into one and the coarse-graining transformation reduces the $L = 18$ sites of \mathcal{L} into two sites using two layers of tensors. A collection of states on these two sites is then encoded in a top tensor \hat{t} , whose upper index $a = 1, 2, \dots, \chi_{\text{top}}$ is used to label χ_{top} states $|\Psi_a\rangle \in \mathbb{V}^{\mathcal{L}}$. This particular arrangement of tensors corresponds to the 3:1 MERA described in (Evenbly and Vidal, 2009a). We will consider a MERA analogous to that of Fig. 6.10 but with Q layers of disentanglers and isometries, which we will use to describe states on a lattice \mathcal{L} made of 2×3^Q sites.

We will use the MERA as a variational ansatz for ground states and excited states of quantum spin models described by a local Hamiltonian \hat{H} . In order to find an approximation to the ground state of \hat{H} , we set $\chi_{\text{top}} = 1$ and optimize the tensors in the MERA

so as to minimize the expectation value

$$\langle \Psi | \hat{H} | \Psi \rangle \quad (6.18)$$

where $|\Psi\rangle \in \mathbb{V}(\mathcal{L})$ is the pure state represented by the MERA. In order to find an approximation to the $\chi_{\text{top}} > 1$ eigenstates of \hat{H} with lowest energies, we optimize the tensors in the MERA so as to minimize the expectation value

$$\sum_{a=1}^{\chi_{\text{top}}} \langle \Psi_a | \hat{H} | \Psi_a \rangle, \quad \langle \Psi_a | \Psi_{a'} \rangle = \delta_{aa'}. \quad (6.19)$$

The optimization is carried out using the MERA algorithm described in (Evenbly and Vidal, 2009a), which requires contracting tensor networks (by sequentially multiplying pairs of tensors) and performing singular value decompositions.

6.1.2 MERA with SU(2) symmetry

An SU(2)-invariant version of the MERA, or SU(2) MERA for short, is obtained by simply considering SU(2)-invariant versions of all of the isometric tensors, namely the disentanglers \hat{u} , isometries \hat{w} , and the top tensor \hat{t} . This requires assigning a spin operator to each index of the MERA. We can characterize the spin operator by two vectors, \vec{j} and \vec{d} : a list of the different values the spin takes and the degeneracy associated with each such spin, respectively. For instance, an index characterized by $\vec{j} = \{0, 1\}$ and $\vec{d} = \{2, 1\}$ is associated to a vector space \mathbb{V} that decomposes as $\mathbb{V} \cong d_0 \mathbb{V}_0 \oplus d_1 \mathbb{V}_1$ with $d_0 = 2$ and $d_1 = 1$.

Let us explain how a spin operator is assigned to each link of the MERA. Each open index of the first layer of disentanglers corresponds to one site of \mathcal{L} . The spin operator on any such index is therefore given by the quantum spin model under consideration. For example, a lattice with a spin- $\frac{1}{2}$ associated to each site corresponds to assigning spin- $\frac{1}{2}$ operators [Eq. (5.24)] to each of the open indices.

For the open index of the tensor \hat{t} at the very top the MERA, the assignment of spins will depend on spin sector J that one is interested in. For instance, in order to find an approximation to the ground state and first seven excited states of the quantum spin model within the spin sector J , we choose $\vec{j} = \{J\}$ and $\vec{d} = \{8\}$.

For each of the remaining indices of the MERA, the assignment of the pair (\vec{j}, \vec{d}) needs careful consideration and a final choice may only be possible after numerically testing several options and selecting the one which produces the lowest expectation value of the energy.

For demonstrative purposes, we will use the SU(2) MERA as a variational ansatz to obtain the ground state and excited states of the spin- $\frac{1}{2}$ antiferromagnetic quantum Heisenberg chain that is given by,

$$\hat{H} = \sum_{s=1}^L \hat{h}^{(s,s+1)}, \quad (6.20)$$

where

$$\hat{h}^{(s,s+1)} = 4 \left(\hat{J}_x^{(s)} \hat{J}_x^{(s+1)} + \hat{J}_y^{(s)} \hat{J}_y^{(s+1)} + \hat{J}_z^{(s)} \hat{J}_z^{(s+1)} \right), \quad (6.21)$$

\hat{J}_x, \hat{J}_y and \hat{J}_z are the spin- $\frac{1}{2}$ operators [Eq. (5.24)]. The model has a global SU(2) symmetry, since the Hamiltonian commutes with the spin operators acting on the lattice \mathcal{L} . This follows from the fact that each local term $\hat{h}^{(s,s+1)}$ in the Hamiltonian commutes with the two site spin operators,

$$[\hat{h}^{(s,s+1)}, \hat{J}_\alpha^{(s)} + \hat{J}_\alpha^{(s+1)}] = 0, \quad \alpha = x, y, z. \quad (6.22)$$

Each spin- $\frac{1}{2}$ degree of freedom of the Heisenberg chain is described by a vector space $\mathbb{V} \cong \mathbb{V}_{\frac{1}{2}}$ that is spanned by two orthonormal states [Eq. (5.23)],

$$|j = \frac{1}{2}, m = -\frac{1}{2}\rangle \text{ and } |j = \frac{1}{2}, m = \frac{1}{2}\rangle.$$

For computational convenience, we will consider a lattice \mathcal{L} where each site contains two spins. Therefore each site of \mathcal{L} is described by a space $\mathbb{V} \cong \mathbb{V}_0 \oplus \mathbb{V}_1$, where $d_0 = 1$ and $d_1 = 1$, also discussed in Example 6. This corresponds to the assignment $\vec{j} = \{0, 1\}$ and $\vec{d} = \{1, 1\}$ at the open legs at the bottom of the MERA. Thus, a lattice \mathcal{L} made of L sites corresponds to a chain of $2L$ spins.

Table 6.1 lists some of the spin and degeneracy dimensions assignment (for the internal links of the MERA) that we have used in the numerical computations for $L = 54$ (or 108

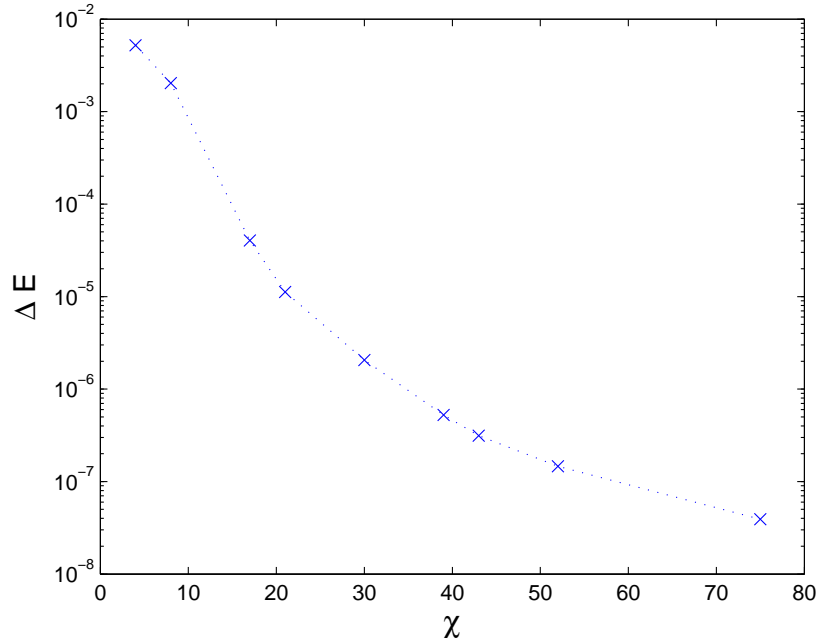


Figure 6.11 – Error in ground state energy ΔE as a function of χ for the Heisenberg model with $2L = 108$ spins and periodic boundary conditions, in the singlet sector, $J = 0$. The error is calculated with respect to the exact solutions, and is seen to decay polynomially with χ for the particular choice of spins listed in Table 6.1.

spins). For a given value of \vec{j} and \vec{d} the corresponding dimension χ can be obtained as,

$$\chi = \sum_{j \in \vec{j}} (2j + 1) \times d_j. \quad (6.23)$$

Figure 6.11 shows the error in the ground state energy of the Heisenberg chain as a function of the bond dimension χ , for the assignments of \vec{j} and \vec{d} that are listed in Table 6.1. For the choice of spin assignments listed in the table the error is seen to decay polynomially with χ , indicating increasingly accurate approximations to the ground state.

6.1.3 Advantages of exploiting the symmetry

We now discuss some of the advantages of using the SU(2) MERA.

Total bond dimension, χ	Spins \vec{j}	Degeneracies \vec{d}
4	{0, 1}	{1, 1}
8	{0, 1}	{2, 2}
17	{0, 1, 2}	{3, 3, 1}
21	{0, 1, 2}	{4, 4, 1}
30	{0, 1, 2}	{5, 5, 2}
39	{0, 1, 2}	{6, 6, 3}
43	{0, 1, 2}	{7, 7, 3}
52	{0, 1, 2}	{8, 8, 4}
75	{0, 1, 2, 3}	{9, 9, 5, 2}

Table 6.1 – Example of spin assignment in an SU(2) MERA for the anti-ferromagnetic spin chain with $L = 54$ sites (or 108 spins).

Selection of spin sector

An important advantage of the SU(2) MERA is that it exactly preserves the SU(2) symmetry. In other words, the states resulting from a numerical optimization are exact eigenvectors of the total spin operator $\mathbf{J}^2 : \mathbb{V}(\mathcal{L}) \rightarrow \mathbb{V}(\mathcal{L})$. In addition, the total spin J can be pre-selected at the onset of optimization by specifying it in the open index of the top tensor \hat{t} .

Figure 6.12 shows the low energy spectrum of the Heisenberg model \hat{H} for a periodic system of $L = 54$ sites (or 108 spins), including the ground state and several excited states in the spin sectors $J = 0, 1, 2$. The states have been organized according to spin projection m_J . We see that states with different spin projections m_J (for a given J) are obtained to be exactly degenerate, as implied by the symmetry.

Similar computations can be performed with the regular MERA. However, the regular MERA cannot guarantee that the states obtained in this way are exact eigenvectors of \mathbf{J}^2 . Instead the resulting states are likely to have total spin fluctuations. This is shown in inset of Fig. 6.12, which corresponds to the zoom in of the region in the plot that is

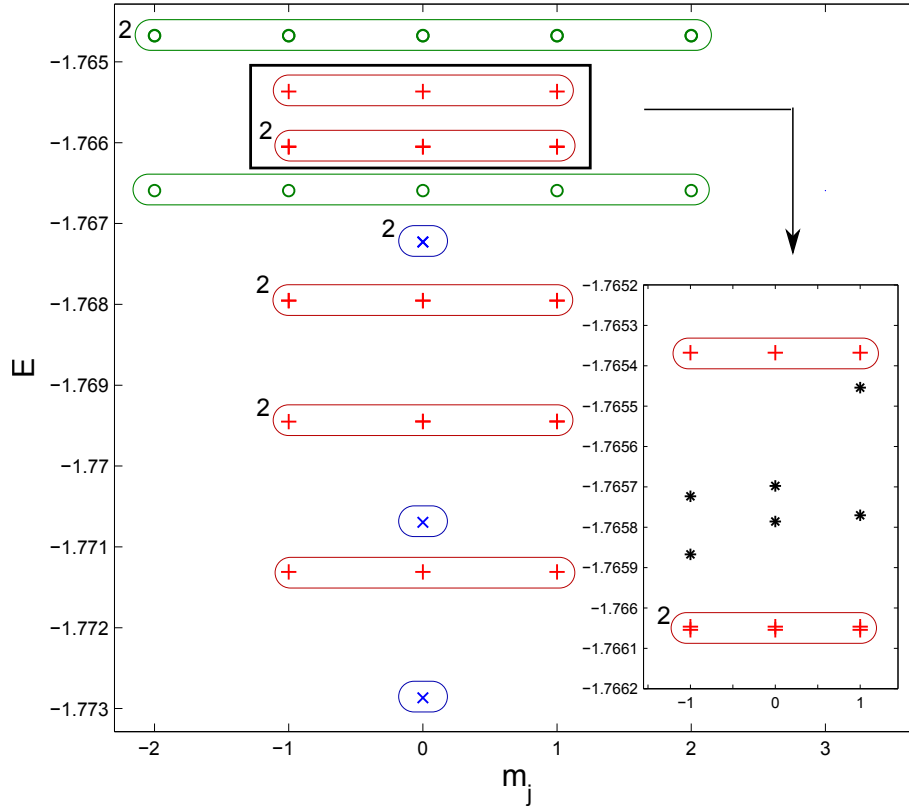


Figure 6.12 – Low energy spectrum of \hat{H} with $L = 54$ sites ($=108$ spins). Depicted states have spin J of zero (\times , blue loops), one ($+$, red loops), or two (\circ , green loop). The superscript 2 close to the boundary of a loop indicates that the loop encloses two-fold degenerate states e.g., the second, third and fourth spin-1 triplets are twofold degenerate. The inset shows a zoom in of the region enclosed within the box. It compares the energies of the two-fold degenerate spin-one states within the box with those obtained using the regular MERA (black asterisk points). Since the symmetry is not protected, the states obtained with the regular MERA corresponding to different m_J do not have the same energies.

enclosed within the box. The inset shows (black asterisk points) the corresponding energies obtained for the enclosed two-fold degenerate $J = 1$ states using the regular MERA. We see that the states corresponding to different values of m_J are obtained with different energies.

Also note that by using the $SU(2)$ MERA, the three sectors $J = 0, 1$ and 2 can be addressed with independent computations. This implies, for instance, that finding the

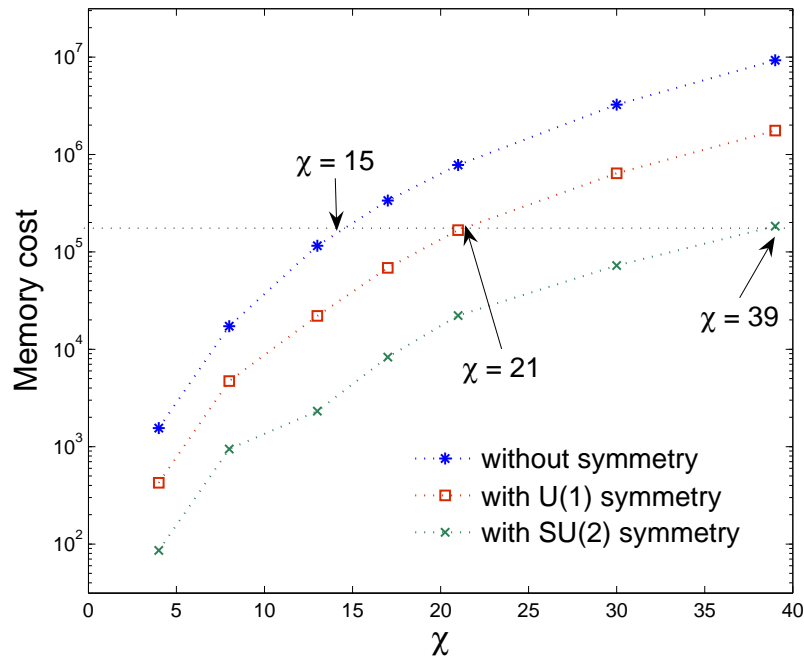


Figure 6.13 – Memory cost (in number of components) for storing the MERA as a function of the bond dimension χ . The horizontal line on this graph shows that this reduction in memory cost equates to the ability to store MERAs with a higher bond dimension χ : For the same amount of memory required to store a MERA with bond dimension $\chi = 15$, one may choose instead to store a U(1)-symmetric MERA with $\chi = 26$ or an SU(2)-symmetric MERA with $\chi = 39$.

gap between the first singlet ($J = 0$) and the first $J = 2$ state, can be addressed with two independent computations by respectively setting ($J = 0, \chi_{\text{top}} = 1$) and ($J = 2, \chi_{\text{top}} = 1$) on the open index of the top tensor \hat{t} . However, in order to capture the first $J = 2$ state using the regular MERA, we would need to consider at least $\chi_{\text{top}} = 20$ (at a larger computational cost and possibly lower accuracy), since this state has only the 20th lowest energy overall.

Reduction in memory and computational costs

The use of SU(2)-invariant tensors in the MERA also results in a reduction of computational costs. We compared the memory and computational costs associated with using

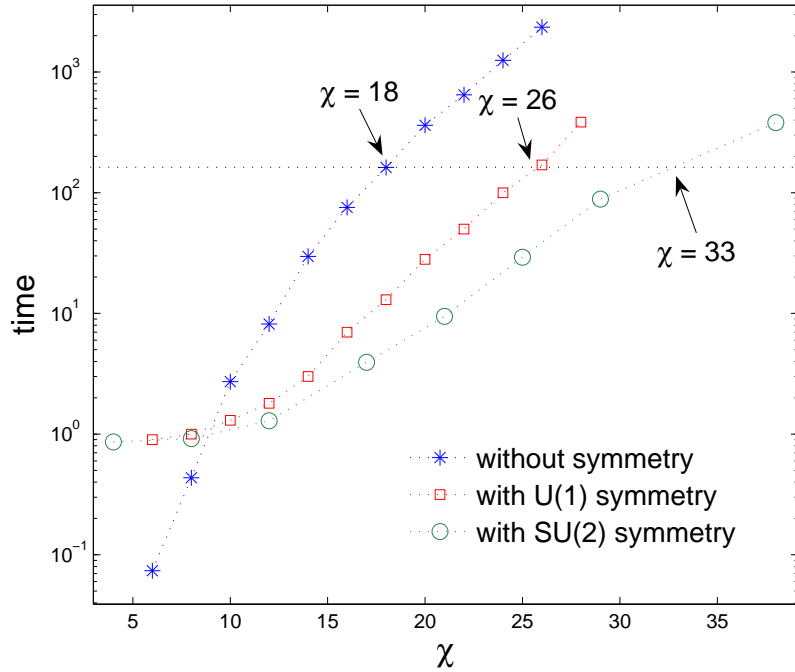


Figure 6.14 – Computation time (in seconds) for one iteration of the MERA energy minimization algorithm, as a function of the bond dimension χ . For sufficiently large χ , exploiting the SU(2) symmetry leads to reductions in computation time. The horizontal line on this graph shows that this reduction in computation time equates to the ability to evaluate MERAs with a higher bond dimension χ : For the same cost per iteration incurred when optimizing a regular MERA in MATLAB with bond dimension $\chi = 18$, one may choose instead to optimize a U(1)-symmetric MERA with $\chi = 26$ or an SU(2)-symmetric MERA $\chi = 33$.

the regular MERA and the SU(2) MERA. We also found it instructive to compare the analogous costs associated with a MERA that is made of tensors that remain invariant under only a subgroup U(1) of the symmetry group. This entails introducing the spin projection operators \hat{J}_z on the links of the MERA and imposing the invariance of constituent tensors under the action of these operators. For such a U(1)-MERA, imposing such constraints corresponds to conservation of the total spin projection m_J , while the total spin may fluctuate. (The explicit construction of the U(1)-MERA was discussed in Chapter 4).

Figure 6.13 shows a comparison of the total number of complex coefficients that are required to be stored for $L = 54$ sites (corresponding to 108 spins) in the three cases: regular MERA, U(1) MERA and the SU(2) MERA. U(1)-invariant tensors (see Chapter 4) have a block structure in the eigenbasis of \hat{J}_z operators on each index of the tensor, and therefore they incur a smaller memory cost in comparison to regular tensors. For example, it can be seen that for the same memory required to store a regular MERA with $\chi = 15$, one can instead consider storing a U(1)-MERA with $\chi = 21$. On the other hand, SU(2)-invariant tensors are substantially more sparse. When written in the canonical form, SU(2)-invariant tensors are not only block-sparse but each block, in turn, decomposes into a degeneracy part and a structural part such that the structural part need not be stored in memory. With the same amount of memory that is required to store, for example, a $\chi = 15$ regular MERA, one can already store a $\chi = 39$ SU(2) MERA.

In Fig. 6.14 we show an analogous comparison of the computational performance in the three cases. We plot the computational time required for one iteration of the energy minimization algorithm of (Evenbly and Vidal, 2009a) (during which all tensors in the MERA are updated once), as a function of the total bond dimension χ for the cases of regular MERA, U(1) MERA and SU(2) MERA. We see that for sufficiently large χ , using SU(2)-invariant tensors leads to a shorter time per iteration of the optimization algorithm. In the case of symmetric tensors we considered pre-computation of repeated operations, see Sec. 6.0.8.

Conclusions and Outlook

In this thesis we have described how to incorporate global internal symmetries into tensor network states and algorithms.

On the theoretical side we developed a framework to characterize and manipulate symmetric tensors. Any given tensor network can be adapted to the presence of a symmetry by imposing the constituent tensors to be symmetric. Symmetric tensors are very sparse objects. Their judicious use and careful manipulation can lead to an enormous computational gain in numerical simulations. This has been extensively demonstrated in this thesis by means of our reference MATLAB implementation.

On the implementation side, we have described a practical scheme for protecting and exploiting the symmetry in numerical simulations. We proposed the use of *tree decompositions* of a symmetric tensor. Several advantages of this scheme were discussed, not excluding the overall simplicity and elegance of the method. We hope to have provided a suitable implementation framework for researchers who are familiar with the theoretical aspects of incorporating the symmetries into tensor network algorithm but nonetheless find the practical implementation challenging.

In implementing symmetries we have gone beyond the case of MPS, which being a trivalent tensor network is simpler to handle. We described the construction of the $U(1)$ and $SU(2)$ symmetric versions of the MERA. Our Abelian implementation led to computational gains

measuring up to an increase of ten to twenty times. The analogous gain from the non-Abelian implementation was much larger, measuring up to an increase of forty to fifty times. These gains may be used either to reduce overall computation time or to permit substantial increases in the MERA bond dimension χ , and consequently in the accuracy of the results obtained. Therefore the exploitation of symmetries, especially non-Abelian symmetries, can be an invaluable tool for numerically challenging systems. This is more so the case in two dimensional lattice models where simulation costs are much more severe. An example of a potential application is to a system of interacting fermions that appears in the context of high temperature conductivity. Here even though symmetries are present in the model, they have not been thoroughly exploited in the context of tensor network algorithms.

Although we have given special attention to specific symmetry groups, $U(1)$ and $SU(2)$, the formalism presented in this thesis may equally well be applied to any reducible compact non-Abelian group that is multiplicity free. In particular, one can consider composite symmetries such as $SU(2) \times U(1)$, corresponding to spin isotropy and particle number conservation and $SU(2) \times SU(2)$ corresponding to conservation of spin and isospin etc. Such a symmetry is characterized by a set of charges (a_1, a_2, a_3, \dots) ; when fusing two such sets of charges (a_1, a_2, a_3, \dots) and $(a'_1, a'_2, a'_3, \dots)$, each charge a_i is combined with its counterpart a'_i according to the relevant fusion rule. Once again, this behaviour may be encoded into a single fusing tensor Υ^{fuse} .

Our implementation scheme can also be readily extended to incorporate more general symmetry constraints such as those associated with conservation of total fermionic and anyonic charge. One proceeds by defining the following tensors for the relevant charges,

- the fusing tensor Υ^{fuse} that encodes the fusion of two charges,
- the recoupling coefficients \hat{F} that relate various ways of fusing three charges, and
- the swap tensor \hat{R}^{swap} that encodes the swap behaviour of two charges.

Note that within our specific implementation framework, one may instead just define the linear maps $\hat{\Gamma}$ that mediate tensor manipulations for the respective charges.

As an example, consider fermionic constraints where the relevant charge, p , is the parity of fermion particle number. Charge p takes two values, $p = 0$ and $p = 1$ corresponding to even or odd number of fermions. The fusing tensor Υ^{fuse} encodes the fusion rules that specify how charges p and p' fuse together to obtain a charge p'' . These correspond to the fusion rules for the group Z_2 , given as,

$$\begin{aligned}(p = 0) \times (p' = 0) &\rightarrow (p'' = 0), \\(p = 0) \times (p' = 1) &\rightarrow (p'' = 1), \\(p = 1) \times (p' = 0) &\rightarrow (p'' = 1), \\(p = 1) \times (p' = 1) &\rightarrow (p'' = 0).\end{aligned}$$

The recoupling coefficients $\hat{F}_{p_a p_b p_c p_d}^{p_e p_f}$, associated with the fusion of three charges p_a, p_b and p_c are simple in this case owing to the Abelian fusion rules. They take a value $\hat{F}_{p_a p_b p_c p_d}^{p_e p_f} = 1$ for all values of intermediate charges p_e and p_f that appear when fusing the three charges one way or the other.

The final ingredient is the tensor \hat{R}^{swap} , which in this case is defined as,

$$\begin{aligned}\hat{R}_{p=0, p'=0 \rightarrow p''=0}^{\text{swap}} &= 1, & \hat{R}_{p=0, p'=1 \rightarrow p''=1}^{\text{swap}} &= 1, \\ \hat{R}_{p=1, p'=0 \rightarrow p''=1}^{\text{swap}} &= 1, & \hat{R}_{p=1, p'=1 \rightarrow p''=0}^{\text{swap}} &= -1.\end{aligned}$$

In a similar way, one can encode the corresponding fusion rules for anyonic charges into the fusing tensor Υ^{fuse} . In the case of anyons, the recoupling coefficients \hat{F} are obtained as solutions to the *pentagon equations* whereas the tensors \hat{R}^{swap} are replaced with the anyonic braid operators that are obtained as solutions to the *hexagon equations*, see (Feiguin et al., 2007; Pfeifer et al., 2010; Trebst et al., 2008). Thus, having defined these tensors for the relevant charges, the formalism and the implementation framework presented in this thesis can be readily adapted to incorporate the constraints corresponding to the presence of fermionic or anyonic charges.

In a different context, preservation of symmetry can be crucial even without demanding a computational gain. Recently, a novel classification of symmetric phases in 1D gapped spin systems was undertaken in (Chen et al., 2011). In the absence of any symmetry, in

this classification all states are equivalent to trivial product states. However, by preserving certain symmetries many phases were reported to exist with a different *symmetry protected topological order*. As an alternative, such a classification could potentially be addressed with the symmetric version of the MERA, since the MERA is adept at characterizing fixed points of the renormalization group flow which correspond to different phases.

Symmetries are a fundamental aspect of nature. Nearly all physical phenomenon can be explained by the presence or the absence of a symmetry. In numerical methods, the preservation of symmetries may well be a necessary requirement for simulating certain aspects of the system. As a computational aid, symmetries will play a crucial role in pushing forward the frontiers of tensor network algorithms in the coming years.

References

- M. Aguado and G. Vidal. *Phys. Rev. Lett.*, 100:070404, 2008. 3
- P. W. Anderson. *Science*, 235.:1196, 1987. 2
- J. Baez. Notes on quantum gravity. <http://math.ucr.edu/home/baez/>. 112
- T Barthel, C. Pineda, and J. Eisert. *Phys. Rev. A*, 80:042333, 2009. 4
- S. Bergkvist, I. P. McCulloch, and A. Rosengren. *Phys. Rev. A*, 74:053419, 2006. 6
- J. D. Biamonte, S. R. Clark, and D. Jaksch. *arXiv:1012.0531v1*, 2010. 112
- Z. Cai, L. Wang, X. C. Xie, and Y. Wang. *Phys. Rev. A*, 81:043602, 2010. 6
- X. Chen, Z.-C. Gu, and X.-G. Wen. *Phys. Rev. B*, 83:035107, 2011. 155
- L. Cincio, J. Dziarmaga, and M. M. Rams. *Phys. Rev.Lett.*, 100:240603, 2008. 3
- P. Corboz and G. Vidal. *Phys. Rev. B*, 80:165129, 2009. 4
- P. Corboz, G. Evenbly, F. Verstraete, and G. Vidal. *Phys. Rev. A*, 81:010303(R), 2010a.
4
- P. Corboz, R. Orus, B. Bauer, and G. Vidal. *Phys. Rev. B*, 81:165104, 2010b. 4
- J. F. Cornwell. *Group Theory in Physics*. Academic Press, 1997. 4, 6, 67, 93
- A.J. Daley, C. Kollath, U. Schollwock, and G. Vidal. *J.Stat. Mech. Theor. Exp.*, page
P04005, 2004. 3, 6
- A.J. Daley, S.R. Clark, D. Jaksch, and P. Zoller. *Phys.Rev. A*, 72:043618, 2005. 6

- I. Danshita, J.E. Williams, C. A. R. Sa de Melo, and C. W. Clark. *Phys. Rev. A*, 76:043606, 2007. 6
- G. Evenbly and G. Vidal. *Phys. Rev. B*, 79:144108, 2009a. 3, 143, 144, 151
- G. Evenbly and G. Vidal. *Phys. Rev. Lett.*, 102:180406, 2009b. 3
- G. Evenbly and G. Vidal. *Phys. Rev. B*, 81:235102, 2010a. 3
- G. Evenbly and G. Vidal. *New J. Phys.*, 12:025007, 2010b. 3
- H.G. Evertz. *Adv.Phys.*, 52:1, 2003. 1
- M. Fannes, B. Nachtergaele, and R. Werner. *Commun. Math. Phys.*, 144:443, 1992. .. 3
- A. Feiguin, S. Trebst, A.W.W. Ludwig, M. Troyer, A. Kitaev, Z. Wang, and M. H. Freedman. *Phys. Rev. Lett.*, 98:160409, 2007. 155
- V. Giovannetti, S. Montangero, and R. R. Fazio. *Phys. Rev. Lett.*, 101:180503, 2008. . 3
- Z.-C. Gu, M. Levin, and X.-G. Wen. *Phys. Rev. B*, 78:205116, 2008. 3
- Z.-C. Gu, F. Verstraete, and X.-G. Wen. *arXiv:1004.2563v1 [cond-mat.str-el]*, 2010. .. 4
- P. Henelius and A. W. Sandvik. *Phys. Rev. B*, 62:1102, 2000. 1
- H. C. Jiang, Z. Y. Weng, and T. Xiang. *Phys. Rev. Lett.*, 101:090603, 2008. 3
- J. Jordan, R. Orus, G. Vidal, F. Verstraete, and J. I. Cirac. *Phys. Rev. Lett.*, 101:250602, 2008. 3
- A. Y. Kitaev. *Annals of Physics*, 303:2, 2003. 1
- R. Konig, B. W. Reichardt, and G. Vidal. *Phys. Rev. B*, 79:195123, 2009. 3
- C. V. Kraus, N. Schuch, F. Verstraete, and J. I. Cirac. *Phys. Rev. A*, 81:052338, 2010. 4
- E. Y. Loh and J. E. Gubernatis. *Phys. Rev. B*, 41:9301, 1990. 1
- S.A. Major. *American Journal of Physics*, 67:972, 1999. 25
- I. McCulloch. *J. Stat. Mech.*, page P10014, 2007. 6

- I. P. McCulloch. *arXiv:0804.2509v1 [cond-mat.str-el]*, 2008. 2
- I. P. McCulloch and M. Gulacsi. *Europhys. Lett.*, 57:852, 2002. 6
- R.V. Mishmash, I. Danshita, C. W. Clark, and L. D. Carr. *Phys. Rev. A*, 80:053612, 2009. 6
- V. Murg, F. Verstraete, and J. I. . Cirac. *Phys. Rev. A*, 75:033605, 2007. 3
- V. Murg, F. Verstraete, and J. I. Cirac. *Phys. Rev. B*, 79:195119, 2009. 3, 4
- V. Murg, O. Legeza, R. M. Noack, and F. Verstraete. *Phys. Rev. B*, 82:205105, 2010. . 3
- D. Muth, B. Schmidt, and M. Fleischhauer. *New J. Phys.*, 12:083065, 2010. 6
- C. Nayak, S. H. Simon, A. Stern, M. Freedman, and S.D. Sarma. *Rev. Mod. Phys.*, 80:1083, 2008. 1
- T. Nishino and K. Okunishi. *J. Phys. Soc. Jpn.*, 67:3066, 1998. 3
- Y. Nishio, N. Maeshima, A. Gendiar, and T. Nishino. *arXiv:cond-mat/0401115v1*, 2004. 3
- S. Ostlund and S. Rommer. *Phys. Rev. Lett.*, 75:3537, 1995. 3, 6
- R. Penrose. Angular momentum: an approach to combinatorial space-time. <http://math.ucr.edu/home/baez/penrose/>, 1971. 26
- D. Perez-Garcia, F. Verstraete, M.M. Wolf, and J. I. Cirac. *Quantum Inf. Comput.*, 7:401, 2007. 3
- D. Perez-Garcia, M.M Wolf, M. Sanz, F Verstraete, and J.I. Cirac. *Phys. Rev. Lett.*, 100:167202, 2008. 6
- R. N. C. Pfeifer, G. Evenbly, and G. Vidal. *Phys. Rev. A*, 79:040301(R), 2009. 3
- R.N.C Pfeifer, P. Corboz, O. Buerschaper, M. Aguado, M. Troyer, and G. Vidal. *Physical Review B*, 82:115126, 2010. 155
- C. Pineda, T. Barthel, and J. Eisert. *Phys. Rev. A*, 81:050303(R), 2010. 4

- S. Pittel and N. Sandulescu. *Phys. Rev. C*, 73:014301, 2006. 6
- I. Pizorn and F. Verstraete. *Phys. Rev. B*, 81:245110, 2010. 4
- N. V. Prokofev, B. V. Svistunov, and I. S. Tupitsyn. *Zh. Eks. Teor. Fiz.*, 114:570, 1998.
1
- S. Ramasesha, S. K. Pati, H.R. Krishnamurthy, Z. Shuai, and J. L. Bredas. *Phys.Rev. B*,
54:7598, 1996. 6
- C. Rovelli. *LivingRev.Rel.* 1:1, 1998. 26
- C. Rovelli and L. Smolin. *Phys. Rev. D*, 53:5743, 1995. 26
- S. Sachdev. *Quantum Phase Transitions*. Cambridge University Press, 1999. 1
- J.J. Sakurai. *Advanced Quantum Mechanics*. Addison-Wesley Publishing Company, 1994.
67
- A. W. Sandvik. *Phys. Rev. Lett.*, 95:207203, 2005. 1
- M. Sanz, M.M. Wolf, D. Perez-Garcia, and J.I. Cirac. *Phys. Rev. A*, 79:042308, 2009. 6
- U. Schollwock. *Rev. Mod. Phys.*, 77:259, 2005a. 2
- U. Schollwock. *J. Phys. Soc. Jpn.*, 74S:246, 2005b. 3, 6
- Q.-Q. Shi, S.-H. Li, J.-H. Zhao, and H.-Q. Zhou. *arXiv:0907.5520v1 [cond-mat.str-el]*,
2009. 4
- Y. Y. Shi, L.-M. Duan, and G. Vidal. *Phys. Rev. A*, 74:022320, 2006. 3
- G. Sierra and M.A. Martin-Delgado. *arXiv:condmat/ 9811170v3*, 1998. 3
- G. Sierra and T. Nishino. *Nucl. Phys. B*, 495:505, 1997. 6
- S. Singh, H.-Q. Zhou, and G. Vidal. *New J. Phys.*, 12:033029, 2010a. i, iii, 6
- Sukhwinder Singh, Robert N. C. Pfeifer, and Guifre Vidal. *Phys. Rev. A*, 82:050301(R),
2010b. ii, iii

- Sukhwinder Singh, Robert N. C. Pfeifer, and Guifre Vidal. *Phys. Rev. B*, 83(11):115125, Mar 2011. doi: 10.1103/PhysRevB.83.115125. ii, iii
- O. F. Syljuasen and A. W. Sandvik. *Phys. Rev. E*, 66:046701, 2002. 1
- L. Tagliacozzo, G. Evenbly, and G. Vidal. *Phys. Rev. B*, 80:235127, 2009. 3
- W. Tatsuaki. *Phys. Rev. E*, 61:3199, 2000. 6
- S Trebst, M. Troyer, Z. Wang, and A.W.W. Ludwig. *Prog. Theor. Phys. Supp.*, 176:384, 2008. 155
- F. Verstraete and J. I. Cirac. *arXiv:cond-mat/0407066v1*, 2004. 3
- G. Vidal. *Phys. Rev. Lett.*, 91:147902, 2003. 3
- G. Vidal. *Phys. Rev. Lett.*, 93:040502, 2004. 3, 6
- G. Vidal. *Phys. Rev. Lett.*, 98:070201, 2007a. 3, 6
- G. Vidal. *Phys. Rev. Lett.*, 99:220405, 2007b. 3
- G. Vidal. *Phys. Rev. Lett.*, 101:110501, 2008. 3
- G. Vidal. *in Understanding Quantum Phase Transitions*. Taylor & Francis, Boca Raton, 2010. 3
- S. R. White. *Phys. Rev. Lett.*, 69:2863, 1992. 2, 6
- S. R. White. *Phys. Rev. B*, 48:10345, 1993. 2
- S.R. White and A.E. Feiguin. *Phys. Rev. Lett.*, 93:076401, 2004. 3, 6
- K. G. Wilson. *Rev. Mod. Phys.*, 47:773, 1975. 3
- Z. Y. Xie, H. C. Jiang, Q. N. Chen, Z. Y. Weng, and T. Xiang. *Phys. Rev. Lett.*, 103:160601, 2009. 3